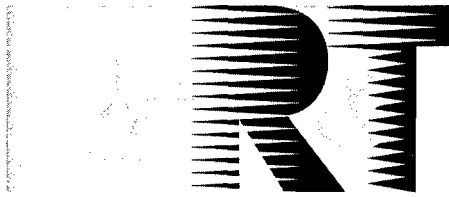


NORTH ATLANTIC TREATY ORGANIZATION



RESEARCH AND TECHNOLOGY ORGANIZATION

BP 25, 7 RUE ANCELLE, F-92201 NEUILLY-SUR-SEINE CEDEX, FRANCE

RTO MEETING PROCEEDINGS 17

Qualification of Life Extension Schemes for Engine Components

(Homologation des programmes de prolongation du cycle de vie des organes moteur)

Papers presented at the Workshop of the RTO Applied Vehicle Technology Panel (AVT) – organised by the former AGARD Structures and Materials Panel – held in Corfu, Greece, 5-6 October 1998.



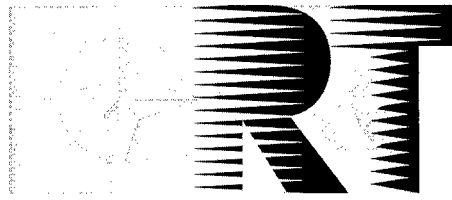
DISTRIBUTION STATEMENT A
Approved for Public Release
Distribution Unlimited

19990324 041

Published March 1999

Distribution and Availability on Back Cover

NORTH ATLANTIC TREATY ORGANIZATION



RESEARCH AND TECHNOLOGY ORGANIZATION

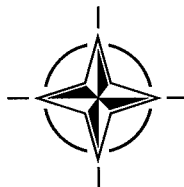
BP 25, 7 RUE ANCELLE, F-92201 NEUILLY-SUR-SEINE CEDEX, FRANCE

RTO MEETING PROCEEDINGS 17

Qualification of Life Extension Schemes for Engine Components

(Homologation des programmes de prolongation du cycle de vie des organes
moteur)

*Papers presented at the Workshop of the RTO Applied Vehicle Technology Panel (AVT) –
organised by the former AGARD Structures and Materials Panel – held in Corfu, Greece,
5-6 October 1998.*



DISTRIBUTION STATEMENT A
Approved for Public Release
Distribution Unlimited

DTIC QUALITY INSPECTED 4

AQF99-06-1206

The Research and Technology Organization (RTO) of NATO

RTO is the single focus in NATO for Defence Research and Technology activities. Its mission is to conduct and promote cooperative research and information exchange. The objective is to support the development and effective use of national defence research and technology and to meet the military needs of the Alliance, to maintain a technological lead, and to provide advice to NATO and national decision makers. The RTO performs its mission with the support of an extensive network of national experts. It also ensures effective coordination with other NATO bodies involved in R&T activities.

RTO reports both to the Military Committee of NATO and to the Conference of National Armament Directors. It comprises a Research and Technology Board (RTB) as the highest level of national representation and the Research and Technology Agency (RTA), a dedicated staff with its headquarters in Neuilly, near Paris, France. In order to facilitate contacts with the military users and other NATO activities, a small part of the RTA staff is located in NATO Headquarters in Brussels. The Brussels staff also coordinates RTO's cooperation with nations in Middle and Eastern Europe, to which RTO attaches particular importance especially as working together in the field of research is one of the more promising areas of initial cooperation.

The total spectrum of R&T activities is covered by 6 Panels, dealing with:

- SAS Studies, Analysis and Simulation
- SCI Systems Concepts and Integration
- SET Sensors and Electronics Technology
- IST Information Systems Technology
- AVT Applied Vehicle Technology
- HFM Human Factors and Medicine

These Panels are made up of national representatives as well as generally recognised 'world class' scientists. The Panels also provide a communication link to military users and other NATO bodies. RTO's scientific and technological work is carried out by Technical Teams, created for specific activities and with a specific duration. Such Technical Teams can organise workshops, symposia, field trials, lecture series and training courses. An important function of these Technical Teams is to ensure the continuity of the expert networks.

RTO builds upon earlier cooperation in defence research and technology as set-up under the Advisory Group for Aerospace Research and Development (AGARD) and the Defence Research Group (DRG). AGARD and the DRG share common roots in that they were both established at the initiative of Dr Theodore von Kármán, a leading aerospace scientist, who early on recognised the importance of scientific support for the Allied Armed Forces. RTO is capitalising on these common roots in order to provide the Alliance and the NATO nations with a strong scientific and technological basis that will guarantee a solid base for the future.

The content of this publication has been reproduced directly from material supplied by RTO or the authors.



Printed on recycled paper

Published March 1999

Copyright © RTO/NATO 1999
All Rights Reserved

ISBN 92-837-1012-6



*Printed by Canada Communication Group Inc.
(A St. Joseph Corporation Company)
45 Sacré-Cœur Blvd., Hull (Québec), Canada K1A 0S7*

Qualification of Life Extension Schemes for Engine Components

(RTO MP-17)

Executive Summary

A significant fraction of the life-cycle cost of an aircraft engine can be attributed to the high replacement cost of engine components that are damaged in service. This Workshop addresses component damage management and ways to reduce operating costs by extending component lives without sacrificing safety. Life extension options available to life cycle managers include (1) improving the durability of components through material substitution, or the addition of protective coatings, (2) returning damaged parts to service after welding or brazing of cracks, (3) eliminating microstructural damage by reconditioning treatment, and (4) implementing new, more efficient lifing techniques for critical parts, such as turbine discs, based on the condition of the parts.

Of the eighteen papers presented at the Workshop, three discuss military needs and benefits accruing from engine component life extension. Three papers describe treatment for enhancing durability of engine materials, another three describe specific repair technologies, while three papers discuss the procedures and testing requirements to qualify life extension technologies for aircraft applications. The remaining six papers deal with analytical methods of life cycle calculation enabling life extension of critical parts beyond conventional "safe life" limits, within acceptable safety limits.

Engine life cycle managers should remain well aware of factors responsible for component damage in their fleet, and the options available to them for achieving component life extension. In this respect, software for failure mode and effect criticality analysis is a powerful tool to help decide which life management option to choose. Several factors influence the decision to either repair or replace components, or to implement new life cycle management procedures for critical parts. The overriding factors, for both critical and non-critical parts in military aircraft engines, are (i) expected cost benefits, (ii) system safety and (iii) cost effectiveness of engine removal frequency for inspections.

The implementation of repairs for damage that exceeds manufacturers' recommended limits is possible in some cases. Such implementation requires a careful analysis of design issues, as well as access to engineering expertise and facilities to qualify the repair technology. Sometimes, simple inexpensive recycling solutions can be developed to avoid having to scrap slightly damaged parts. Also, on occasion, qualification by analysis may be possible, but most often, extensive testing at the material sample and component levels, including in service trials, is required to demonstrate that the repaired and/or modified component is safe to use and remains so once returned to service.

Life extension of critical parts beyond conventional "safe life" limits based on damage tolerance and inspection concepts is not only feasible, but also applicable to older engines. Reliable life prediction models and accurate fracture mechanics data, coupled with a statistical approach, are required for safe implementation of damage tolerant methodologies. Implementation is complex and often compromised by a lack of detailed information on the thermal-mechanical loading conditions for critical components

and by uncertainties in material properties. Finally, it is shown that no proven methods exists at present for designing around high cycle fatigue (HCF) problems, triggered by other forms of service-induced damage, such as low cycle fatigue (LCF), foreign object damage (FOD) or fretting. Damage tolerance concepts are being considered for minimizing risks of failures, but have yet to be proven. An indirect way of dealing with the HCF issue would be to increase the resistance of engine materials to LCF, FOD or fretting.

Homologation des programmes de prolongation du cycle de vie des organes moteur

(RTO MP-17)

Synthèse

Une part importante des coûts d'exploitation d'un moteur d'avion provient du prix élevé de remplacement des pièces endommagées en service. L'atelier traite de la gestion de cet endommagement et de l'application de techniques permettant de prolonger la vie de pièces coûteuses, afin de réduire les coûts d'exploitation des moteurs, sans en compromettre la sécurité. Les options de prolongement de vie mis à la disposition des responsables de la gestion du cycle de vie des moteurs comprennent (1) l'augmentation de la durabilité des pièces par substitution de matériaux ou l'ajout d'un revêtement protecteur, (2) la remise en service de pièces après réparation de fissures par soudage ou brasage, (3) l'élimination de l'endommagement de la microstructure par traitement de remise en état et (4) la mise en pratique de nouvelles techniques de gestion de vie plus efficaces pour les pièces critiques, telles les disques de turbine, fondées sur la condition des pièces.

Trois des dix huit présentations de l'atelier traitent des besoins militaires et des bénéfices à retirer de la mise en pratique des technologies de prolongement de vie pour pièces de moteurs. Trois articles discutent de modifications de surface visant à augmenter la durabilité des matériaux utilisés, trois autres décrivent des méthodes spécifiques de réparation, tandis que trois autres encore se penchent sur les procédures et les exigences des essais d'homologation pour applications aéronautiques. Les six autres articles couvrent les méthodes analytiques de calcul de vie permettant de prolonger la durée de vie de pièces critiques au delà des limites conventionnelles de la durée de vie sûre, dans des conditions de sécurité acceptables.

Les responsables de la gestion du cycle de vie des moteurs se doivent de bien comprendre les modes d'endommagement associés au vieillissement des pièces, ainsi que les options disponibles pour prolonger leur durée de vie. Dans ce contexte, un logiciel d'analyse des modes de défaillance et de la criticité des effets est un outil puissant permettant aux responsables de choisir parmi plusieurs options. Plusieurs facteurs influencent la décision de réparer ou de remplacer des pièces, ou encore d'introduire une nouvelle méthode de gestion de vie pour pièces critiques. Les principaux facteurs qui s'appliquent à la fois aux pièces critiques et non critiques dans les moteurs militaires sont (I) les bénéfices attendus en terme de coûts, (II) la sécurité des systèmes et (III) la rentabilité de la fréquence de démontage des moteurs pour l'inspection des pièces.

Il est parfois possible de réparer des pièces endommagées au delà des limites autorisées par les motoristes. Dans ce cas, il est important d'aborder les questions de conception et d'avoir accès aux installations et à l'expertise nécessaire pour l'homologation du procédé de réparation, et de la firme qui compte l'appliquer. Parfois, des solutions simples et peu coûteuses peuvent être élaborées afin de recycler des pièces qui ne sont que légèrement endommagées. Enfin, bien qu'une homologation par analyse soit quelquefois possible, dans la plupart des cas, des essais d'homologation sur éprouvettes ou sur pièces, y compris des essais de pièces sur moteur, sont nécessaires afin d'assurer une remise en service de pièces réparées ou modifiées de façon sûre et fiable.

La gestion de vie des pièces critiques fondée sur la tolérance à l'endommagement et sur l'inspection, qui permet de prolonger leur durée de vie utile au delà des limites conventionnelles de la durée de vie sûre, est non seulement faisable mais aussi applicable rétroactivement à des moteurs anciens. Pour assurer la sécurité, des modèles fiables de prévision de durée de vie et des données précises en mécanique de la rupture, associées à une approche statistique, sont nécessaires. La mise en pratique de telles méthodes de gestion de vie est complexe, et souvent compromise par le manque de données précises sur les contraintes thermo-mécaniques auxquelles sont soumises les pièces critiques et par les incertitudes concernant les propriétés des matériaux. Enfin il a été souligné qu'il n'existait aucune méthode reconnue pour faire face aux problèmes de fatigue vibratoire engendrés par d'autres formes d'endommagement, telles la fatigue oligocyclique, l'impact par objet externe ou le frettage. Des concepts de tolérance à l'endommagement ont été suggérés pour minimiser les risques de défaillance qui en découlent, mais rien n'a été encore démontré en pratique. Une solution indirecte au problème serait d'augmenter la résistance des matériaux pour moteurs à la fatigue oligocyclique, à l'impact par objet externe et au frettage.

Contents

	Page
Executive Summary	iii
Synthèse	v
Preface	ix
Sub-Committee Membership	x
	Reference
Summary of the Workshop and the Round Table Discussion by A. Lasalmonie and J.-P. Immarigeon	S
Technical Evaluation Report by A. Lasalmonie	T
SESSION I: COMPONENT LIFE EXTENSION - NEEDS AND BENEFITS	
Aero-Engine Component Repair/Replacement Decision Factors by R.R. Hastings	1
Cost Effectiveness of Modern Lifting Concepts - Consideration of Economical Aspects Concentrating on Group A Parts of Military Aircraft Engines by K.U. Tschirne and W. Holzbecher	2
International Acceptance of Commercial Repair Approvals by W. Thomas and B. Junkin	3
High Cycle Fatigue Life Management in Gas Turbine Engines by T. Nicholas	4
Cost Benefit Analysis for the Use of Better Turbine Materials and Technology Including Predicted Life Improvements by T.J. Williams	5
Repair Developments to Fit Customer Needs (Presented in Session I) by D. Burlon (See Paper 15)	15
SESSION II: LIFE EXTENSION THROUGH USE OF SURFACE MODIFICATION TREATMENTS	
Low Friction Diamond-like Carbon Coatings for Engine Applications by J. Smeets	6
Life Extension of IN706 Type Disc Materials by Surface Modification with Boron by J. Rösler and S. Müller	7

TBC and Other Surface Coatings; Benefits and Lining Procedures by D.L. Shaw	8
---	----------

Paper 9 withdrawn

Paper 10 withdrawn

SESSION III: LIFE EXTENSION THROUGH USE OF REPAIRS/REFURBISHMENT PROCEDURES

Enabling Technologies for Turbine Component Life Extension by J. Liburdi	11
--	-----------

Development of a Qualification Methodology for Advanced Gas Turbine Engine Repairs/Reworks by P.C. Patnaik and R. Thamburaj	12
---	-----------

Advanced Recontouring Process for Compressor Blades by M. Panten and H. Hönen	13
---	-----------

Paper 14 withdrawn

Repair Developments to Fit Customer Needs (Presented in Session I) by D. Burlon	15
---	-----------

Fracture Mechanics Evaluation of Weld Repaired Seal Teeth for Life Extension of Aircraft Gas Turbine Engine Components by P.A. Domas	16
--	-----------

Propeller Barrel Cam Life Extension by K. Tandon, B. Junkin and W. Thomas	17
---	-----------

SESSION IV: COMPONENT LIFE EXTENSION THROUGH IMPROVED LIFE MANAGEMENT

The Development of Life Extension Methods for Fracture Critical Aero-Engine Components by A.D. Boyd-Lee and G.F. Harrison	18
---	-----------

Critical Parts' Life Extension Based on Fracture Mechanics by P. Blüml and J. Broede	19
--	-----------

Damage Tolerance and Reliability of Turbine Engine Components by C.C. Chamis	20
--	-----------

Life Extension Methodology Based on Creep-Fatigue Models by C. Moura Branco, A. Sousa e Brito and J. Byrne	21
--	-----------

Preface

Turbine components incur damage in service as a result of their demanding operating environments. The damage may be external, affecting surface finish and component dimensions, which is detrimental to aerodynamic performance and load bearing capacity of gas path components. External damage also provides sites for crack initiation, thereby reducing lives of affected parts. The damage may be internal, affecting microstructure in highly stressed components and hot parts, which may fail by fatigue or by creep. When damage becomes excessive, as dictated by design, the components are replaced with new ones. A significant fraction of the life cycle cost of aero-engines is associated with replacement of service-damaged parts.

The objective of the two-day Workshop was to bring together military turbine engine life cycle managers and technical experts from the various NATO countries to discuss component damage management, and techniques for extending lives of service-damaged parts to achieve engine life cycle cost reductions. Operator's needs and various technologies available, including protective surface treatments and coatings, repairs and refurbishment procedures, as well as improved component life cycle management practices, are discussed. Implementation of these technologies in older engine as retrofits is addressed. Emphasis is placed on the qualification testing requirements that must be satisfied to ensure that repaired or modified parts, or parts for which new life cycle management practices are applied, remain safe and reliable when returned to service.

Dr. J.P. IMMARIGEON
Sub-Committee Chairman

Préface

Les pièces de turbine s'endommagent en cours de service dû à l'agressivité de leur environnement d'exploitation. L'endommagement peut être externe, affectant les finis de surface ou les dimensions, qui affectent à leur tour, les performances aérodynamiques et la capacité de charge de l'aubage de turbine. Le dommage externe peut aussi engendrer des amorces de fissures, réduisant ainsi la durée de vie des pièces affectées. Le dommage peut également être interne, affectant la microstructure dans les pièces hautement sollicitées en charge et en température, qui peuvent faire défaut par fatigue ou fluage. Lorsque l'endommagement est jugé excessif, selon les critères de conception, les pièces doivent être remplacées. Une proportion importante des coûts d'exploitation des moteurs d'avion provient du remplacement des pièces endommagées en service.

Cet atelier de deux jours a rassemblé des responsables de la gestion de vie de moteurs militaires et des spécialistes de différent pays de l'OTAN afin de discuter de la gestion de l'endommagement des composants de moteurs et des techniques de prolongation de durée de vie pour pièces endommagées, en vue de réduire les coûts de remplacement. L'atelier examine les besoins des exploitants et discute des différentes technologies disponibles, y compris, l'utilisation de traitements de surface ou de revêtements protecteurs, les réparations et remises en état des pièces, ainsi que les techniques améliorées de gestion du cycle de vie des composants critiques. L'application de ces technologies à des moteurs anciens est également envisagée. L'accent est mis sur les exigences en matière d'homologation qui doivent être satisfaites afin d'assurer la remise en service de façon sûre et fiable de pièces réparées ou modifiées, ou ayant fait l'objet de nouvelles techniques de gestion du cycle de vie.

Dr. J.P. IMMARIGEON
Président du Sous-Comité

Sub-Committee Membership

Chairman

Dr. J-P. IMMARIGEON
Chief, Materials
Institute for Aerospace Research
National Research Council of Canada
Montreal Road
Ottawa, Ontario, K1A 0R6
CANADA

Members

J-M Dauphant	-	FR	S. Sampath	-	US
H. Goncalo	-	PO	R. Servent	-	SP
P. Heuler	-	GE	J. Vantomme	-	BE
L. Kompotiatis	-	GR	J. Waldman	-	US
H.H. Ottens	-	NE	M. Winstone	-	UK

Panel Executive

Dr. J.M. CARBALLAL, SP

Mail from Europe:

RTA-OTAN/AVT
BP 25
7, rue Ancelle
F-92201 Neuilly-sur-Seine Cedex
France

Mail from US and
Canada:

RTA-NATO/AVT
PSC 116
APO AE 09777

Tel. 33 (0) 1 55 61 22 90 & 92

COMPONENT LIFE EXTENSION NEEDS AND BENEFITS

SUMMARY OF THE WORKSHOP AND OF THE ROUNDTABLE

A. LASALMONIE

SNECMA

Etablissements de Villaroche

77550 Moissy-Cramayel - France

JP. IMMARIGEON

Institute for Aerospace Research, NRC

Montreal Road

Ottawa, Ontario K1A 0R6, Canada

THE ISSUE AND CHALLENGES

The armed forces of NATO are faced to the problem of aging systems, the life of it must be extended at optimum cost. The motivation is to reduce the LCC (Life Cycle Cost) ; a concept which is now the practice for commercial engines.

The problem is different for non critical parts which are sold by the manufactures « on condition » or for the critical parts which are « lifed » for a given time.

THE PROCESS IN MAINTENANCE AND REPAIR

All the presentations stressed the importance of close relations between all the actors involved in maintenance strategy :

- 1 The users which need to be « smart users » whether they are commercial or military Cost effective maintenance and life extension strategies need strong input of the users to set knowledge based expert systems, necessary to take decisions on the strategy
- 2 The players are :
 - The repair shops
 - The engineering
 - The O.E.M. (Original Engine Manufacturer)
 - The Approval authorities

The decision to introduce new technologies such as :

 - the replacements of old parts :
 - The repair/rework
 - The life management

depend of a comparative cost analysis of these three possibilities
- 3 The output :
 The output of the process is a cost analysis of the various possibilities to extend life and a conclusion on the cost effectiveness of the best solution.
 The point was raised of the possibilities of conflicting interests between the various solutions since the conclusion of a cost effectiveness analysis can be different if the repair shop is independent or related to an OEM or an user ; the dependence of the Engineering which contribute to the decision is also a key factor

THE TECHNICAL ASPECTS

The main general conclusions of the workshop are as follows :

1 Failure modes of the parts

- They are not always clearly understood or documented for specific components, which make choices for new technologies difficult
- HCF, LCF, Fretting and FOD are increasingly important as life is now extended beyond the original target

2 Rejection criteria

The controllers are faced with unclear criteria due to the fact that the problems are not anticipated or studied. Input from experience can help to find unexpensive solutions and avoid unnecessary scrap of slightly damaged parts

3 Surface modification treatments

It was found that more discussions between people working on the surface treatments and designers are necessary to have a clear view on the influence of these treatments on the properties and design.

A good example is the addition of a TBC which is favourable to the life only if the TBC has been integrated in the design (TBC adds weight and has no mechanical function).

4 Repair and rework

It was again emphasized that process control was important to ensure consistency and repeatability

5 improved life management for critical components

- Several papers showed clearly that life extension beyond the safe service life was possible. however this assumes good lifing models and accurate fracture mechanics data coupled with a statistical approach
- Obviously life management beyond safe service life also needs accurate stress and temperature measurements on the parts. It is also dependent of the capability to introduce in the models stress and temperature cycles representing the actual service conditions.
- This last condition is not easy to fulfill for military planes and raises the problem of reliable usage monitoring systems
 - The necessity of good NDT techniques to allow life management was also raised ; the problem being the cost of such controls.

MAIN POINTS RAISED DURING THE DISCUSSION

1 THE PROCESS

A component Improvement Programme exists in North America where founding coming from national and foreign military common customers is used to address common durability problems and identify new technologies for extending component lives. Such multi-client program concepts do not exist in other Nato countries (Germany, France...)

2 SURFACE TREATMENTS/REPAIRS/REWORK

J. LIBURDI explained that for the non critical parts, life extension is usually managed on a comparative basis ; most of the effort is focused on restoration of the metallurgical and geometrical characteristics. However, restoring the initial structures is not always possible ; i.e. : high temperature solutioning treatments are sometimes impossible due to interdiffusion effects. Sometimes repair shops are able to improve the properties of the parts when they have a good understanding of the physical metallurgy principles governing alloy properties and its service degradation. An exemple is tip rebuilding of turbine blades using a material more oxidation resistant than the original one.

However the repair shop has not always a clear view on the interaction between the repaired parts and the engine environment.

LIFE MANAGEMENT

The following problems were raised :

1 AVAILABILITY OF THE ENGINES

The extension of « on wing life » may not be the highest-priority for armed forces. For some representatives the most important aspect was claimed to be the predictability of repair frequency to guarantee the availability of the engines.

2 IN SERVICE MONITORING

In service monitoring is difficult to implement especially for older engines. It was pointed out that, for civil engines, the engine cycles are usually well known and very reproducible ; this is not the case for military engines.owing to wide differences in ways the engines are used.

3 MANAGEMENT OF REPAIRED PARTS

M. WINSTONE (DERA) raised the issue of the tracking of repaired parts : is there a management system ? Can the same part be repaired several times ?

For GEAE and SNECMA all the engines have documented histories. The manual indicates how to mark and follow a part although it is not always detailed (it may just indicate that a repair was made but not provide details).

The various Air Force representatives expressed that documentation was compulsory with clear visibility. The canadian Air Force applies the same process as commercial companies.

In conclusion a part management system is important, but it cannot be detailed and may be difficult to exploit over extended periods of times.

4 LIFE EXTENSION OF CRITICAL PARTS

Damage tolerance models and retirement for cause are solutions to extend the life.

However many problems arise :

- The theoretical bases are not always well established : long cracks behaviour is reasonably described in fracture mechanics ; on the contrary short cracks are much more difficult to study and introduce large scatter in the properties.

C.C. CHAMIS (NASA) emphasized that if failure mechanisms are unique for a given material, the failure modes will change with the operating conditions which makes the predictions difficult.

G. HARRISON (DERA) explained that materials with strong anisotropy made stress redistributions more difficult to calculate. He gave the example of single crystals with the possible influence of anisotropy on surface strains and TBC spalling.

- Retirement for cause need efficient NDT techniques ; very small defects must be found with high confidence ; the inspections will be very costly: this has to be included in the cost analysis

- Evaluation of the risk due to life extension : if life extension is applied only to the fleet leader, the induced risk is very low and can be accepted (G. HARRISON, DERA)

To increase the statistical basis it is also possible to test to rupture the components which were retired early.

- JP. IMMARIGEON remarked that in some cases the damage tolerance philosophy cannot be avoided when no more spare parts are available for very old engines

SUGGESTION FOR FUTURE ACTIVITIES

From this discussion, the following subjects related to life extension are considered important :

- Retirement for cause of critical parts
- Usage monitoring systems
- Repaired parts documentation methodology

Recorder's report on the workshop :

QUALIFICATION OF LIFE EXTENSION SCHEMES FOR ENGINES COMPONENTS

Alain Lasalmonie
Département YKO - SNECMA
Etablissements de Villaroche
77550 Moissy-Cramayel - France

I. INTRODUCTION

There is a continuing need for NATO forces to reduce the cost of operating military equipment. A major part of the life-cycle cost of an aircraft can be attributed to the powerplant and its components. The replacement cost of service-damaged engine components is a significant contributing factor. Such figures are probably similar to those experienced by other NATO nations. Therefore, from an operational cost point of view, techniques for extending the usable life of engine components should be very attractive to NATO forces.

Engines components incur damage in service as a result of their demanding operating environments. The damage may take many forms, depending on type of component and operating conditions. For gas path components, it may be external, affecting surface finish or dimensions, which tends to adversely affect aerodynamic performance. The damage may also be internal, in the form of creep or thermomechanical fatigue damage, and may involve cracking, as a result of which component structural integrity is reduced. When operating conditions prove to be more severe than originally anticipated, and materials capabilities are exceeded, premature unforecast failures may occur. Such failures affect powerplant reliability, which in turn has a significant impact on aircraft operational cost and capabilities.

In order to reduce aircraft engine operating costs, operators may :

- a) extend the usable life of gas path components by providing increased

protection against environmental attack through such means as the application of protective coatings or other forms of surface modification treatments (to new or service-exposed parts) ,

- b) return excessively damaged parts to functional serviceability through welding or brazing of thermal fatigue cracks ; surfaces can also be rebuilt and internal damage, such as creep voids or fatigue damage, can be eliminated by HIP rejuvenation or heat treatments.

Whichever life extension technology option is pursued, there are airworthiness qualification requirements that must be satisfied to ensure that repaired or modified parts remain safe and reliable when return to service. Furthermore, the introduction of new life extension technologies may require the implementation of new life cycle management approaches for repaired and/or modified components used beyond conventional life limits.

This workshop intended to :

- a) evaluate the state-of-the art in engine component life extension technologies
- b) share experience in methodologies used to qualify the technologies as airworthy for aircraft engine use,
- c) review field experience with life extension technologies, through case studies for cold and hot gas path components, and discuss the life cycle management of repaired/modified engine components.

Several speakers invited to this workshop came from the commercial engines industry since the concerns are more and more similar for the military and commercial business.

The summary of the 4 sessions will be given below, with the main point raised during the discussions.

The conclusions of the roundtable are detailed at the end of this proceeding.

II. COMPONENT LIFE EXTENSION : NEEDS AND BENEFITS

Several papers (papers 1, 2) stressed the importance of a cost Effectiveness Analysis (CEA) before deciding between repair and replacement of used components.

The CEA is not a trivial task since it includes technical costs and the cost of the certification process, which needs appropriate structures when life improvement must be substantiated.

- Other papers (paper 3, 15) evinced the benefits which should be gained by military operators by adopting methodologies similar to commercial standards : repair schemes and delegation with maintenance contractors; participation of the customers to repair programs ;
- Life management, life cycle cost were discussed in papers 2, 4, 5.

The interest of reliable life usage monitoring systems was discussed in paper 2 ; one interesting conclusion was that scrapping of parts with remaining life is not a waste of money when carefully planned.

Paper 4 showed how a damage tolerant approach could be efficient to manage the life of fracture limited parts. However

knowledge is still limited on LCF-HCF interactions.

III. LIFE EXTENSION THROUGH USE OF SURFACE MODIFICATION TREATMENTS

This session was devoted to protective coatings (papers 6, 8, 10) and to surface modifications (paper 7) in order to improve the environmental resistance.

DLC coatings (paper 6) have been known for a long time, without finding extensive applications in aeroengines, although their tribological properties are good.

Paper 8 argued that life extension by the addition of TBC is difficult to demonstrate through laboratory testing ; full use of the TBC depends of the understanding of the failure mechanisms of both the barrier and the component.

IV. LIFE EXTENSION THROUGH USE OF REPAIRS / REFURBISHMENT PROCEDURES

An interesting methodology was presented by Orenda (paper 12) for repair/rework/design change of gas turbine engines.

This methodology addresses an organised approach including :

- failure mode analysis
- coupon testing
- component rig testing
- engine testing
- design change approval

This approach is very similar to that used for commercial engines.

Paper 11 (J. Liburdi) detailed technologies developed for repairing turbine components. The complexity of the components and the cost of the repair technologies are such that cooperations between the repair facilities and the engine manufacturers is increasingly important.

Papers 13, 16, 17 gave practical example of life extension.

In the case of recontouring compressor blades (paper 13) the question was raised of the efficiency of the new profile compared to the original one. This is a general problem which emphasises the importance of linking design and repair.

Another interesting question raised in paper 17 is that, inspectors in the maintenance shops have sometimes no clear guidelines for the rejecting criteria ; as a result they may have a tendency to scrap many parts. There is thus, a need for improved inspection capabilities and for standards (Typical defects...)

Starting from an example on seal teeth, paper 16 highlights the process variability and the need to characterise process capability in terms of margins and specifications limits.

V. COMPONENT LIFE EXTENSION THROUGH IMPROVED LIFE MANAGEMENT

Paper 18 discusses the safe service life for fracture critical components.

Life extension beyond the safe value is sometimes possible and 3 ways are described in the paper :

1. Exploitation, of the full safe life capability in crack-tolerant components,
2. Exploitation if non finite fatigue test results
3. Acceptance of a risk at a limited level

The average life extension found possible is 20 %.

Paper 19 is complementary of the previous one since it compares two methods : "The safe crack initiation life approach" and "the safe crack propagation life approach".

The second approach can significantly extend the authorised life.

Paper 20 describes a formal method to quantify structural damage tolerance and reliability. The results indicate that the method is suitable for predicting remaining life in aging structures.

However for all methods, one of the practical problems is the weak correlation between flight time and cyclic life : better application of the modelling could be achieved with better on-board monitoring of the engine cycles.

IV. ROUNDTABLE DISCUSSION

The main point raised in the roundtable are :

1. a close relationship between all the actors of the maintenance strategy is increasingly important. The players involved are : the users, the repair shops, the engineering, the O.E.M. and the approval authorities.
2. The failure modes of the parts are not clearly documented
3. The rejection criteria for the controllers are, often, not clear enough
4. Full advantage of the surface treatments depend of closer discussions with engineering
5. Improved life management would need reliable usage monitoring systems to have realistic stress and temperature cycles,

6. Financial gains would be possible by generalising components Improvement multiclient programs.

The long discussions on life management showed the difficulty of this problem ; various aspects of it are detailed in the roundtable summary.

The following activities were suggested for the future :

- retirement for cause
- usage monitoring systems
- repaired parts documentation methodology

AERO-ENGINE COMPONENT REPAIR/REPLACEMENT DECISION FACTORS

R.R. Hastings

Director of Marketing, Atlantis Aerospace Corporation
1 Kenview Blvd, Brampton, Ontario, Canada L6T 5E6

1. SUMMARY

The high cost of ownership of military weapons systems coupled with shrinking defence budgets is encouraging the pursuance of alternative management strategies for cost control. Aero-engines which typically consume 30% of the life cycle costs of a fighter aircraft platform are a prime target for initiatives including: damage tolerant design practices, on-condition maintenance and the repair, refurbishment or rejuvenation of components as opposed to their replacement. While the foregoing issues address cost issues in a very direct manner, there are a number of other factors which may motivate owners of large fleets of aircraft to pursue management by repair/refurbishment.

2. ABBREVIATIONS

CEA	Cost Effectiveness Analysis
CF	Canadian Forces
DND	Canadian Department of National Defence
DRDB	Canadian Defence Research and Development Branch
FMECA	Failure Mode, Effects, and Criticality Analysis
FOD	Foreign Object Damage
HF	Hydrogen Fluoride (Ion Cleaning)
HIP	Hot Isostatic Pressing
HPC	High Pressure Compressor
HPT	High Pressure Turbine
IAR	Institute for Aerospace Research (of NRCC)
LCF	Low Cycle Fatigue
NRCC	National Research Council of Canada
OEM	Original Equipment Manufacturer
R&O	Repair and Overhaul
ROI	Return on Investment
TCA	Transport Canada Aviation

3. INTRODUCTION

The Canadian Forces (CF), through the Defence Research and Development Branch (DRDB) initiate a focussed research and development program in 1978 to develop the capability of performing unique repairs or life extension processes on aero-gas turbine parts including those components considered to be flight critical. This program culminated in 1998 with the generation of an engine repair qualification process and the demonstration of that process using parts from the F404-GE-400 engines used in Canada's CF18 aircraft. This 20 year program has been a partnership between the Department of National Defence (DND), the National Research Council of Canada (NRCC) and Canadian industry lead by the repair and overhaul (R&O) contractor for CF F404 engines, the Orenda Division of Magellan Aerospace. Without this partnership, and investment by these two primary partners, DND could not have pursued this ambitious project.

The operational and cost impact of aero-engines on weapon system programs from a Canadian context is first provided. Next discussed are the factors which motivate an operator of aircraft engines to pursue repair technique development. These considerations include not only the contracted cost of repair and overhaul but also such issues as military maintenance personnel overheads, flight safety, security of supply, and industrial support base considerations. The discussion of cost and operational benefit motivators is followed by a description of the prerequisites considered necessary by the CF for the pursuance of a repair process development. These include: fundamental metallurgical competence, an understanding of the operating environment of the components, facility requirements, and a qualification or certification process for the assurance that airworthiness standards are being maintained. In concluding, a brief description of the conduct of the F404-GE-400 qualification process development is provided that includes a summary of some of the benefits derived both from the targeted program as well as those identified as a result of the change in management philosophy.

4. BACKGROUND - THE CANADIAN CONTEXT

The CF typically operate their aircraft in a manner which is at least as extreme as any other user of the aircraft in terms of both mission severity and service longevity. Environmental conditions such as extreme low temperature conditions complicate matters from perspectives of operability as well as aircrew survivability following serious air incidents. By way of example of utilization rates, the CC130 Hercules fleet has historically exceeded manufacturer specified maximum wartime utilization rates every year of operation, flying at an average rate that is approximately 2.5 times that of the USAF. Additionally, for reasons of cost avoidance, the CF has periodically chosen not to introduce Original Equipment Manufacturer (OEM) specified modifications to aircraft or engines, and this has resulted in the requirement to manage unique CF configurations. Often these unique configurations have not received full OEM test or qualification support. Finally, DND has endeavored to utilize a very capable Canadian industrial base to repair and overhaul military aircraft and components in order to establish and enhance an indigenous support base necessary both in peacetime and in periods of heightened tension.

To assist in identifying R&D investment priorities, the DRDB conducted a study [1] to assess the impact of aeropropulsion systems on in-service life cycle costs and operational availability. At the time of the study, the cost of contracted-

out support of DND equipment approached Can\$1.4B of which approximately Can\$800M, or 57%, was devoted to contracted R&O on air weapon systems. This high cost of aircraft R&O reflects the high cost of advanced technology combined with stringent flight safety requirements. A total of eight CF aircraft were included in the study. Four commercial aircraft having CF military equivalents were also analyzed for data normalization purposes. For the CF aircraft, the powerplant was found to cause from 27% (CF18) to 46% (CH124 Sea King Maritime Helicopter) of materiel failure initiated flight safety occurrences. The commercial aircraft data were very similar to those of their military equivalents. In terms of unscheduled maintenance man-hours, which was taken to correlate with non-planned aircraft unavailability, the powerplant consumed 10% (CH124 Sea King) to 37% (CF-5) of resources. Replenishment spares, contracted R&O, CF maintenance labour, petroleum, oil, lubricants, and expendable stores cost data is provided in [1], although only the initial three factors are used for sub-systems comparative cost analysis. Based on replenishment spares, contract R&O, and fully loaded CF maintenance costs, the aeropropulsion systems typically account for 28% of the in-service life cycle costs of an aircraft. Further analysis identified premature retirement of engine components as the major contributor to this high relative impact of the powerplant on operational availability and aircraft support cost. It was found that in some cases, components were being rejected with as little as 10% of their specified design life realized.

5. REPAIR /REPLACEMENT DECISION FACTORS - MOTIVATORS

Given the foregoing overview of the cost and operational impact as experienced by the Canadian military, and the recognition that components can often be repaired at lower cost than the purchase price of new components, the following factors can be identified as motivators for repair process development and implementation:

5.1 Reduced Program Costs

Perhaps the most obvious repair/replacement decision factor is related to the program cost reductions that can be achieved. As a prerequisite to repair process development for the Canadian program [2], the projected cost of repair would have to be less than one third of the new part replacement cost. This ratio was intended to focus repair development efforts on those areas where the greatest program cost reductions could be generated and to allow some room for repair process cost growth. While this objective also identifies the magnitude of cost reduction which might be expected, it is often difficult to place an economic value on the benefits derived from these repair processes within a military context. In an organization whose primary purpose is revenue generation, such as a commercial airline, a dollar value can be readily determined which relates to aircraft availability at the gate. Conversely, in a military organization, aircraft availability may be of less concern during peacetime than in the midst of a confrontation. Nevertheless, this issue can be addressed for engine components if a sufficient understanding of current cost drivers exists. The US Department of Defense

Cost Effectiveness Analysis (CEA) process, described at [3], is an excellent and available tool for full cost/benefit analysis of repairs. This CEA, or an equivalent procedure, is a necessary prerequisite to understanding which repairs are economically desirable.

5.2 Increased Component Service Life

Although it is generally assumed that a repaired component will have a service life following repair which is a fraction of that of a new component, research undertaken by Canadian industry and the NRCC identified a number of opportunities where the service life of a repaired component could actually be greater than that of the original OEM component. It is perhaps worthwhile to provide a few examples of how a repaired or reworked component can offer this expectation of increased service life.

The High Pressure Turbine (HPT) vane segment of the F404-GE-400 suffers from thermal fatigue cracking in both the MA754 vane and in the MM-509 platform or band. The vane and platform cracking is due to complex thermal and gas bending loads during typical military cycles of operation. The repair process developed for the HPT nozzle consists of a vacuum diffusion braze process which is accomplished by filling the service induced cracks with selected and optimized braze material. The OEM HPT nozzle segment has a Codep B-1 aluminide coated platform and uncoated aerofoil or vane segments. The uncoated vanes are subject to cyclic oxidation and thermal fatigue cracking leading to spalling of oxides and subsequent loss of material and functionality. In exploring the metallurgy and the developing a full understanding of the damage mechanisms, it was possible to develop a protective coating for the aerofoils which will result in a service life of the repaired component being twice that of the service life of new HPT nozzles. Ideally, this same coating will also be applied to new HPT nozzles. It is interesting to note that once the coating process is applied to new components, there may not be sufficient parts rejected for these repairs to be economically feasible.

A second example is the HPT blade, which is a directionally solidified René 80 component whose life limiting region is expected to be the leading edge with the life limiting mode being thermal fatigue. This component; however, suffers intergranular corrosion tip damage and cracking which often results in premature retirement with only a fraction of its expected design life of 30,000 equivalent full thermal cycles realized. The repair process that will be used to refurbish the HPT blades will involve damage assessment, HF ion cleaning, and weld repair followed by post weld heat treatment and finish machining. The weld material at the tip provides an interface between the gas stream and the intergrain boundary that serves as a barrier to intergranular corrosion. A service life has been demonstrated for repaired blades in burner rig endurance testing which is far greater than that of new components. A tip coating will also be applied to further address the corrosion attack.

A final example addressing classic fatigue damage relates to the fan blade. It was anticipated that Hot Isostatic Pressing

(HIP) rejuvenation of the titanium Ti-6Al-4V fan blades of the F404-GE-400 engine could recover a conservatively estimated 80% of that component's original Low Cycle Fatigue (LCF) life. This form of rejuvenation is the most obvious demonstration repair or rework cost reduction in that a time expired component which is aero-thermodynamically functional can be retained through the recovery of original materials performance. It is worthwhile noting that the HIP process was developed and demonstrated, then abandoned when the OEM modified the life limiting leading edge radius beneath the blade platform and increased the LCF life by a factor of three. This LCF improvement removed the anticipated HIP rejuvenation Return On Investment (ROI). Unfortunately failures of the modified design have not substantiated the increased design life expectations.

5.3 Improved Safety of Flight

In developing the comprehensive knowledge base pertaining to operational loading and critical damage modes, the user of a gas turbine engine will necessarily improve their ability to anticipate failures of components and to understand the consequences of those failures. An integral part of the CF program was the generation of a Failure Modes and Effects Criticality (FMECA) process for the CF18 engines. Not only is the FMECA the initial decision point for a repair process development, it is also a necessary tool for operational management of fleet assets. The FMECA assists CF headquarters staff in assessing the consequences of unforeseen failures and in determining the most appropriate management action required to ensure that operational commitments can be met without sacrifice to airworthiness.

5.4 Security of Supply

Although the CF often experiences early fleet failures, other users will experience those same failures and will place concurrent demands for replacement parts which exceed normal supply capacity. In an era when fewer aircraft assets are held, unexpected supply shortages or replacement component delivery priorities that are determined by other nations' governments, can have a significant effect on CF operational readiness. In developing a repair/rework capability it becomes possible for Canadian Forces requirements to be met using the repair infrastructure in periods of duress whether they are cost effective or not. If the only means of keeping aircraft functional is to repair damaged components, then that option will be available.

5.5 Industrial Base Development

The development of an industrial base in Canada to design and implement repair processes can perhaps be justified solely on shorter term economic factors. Inherent in the development of this capability; however, is the development or maintenance of competencies necessary to support future military systems. Simply stated, it will be virtually impossible to accept new technologies into operational service, if Canada cannot technically manage existing design concepts and materials performance. Canada's aerospace industry is primarily oriented towards commercial aircraft needs, it is strong, technologically advanced and capable of

also meeting the majority of Canadian military aerospace needs.

6. REPAIR/REPLACEMENT DECISION FACTORS - CONSTRAINTS

6.1 Technology Base and Competency

The most fundamental prerequisite for the repair/replacement option is the understanding of the metallurgical principles which pertain to the gas turbine components of interest. The physical properties of the individual parts of the gas turbine and the damage modes that will affect either the aero-thermodynamic performance or lead to physical failure of these components vary greatly throughout the engine and must be understood in detail. High and Low Cycle Fatigue (HCF and LCF) may predominate as damage modes in the compressor section, while pressure burst or thermal fatigue may be primary considerations in the combustor. The area of greatest duress; however, is in the turbine module where creep, thermal mechanical fatigue, erosion and corrosion combine to generate the most severe of operational environments. The National Research Council, as part of their research program, and as sponsored by DND, have conducted a focused and productive research program in emerging materials and their characteristics. DND engines have provided the stimulus and much of the specific research subjects as they employ advanced materials for which a store of service experience exists or is being continuously generated. This information has been used to develop and validate experimental test methods. Studies and experiments have been conducted on coupons and actual service exposed materials to establish the database necessary for advanced repairs or reworks. International fora and research have also been actively supported by NRC and DND contractor personnel, including the AGARD Structures and Material Panel Sub-Committee 33 on an Engine Disc Co-operative Testing, and the Propulsion and Energetics Panel Working Group 20 on Low Cycle Lifting Analysis Techniques for Gas Turbine Components. These activities have established the necessary understanding and the fundamental capabilities within the Canadian technology base to proceed with the gas turbine repairs anticipated.

A second competency area required for the repair/replacement option relates to the understanding of the actual operating environment in which these components perform their design function. Much of this information is closely guarded proprietary design data which is retained by the Original Equipment Manufacturer (OEM). The design assumptions; however, often do not adequately address the entire operational spectrum and so it is necessary to analyse in-service experience. This expertise has been developed within the NRC and at DND support contractor organizations. This aspect of the knowledge base has been developed through advanced instrumentation development, experimental methods development, analysis of available histories of failed components, special instrumented engine and flight tests, and post failure analyses. Much of this knowledge is necessarily specific to type and has been developed for the F404 engines.

Understanding fleet average service loads is not sufficient to support a comprehensive repair/replacement decision. Individual monitoring of component life usage is also required. Without the ability to track individual engine usage, and from that to infer damage accumulation, it is extremely difficult to adequately understand failure trends and to generate repair processes which safely address the root causes of failure. For this prerequisite function, the Canadian Forces had supported a detailed data capture and analysis program on the CF18 engines. This analysis capability was intended to serve engine usage and health monitoring needs but has also proven instrumental in enabling a more comprehensive understanding of damage mode/operational usage relationships. Without the Maintenance Signal Data Recording System (MSDRS) and In-flight Engine Condition Monitoring System (IECMS) of the F404-GE-400 engines the database could not have been generated.

6.2 Certification Infrastructure

As mentioned previously, a major obstacle to airworthiness certification for many operators is the availability of adequate test facilities for coupon, component and full scale engine verification testing of repair redesigns or reworks. As a part of the collaborative R&D program between DND and NRCC a number of these facilities have been established, or improved, and valuable experience gained in their operation. These facilities are primarily located in the Institute for Aerospace Research (IAR) and are made available to DND. Test capability has been developed for a full spectrum of gas turbine design considerations and includes:

6.2.1 Tensile and Compressive Test Devices

A number of test systems are available for tensile and compressive testing at elevated temperatures up to 1200°C for testing coupons of virgin material or coupons machined from service exposed components.

6.2.2 Bending

Four point bending at up to 1500°C and high cycle rotating bending fatigue testing up to 980°C and 10,000 RPM in corrosive atmospheres can be conducted to simulate operating conditions.

6.2.3 Indentation Testing

This test capability is necessary to assess the performance of corrosion or erosion coating systems as well as to assess the performance of other forms of surface treatment, such as ion implantation, or laser surface treatment. Tests can be conducted at temperatures up to 1000°C.

6.2.4 Low Cycle Fatigue Testing

Stress or strain amplitude controlled LCF testing of compressor or turbine material coupons can be conducted up to 1100°C as necessary to validate the long term life characteristics of compressor components which have been weld repaired or turbine components which have received a protective coating system which can in turn affect substrate characteristics or durability.

6.2.5 Fatigue and Creep Crack Growth Rate

Creep strength up to 1100°C can be demonstrated and fatigue and creep crack growth rates can be studied at temperatures up to 1000°C for damage tolerance testing of coupons or components. The purpose of this type of testing is to gain an understanding of the service time available between initially detectable defects and component dysfunction.

6.2.6 High Temperature Burner Rig Testing

A high temperature burner rig has been established at the Institute for Aerospace Research with DND funding which enables thermal fatigue and erosion testing of coupons or components at temperatures up to 1500°C and at high velocity ($M=0.8$). This test facility was originally intended for erosion/corrosion testing but has been successfully adapted for thermal mechanical fatigue and durability testing of full scale gas turbine components or representative coupons.

6.2.7 Full Scale Engine Testing

A comprehensive complement of full scale engine test facilities with laboratory quality instrumentation also has been established at the NRC/IAR for DND and commercial test purposes. These test facilities were originally established for engine health monitoring and gas path analysis research, as well as DND failure analysis. These test systems now represent a major asset available for DND and industrial use. Engine Block Tests or Accelerated Mission Tests which are similar to the final test requirements for commercial certification of engine designs, have been performed on the CF18/F404 engine in an NRC engine test cell.

6.2.8 Hot Spin Pit Test and Advanced Coating Technologies

Although not employed in the original CF repair development program, the NRCC have added hot spin pit test and an unbalanced magnetron sputtering coating facility for future materials and repair technology development.

6.3 Certification Process

DND has a long and well-established record of flight safety which is on par with, or exceeds civil standards. Repairs to flight critical gas turbine components have not been attempted in the past by DND and no approach had been developed to address the certification of airworthiness for repaired components. Additionally, commercial operators have not attempted repairs to flight critical engine components in the past and accordingly, no commercial certification procedures were found to exist. Civil regulatory guidance was found to be directed primarily toward the design and certification of new engines and components. In order to understand the civil regulatory requirements and to develop a process which was consistent with aerospace industrial practices, a review of regulatory agency requirements in Europe and North America was undertaken. This enabled the generation of a certification process on gas turbine repairs which will ideally be acceptable to civil regulatory agencies in the future.

6.4 Cost Effectiveness Analysis

A Cost Effectiveness Analysis (CEA) approach has been developed by the US Department of Defence in collaboration with their industrial and university partners. This CEA identifies a consistent and engineered approach to cost and benefit assessment and was directly applicable to the DND project on gas turbine repair development. The principles of this CEA analysis have been applied to repairs in the Canadian program. The process essentially identifies each step in a repair process and the total cost picture associated with that step. The CEA inputs are divided into three areas: standard inputs, which define the current environment; incorporation data, which accounts for one time changes caused by the implementation of the repair process; and scheduled/unscheduled inputs which reflect current maintenance schedules, and current unscheduled removal rate. CEA outputs can be given in terms of dollar cost or in investment terms, as NPV, ROI. An important capability of this CEA software is that one can perform a sensitivity analysis to identify and address the critical functions and further optimize costs or benefits. This ability works in reverse, that is, hypothetical events such as fuel cost increase, or parts unavailability can be addressed with respect to costs.

7. CONCLUDING MATERIAL

Having identified the motivators and constraints considered by the Canadian military, it is perhaps worthwhile to briefly summarize the steps taken in developing the repair qualification process and then to identify the cost reductions that are now expected to accrue to the CF18/F404-GE-400 engine program.

7.1 Qualification Methodologies for Gas Turbine Repair/Rework- Program Description

The development of a methodology for the airworthiness verification of gas turbine component repairs or reworks and the exercise of that methodology on a number of CF18 engine repairs has now been completed. That process involved technological, as well as economic considerations. The individual phases of the program are described below:

7.1.2 Preliminary Technology and Economic Feasibility Studies.

Prior to initiation of the major development project and using the CF18/F404 engine as a target of opportunity, component failure and rejection rates at all levels of maintenance, repair and overhaul were analysed. Components which offered potential for significant cost savings were identified and technology needs for repair identified. The economic analysis was fundamental in nature and was subsequently enhanced using the CEA procedures. Technologies were then explored which could address knowledge gaps and the technical feasibility of a number of specific repairs was demonstrated.

7.1.3 Regulatory Agency Review.

The intent of the Regulatory Agency Review was to identify what, if any, existing guidance could be applied to DND initiated repair redesign activities. It was also intended that a Qualification Methodology be generated which would

facilitate the acceptance of the specific repairs generated under this project by other military users, and would encourage the pursuance of these repairs in commercial markets as well. A review was conducted of the procedures followed for design change approvals as specified by Transport Canada Aviation (TCA), The United States Federal Aviation Administration (FAA), the British Civil Airworthiness Authority (BAA), the European Joint Aviation Authority (JAA), the U.S. Department of Defence, and U.K. Ministry of Defence (MOD). In general, the TCA procedures and definitions are being used as they address or surpass the requirements of other regulatory agencies. Differences between TCA and other regulatory agency procedures have been documented in a comprehensive report for future reference. The process for repair certification, and the responsibilities and privileges of accredited personnel such as the Design Approval Representative (DAR) or a Design Approval Organization (DAO) are also specified.

7.1.4 Failure Mode Effects and Criticality Analysis (FMECA)

This element of the Qualification Methodology is of value to fleet repair analysis as well as for repair redesign purposes and will serve as a stand alone tool for DND's Life Cycle Materiel Managers (LCMM). The FMECA is a computerized aid which leads design authorities for aerospace equipment through the types of failures which can occur on each component, identifies the probability of those failures, and explains possible subsidiary consequences of failure.

7.1.5 Qualification Methodology

The Qualification methodology describes how to design and certify a repair as being airworthy following a systematic, consistent and auditable certification process. The methodology addresses repair design, life analysis, verification testing, and personnel qualification requirements. This qualification methodology is applicable to Canadian DND aero-gas turbine engines and is valid for both flight-critical and non-critical components. The certification process specifies requirements for:

- FMECA;
- Coupon level test requirements and process guidelines;
- Component rig testing requirements and process guidelines;
- Full scale Engine Block Test and Accelerated Mission Testing methodologies; and
- Design change approval process and documentation.

7.1.6 Proof-of-Concept Demonstration

The feasibility of a number of advanced repair and life extension techniques for high cost /high rejection rates components had been explored in preliminary studies. In order to fully demonstrate the repair generation and certification process, a comprehensive repair certification program was initiated for the F404-GE-400 components of interest. Contractual issues required that a specified minimum set of repairs was to be demonstrated during the proof-of-concept stage of the program. The repairs which were contractually specified are listed below:

- Stage 1 fan blade FOD repair;
- Stage 1 fan blade dovetail fretting fatigue improvement;
- Stage 3 HPC blade dovetail fretting fatigue improvement;
- HPT vane segment cracking and braze loss repair;
- HPT vane life extension;
- HPT blade tip repair;
- HPT blade life extension; and
- LPT vane segment cracking and braze loss.

7.2 Canadian Repair Program Benefits

Table 1 below identifies both preliminary and rudimentary Cost Benefit Analysis figures, as well as CEA savings projections for the repairs identified above. Both of these figures are provided to identify the much more conservative, but realistic CEA cost avoidance projections. It is felt that the more rigorous CEA is a necessary tool for the identification of realistic cost avoidance potential.

Table 2 below identifies the CEA cost reduction projections for repairs that have been identified for the F404-GE-400 engine subsequent to the initiation of the proof-of-concept demonstration contract. These repairs give an indication of the effect of the change in management philosophy on program costs for this one engine program.

7.3 Conclusion

The savings indicated in Tables 1 and 2 are significant from cost and management perspectives. This proof of concept demonstration phase of this program cost Can\$4.1M and was initiated based on the expectation of Can\$43.3M in program cost savings/cost avoidance. The CEA estimate of Can\$12.3M was considered realistic and provided only a marginally acceptable ROI. The savings anticipated from opportunity repairs that would not have been conceived without this repair process development; however, total an additional Can\$66.4M. Once an organization recognizes the cost and availability impact of repair implementation, and has the infrastructure and process to effect those repairs, significant benefits can be derived. Benefits to the CF resulting from the development of a repair certification process are as follows::

- Program cost reduction/avoidance;
- Increased new and repaired component life;
- Improved safety of flight;
- Improved maintenance management decision tools;
- Security of supply;
- Industrial base preparation for advanced technology concepts

Table 1 - Canadian Repair Program Initial Cost Avoidance Projections

Component/ Repair	Initial Estimated Savings (Can\$M)	CEA Estimated Savings (Can\$M)
1 st Stage Fan Blade FOD	2.9	1.4
1 st Stage Fan Blade Fretting Fatigue	na	.9
1 st Stage Fan Blade LCF Extension	7.4	Cancelled
3 rd Stage HPC Blade Dovetail Fretting Fatigue	na	na
HPT Vane Cracking and Braze Loss *	21.0	1.2
HPT Vane Life Extension		
HPT Blade Tip Repair	na	na
HPT Blade Life Extension	na	na
LPT Vane Cracking and Braze Loss	12.0	8.8
15 Year Program Savings (Can\$M)	43.3	12.3

- Includes recovery of an estimated 2000 HPT nozzle guide vane segments which have previously been rejected and quarantined pending repair process development.

Table 2 -Opportunity Cost Reductions/Avoidance

Component Repair	CEA Estimate of 15 Year Savings (Can\$M)
LPT Nozzle Segment Joint	4.3
Combustion Chamber case	3.2
LPT Nozzle Air Seal	20.9
HPC Vane Segment	.3
LPT Blade Coating	.8
HPT Shroud Support Repair	27.9
Front Frame Repair	9.0
Total 15 Year Cost Reduction	66.4

References

1. Hastings R.R., Macmillan W.L., and Tobin M., "Aircraft Subsystem Cost and Reliability", Canadian DND Publication CRAD Technical Note DRDA/9301/06
2. Development of a Qualification Methodology for Advanced Gas Turbine Repair/Rework - Final Report for Task 4, Orenda Division, Hawker Siddeley Canada Inc., March 1996
3. Dockendorf J.E., Malson M.Z., "Government/Industry Standard Cost Effectiveness (CEA) Model", in "Annual Reliability and Maintainability Symposium, 1996 Proceedings", 22-25 January 1996

COST EFFECTIVENESS OF MODERN LIFING CONCEPTS

Consideration of Economical Aspects Concentrating on Group A Parts of Military Aircraft Engines

K. U. Tschirne and W. Holzbecher

WTD 61 - Federal Armed Forces Engineering Centre for Aircraft
Military Airworthiness Authority
Propulsion Systems Division
Flugplatz
D-85077 Manching
Germany

1. SUMMARY

It is an usual approach of traditional lifing procedures to perform extensive and therefore costly spinning and laboratory tests with subsequent sampling programmes aiming at the maximum usage of fracture critical parts, so called group-A-parts.

Experience on military programmes has shown that this approach does not take into account all the aspects related to the real in-service situation.

In order to avoid engine removals and disassemblies due to life-expired parts, causing major expenses, it becomes necessary to retire parts when they become available on the basis of natural arisings, i. e. at the most economical and suitable point in time.

The aim of the presentation is to encourage both the manufacturer and operator of military engines to instigate a detailed review of their current lifing policy as far as the remaining life at the point of retirement is concerned.

Furthermore, some aspects concerning the philosophy of the required (desired) specified life for an engine and its components are highlighted.

2. INTRODUCTION

The German Air Force/German Navy (GAF/GNY) has implemented a modern lifing concept combined with the introduction of a „Life Monitoring System“ for the RB 199, the engine of the Tornado aircraft.

This paper will review the corresponding procedures, the users effort necessary to cope with the relevant requirements and will highlight associated in-service experience.

It is neither the aim to create new lifing philosophies nor to propose specific changes to stress calculations, to certain laws or to specify mathematic formulae. This task of course is left to the experts and the appropriate fora.

After more than 15 years experience of RB 199 in-service operation it appears prudent to question certain features established in the course of improving the general lifing procedure and to assess its economical value.

Some aspects will be presented which cropped up during the process of reconsidering the present approach because of budgetary restrictions and problems concerning the availability of engines.

Presenting a realistic, clear-headed and unbiased picture from the **users point of view**, supported by trends, statistics and other facts, should be supportive and helpful for the experts during the process of developing living concepts which suit both sides best.

All parties involved are encouraged to reconsider certain aspects and benefits of „old“ and simple lifing procedures in combination with modern features which have already demonstrated their costeffectiveness.

3. CURRENT LIFING PROCEDURE

3.1 Basic Method

The procedure we are talking about, mainly deals with the life of fracture critical parts. This procedure forms a major element of the general lifing policy applied to the RB 199 engine and is covered and documented comprehensively [1].

Initially, this procedure was solely based on the „Safe Crack Initiation Life“ where „Crack Initiation“ is defined as a crack of 0.4 mm.

Release of the full life of the fracture critical parts is subject to the successful completion of cyclic rig testing of ex-service samples at 50 % and 75 % of this safe life. Temperature profiles as close as possible to actual engine in-service environment are simulated during testing of certain fracture critical parts.

The results require support from detailed inspection of parts withdrawn from service engines after equivalent times of operation.

For parts, where meaningful cyclic testing cannot be performed due to technical reasons (installation, geometry) life clearance (extension) is based on satisfactory inspections, cyclic tests on new parts, on modified ex-service parts or on representative specimens.

3.2 Module and Accessory Sampling

Only limited evidence regarding the many possible failure modes is available by the time an engine enters service.

Therefore, the initial lifing procedure is supported by a sampling plan to avoid failures which may remain undetected and become hazardous to the aircraft.

This plan requires a stepwise withdrawal of relevant samples from different operating units for detailed non-destructive inspections.

Evidence from all maintenance facilities is also taken into account. This is to guarantee that all possible effects of operational peculiarities of all users are considered.

3.3 Technical Life Review

Additionally, technical life reviews are established at each stage of life declaration to consider and discuss the technical history and results of regular inspections supported by the evidence obtained from inspections resulting from quite a number of unplanned removals due to natural arisings.

3.4 Cyclic Exchange Rates/Monitoring System

Furthermore, an extensive exercise embracing a comprehensive assessment of a large number of flight recordings (usage survey and mission analysis) has shown how the engines have actually been used in service, resulting in a reduction of the initial cyclic exchange rates.

Cyclic exchange rates, also called β -factors, determine the ratio between cycles of engine components and engine flying hours (EFH).

To allow the safe use of components until their individual life expires and to avoid continuous, frequent evaluation of mission recordings, an on-board engine monitoring system has been introduced.

This system automatically calculates the life consumption in accordance with the mission profiles actually flown.

Hence, a large database containing detailed and reliable information on all individual fracture critical parts of the engine is readily available for the user and the engine industry.

Detailed assessment of the life usage data has shown that significant differences exist between handling procedures and mission profiles. Also differences between right and left hand engines have been established, even pilots' "finger prints" could be identified.

3.5 Safe Crack Propagation Life

In order to overcome quarantining of parts during life progression, interim lives based on preliminary results from not yet completed cyclic tests or on in-service evidence are frequently released.

Despite of that, certain fracture critical parts have to be withdrawn because they have reached their relatively low declared safe service life.

In accordance with the safe life approach, the predicted safe life of the weakest individual part will be the final life for all of these parts in service, which means that a significant amount of residual life of the other individual parts must be wasted.

Hence, the high cost for spare parts requires reconsideration of life extension methods within the frame of the implemented lifing procedure.

Extensive specimen tests, investigation of the crack propagation characteristics and cyclic testing up to the onset of unstable crack propagation to establish the safe cyclic dysfunction life demonstrated that certain discs and their critical areas were significantly damage tolerant.

A detailed finite element analysis using the 3D method was performed to fully understand the stress intensity at critical areas for a limited number of load steps.

Without weakening the primary objective of the lifing philosophy, i. e. to ensure aircraft flight safety, the basic procedure was refined and the safe propagation life of damage tolerant critical areas of fracture critical parts was added to the safe crack initiation life.

3.6 Statistical Analysis

A proposal to use statistical analysis of finite and non-finite lognormally distributed fatigue test results for the lifing of fracture critical parts is under consideration.

It is expected that this statistical method comprising the analysis of samples which contain non-finite results can provide service life extensions up to 40 % [8].

However, had the fatigue testing in the past been continued beyond the occurrence of cracks (no termination of testing after the scheduled test period), this complex approach would not have been necessary.

In consequence, the total life (initiation and propagation) should be established at a very early stage of development (i. e. spin testing of new parts).

4. ON-BOARD LIFE USAGE MONITORING SYSTEM (OLMOS)

4.1 Development of OLMOS

The Tornado aircraft is equipped with an on-board life usage monitoring system integrated into a data acquisition unit which records flight data.

The system is installed on all GAF/GNY Tornado aircraft and used fleetwide.

As part of this system the "Engine Life Consumption Monitoring Programme" (ELCMP) contains the calculation of the low cycle fatigue life consumption of fracture critical parts and additionally, engine performance trending and diagnosis/statistics.

To date, nine updates of the software have been introduced as a result of continued testing, new engine standards, increased experience, better knowledge of temperature distribution taking into account deterioration of the air system and modified engine parts.

Finally, tasks have been initiated to develop crack propagation models (algorithms) which are directly integrated into the structure of the existing life usage monitoring system. The next ELCMP version will feature that scheme.

To cater for changes in engine build standards, additional engine configurations or changes in operational requirements, it is necessary to continuously update the ELCMP software, during the lifetime of the engine.

Those fleetwide software changes incur considerable effort. Therefore, change proposals must be carefully evaluated to avoid that the cost for the update exceed the savings gained by a few more cycles.

However, application of OLMOS means that the life of critical engine parts is individually monitored during in-service operation with the benefit that the scatter of low cycle fatigue life consumption of comparable parts is much smaller than the scatter achieved by using cyclic exchange rates. See figure 1 [7].

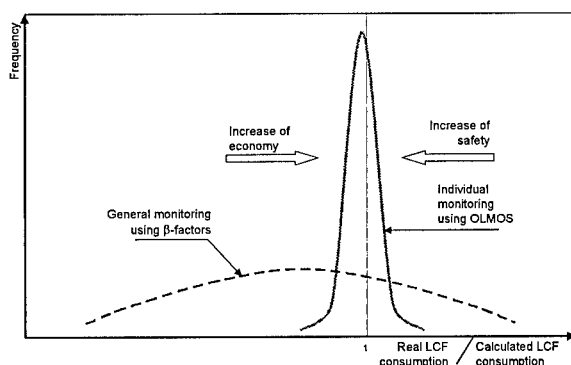


Figure 1 Distribution of LCF life consumption; application of β -factors compared with a life monitoring system

4.2 Lessons Learned

A comprehensive and permanent training of all support and maintenance personnel is mandatory to obtain the expected benefits from the monitoring system (high skill level).

Unfortunately, after years of in-service experience, the link to the central logistic support system is still a route full of possible errors and inconsistencies which requires refinement to synchronize the various activities between the parties involved. Too much manual intervention is necessary in handling the lifing data of spare parts. Additionally, the planning process does not fully exploit the vast amount of information contained in the collected data.

The ground station as part of the life monitoring system should contain all the information necessary for tracking the life usage of each engine of the squadron or of the fleet.

Due to data handling problems, a separate calculation system was installed to check the plausibility of all the data fed into the logistic support system.

Therefore, the full benefit and the expected cost savings could not be realised.

To ascertain that all the positive effects of an individual monitoring system are achieved, the above quoted deficiencies - human errors in particular - have to be avoided by all means.

It is absolutely essential, to **completely** design and establish the whole structure of such a system during the stage of development. This has to include all details on the data transfer process from the on-board monitoring via any hand held device and ground station to the different logistic centres at the end of the line.

Furthermore, by only recording and storing the mission related data on aircraft and calculating the low cycle fatigue life consumption in a ground station, the on-board system can be kept quite simple. On-board processing, on-board storage of results and on-board bookkeeping of engine life consumption would not be required.

Should the calculation process of the life consumption be changed, a reassessment of the life usage of the individual component would be possible more easily and accurately due to the availability of the complete mission data in a ground station instead of introducing additional correction factors.

In addition, software updates would be less complex and costly due to the simplified software clearance requirements for ground stations.

5. EXPERIENCE WITH THE CURRENT PROCEDURE

In an international programme where each nation uses individual methods and different monitoring systems for the calculation of the life consumption of their fracture critical parts, the assessment and evaluation of relevant test results can be a painful, engineering capacity binding, time consuming and costly exercise.

Because of the above, the customer has hardly any other choice than to accept and implement updates to the lifing procedure depending on the latest findings from further research and development programmes.

The highest priority is dedicated to flight safety and the avoidance of any hazardous flight situation, this means that all improvements e. g. in disc design, material properties or manufacturing processes, consequently require an update of the lifing procedure.

Special programmes have been established to fully assess the effects of corrosion, fretting, wear etc. on the predicted life.

The high number of unplanned removals provides a lot of data regarding the status of fracture critical parts that can be collected from the repair and overhaul line.

This data is used to identify potentially critical areas and to take any necessary action in due time.

Despite the useful and risk minimising effort to streamline and to optimise the lifing procedure by taking on board new technologies and methods to reflect the latest state of the art, the customer is still confronted with certain **life reductions** which leads to the question if the original approach has completely taken all safety aspects associated with lifing into account.

Furthermore, human errors in the interface between ground station and logistic system have led to an extra programme to recalculate the life consumption and to check the plausibility of the recorded hours/cycles for the individual parts (see para 4.2 above).

The fact that the total cost for the replacement of components exceed the price of a new part by far, leads to the conclusion that all economic aspects are to be considered before a part is replaced. Even very early withdrawals can be costeffective.

In summary, the implemented procedure with its staged life release to the maximum usable life supported and confirmed by spin tests, confirmatory samples and unplanned removals taking into account all unforeseen "In-Service Effects" which could severely influence the final life of a component is a **rather cost intensive method**.

In conjunction with an intelligent on-board life monitoring system the total life potential of an individual part can be entirely used in service. Furthermore, "real life" exchange rates can be derived and the exact knowledge of the life consumption of each individual fracture critical part is in hand. The **real** overall situation and distribution of the remaining life of the parts within the fleet is available at any point in time.

The availability of all this data allows a specific module and/or engine removal management and the use of additional life potential if, for instance, a crack propagation life is calculated.

Despite the high level of confidence and safety gained, the procedure requires a sophisticated management system for life monitoring, logistics and parts.

Additionally, the necessary high skill of the staff requires permanent training which is aggravated by the frequent fluctuation of military personnel.

One special problem needs mentioning, in case of a **reduction** of the released life due to unforeseen changes, there are no life reserves to compensate for. This is a very sensitive and costly (additional removals!) area of the lifing procedure.

6. IN-SERVICE SITUATION

6.1 Definition of a Remaining Life

Every year, a summary of operation is issued which reviews in great detail the causes for engine rejections including the individual modules and accessories and shows statistically the overall situation.

During the last 10 years of service operation, the different fleets (GAF/GNY) suffered a total of approx. 3660 unplanned engine removals followed by extensive repair and overhaul activities (distribution see figure 2).

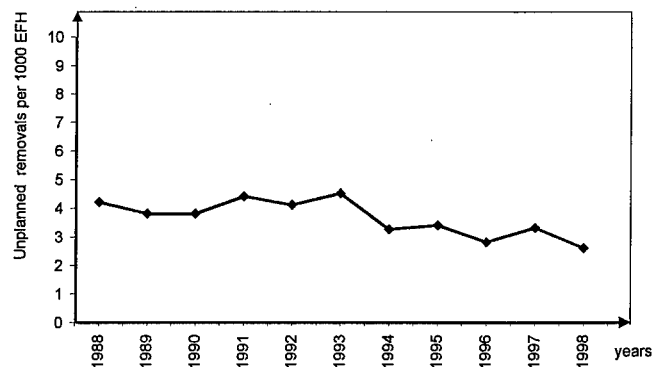


Figure 2 Distribution of unplanned engine removals

Because of the modularity of the engine, complete modules have to be replaced which means that every year a very high number of individual modules require rectification causing high repair and spare part costs.

It is not always easy to determine which module is the one causing the problem. Often the deterioration of a number of modules contributes to the failure of an engine (e. g. vibration).

Studies have shown that the most significant contributor to the life cycle costs of fighter engines are the costs for parts and labour associated with repair and overhaul.

In an ideal world, only rejections of engines caused by the expiration of the released service life of parts and components would be expected.

Unfortunately, in addition to the planned removals (life-ex) the high number of unplanned removals (natural arisings) leading to shortage of repair capacity, grounding of aircraft and costs which are not necessarily covered by the released annual budget has to be taken into account.

Detailed assessments have shown that the actual cost for engine removal, disassembly, repair and assembly can be more than ten times higher than the cost for a new fracture critical part. Practically, the cost for the new part can be ignored and a new approach has to be explored.

To minimise the cost, both, the unplanned and planned removals have to be combined and optimised. Fracture critical parts due for retirement should be replaced when they become available on the basis of an unplanned removal caused by natural arisings (see figure 3).

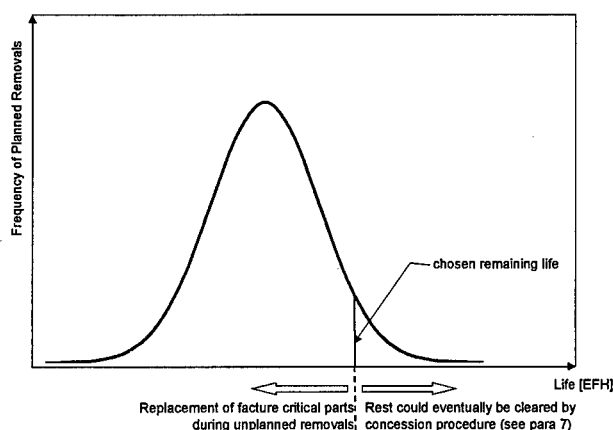


Figure 3 Replacement of fracture critical parts

A compromise is to be found between the probability of an event causing an engine disassembly and the cost and logistic implications of removing and retiring serviceable parts before their lives are expired.

The value of the "wasted" life of a fracture critical part and the cost for engine removal and repair have to be balanced. The possible effects and implications resulting from a lifing procedure where fracture critical parts with different periods of remaining life are retired have been investigated. The results are shown below.

6.2 Optimisation of the Remaining Life

In the early service phase engines are rejected more frequently due to reliability problems. Usually, the remaining life at retirement is relatively low as the parts concerned become available quite often.

At a later stage, the reliability increases due to introduced modifications. The number of engine removals and consequently the opportunity to review the remaining life of a fracture critical part in order to decide on its reuse on an economical basis is reduced.

Hence, each time an engine is removed and disassembled and the fracture critical part becomes available, a decision must be made whether to reuse the individual item or to retire it due to its remaining life being too low.

To illustrate the possible differences in module availability and the resulting effect on how an appropriate time for retirement is defined, three engine modules are exemplarily considered:

- Low Pressure Compressor (**LPC**) - a module the removal of which does not require removal of other modules
- High Pressure Compressor (**HPC**) - a module requiring very extensive strip of the engine
- High Pressure Turbine (**HPT**) - a module of the "hot end" requiring removal of several other "hot end" modules.

Each time an engine is rejected from the aircraft and disassembled for rectification, the aircraft downtime affecting the operational readiness, the manhours required at all maintenance levels the transportation-, administration-, repair- and spare part costs as well as the spares availability have to be considered.

Summary of Influences

The various influences affecting the definition of an acceptable remaining life at retirement are:

Part Costs

The relatively high cost of the **LPC** (3 stage welded drum) requires that the maximum possible life is used.

Effect: - Reduce the remaining life at retirement maximise the usage.

The relatively low cost of the **HPT** (single stage disc) does not require that the maximum possible life is used.

Effect: - Increase the remaining life at retirement.

Removal/Replacement Cost

The **LPC** module is easily and quickly removed and replaced no disturbance of other modules. Therefore the costs involved are relatively low.

Effect: - Reduce the remaining life at retirement.

To access the **HPT** several modules require removal therefore, the costs for removal and replacement of this module are comparatively high.

Effect: - Increase the remaining life at retirement.

Module Repair Cost

The relatively high cost for repair of the **LPC** suggest that the number of removal/replacements should be minimised.

Effect: - Reduce the remaining life at retirement.

The relatively low cost for repair of the **HPT** implies that the number of removal/replacements has little effect on costs.

Effect: - Increase the remaining life at retirement

Look in Damage

As the **LPC** can be removed without disturbing other modules, the opportunity to discover look in damage is minimised.

Therefore, additional costs are low.

Effect: - Reduce the remaining life at retirement.

As several modules require removal to access the **HPT**, the possibility of finding a large amount of look in damage during removal/replacement is high.

The resulting repair cost should be avoided.

Effect: - Increase the remaining life at retirement.

The **HPC** is the most expensive component requiring a complete strip of the engine, and is a very expensive spare part due to the number of discs involved (6 stages). Furthermore grouping of the discs lives is necessary since each of the discs has been released for a different service life.

The various influences affecting the definition of a suitable remaining life are shown in table 1.

Criteria	Module	Remaining Life (RL)		Comments
		-	+	
Removal Distribution (see figure 1)	LPC	✓		With no clear peak a lower RL can be used
	HPC		✓	Clear peak indicates higher RL
	HPT		✓	Clear peak indicates higher RL
Cost of Spare Parts and Module Repair	LPC	✓		High cost require lower RL
	HPC	✓		High cost requires lower RL
	HPT		✓	Relatively low cost allows higher RL
Cost for Removal/Replacement, Look In Damage and Additional Module Spares ¹⁾	LPC	✓		Low cost allows lower RL
	HPC		✓	High cost requires higher RL
	HPT		✓	High cost requires higher RL

Table 1: Criteria affecting the definition of the most suitable remaining life.

Removal Distribution

Figure 4 below, shows the number of removals of the LPC, HPC and HPT versus the time between two consecutive removals in engine flying hours [6].

All unplanned removals from entry into service until end of 1997 are included (GAF/GNY).

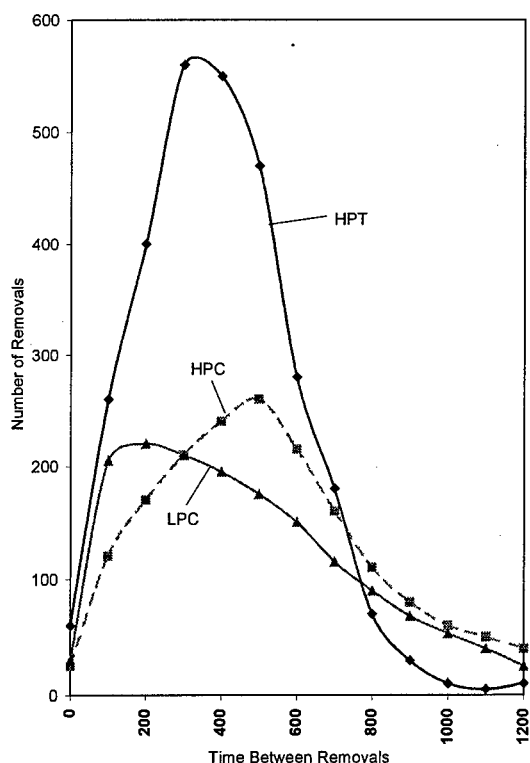


Figure 4 Distribution of LPC, HPC and HPT removals

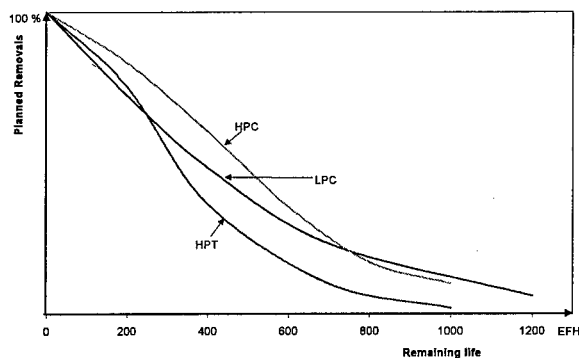


Figure 5 Frequency of planned removals versus Remaining Life

Figure 5 above illustrates the reduction of planned removals (life-ex) with increasing remaining lives. The figure is based on the removal distribution shown in figure 4.

Causes for Removal

The LPC is subject to a high rate of non-basic removals caused by foreign object damage (FOD) which has no major overall effect on the rest of the engine.

The HPC is subject to a fairly high rate of non-basic removals caused by FOD similar to the LPC.

¹⁾ Definition: Cost for module pool

The primary causes for HPT removals are basic failures related to design and material of the turbine blades.

A small percentage of removals are due to secondary damage.

Maintenance Effects

The LPC module is easily and quickly removed and replaced without disturbing other modules.

Unrelated modules hardly ever require removal, repair or replacement. Therefore, most of the LPC replacements do not incur any additional cost.

The HPC module requires the highest maintenance effort for removing and replacing all the fracture critical parts.

The cost for removal and replacement of the HPC is the highest of all engine modules and requires almost a complete engine disassembly.

On these grounds any unnecessary removal and replacement should be avoided.

Several modules require removal to access the HPT and therefore, a high amount of unrelated damage can be identified which requires repair (look in damage).

The cost for removal, repair and replacement of this module is comparatively high.

Look In Damage

Using a sample of LPC, HPC and HPT module removals, the following average percentage of other modules requiring repair (look in damage) has been established (see table 2, repair due to secondary damage is excluded).

Matrix of Look In Damage			
Module	LPC (01)	HPC (03)	HPT (08)
01	100%	35%	45%
02	21%	20%	45%
03	21%	100%	25%
04	7%	25%	20%
05	0%	25%	20%
06	14%	30%	45%
07	14%	85%	95%
08	21%	75%	100%
09	0%	60%	35%
10	7%	65%	25%
11	7%	40%	0%
12	7%	35%	35%
13	0%	5%	0%
14	0%	30%	5%
15	14%	0%	35%
16	7%	10%	10%

Table 2: Amount of damage to other modules (look in damage) identified during removal of the LPC (module 01), the HPC (module 03) or the HPT (module 08). Modules 02, 04 to 07 and 09 to 16 form the rest of the RB 199 engine.

Removal Cost

Based on the distribution of look in damage an additional cost element for the repair of the associated modules has to be added when estimating the total average cost for removal of the LPC, HPC or HPT, respectively.

Summing up all aspects which have an monetary effect on the overall cost for the replacement of an engine module leads to the following correlation:

Module	Cost for Removal
LPC	1.0
HPC	2.4
HPT	1.8

Table 3: Correlation of total removal costs.

Establishment of the Remaining Life

Considering the findings of the cost evaluation and the situation concerning various influences like removal distribution, extent of engine strip/repair and spare parts availability the following individual remaining lives have been allocated to the three different modules:

LPC = 200 EFH
HPC = 800 EFH
HPT = 700 EFH.

6.3 Concluding Remarks

Several factors must be taken into account when reviewing the most cost effective remaining life at retirement of a fracture critical part. A continuous update is required reflecting the actual in-service situation.

The most crucial factor is the actual time of and time between removals currently evident in the fleet since this rate determines the period when parts to be replaced become available at no extra cost.

As seen from the three examples (LPC, HPC, HPT) above, an allocation of a single remaining life for all modules does not result in the most costeffective approach.

A lifing policy of retiring fracture critical parts by “sacrificing” remaining life, requires a compromise between several contradictory features. However, a sensible assessment will ultimately reduce the cost. Consequent application of this policy, a thorough updating procedure in conjunction with a reliable and flexible life management (e. g. spare part provisioning) would widely exclude that an engine had to be removed and disassembled just to replace a life-ex fracture critical part.

Nevertheless, in certain cases a selective use of a life potential on the basis of concessions cleared through additional calculations/testing should be allowed to avoid planned removals (see para 7 below and figure 3).

One might argue that this procedure cannot be used successfully in other projects due to differences in rejection rates.

Agreeably, the rate of rejections may vary and the remaining lives must be adjusted accordingly, but rejections caused by basic or non-basic failures (e. g. FOD) are, by nature of the design and the operation of all weapon systems, unavoidable (see figure 6).

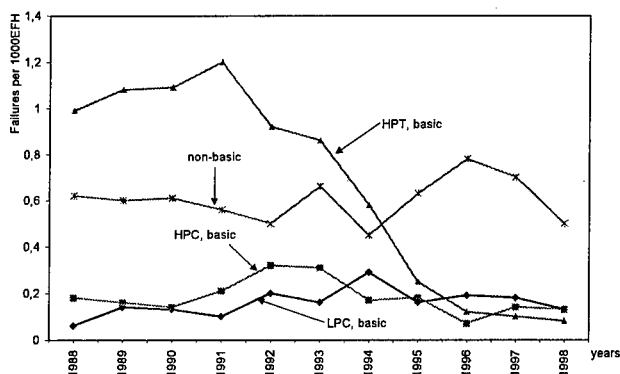


Figure 6 Distribution of rejections caused by basic and non-basic failures

Based on statistics and experience those removals can be predicted and hence reflected in a lifing procedure tailored to any other engine programme.

7. PROPOSAL TO EXTEND THE INDIVIDUAL LIFE OF FRACTURE CRITICAL PARTS

The chapters above describe how useful it can be to extend the remaining life of a fracture critical part i. e. scrapping of parts considerably far away from their released lives just for overall costeffectiveness.

In some cases, however, just the opposite might be necessary when the expiration of the life of an individual fracture critical part affects the operation of the weapon system unacceptably.

When fracture critical parts are retired prior to the expiration of their released life, a portion of the accepted failure risk remains "unused". It is the intention to use this portion, or reserve, for the extension of the released life of the remaining individual parts.

The assumption is currently held that 100 % of the parts entering service will reach their released service life. There is a risk of failure, albeit very small, due to the scatter in material properties, and an accumulated failure risk of 1 in 750 is admissible. This is felt to be acceptable, taking into account the fact that, on the one hand unfavourable geometric and material properties are assumed, and on the other hand a certain degree of statistical safety is implied when calculating released life figures from test results.

If not all fracture critical parts reach their released life, the accumulated failure risk of the population decreases. There are essentially two factors which contribute to this effect:

- fracture critical parts are rejected due to wear or other unacceptable damage - such parts are not repaired.
- fracture critical parts are rejected due to lack of remaining service life - in accordance with the life management detailed above.

In retrospect, the portion of components, based on particular parts, still in service can be transformed into a function of service life defined as the "in service rate".

Multiplication of this "in service rate" with the failure probability density, i. e. the assumed log-normal population, and integration of the resulting function up to conventionally released life, leads to an accumulated overall probability of less than 1 in 750.

The remaining "potential" can be used for an individual life extension without exceeding the accepted limits of overall failure probability.

Assumptions

- With regard to parts with a high replacement rate, it is assumed that the points of retirement are equally distributed. With regard to other parts, it was assumed that there is a 100 % survival rate up to the point "released life less remaining life".
- The population of parts within the period of the remaining life is linearly reduced by 50 %.
- The removal rate remains unchanged beyond the initially released service life until the "new" service life is reached.

Results

By fully using the accepted accumulated risk of 1 in 750 and based on the above assumptions, the maximum admissible lives shown in table 4 can be obtained [9].

Component	$S_{min}^{1)}$ (EFH)	Scrap p/A ²⁾	RL ³⁾ (EFH)	$S_{min} + X^{4)}$ (max) (EFH)	Gain ⁵⁾ (%)
HPC 3	1878	2	450	2010	7,0
HPC 4	3223	1,5	450	3396	5,4
IPC ⁶⁾	1520	1,75	400	1.596	5,0

Table 4: Gain in life of fracture critical parts (examples) by utilising the "failure risk potential" of prematurely retired parts.

¹⁾ S_{min} : Initially released life

²⁾ Scrap p/A: Number of retired components per year

³⁾ RL: Remaining Life; the figures are random, chosen for calculation only

⁴⁾ $S_{min} + X$: Revised max. admissible life ("new" service life)

⁵⁾ Gain is variable, depending on RL

⁶⁾ IPC: Intermediate Pressure Compressor

8. CONCLUSIONS

The implemented life procedure for fracture critical parts in conjunction with the integrated on-board life usage monitoring system has been successful, despite the high cost involved, with respect to the following:

- Very high confidence in flight safety
- Optimal use of the life potential of a fracture critical part
- Extension of the released life and flexibility to cope with changes in the requirement e. g. performance increase (temperatures) during the in-service phase.
- Considerable reduction in life consumption in conjunction with an advanced digital engine control unit (e. g. avoidance of overswing of temperatures and speeds).

But nevertheless, the user is faced with hardly affordable costs caused by a high number of unplanned removals additionally followed by planned removals due to life-ex fracture critical parts.

With the introduction of an individually tailored remaining life policy reflecting the actual in-service situation the number of planned removals as one of the cost drivers has significantly been reduced. But the optimum could not yet be achieved because of its late application.

Furthermore, deficiencies in certain procedures and the possibility of manual intervention (human errors) have reduced a considerable portion of the envisaged savings.

This leads to the idea that less sophisticated, simplified and less costly concepts may result in similar or even better overall achievements.

Our assessments allow the conclusion that scrapping of remaining life under certain circumstances is not a waste of money from an overall point of view.

Retired parts can be stored and reinstalled to bridge the phasing-out period of an engine system.

The evaluation of the Tornado engine programme has demonstrated considerable potential for improvement even after more than 15 years of in-service operation.

Future budget restraints dictate a more costeffective approach (see para 4.2, 6.1, 6.2) for the next engine generation (e. g. EJ200).

Referring to the introduction of this paper it should be the common interest of all parties involved (contractor and customer) to further improve the whole lifing concept. The aim must be the achievement of the best costeffectiveness by keeping the highest level of safety.

This goal can only be reached when all associated lifing aspects are continuously born in mind from the writing of the specification, the first line on the drawing board, during the complete development, production and in-service period.

All associated lifing issues of the different programme phases must adequately be covered from the very beginning of a lifing concept. This concept is put forth and controlled by a comprehensive life management plan which is continuously updated in an iterative process.

It might be worth to consider an engine project where - from the onset - fracture critical parts are designed only for a certain period of the overall life of the engine (e. g. 50 % or 10 to 12 years) but this design is based exclusively on proven technology. After that period those fracture critical parts could be replaced at no extra cost during a major engine upgrade programme where advanced - state of the art - technology could be embodied for the remaining period of in-service life. This standard procedure is widely and successfully applied by civil engine operators.

ACKNOWLEDGEMENTS

The authors wish to thank H. Eidenschink, A. Gallersdörfer and P. Blüml for their engineering support and significant contribution towards the preparation of this paper.

Additionally, many thanks to Mrs. M. Lang and Mr. K. Zanker for the perfect layout.

REFERENCES:

1. TU346 issue 3; "Lifing Procedure for RB 199 Group A Parts" [TU private data]
2. Broede, I. and Köhl, M.; "Methods of Modern Lifing Concepts Implemented in O-Board Usage Monitoring Systems"
3. Broede, I. and Pfoertner, H.; "OLMOS in FAG MRCA Tornado - 10 Years of Experience with On-Board Life Usage Monitoring"; AIAA 97-2905
4. Harrison, F. G.; DERA, UK; "Recommended Practices for Monitoring Gas Turbine Engine Life Consumption"
5. Henderson, M. B. and Harrison, F. G.; "Development and Validation of Algorithms for Engine Usage Monitoring Systems"
6. MTU-MKTR/DC/12-97; "RB 199 Minimum Issue Service Life"
7. Broede, I.; "Engine Life Consumption Monitoring Program for RB 199 Integrated in the On-Board Life Monitoring System"; Conference Proceedings No. 448 (AGARD)
8. A. D. Boyd-Lee; "Statistical Analysis of Finite and Non-Finite Lognormally Distributed Fatigue Lives"; DRA/SMC/CR 962231 13. Sept. 1996
9. Minutes of the 47th RB 199 Local Technical Committee, Feb. 1998 (MOD GE, DASA/MTU private data)

INTERNATIONAL ACCEPTANCE OF COMMERCIAL REPAIR APPROVALS

Wayne Thomas
Brent Junkin

STANDARD AERO LTD
33 Allen Dyne Road
Winnipeg, Manitoba, Canada R3H 1A1

SUMMARY

As the military increasingly adopts commercial standards for the maintenance of "dual use" aircraft, commercial repair approval and its methodology is becoming increasingly relevant in the military world. Component repair development is not limited to the MANUFACTURER. The repair marketplace is global with independent facilities operating around the world.

The authority to issue approvals for aeronautical product repair procedures lies with the National Aviation Authority (NAA). Some NAA's have implemented a system of delegation to enhance the efficiency and effectiveness of the approval process. The privileges and responsibilities of delegated authority may be granted to operators, independent repair stations, qualified individuals, or the manufacturer.

This paper describes how the commercial system works to obtain approval for a new repair scheme, and describes some delegation systems.

1.0 AVIATION REGULATIONS

National aviation regulations enable governments to establish procedures and standards to control all aspects of the aviation industry.

Most countries introduced legislation in the early days of aviation, empowering the governments to set "Minimum Standards of Airworthiness". NAA were established to create and enforce these regulations. Today, some examples of these are:

- United States Federal Aviation Regulations (FAR)
- Joint Aviation Authorities* – Joint Aviation Regulations (JAR)
- Canadian Aviation Regulations (CAR)

*Footnote: *JAA member countries are working on the development and acceptance of the JARS. Member countries still have some national regulations in use. Other countries also have similar regulations.*

The regulations also define the requirements for the approval of maintenance data and repair procedures. The authority for approval of all aeronautical product designs, and procedures for repairs and modifications thereof originates from the applicable NAA.

2. THE TYPE CERTIFICATION PROCESS

The Type Certification Process requires the manufacturer of a new civilian aeronautical product, i.e. an aircraft, aircraft engine, or propeller, to demonstrate that their product meets these minimum standards of airworthiness. For example, a partial list from FAR 33 for engines includes:

- Design Features
- Materials
- Fire Prevention
- Durability
- Engine Cooling
- Engine Mounting Attachments
- Accessory Attachments
- Turbine Rotors
- Vibration Tests
- Surge Characteristics
- Fuel and Induction System
- Ignition System
- Lubrication System
- Endurance Tests (block tests)
- Bird Ingestion Tests
- Rain and Hail Ingestion tests
- Engine Component Tests

These regulations define the minimum standards and form the "Type Approval Basis" for the product.

The NAA and manufacturer work closely together during this phase. The manufacturer will generally submit a compliance program to the NAA. This is a document that addresses each airworthiness requirement, and proposes how the product will be demonstrated to comply. The NAA interacts with the manufacturer, and may require additional test procedures or alternative means of demonstrating compliance. The NAA may also require that their representative be permitted to witness tests or procedures that they consider critical.

When compliance has been demonstrated with the applicable standards of airworthiness the NAA issues the Type Certificate. The Type Certificate is the NAA's certification that the aeronautical product has met the minimum standards for use in certificated aircraft. The Type Certificate also provides key specifications, ratings and operating limits.

The drawings and specifications that define the product (called the Type Design) and the manuals that specify

the proper operation, maintenance and recondition thereof are submitted to the NAA at the time of initial certification. These data are an integral part of the Type Certification process.

3. MANUFACTURER'S MANUALS

The manufacturer's maintenance and overhaul manuals contain data that define the requirements to maintain the aeronautical product in an airworthy condition. These manuals are approved or specified as acceptable by the NAA. By law, maintenance must be performed in accordance with the requirements of these manuals to maintain the Certificate of Airworthiness of the aircraft.

The manuals are written by the manufacturer at the time of initial certification. The manufacturers use their best judgment and Type Certification test program experience to establish:

- Tooling and Equipment Requirements
- Process Specifications, i.e. cleaning, non-destructive inspection, welding, Brazing, metallizing, plating etc.
- Inspection Methods
- Serviceable Limits
- Component Repair Requirements
- Repair Procedures and Repairable Limits

The manuals reflect the manufacturer's level of knowledge at the time of initial Type Certification. The repairs are generally basic, and utilize common processes and equipment that will be available in a typical repair station or approved maintenance organization. While service bulletins and manual revisions are issued from time to time the revision of repair procedures, and addition of new repair procedures tends to fall behind advancements in technology. The manufacturers may also leave the details of specialized repair processes out of the overhaul manuals for proprietary/competitive reasons.

4. MAINTENANCE IN SERVICE

Once the product enters service the operator is responsible for maintaining the product in accordance with the manufacturers maintenance and overhaul manuals. Operators seek the most cost effective approach to maintain their equipment. This may be by performing the work in an in-house maintenance facility, or by subcontracting the work to a NAA authorized facility. Independent repair facilities and the manufacturer compete for this business

As the product matures and service experience is accumulated the components suffer service degradation and wear in ways that the manufacturer could not foresee. Since repair schemes for these conditions are not provided in the manufacturers manuals, new approved repair procedures must be produced or the parts will be deemed scrap. Additional repair procedures must be added to economically maintain the product.

In addition, advances in technology make new repair procedures possible. Companies that effectively apply these technologies to component repair extend the safe service life of components and reduce maintenance costs by reducing new material costs.

5. DELEGATION OF REPAIR DATA APPROVAL

Delegation is defined as "*the art of achieving specific, predefined results through the empowerment and motivation of others*".

As previously noted, the NAA is the source of authority for all approvals to aeronautical products. This includes the approval of new repair procedures.

The NAAs recognize that companies must supplement the manufacturer's manuals with additional data to maintain aeronautical products. The NAAs make provisions for this in the regulations. For example, JAR 145.45 (b) states:

"Where the JAR-145 approved maintenance organization produces it's own airworthiness data additional to that specified in paragraph (a) such additional airworthiness data must be produced in accordance with a procedure acceptable to the Authority."

NAA's do not have the resources to directly review and approve all of the modifications and repairs generated by industry for previously Type Certificated Aeronautical Products. To meet this need, some NAAs have established systems to delegate authority.

The delegation of authority enables the delegate to fulfill obligations charged to the NAA under the aviation regulations. Delegates act as an extension of the NAA, and apply the same rules as the NAA. Privileges may be granted to qualified individuals, independent maintenance or design organizations, and the manufacturer.

Delegation systems enable the NAA to have a large number of highly qualified technical people perform the enormous amounts of examinations, testing, and inspections necessary to determine compliance with pertinent regulations.

6. DELEGATION SYSTEMS

FAA - Designated Engineering Representative (DER)

The DER system is described in FAA Order 8110-37. There are two categories of DERs that approve data, Company DERs and Consultant DERs. In either case, the delegation is issued to the **individual** via a FAA 8110-25 Certificate of Authority.

The minimum DER qualifications are:

- 8 years of progressively responsible engineering experience as appropriate to the designation sought
- an engineering degree from a college of recognized standing
- 1 year direct working relationship working with the FAA where the applicant
- continuously and actively is engaged in processing engineering work for FAA
- approval of the type in which the applicant is seeking appointment

The DER delegation is given in the particular area of designation in which the applicant has expertise. For example Engines, Structures, Propellers etc.

The privileges differ slightly for each designation, but generally consist of the authority to prepare and/or approve:

- Engineering Reports
- Drawings
- Other data related to durability, materials, and processes employed in design, operation, and maintenance provided these items comply with the pertinent regulations

A typical project sequence for a repair approval is as follows:

- Data are submitted to the DER for review
- DER assesses whether repair is major or minor.
- If major, the DRE consults with their FAA advisor and obtains permission to proceed with the project.
- DER identifies the applicable airworthiness requirements. Normally these are at the amendment level defined in the Type Certificate for which the product was originally approved.
- DER evaluates data against applicable airworthiness requirements. Technical data for a major repair must show that the condition of the repaired product will be at least equal to its original or properly altered condition. To accomplish this, the data must show compliance with the applicable airworthiness standards. This is commonly shown through engineering analysis and physical testing. Data must show the repaired product will function reliably through its established inspection interval.
- DER makes a determination if data are adequate to demonstrate compliance. If a finding of compliance is made, the DER approves the data by issuing a completed FAA 8110-3 form.

The FAA holds recurrent DER "Standardization Seminars" which help achieve consistency in the DER system. However, as the DER program is managed by the ACOs in the regions, there is some variation in the practices for appointment and oversight of DERs through the USA. With special permission DERs may

perform work outside their region, including at foreign FAA repair stations.

FAA Special Federal Aviation Regulation (SFAR) 36

SFAR 36 permits certain Part 121 and 145 operators to develop their own technical data for performing major repairs on aircraft, engines, propellers, and appliances when approved data does not exist.

The operator produces and approves data in accordance with a FAA approved SFAR 36 procedures manual. The manual specifies the procedures for developing and determining the adequacy of technical data for major repairs. The manual also specifies the names and responsibilities of each person whom:

- Has authority to make changes in procedures that require a revision to the procedures manual
- Prepares or determines the adequacy of technical data
- Plans or conducts tests
- Approves the results of tests

The FAA plans to eliminate SFAR 36, but this has been delayed several times. SFAR 36 is still in effect. Some consider the SFAR 36 system to be less rigorous than the FAA DER system.

Transport Canada Design Approval Representative (DAR)

The Transport Canada DAR system was structured to be the equivalent of the DER system used in the USA.

Like FAA DERs, the DARs review engineering data to determine compliance with the applicable standards of airworthiness. The DAR system is still active for individuals, i.e. a consultant DER.

Transport Canada Design Approval Organization (DAO) and Approved Engineering Organization (AEO)

The DAO/AEO systems were introduced after the DAR system. The DAO/AEO introduce the concept that the corporation is responsible for having adequate resources and program management to support and maintain the delegation. Under the DAO/AEO the corporation receives the delegation, **not** the individuals. Transport Canada Airworthiness Manual Chapter 505 refers.

The DAO and AEO systems are similar. A DAO is established in an Approved Maintenance Organization (equivalent of a repair station). An AEO is established in a Commercial Air Service. Persons in the DAO and AEO have a similar role to the DAR as described above.

The DAO/AEO is effectively an organization within the Approved Maintenance Organization/Commercial Air Service. The DAO/AEO has its own Transport Canada approval separate from the parent organization. The DAO/AEO operates in accordance with an approved procedure manual, which includes (in part):

- A statement of DAO/AEO purpose
- Management commitment to:
- provide adequate resources to perform the delegated functions
- grant adequate authority to perform the delegated functions
- ensure staff remain knowledgeable in their technical specialty with respect to
- airworthiness standards and procedures
- DAO/AEO description and lines of responsibility
- A description of the functions the DAO/AEO is authorized to perform
- A description of the airworthiness control system utilized for determining the
- adequacy of technical data approved by the DAO/AEO
- A description of the system used to audit the performance of the DAO/AEO
- A description of the record keeping system
- The names and titles of persons appointed to perform airworthiness functions, and sample signatures

The DAO/AEO systems offer advantages over the DAR system. The procedures to generate, review and approve data are specified in more detail, and more widely known through the organization.

Transport Canada exercises control through the approved procedures manual, compliance programs, and conditions specified by the Regional Office when issuing approval numbers.

JAA Design Organization Approval (DOA)

The JAA is moving toward implementation of an organization delegation system called a DOA. The regulations will be specified in JAR 21, subpart M. The procedure is currently in draft form, with expected implementation June 1, 1999. Note that while the individual countries will adopt the JAR, individual NAAs may choose to add requirements. Pending acceptance of JAR 21, subpart M the individual member countries of the JAA utilize their own NAA regulations that may be applicable.

7. INTERNATIONAL ACCEPTANCE OF REPAIRS

The international acceptance of repairs involves two issues, the acceptance of maintenance performed in the other country, and the acceptance of repair data approved by delegation.

The issue of acceptance of maintenance (performed in accordance with the manufacturer's overhaul and maintenance manuals) is usually dealt with by a Bilateral Airworthiness Agreement, Memorandum of Understanding, or other agreement between the countries.

JAA countries generally accept manufacturer's repairs, but there are no regulations yet for acceptance of other repairs approved by delegation. There are however JAA General policies that apply. General JAA Policy-1 states: "*Member states accept repairs approved within the regulatory system of the Type Certifying Authority.*" General JAA Policy-2 states: "*Involvement of the manufacturer with such repairs is desirable, but not mandatory.*"

Practical acceptance of repairs (from sources other than the manufacturer) approved by delegation is by member states, but most JAA states are following General JAA Policy-1. The aircraft operator must also accept the repair. The degree of acceptance varies between countries, airworthiness inspectors, and operators.

The concept of the NAA issuing approval (not the manufacturer) is not well understood. Likewise, the concept of delegation to approve repairs is not well understood in many JAA states.

These considerations impact maintenance not only at the time the maintenance is performed, but also when an aircraft is moved from one country of registration to another. If the receiving state does not accept the repair approvals embodied in the aircraft costly remedial work may be required to satisfy the receiving state.

8. CONCLUSIONS

- The NAA issues approvals for Civilian Aeronautical Products
- The manufacturers maintenance and overhaul manuals must be supplemented with additional repair data to economically maintain aeronautical products
- Some NAA appoint delegates to act on their behalf and issue approvals for repair procedures
- NAA delegates increase the capacity of the NAA to review and approve large volumes of data
- Military operators can gain similar benefits by adopting a system of delegation with their maintenance contractors.

References:

1. JAA JAR 145.45 Airworthiness Data
2. FAA FAR 145 Repair Stations
3. FAA SFAR 36 Development of Major
Repair Data
4. FAA Order 8110-37, Designated Engineering
Representative Guidance Handbook
5. Transport Canada Airworthiness Manual Chapter
505 - Delegations

HIGH CYCLE FATIGUE LIFE MANAGEMENT IN GAS TURBINE ENGINES

T. Nicholas

U.S. Air Force Research Laboratory
Materials and Manufacturing Technology Directorate
Wright-Patterson AFB, OH 45433-7817, USA

SUMMARY

HCF failures in materials used in rotating components of gas turbine engines have often been found to be attributable to fatigue loading on materials which have sustained damage from other sources. Damage can be present in the form of initial material or manufacturing defects, or can develop during service operation. Three major sources of in-service damage have been identified which can alter the HCF resistance individually or in conjunction with one another: low cycle fatigue (LCF), foreign object damage (FOD), and fretting. Methodologies for treating such damage in establishing material allowables are considered. Some recent results on the effects of damage on the Haigh (Goodman) diagram and a discussion of the life management aspects of HCF are presented.

1. INTRODUCTION

The high incidence of HCF related failures over the past several years in U.S. Air Force gas turbine engines, combined with the substantial maintenance costs and potential detrimental effects on operational readiness, have led the Air Force to re-evaluate the design and life management procedures for HCF. In attempting to assess the root cause of HCF failures and find methods for reducing the incidence of such failures, the relatively empirical nature of the procedures now in place becomes abundantly clear. Further, the lack of detailed information on vibratory loading and dynamic response of components as well as material capability under HCF, particularly in the presence of initial or in-service damage, makes anything but a highly empirical approach impractical at this time. To address these

shortcomings, the U.S. Air Force initiated a National High Cycle Fatigue Program to develop a technology base for implementation of damage tolerance procedures for HCF in gas turbine engines. This paper focuses on the material capability aspects of the damage tolerant approach for design and life management of components subjected to HCF.

2. DAMAGE TOLERANCE

The natural tendency in the implementation of a "damage tolerant" approach to fatigue would be to relate remaining life based on predictions of crack propagation rate to inspectable flaw size. In LCF, this has been shown to work well, and such an approach was adapted by the U.S. Air Force in 1984 as part of the ENSIP Specification [1]. For HCF, direct application of such an approach cannot work for "pure" HCF because required inspection sizes are well below the state-of-the-art in non-destructive inspection (NDI) and the number of cycles in HCF is extremely large because of the high frequencies involved. The basic problem is illustrated schematically in Fig. 1 which shows that LCF involves early crack initiation and a long propagation life as a fraction of total life. In addition, LCF cracks are typically of an inspectable size early enough in total life so that there is a considerable fraction of life remaining during which an inspection can be made. HCF, on the other hand, requires a relatively large fraction of life for initiation to an inspectable size, or the creation of damage which can be detected, to occur. This results in a very small fraction of life remaining for propagation. It must be pointed out that considerable research is being conducted at the present time to identify and detect HCF damage in the early stages of total fatigue life.

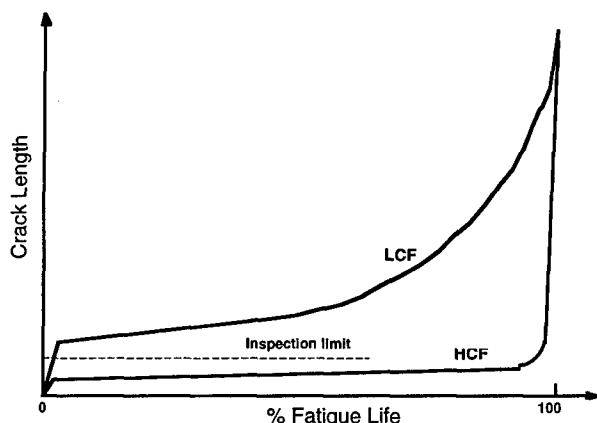


Fig. 1 Schematic showing difference between HCF and LCF.

While a damage tolerant approach may seem out of the question at present for HCF, the most pressing problems in field failures are not related to material capability under pure HCF. Rather, the problems fall into two categories. First, and foremost, is the existence of vibratory stresses from unexpected drivers and structural responses which exceed the material capability as determined from laboratory specimen and sub-component tests. Design allowables are normally obtained on material which is representative of that used in service including all aspects of processing and surface treatment and are often represented as points on a Haigh or "Modified Goodman diagram". (This point is qualified in the following paragraph.) The second category involves the introduction of damage into the material during production or during service usage. The three most common forms of damage, either alone or in combination, are LCF cracking, foreign object damage (FOD), and fretting fatigue. To account for this damage, or to design for pure HCF, the concept of a threshold below which HCF will not occur is necessary because of the potentially large number of HCF cycles which can occur over short service intervals. This is due to the high frequency of many vibrational modes, often extending into the KHz regime. In fact, current design for HCF through the use of a Haigh diagram seeks to identify maximum allowable vibratory stresses so that HCF will not occur in a component during its lifetime. The current ENSIP specification requires this HCF limit to

correspond to 10^9 cycles in non-ferrous metals, a number which is hard to achieve in service and even harder to reproduce in a laboratory setting. Consider that a material subjected to a frequency of 1 KHz requires nearly 300 hours to accumulate 10^9 cycles.

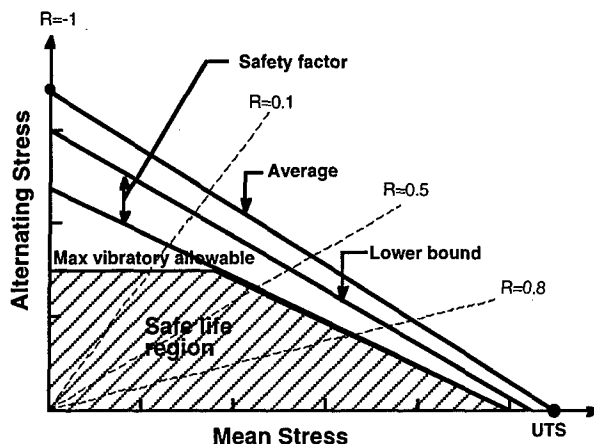


Fig. 2 Constant life diagram.

3. CONSTANT LIFE DIAGRAMS

The diagram most used for design purposes is a constant life diagram as illustrated in Fig. 2, where available data are plotted as alternating stress as a function of mean stress for a constant design life, usually 10^7 or higher. This diagram, which can be correctly called a Haigh diagram, is commonly and incorrectly referred to as a Goodman diagram or a Modified Goodman diagram [2]. In the absence of data at a number of values of mean stress, it is often constructed by connecting a straight line from the data point corresponding to fully reversed loading, $R=-1$, with the ultimate tensile strength (UTS) of the material. Data at $R=-1$ can be obtained readily from a number of techniques using shaker tables to vibrate specimens or components about a zero mean stress, while data at other values of mean stress are often more difficult to obtain, particularly at high frequencies. Alternatives to the straight line approximation in Fig. 2 involve various curves through the yield stress or UTS point on the x-axis, or through actual data if available, to represent the average behavior. Scatter in the data can be handled by statistical analysis which

establishes a lower bound for the data. On top of this, a factor of safety for vibratory stress can be included to account for the somewhat indeterminate nature of vibrations, particularly those of a transient type. Finally, design practices or specifications may limit the allowable vibratory stress to be below some established maximum value, independent of the magnitude of the mean stress. The safe life region, considering all of these factors, is shown in Fig. 2. What the shaded region provides, therefore, is an allowable threshold vibratory stress as a function of mean stress, the latter being fairly well defined because it is closely related to the rotational speed of the engine. If the vibratory stress is maintained within the allowable region on the Haigh diagram, there should be no failure due to HCF and, further, no periodic inspection required for HCF. Provided that the maximum number of vibratory cycles experienced in service does not exceed the number for which the Haigh diagram is established, 10^9 for example, then such a design procedure is one of "infinite" life requiring no periodic inspection.

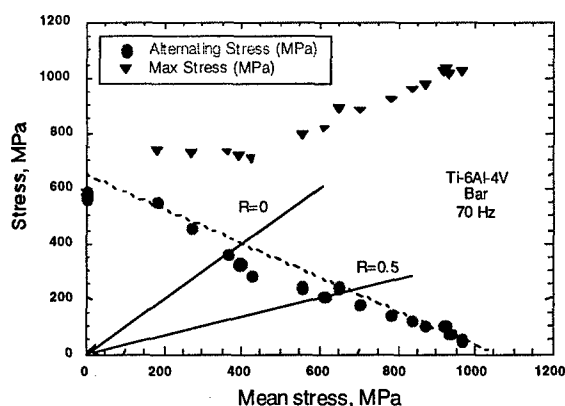


Fig. 3 Haigh diagram for Ti-6Al-4V bar.

There are some pitfalls in the use of a Haigh diagram in design, particularly when basing it only on data at $R=-1$. For example, Figs. 3 and 4 show such diagrams for the same material, Ti-6Al-4V, processed into two different product forms, hot rolled bar, and forged plate, respectively. In addition to the alternating stress, the peak or maximum stress is also shown. The data in Fig. 4 are obtained from two independent sources on the same material,

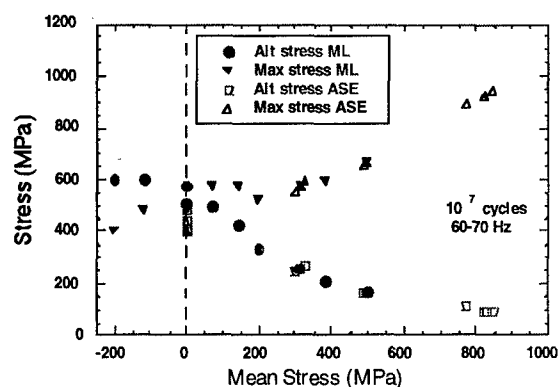


Fig. 4 Haigh diagram for Ti-6Al-4V plate.

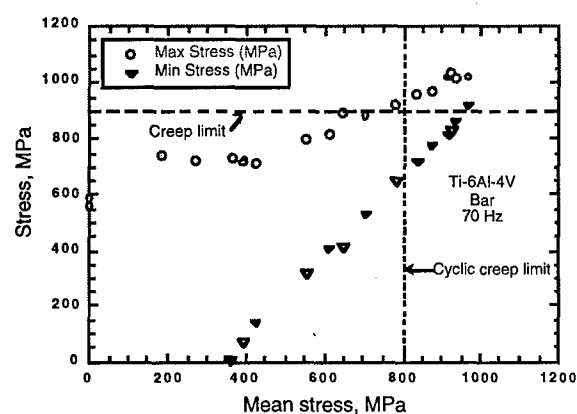


Fig. 5 Haigh diagram showing region of transition in mechanism for high mean stress.

yet an unusual feature of the data is the relatively large amount of scatter which occurs under $R=-1$ (fully reversed, zero mean stress) loading. This phenomenon has been observed in several other alloys and is under further investigation. Note also that a straight line does not provide a good representation of the alternating stress data. Note, further, that for high values of mean stress, the maximum stress is quite high, approaching the static ultimate stress of 1030 and 980 MPa for the bar and plate material, respectively. Recent research on fatigue life at high mean stresses [3] has shown that at high mean stress, the fracture mode changes from one of fatigue to one of creep. A plot of maximum and minimum stress, Fig. 5, shows the range of vibratory stresses (min to max) at each mean stress tested. The stress above which creep occurs is shown along with the line which delineates the region of fatigue, at

low mean stresses, from the region of creep, at high mean stresses. Thus, in the creep regime, consideration should be given to the amount of time during which such vibrations occur, not only to the number of cycles. Allowable vibratory stresses, while very low in this region, should also be supplemented with consideration of maximum stresses. It is for these reasons that designers shy away from the high mean stress regime, often for reasons that cannot be quantified.

4. DAMAGE CONSIDERATIONS

While methods appear to be available to quantify the fatigue limit of a material, and to establish a threshold for a crack of an inspectable size, there are still issues remaining over how severe is the damage induced by FOD and fretting fatigue. Other modes of service-induced damage, such as creep, thermo-mechanical fatigue, corrosion, erosion, and initial damage from manufacturing and machining, must also be taken into account in establishing material capability and inspection intervals. The following sections provide a brief description of the issues associated with FOD and fretting.

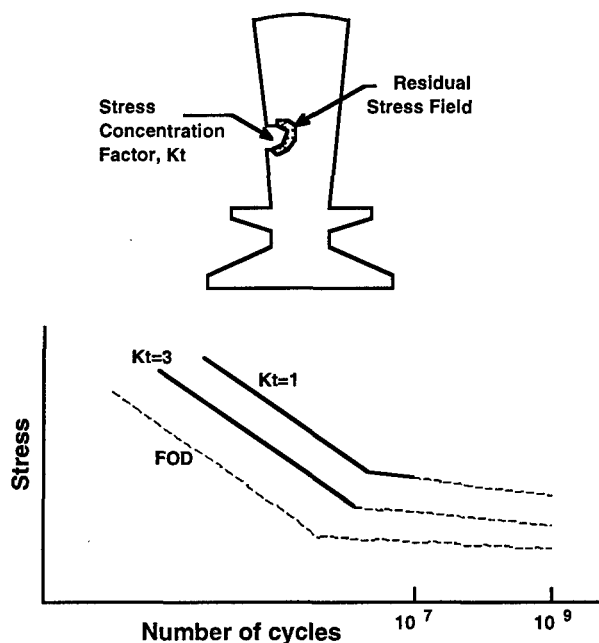


Fig. 6 Schematic of concerns in FOD.

4.1 FOD and Notches

Foreign objects impacting leading edges of rotating blades or static structures can produce damage in the form of notches or tears as shown schematically in Fig. 6. Attempts have been made to quantify such damage in the form of an equivalent K_t , but relating that to actual material behavior is difficult. First, it is difficult to establish the effective value of K_t , particularly when residual stresses are produced and when small cracks are formed at the tip of the notch. Second, there are an unlimited number of notch geometries involving combinations of depth and radius of notch which will produce the same value of K_t for a given loading condition. Third, while some data exist on the reduction of fatigue life at a given stress due to FOD, there are few data available on the reduction of the fatigue limit, particularly in the very high cycle regime.

These "regions of ignorance" are shown schematically in Fig. 6 as dashed lines. Recent work has provided some quantitative results on the fatigue notch factor, K_f (unnotched fatigue limit stress/notched fatigue limit stress) for machined notches in Ti-6Al-4V. Bellows et al. [4] report values of $K_f = 1.8$ and 2.1 for $R = -1$ and $R = 0.1$ respectively using specimens with a notch having a $K_t = 2.5$. The fatigue limit is established for 10^7 cycles at 60 Hz. Lanning et al. [5] report values of $K_f = 2.1, 1.8$, and 1.3 for

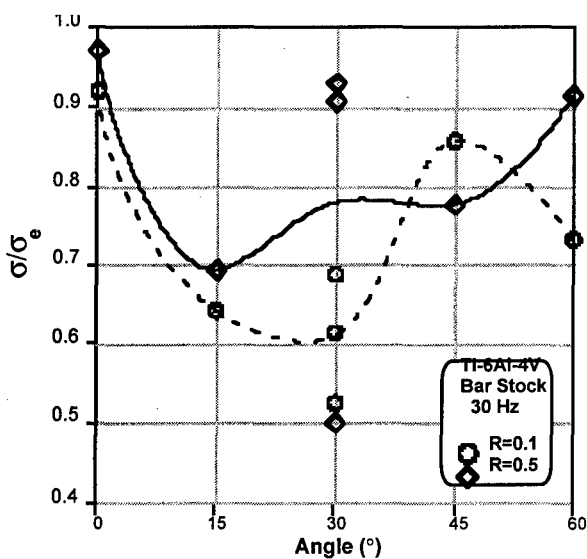


Fig. 7 Effect of incidence angle on fatigue limit for FOD from 1 mm diam. particles.

10^6 cycles for $R=0.1$, 0.5 and 0.8 respectively, for $K_t=2.8$ at 50 Hz. These type of data allow design limits for vibratory stress to be established for notches of a known K_t . But how do these relate to the performance of a material which has suffered FOD from a particle impacting at high velocities? Results for values of the fatigue limit in Ti-6Al-4V have recently been obtained using tension specimens which have a leading edge geometry similar to a fan or compressor blade. Tests on a leading edge (LE) specimen whose LE thickness is 0.75 mm (radius = 0.38 mm) have been conducted by impacting the LE with 1 mm diam. glass spheres at a velocity of 300 m/s and at incident angles between 0° and 60° [6]. Results are shown in Fig. 7 which shows the 10^7 cycle fatigue limit for the various conditions normalized with respect to the undamaged material at 2 values of R . It can be seen that normal incidence, 0° , is the least damaging for these impacts. The worst condition is when the impact angle is around 30° although a large amount of scatter is seen in the data. It is clear that experimental and analytical methods for assessing the extent of FOD damage must consider angle of incidence as an important parameter.

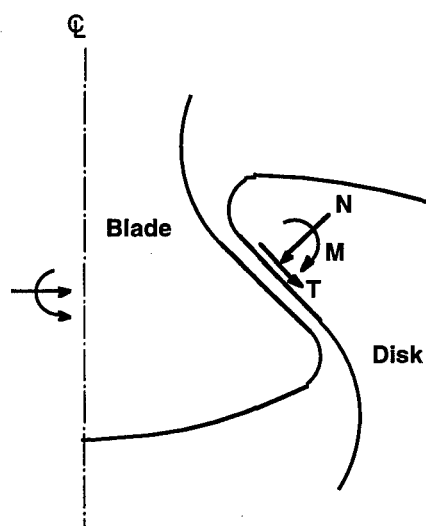


Fig. 8 Schematic of loads in dovetail region.

4.2 Fretting

Fretting fatigue in dovetail joints is one of the most difficult and one of the costliest problems in the U.S. Air Force related to HCF. Fretting

fatigue occurs when there is relative motion in the contact region between two surfaces. In the schematic of a dovetail, Fig. 8, it is seen that the contact region involves normal and shear loads as well as bending moments across the interface. In addition to the loads shown, there are axial stresses in both the blade and disk parallel to the contact plane. Superimposed on the loads from the steady centrifugal loading of the blade are vibratory stresses which can result from blade vibrations. Because of the nature of the stress fields in contact regions, there is always a region of relative slip near the edge of contact, shown schematically in Fig. 9. The general problem, therefore, involves normal contact forces, N , tangential contact forces, T , axial loading of the material, P , regions of stick and slip, and a relative displacement in the slip region. Depending on the magnitude of this relative motion and the stress fields produced by the steady and vibratory stresses, fretting fatigue can occur near the edges of the contact region. Whether fretting fatigue is due entirely to the relative motion, or whether the complex stress field contributes significantly to the process, is still debated. Nonetheless, laboratory experiments and field usage demonstrate that fretting fatigue can reduce the HCF material capability significantly.

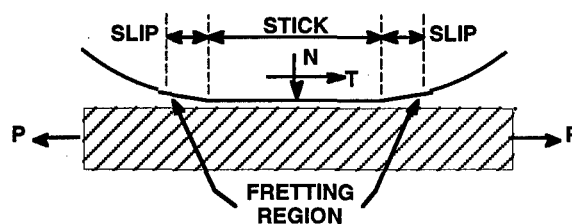


Fig. 9 Schematic of loads in contact region under fretting fatigue conditions.

Results for the fatigue limit stress corresponding to 10^7 cycles for specimens held in a fretting pad fixture [7] are presented in Fig. 10. The data shown represent the maximum stress, denoted by "Goodman stress", for tests conducted at two stress ratios using fretting pads with two different radii at the edge of contact. The data are plotted against the average normal (clamping) stress of the pad on

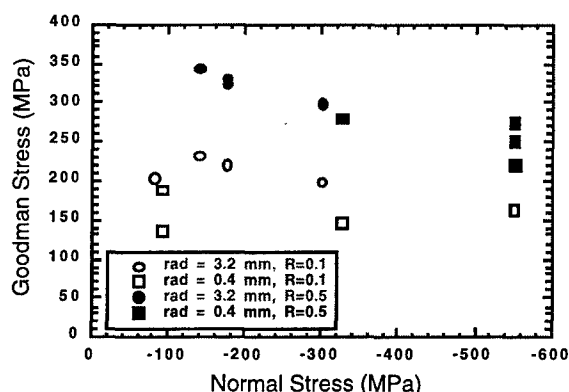


Fig. 10 Fatigue limit stresses under fretting.

the specimen. For comparison purposes, typical Goodman stress values for the Ti-6Al-4V used as the specimen and pad material are 600 and 825 MPa for $R=0.1$ and $R=0.5$, respectively. It can be seen from the figure that the values under fretting conditions are significantly lower than for the unfretted material. To quantify the reduction in fretting capability, an average knockdown factor (KF) is calculated as the unfretted fatigue limit stress divided by the fretting fatigue limit stress. This definition is similar to the one used for notches, K_f . The results are presented in Table 1 and show that the larger contact radius produces the larger value of KF for both values of $R=0.1$ and 0.5 . Second, tests at $R=0.1$ produce a higher value of KF than those conducted at $R=0.5$. While these trends and corresponding values of KF are significant and should be taken account of in design, there appears to be no systematic change in Goodman stress with value of clamping stress over the range of clamping stresses which cover roughly a factor of six in this investigation as seen in Fig. 10. The authors conclude tentatively that the normal stress may not have much affect on the relative slip length in the contact region, but clearly more work has to be done to quantify all such effects. These results show, however, that use of a single factor of safety on the allowable alternating stress in a Haigh diagram, a procedure that has been used in design more than once, is not a rational approach and may be non-conservative for some contact stress conditions if the factor of safety is obtained

empirically for one specific condition. Note that the values in Table 1 for KF range from 2.6 to 4.2 for the limited range of conditions studied.

σ_{fret} (MPa)	radius (mm)	Stress Ratio	σ_{ref} (MPa)	KF
144	3.2	0.1	600	4.2
214	0.4	0.1	600	2.8
258	3.2	0.5	825	3.2
323	0.4	0.5	825	2.6

Table 1. KF values for fretting fatigue.

5. HCF DAMAGE TOLERANCE

The ultimate goal is to be able to design for HCF in the presence of any type of damage or service usage which degrades the properties of materials under HCF loading. The concept is illustrated in Fig. 11 which shows, schematically, some type of damage which might affect material capability. Such damage state, denoted by D , will have a design life which is some fraction of the actual life under those conditions. The damage may be a continually increasing function, such as LCF, or may be a step function such as FOD. In either case, the material would be removed from service for cause (inspection) or because the design life is reached. Just prior to removal, the material has its least resistance to HCF. A damage tolerant design should address the HCF capability under the most severe and probable damage state, shown schematically in Fig. 11 as the critical damage state. Various approaches to implementing such an approach are discussed in the following sub-sections.

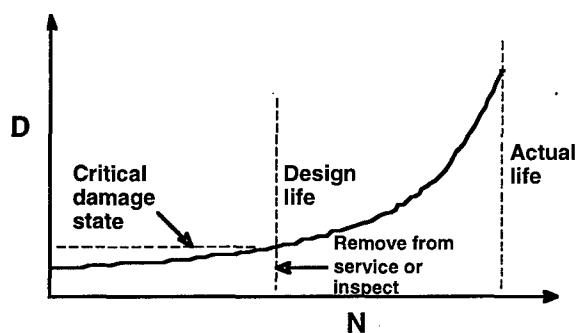


Fig. 11 Schematic of damage accumulation.

5.1 Crack growth thresholds

For damage in the form of cracks, from FOD, fretting, or LCF, the use of a fracture mechanics threshold to determine the allowable vibratory stress seems to be a promising approach for HCF, and follows the concept now being used successfully for LCF. Provided that an inspection can be made, and crack lengths measured, knowledge of the threshold for crack propagation can be used to assess the susceptibility of the material to HCF crack propagation. If the stresses are maintained below this limit, and the limit corresponds to a sufficiently low growth rate, perhaps 10^{-10} m/cycle or lower, then safe HCF life is assured. The potential growth of such cracks under LCF, and the time interval where such growth produces a crack where HCF might occur, must also be considered. This would establish the required inspection interval. One key issue in this proposed scenario is the determination of a suitable threshold for the types of cracks which may occur in service, some of which could be quite small. Various types of loading conditions can be used to determine a threshold, most of which are for long cracks. Lenets and Nicholas [8] used two methods, shown schematically in Fig. 12, where thresholds were obtained from increasing and decreasing ΔK experiments after growing the crack under large amplitude loading. Fig. 13 shows the results which show that the decreasing ΔK threshold (Jump A) is smaller than the increasing ΔK threshold (Jump B), although the authors feel that the lower threshold is not realistic because service conditions usually produce loadings below threshold until a severe event occurs in which HCF becomes critical, as in Jump B. Boyce et al. [9] conducted tests at 1 KHz frequency and found that a lower bound threshold for small crack propagation could be established from long crack threshold tests at high R under constant- K_{max} /increasing K_{min} conditions. For Ti-6Al-4V, at $R=0.92$, this lower bound was found to be $\Delta K=2.2$ MPa \sqrt{m} whereas small crack growth behavior from naturally initiated and FOD induced small cracks was not observed below a ΔK of 2.9 MPa \sqrt{m} .

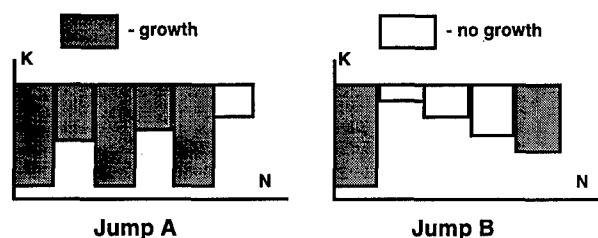


Fig. 12 Schematic of jump loading history

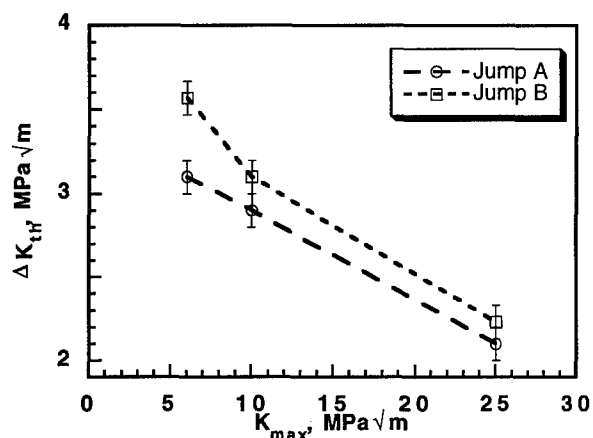


Fig. 13 Threshold data for jump tests.

5.2 Surface treatments

In addition to the implementation of damage tolerance to improve the reliability of HCF design when other damage may occur, procedures are being developed to decrease the materials susceptibility to in-service damage. In addition to shot peening, which improves the fatigue resistance of materials when initiation takes place near the surface, a laser shock peening (LSP) process has been introduced into service to improve the material resistance to FOD. A schematic of the process is shown in Fig. 14 where a pulsed laser impinges on the surface of a material. In actual practice, two pulses impinge simultaneously on both sides of the leading edge of a blade. The rapid ablation of the surface coating generates intense, short duration shock pulses which interfere with each other within the blade and produce a high compressive residual stress at the surface down to depths of the order of nearly 1 mm. Water on the surface acts as an impedance mismatch and serves to constrain the shock pulse within the blade. The compressive residual stresses, which are more intense and much deeper than

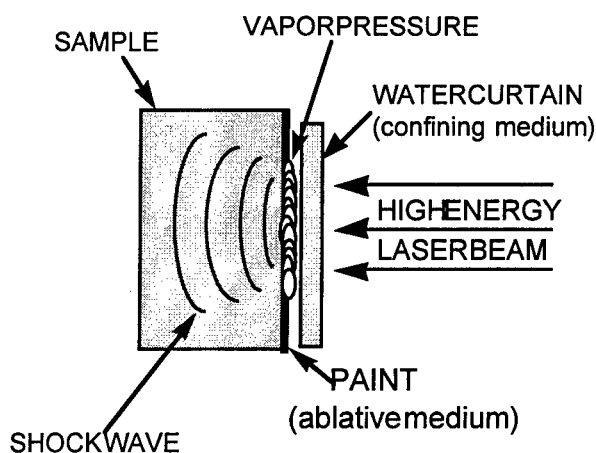


Fig. 14 Schematic of LSP process.

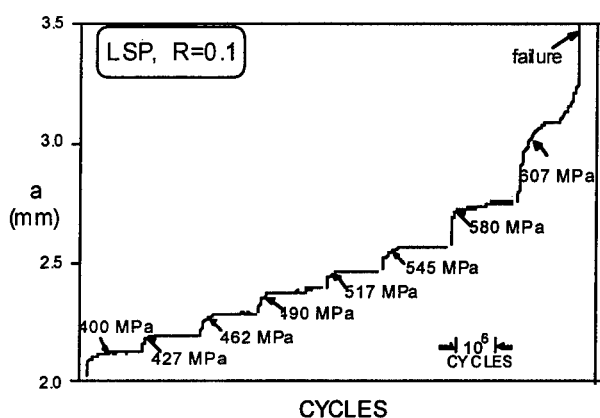


Fig. 15 Sample LSP crack growth data.

those developed under conventional shot peening, retard both the initiation and growth of cracks from foreign body impacts or machined notched in the leading edge. An illustration of the benefits of LSP is shown in Fig. 15 where crack length in a three-point bend specimen is shown for various increments of loading [10]. For each load step, the crack grows and then arrests. This happens as the load is increased from 400 to 580 MPa and failure only occurs when a stress of 607 MPa is applied. By contrast, a specimen without LSP fails upon loading at the lowest load level where the crack continues to grow without arrest. The retardation of crack growth for the LSP samples is attributed to the compressive residual stresses which, in turn, provide the equivalent of a superimposed negative K [10].

6. CONCLUDING REMARKS

Damage tolerant approaches for HCF are still in the development stage. Whatever their final form, it seems clear that they will involve the use of a threshold concept, a criterion for a smooth or damaged material below which HCF will not occur. The criterion could be in the form of a stress or a stress intensity. From a maintenance and life extension point of view, it is important to be able to quantify the level of damage that may be present from other than HCF, such as from LCF, FOD, or fretting. This may be accomplished by inspection, analysis, probabilistics, or some combination of these. In addition, methods need to be established to predict the growth or extension of any such damage so that material capability limits are not exceeded before the next inspection or the component is removed from service.

7. REFERENCES

1. Engine Structural Integrity Program (ENSIP), MIL-STD-1783 (USAF), 30 November 1984.
2. Sendekyj, G.P., "History of Constant Life Diagrams," High Cycle Fatigue of Structural Materials, T.S. Srivatsan and W.O. Soboyejo, Eds., TMS, 1998, pp. 95-107.
3. Morrissey, R.J., "Frequency and Mean Stress effects in High Cycle fatigue of Ti-6Al-4V", WL-TR-97-4100, Wright-Patterson AFB, OH, 1997.
4. Bellows, R.S., Bain, K.R. and Sheldon, J.W., "Effect of Step Testing and Notches on the Endurance Limit of Ti-6Al-4V," Proceedings of ASME Winter Annual Meeting, Anaheim, CA, Nov. 15-20, 1998.
5. Lanning, D., Haritos, G.K. and Nicholas, T., "Notch Size Effects in HCF Behavior of Ti-6Al-4V," Int. J. Fatigue, (in press).
6. Ruschau, J., University of Dayton Research Institute, Dayton, OH, unpublished data.

7. Hutson, A. and Nicholas, T., "Fretting Fatigue of Ti-6Al-4V Under Flat on Flat Contact," Int. J. Fatigue, (in press).
8. Lenets, Y.N. and Nicholas, T., "Load History Dependence of Fatigue Crack Growth Thresholds for a Ti-Alloy," Engineering Fracture Mechanics, 60, 1998, pp. 187-203.
9. Boyce, B.L., et al., "Thresholds for High-Cycle fatigue in a Turbine Engine Ti-6Al-4V Alloy, Int. J. Fatigue, (in press).
10. Ruschau, J.J., John, R., Thompson, S.R. and Nicholas, T., "Fatigue Crack Growth Rate Characteristics of Laser Shock Peened Titanium ASME J. Eng. Mat. Tech., (in press).

Cost benefit analysis for the use of better turbine materials and technology including predicted life improvements.

T J Williams BEng (Hons) CEng MIMechE

Turbine Systems - Engineering
Rolls-Royce plc
PO Box 3
Filton
Bristol BS34 7QE

ABSTRACT

The new materials and technologies being identified to give an improved engine product have a number of interacting effects. For example, a more advanced turbine blade cooling system may offer improved performance and/or life but may also increase the cost of each blade.

Life cycle cost methods are used in the aero engine industry to establish the overall operating cost for a particular engine / airframe combination. As the name implies the total cost of operation of the engine over its scheduled service life can be established.

This paper will demonstrate how the use of life cycle costing techniques at the early stage of life extension proposals can influence the design and lead to a more economic design solution. In the study the effect of initial costs (material and manufacture) were traded against performance and life improvement to optimise the most cost effective design. The results of the study have been used to identify what manufacturing cost reduction must be achieved to benefit fully from performance and life improvements during the overall life of the engine.

INTRODUCTION

Life Cycle Cost (LCC) can be defined as the total cost of acquisition and ownership of a system over its useful life. It includes the cost of development, acquisition, support and where applicable disposal. Figure 1.

The current methodology employed by Rolls-Royce in life cycle cost analysis has been developed over many years and is the product of a great deal of effort aimed at achieving customer performance and operational requirements, at minimum cost, in both civil and military engine applications. The LCC models used within Rolls-Royce are based upon industry standards as recommended in SAE ARP 4294.

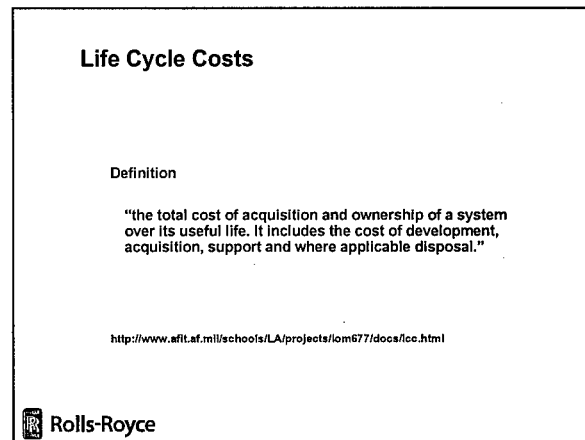


Figure 1. Definition of Life Cycle Costs

It has long been recognised that to be truly competitive in the global aerospace market it is essential to provide cost effective products. To meet this aim the company has sought to develop LCC methodologies to enable the following;

- 1) To respond to customer demands for information on costs associated with the purchase and most economic use of our products, either as a complete engine acquisition programme or a limited module / component improvement package.
- 2) To identify areas of technology development and engine design to give the optimum return in terms of increased marketability and reduced cost of ownership. Additionally the methodology used should help in the identification of design solutions to maximise Rolls-Royce profit potential. As has been mentioned previously the LCC methodology used must have sufficient range of applicability to be used across a wide range of study scenarios, from the sale of an existing engine/airframe combination to an existing customer, the assessment of cost of ownership issues of a component modification / enhancement through to the LCC analysis at the initial design stage of a new engine. In each case the content of the LCC study

and data available is different, maximum benefit is offered by the use of LCC techniques at the initial design stage.

In adopting a process of design to minimum LCC for a new engine project, the contributions of operational and support costs to overall LCC are evaluated. A trade off of component design parameters, life, performance, cost etc. is performed to establish the means of identifying the optimum balance between all contributing LCC elements for the achievement of design to minimum LCC. For example, a component's life improvement through the use of a more expensive material can be assessed against an increase in acquisition and higher replacement costs. In the same way the potential for improved engine performance and reduced fuel burn can be weighed against the cost increase associated with a design change and the effect of increased cycle temperature on component usage.

The highly complex interactions and variability of the large number of parameters that influence overall LCC makes the trade off comparison a difficult calculation. The major factors considered in the assessment are;

- 1) Cost of new and repaired parts fitted
- 2) Cost of labour associated with engine strip, overhaul and repair
- 3) Cost of fuel and other consumables used during operational service

To analyse maintenance material costs (MMC) and maintenance man hours (MMH) Rolls-Royce has developed a wide range of deterministic and probabilistic simulation models to assess the impact of, for example, component life, inspection rates overhaul periods and unit cost on the overall LCC. Examples of use include the successful development of maintenance policies to reduce the operating cost and to improve reliability and military and civil engines and the identification of the optimum design solutions for modifications to in-service products.

The intention behind the generation of these LCC models is based upon the development of a logical process linking design principals and overhaul / maintenance policy through to the generation of a cost breakdown and an understanding of the principal cost drivers of the design solution. The modelling is based upon an assumed mission usage profile, operating environment aircraft type etc., for the most accurate simulation this data has to be agreed with and clearly defined by the customer and is used to

proved additional data on component lifing, flying hours removal and overhaul time, etc. The models generate data on total labour and spares costs, engine removal rates and a forecast of the number of spare engine/modules investment requirements. The process of LCC simulation is improved by continual feedback of service experience data from the customer.

Within Rolls-Royce, experience has shown that the typical breakdown of military engines LCC is as shown in Figure 2 and is broadly similar to that for the industry as a whole, Figure 3.

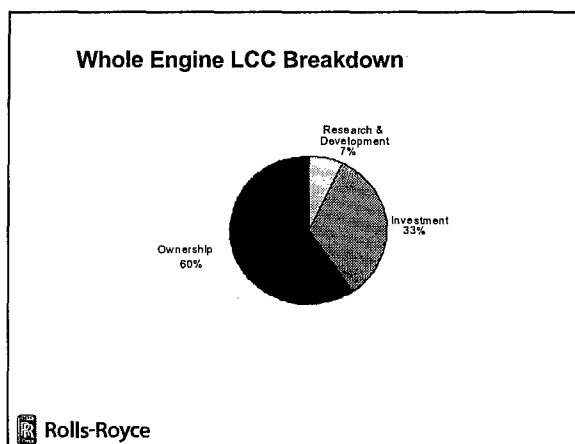


Figure 2. Breakdown of engine LCC.

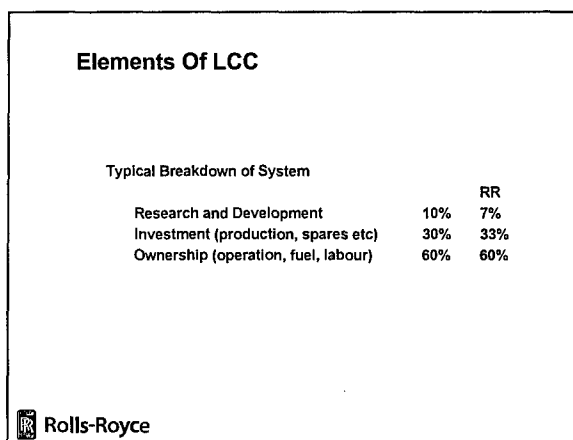


Figure 3. RR Vs Industry LCC breakdown

The data in Figures 2 & 3 indicates that if one were to undertake a study to optimise LCC then the best improvement should be achieved by addressing design features which have the highest influence on the cost of ownership. Exploring the data further it can be shown that within the category of ownership, fuel, oil and lubrication accounts for some 31% of the total LCC and replenishment spares 18%, Figure 4 & 5.

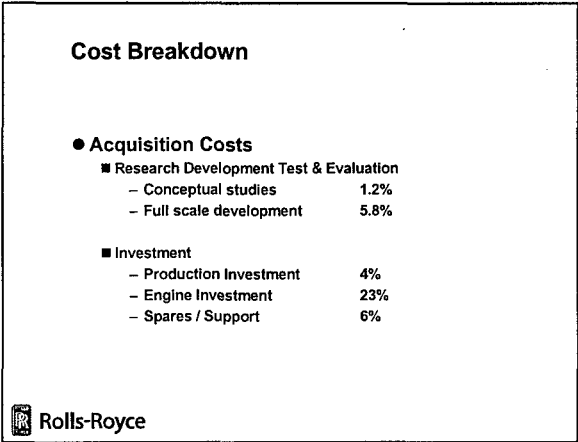


Figure 4. Breakdown of acquisition costs

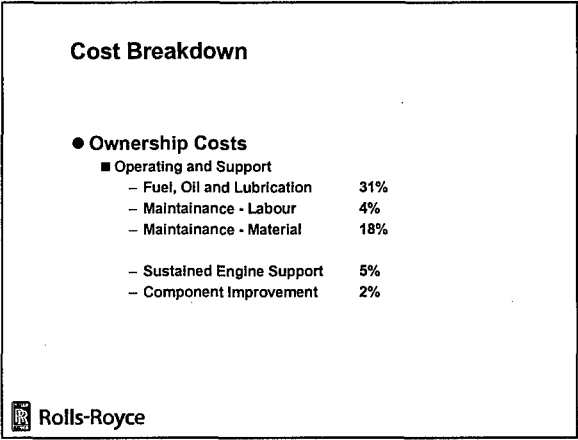


Figure 5. Breakdown of ownership costs

Based upon the data contained in Figures 4 & 5, the following design issues can be interpreted as design guides to produce a cost effective turbine design.

- 1) Low fuel burn
- 2) Increased life, minimises number of spares required and reduced labour costs
- 3) Low component cost

USE OF LCC AT INITIAL DESIGN STAGE

During the concept definition stage of a new Turbine blade design for an engine upgrade, an assessment of the cost benefit analysis, using LCC techniques has been completed. A typical HP turbine blade is shown in Figure 6.

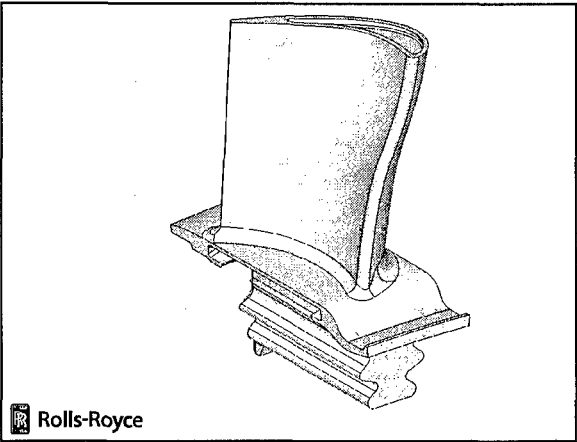


Figure 6. Typical HP Turbine Blade

The objective of the study was to explore the influence of various design options, e.g. component efficiency, material, cooling system and manufacturing process on the overall life cycle cost of the engine. It was anticipated that the results from the study would give a clear indication of the design style that should be incorporated in the full design, additionally the study could offer pointers to indicate future technologies and cost reduction strategies that should be explored to further reduce the engine LCC. The study was completed using a cross discipline approach incorporating engineers from the turbine, performance and commercial departments.

The initial design proposal considered was that for the growth engine a reduction in blade numbers should be incorporated to reduce unit cost. However, what needs to be understood from this strategy is,

'If we reduce the number of rotor blades, thus affecting cost, efficiency and cooling air - do we win on LCCs ?'

In addition to offering an understanding of the technology requirements to minimise LCC, any design solutions must also meet the Rolls-Royce commercial strategic objectives, which can be summarised as follows;

- 1 Rolls-Royce strives to be the industry leader in low cost of ownership. Reducing the number of blades per set will reduce the set cost and hence LCC.
- 2 Rolls-Royce wishes to reduce its product costs.
- 3 The objective of growing market share should be achieved based upon the argument that a lower LCC engine should attract more customers.

- 4 A reduction in blade numbers should translate into lower strip and rebuild times and less man-hours to repair and overhaul. This should contribute to the reduction in LCC as reduced Maintenance labour Costs
- 5 The order book, although potentially larger due to increased demand for a LCC optimised engine, may suffer due to lower spares orders as a result. However, the other objectives tend to override this.

The scenario investigated was based upon an existing simplified LCC model developed for a modern military airframe/engine combination. The investigation is based upon an assumed fleet of 250 aircraft flying approx. 355 hours per year over a 25-year period. The component life data used in the LCC model is based upon the lives that are broadly in line with those that modern military engines can achieve. For the turbine module, the current expectations would be approx. 1500 engine flying hours (EFH) for the blades (and other hot gas path components) and the remainder of the module around 3000 EFH.

To begin the process of design to LCC optimisation, the initial analysis completed in the study was aimed at gathering an understanding of the 'influence factors' for the main turbine design changes that were under consideration. The LCC model used was a simplified version of an existing whole engine LCC model, in that only the influence of turbine module components was included. For the sake of simplicity the model was based upon the cost of the turbine module, the maintenance cost of the module and the influence on total fuel burn of performance changes to the HP turbine blade.

These factors that were evaluated are as follows;

- 1) The effect of a 1% efficiency improvement
- 2) A 1% reduction in turbine blade cooling air usage
- 3) 10 % reduction in turbine blade set cost

Many of these proposed design changes may have an influence in direct opposition to each other, for example the proposed 10% reduction in turbine blade set cost could be achieved by a reduction in blade numbers, however this could lead to a decrease in

turbine efficiency and hence an increase in fuel burn rate. In this instance it is anticipated that this could be recovered by the use of technological improvements

e.g. high lift aerodynamics to recover aerodynamic performance.

During the design study an initial design objective was to increase the blade life by 25%, at the same time as designing a blade capable of operating at an SOT approximately 150° hotter than today's baseline engine. The requirement to increase blade life is based upon the fact that operating costs for the engine account for 60% of the overall LCC, of this 31% is attributed to fuel and lubrication and 22% to maintenance (spares and labour). From these figures, it is clear to see that a 25% increase in blade life will reduce the number of spare turbine components used during the engines operational life and as a result the labour costs will also reduce. However, the LCC analysis indicated that solely increasing the HP turbine blade life actually increased the overall operating cost of the engine. An investigation into this indicated that this would actually require more engine strips, as the overhaul period for the turbine blades would be out of sync with other components. This demonstrates that a component life increase is really only of benefit when combined with at least a whole module life increase, or a degree of harmonisation of inspection periods. However, in the overall interests of reducing engine LCC it is worth pursuing a strategy to generally increase the life of the engine. The effect of the influence factors on the overall engine LCC are as follows;

Change	Effect on Turbine Operating Costs
+1 % Turbine Efficiency	-0.86 %
-1 % Turbine cooling air usage	-0.5 %
-10 % blade set cost	-0.4 %

From the figures quoted above, it can be seen that from the "influences" studied, the most beneficial influence on the overall operating cost of the turbine module would be an increase in turbine efficiency. However there is in reality, very little to distinguish between the three options. We have already highlighted that we would like to reduce number of turbine blades, hence set cost decreases but the potential loss in turbine efficiency may offset this benefit. Another point worthy of note, is that the simplified nature of the model used does not take account the effect of turbine blade changes on other components e.g. a reduction in blade numbers should also reduce the cost of the disc, since fewer blades

will require fewer slots to be broached on the discs and cost should drop accordingly.

DESIGN FOR 25% INCREASE IN BLADE LIFE

The study continued with an evaluation of the effect on LCC of the available technologies that may be incorporated in the growth engine design to achieve the required life increase of the HP turbine blade. In order to increase the design life of the blade, there are several design changes that can be incorporated, typically these would involve a reduction in metal temperature, a change to an alternative material with better temperature capability or both. Unfortunately many of these changes are in direct opposition to the objective of cost reduction. In order to investigate the specific influence of design changes on LCC a study evaluating the influence of potential design solutions was undertaken.

COST REDUCTION TECHNOLOGY - REDUCTION IN BLADE NUMBERS

A prime objective of the growth engine study was to reduce both unit cost and parts count, in the turbine module this has been achieved by a reduction in blade numbers. To maintain low weight the axial width of the blade and disc rim cannot increase, hence each blade must generate a higher lift force. It was felt that a 15% reduction in blade numbers would be achievable, based upon recent rig test results and an improved understanding of aerodynamic performance through the use of computational fluid dynamic analysis of the turbine stage. The proposed reduction in blade numbers will also have an effect on the overall turbine blade cooling air utilisation since fewer blades will require less cooling air. The downside of a reduction in blade numbers is a potential decrease in turbine efficiency, although the use of high lift aerodynamics was proposed to recover component efficiency. In the study, the decrease in turbine efficiency has been included along with a corresponding increase in SOT.

TECHNOLOGIES TO INCREASE LIFE

There are several technologies that can be employed to increase the life of the blade, the following options were evaluated in the study;

- i) A reduction in metal temperature achieved by an increase in cooling flow.
- ii) The introduction of an advanced internal blade cooling system.

iii) Utilising the improved life capability of the more advanced blade alloy, CMSX-4.

iv) The application of a thermal barrier coating (TBC) to the blade to insulate the parent metal from the hot gas flow.

The relevant data for each of these changes was entered into the Rolls-Royce LCC programme to evaluate the overall effect. The matrix of design options that has been evaluated using the LCC program is as shown in Figure 7.

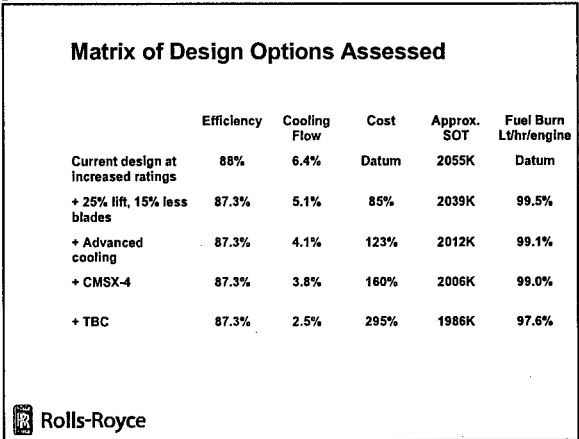


Figure 7

RESULTS

The LCC simulation was analysed for each of the design options quoted above; the results of the analysis are summarised in Figures 8 & 9.

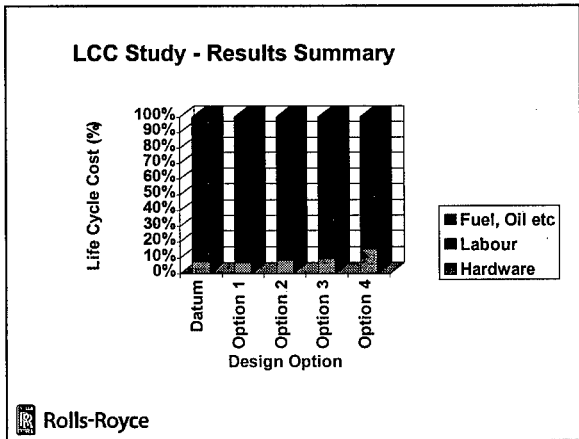


Figure 8

Evaluating the results it can be seen that the most beneficial solution in terms of LCC is the design incorporating a 15% reduction in blade numbers. Even with an assumed reduction in component efficiency, a lower overall LCC is achieved by virtue

of the lower initial blade set cost and a reduction in cooling air used, due to the reduced number of blades that need cooling.

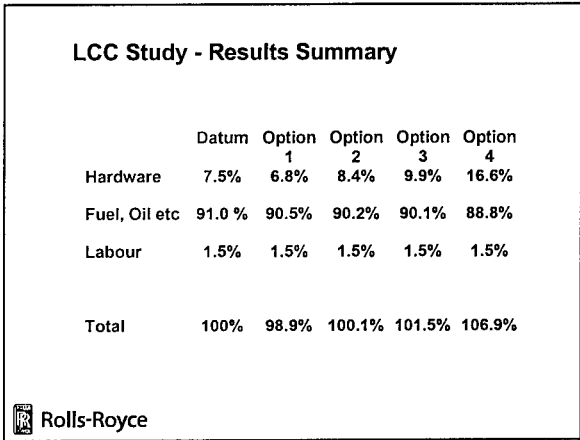


Figure 9

However, the choice of an optimum solution is not clear cut and cannot be based solely on the basis of LCC figures alone. The prime objective of the engine being designed must be the capability to fulfil its operational requirements. A design solution can only be truly optimised on a LCC basis if range and payload requirements are also considered. Bearing this in mind though, the results do indicate that the optimum design solution does indeed offer an improvement over the current datum design and as such would contribute towards improved overall weapons system performance. The results of the other options studied, whilst not actually demonstrating a reduced LCC, do give a pointer to cost reductions that should be pursued to further reduce LCC. The study indicates that options incorporating an advanced cooling system and the application of a TBC coating offers the best overall fuel burn rate, but the costs are too high. If it were possible to reduce the cost of this option 4 closer to that of the other options, then we would make significant contribution towards the reduction in overall LCC. The figures indicate that a potential

saving of some £M24,9 could be achieved over the overall life of the fleet. Target costs for these new technologies can be set in order to achieve an overall saving in LCC. This clearly feeds into the technology acquisition programme to set the standards for affordability as well as performance. This approach has proved to be very successful, particularly with thermal barrier coatings, the cost of which has been driven down over the last few years since the study was undertaken, to make their application a far more commercially viable option.

CONCLUSIONS

For the growth engine being evaluated in the study, a reduction in turbine operating cost is achieved by increasing the life capability of the blade. However, the increase in life cannot be achieved without the utilisation of a combination of several advanced technologies, many of which have contradicting influences on LCC. For a blade of a given life, the most beneficial effect on LCC is achieved by technologies that directly reduce the engine fuel burn rate, remember fuel and oil costs directly account for some 30% of the total LCC. If this can be achieve at a reduced cost, spares etc. are 18%, then a significant reduction in LCC is possible.

In the study completed, the design solution giving the best LCC reduction is that with a reduced blade count and a corresponding reduction in blade cooling air. The solution identified incorporating an advanced cooling system and the application of a thermal barrier coating, offers the best reduction in fuel burn, but is unattractive from a LCC viewpoint because of the high cost of manufacture and repair of the blade. LCC has been used to generate cost targets for these technologies to ensure that their affordability and performance will yield a benefit to the customer. The figures quoted in this study are based upon 1995 cost estimates. Since the study was completed, the cost of TBC application has dropped significantly such that today the use of TBC looks to be a far more attractive proposition.

Low friction diamond-like carbon coatings for engine applications

Mr. J. Smeets
VITO
Boeretang 200
B-2400 MOL, Belgium



NATO RTA-AVT WORKSHOP ON QUALIFICATION OF LIFE
EXTENSION SCHEMES FOR ENGINE COMPONENTS

Low Friction Diamond-like Carbon Coatings for Engine Applications

J. Smeets
Materials Technology



Coating types

- Pure diamond-like carbon (DLC): a-C:H
- Doped diamond-Like carbon: a-C:H:Si, a-C:H:F, a-C:H/a-Si:O (Dylyn®)
- Gradient and multilayer coatings



Deposition methods

Vapour-based deposition technology:

- vacuum technology
- Physical Vapour Deposition (PVD): starting from solids
- Chemical Vapour Deposition (CVD): starting from gases
- flux of radicals and ions to the substrate
- Ion flux/ion energy determines film properties

VITO ⇒ plasma-assisted CVD (PACVD)



Plasma-assisted CVD (PACVD)

- starting from hydrocarbon precursor (gases, liquids)
- plasma generation by r.f. or pulsed d.c. discharge
- conducting or insulating substrates
- deposition temperature < 200°C
- no line-of-sight deposition: complex part coating possible
- plasma etching before coating
- typical thickness 2-3 µm
- deposition rate 1-3 µm/hr
- high deposition rates using ICP-plasma



Coating properties

Diamond-like carbon (DLC, a-C:H)

- high hardness (20-25 GPa)
- high elasticity (Young's modulus 150-200 GPa)
- low coefficient of friction (0.05 ± 0.15)
- high wear resistance (< 10⁻⁷ mm³/Nm in ball-on-disk test)
- wear resistance of counterbody
- amorphous and conformal coating
- chemical inertness
- max. working temperature 300 °C
- low surface energy (40-50 mN/m)
- contact angle of water 60-70°
- highly IR transparent, UV opaque
- low deposition temperature ⇒ adhesion (use of interlayers)



Coating properties

a-Si:C:H, a-C:H/a-Si:O(Dylyn®)

- reduction of internal stress ⇒ adhesion improvement
- working temperature up to 400°C
- lower coefficient of friction (0.05-0.1)
- coefficient of friction independent of air humidity
- hardness 12-17 GPa
- wear factor 2-40 x 10⁻⁷ mm³/Nm
- surface energy 20-30 mN/m
- contact angle of water 90-95°
- higher transparency for visible light



Possible applications

- protective coatings on optical components
- protective coatings on magnetic and electronic components
- tribological parts (wear resistance, low friction)
- protective coatings in aggressive chemical environments
- biomedical applications
- electronic applications
-

DATE: 1994-01-10 10:00:00

0.000



Applications

Optical applications: scratch resistant coatings

- laser bar code scanners
- sun glasses
- polycarbonate substrates (e.g. ophthalmic lenses)
- IR components

Non-sticking applications: wear resistant release coatings

- plastic injection moulds
- Al forming tools
- compressing tools (e.g. pharmaceuticals)
- food and medical tooling

DATE: 1994-01-10 10:00:00

0.000



Applications

Tribological applications: dry running, self-lubricant coatings for wear protection of machine components

- shafts, bearings, ...
- moving mould parts

Abrasion resistance

- textile machinery components

Corrosion resistance

Barrier coatings

DATE: 1994-01-10 10:00:00

0.000



Applications

Cold forming (dry) of ferro and non-ferro metals

- reduction of cold welding combined with low friction (even dry)
- moulds for production of cans
- moulds for dry forming of Al-parts

Medical applications :

- non-sticking coatings on surgical tools and knives
- biocompatible coatings on implants

Electronic applications :

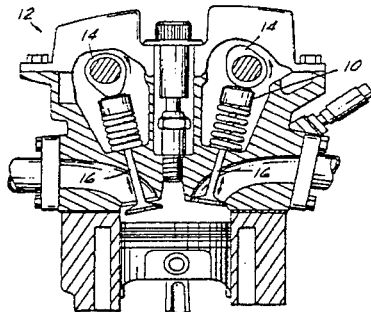
- wear resistant coatings for data storage media
- high dielectric strength coatings
- electromechanical contacts with tunable resistivity

DATE: 1994-01-10 10:00:00

0.000



Powertrain Components

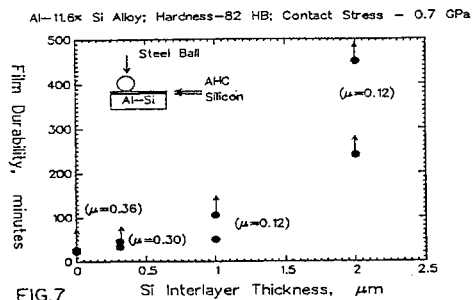


DATE: 1994-01-10 10:00:00

0.000



Powertrain Components



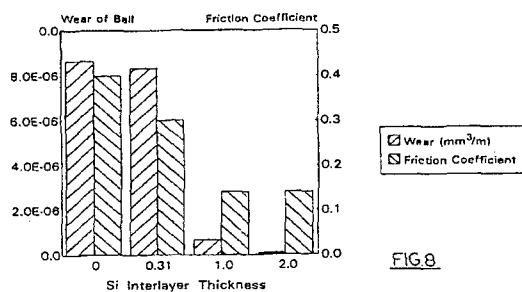
DATE: 1994-01-10 10:00:00

0.000

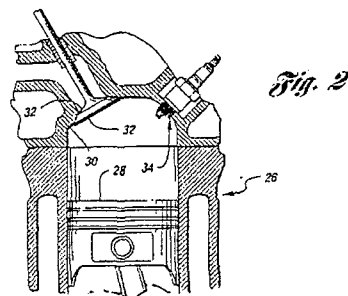


Powertrain Components

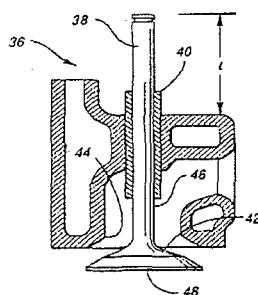
Friction and Wear of Steel Ball Sliding Against AHC on Al-Si Alloy with Si Interlayer



Carbonaceous deposit-resistant coating



Carbonaceous deposit-resistant coating



Conclusions

Diamond-like carbon coatings display:

- high hardness
- high wear resistance
- high elasticity
- low friction

Surface energy (wettability) can be tuned

Engine applications:

- power train components
- gear boxes, transmission systems
- preventing carbonaceous-deposits

Limited working temperature

Life Extension of IN706 Type Disc Materials by Surface Modification with Boron

J. Rösler

S. Müller

Technische Universität Braunschweig

Institut für Werkstoffe

D-38106 Braunschweig, Langer Kamp 8, Germany

SUMMARY

A novel process is described which is capable of protecting Ni-base superalloys against stress accelerated grain boundary oxidation by chemical modification of a surface zone with boron. The potential of the proposed technique in extending the lifetime of wrought Ni-base alloys is discussed performing creep crack growth, constant strain rate and LCF experiments at 600°C and 700°C. Significant life extension under static loading conditions is demonstrated. Under cyclic loading, care has to be taken to avoid brittle boride layers on the component surface to make full use of the protective effect against SAGBO.

1. INTRODUCTION

In order to fulfill future thrust and efficiency requirements, aeroengine components are subjected to ever increasing temperatures. In addition to design improvements, advanced material solutions are therefore needed for critical engine parts. Discs are one example. Today, typical service temperatures are around 650°C with increasing demand for temperatures beyond 700°C. One challenge is to meet the conflicting requirements between rim and bore. While yield- and LCF strength at moderate temperatures are key requirements for the bore, creep strength and crack growth resistance at high temperatures are needed at the rim. Because Ni-base disc materials show the so-called SAGBO (= stress accelerated grain boundary oxidation) phenomenon, insufficient resistance against crack propagation at elevated temperatures is one of the main hurdles to overcome.

An intriguing effect of SAGBO is the acceleration of the crack propagation rate by up to two orders of magnitude in air relative to vacuum environment /1-3/. It is associated with the embrittlement of grain boundaries by oxygen in the presence of tensile stresses /4,5/. A number of approaches have been proposed to alleviate the environmental effect. The most important are enlargement of the grain size /1,6/ and overaging of the microstructure /2, 7/. However, it is clear that these measures adversely affect other important properties such as ambient temperature yield and fatigue strength. One potential solution is the fabrication of so-called dual alloy discs comprised of two individual parts /8/. Due to the complicated manufacturing process, this procedure is however expensive which, in today's world, is an important factor to be considered.

One cause for the sensitivity of wrought Ni-base alloys to SAGBO is that highly segregating elements such as boron or zirconium have been reduced to very low levels for improved forgeability and weldability /9/. It is well known, on the other hand, that these elements act as grain boundary strengtheners and are capable of improving the elevated temperature crack growth resistance /10/. Based on this knowledge, a new approach is presented here which reconciles the requirements on manufacturability and mechanical performance. Because

crack growth resistance is of concern at the rim surface where high temperatures and the environment are present simultaneously, the basic idea is to increase the content of grain boundary strengthening elements locally by a deposition and heat treatment process after manufacturing of the turbine disc /11/. As a result, chemically exposed grain boundaries can be chemically modified for improved resistance against SAGBO. In this paper the details of this novel process are described and its effect on elevated temperature performance is discussed.

2. EXPERIMENTAL TECHNIQUES

2.1 Test Material and Metallography

INCONEL 706 has been selected as base material for this study. It is a typical representative of wrought Ni-base superalloys and similar to INCONEL 718 which is more widely used in aeroengine applications. The chemical composition is given in Table 1.

Table 1: Chemical Composition of IN 706 (in wt.-%).

Element	Ni	Cr	Nb	Al	Ti
wt.-%	41.5	16.0	2.9	0.2	1.8
Element	Si	C	B	Fe	
wt.-%	0.05	0.01	0.003	bal.	

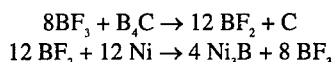
Test material was supplied by Inco Alloys International Inc. and ABB Power Generation. A standard heat treatment involving 1000°C/2 h/AC solutioning and two-step 720°C/8 h (cooling rate: 1 K/min), 620°C/8 h/AC precipitation heat treatment was used. An ASTM 3 grain size was obtained after heat treatment.

For metallographic examination, the specimen were polished mechanically and etched with a mixture of 100 ml HCl, 10 ml HNO₃, 0.3 ml Sparbeize (tradename of Wirtz-Buehler GmbH Düsseldorf, Germany) and 100 ml H₂O at a temperature of 40°C. The boron concentration profile was measured quantitatively by glow discharge optical spectroscopy (GDOS). Surface layers of approx. 20 µm thickness were removed by grinding after each measurement to gain adequate depth resolution.

2.2 Surface modification

As boron is probably the most powerful grain boundary strengthener and a fast diffusing element in nickel, it was decided to chemically modify the surface zone in this study with boron. Amongst the large number of potential boron deposition processes, boronizing in a boron containing powder pack was selected. This method is widely used for producing wear resistant coatings on steels /13/. Recently a powder was developed for boronizing nickel based superalloys /14/ which was used in this study. Finished tensile test specimens were packed in a box and completely covered

with powder. The pack was heat treated at 850°C/3 h in argon atmosphere. The basic reaction sequence is as follows:



After boron deposition, the test specimens were removed from the powder pack and diffusion heat treated at 1000°C for 0.5 h. Because of the solutioning effect of this heat treatment, the standard precipitation heat treatment was repeated afterwards.

2.3 Mechanical testing

Three types of tests and test specimen were used. 1" CT specimen according to ASTM 1457 with 2.5 mm deep side grooves were taken to determine the creep crack growth resistance at T=600°C and 700°C. The specimen were machined from a forged pancake such that the crack propagates in the tangential plane in radial direction (LR orientation). A fatigue pre-crack was introduced at room temperature. Crack propagation was monitored by a DC potential drop technique. Johnson's formula according to ASTM 1457 was used to convert the monitored potential into crack length. All tests were performed under load control in an electromechanical testing machine (Walter und Bai AG, Switzerland) using resistance heating. The temperature was controlled to $\pm 1^\circ\text{C}$ by thermocouples which were directly mounted at the specimen.

For constant strain rate (CSR) testing, smooth tensile test samples of diameter $d = 8$ mm and 25 mm gage length have been machined from IN706 sheets with the specimen axis oriented perpendicular to the rolling direction. Testing was performed under strain rate control in a MTS servohydraulic testing machine at 600°C using induction heating. A strain rate of $d\epsilon/dt = 5 \cdot 10^{-4} \text{ s}^{-1}$ was selected for all tests. The temperature was controlled to an accuracy of $\pm 2^\circ\text{C}$ within the gage section.

Identical test specimen as for CSR testing were used for investigation of the LCF behaviour. All tests were performed under strain control with $\Delta\epsilon = 1\%$, $R=0$, $T=600^\circ\text{C}$ and 0.05 Hz. As shown in Table 2, two specimen each were tested for the following material conditions: unmodified IN706 (group A), boronized IN706 with hard boride layer (group B) and boronized IN706 with chemically removed boride layer (group C). All specimen were ground with 400 mesh grinding paper to obtain identical surface roughness of approx. $1.5 \mu\text{m}$.

Table 2: Overview of material conditions for LCF testing.

	Condition	Remarks
Group A	unmodified	
	unmodified	
Group B	boronized with hard boride layer	
	boronized with hard boride layer	
Group C	boronized without boride layer	Boride layer and parts of diffusion zone removed
	boronized without boride layer	Boride layer removed

3. MICROSTRUCTURE

The microstructure of the modified surface zone after boron deposition and diffusion heat treatment is shown in Fig. 1. Clearly visible are the boride layer (thickness $\approx 35 \mu\text{m}$), a matrix zone containing boride precipitates and the metallographically unmodified matrix. The boride layer itself contains different boride types. According to /15/ the outermost layer is a Fe-rich boride in which Ni-rich borides are embedded. It is followed by a Ni-rich boride layer in which Cr-rich and Fe-rich borides are embedded.

It is important to note, that the outer boride layer is a by-product which is not essential here. In fact, as shown below, the boride layer should be mechanically removed or avoided by further process optimization as it can impede the fatigue performance due to its brittleness. Of key importance here is the boron enriched matrix. The boron concentration profile after diffusion heat treatment has been measured by glow discharge optical spectroscopy in /15/ and is reproduced in Fig. 2. Considering the initial IN706 concentration of 30 ppm boron, the boron modified surface zone is approx. $150 \mu\text{m}$ deep. It by far exceeds the depth of the Ni-matrix containing boride precipitates (compare with Fig. 1).

4. MECHANICAL BEHAVIOR

In Fig. 3, the results of the creep crack growth measurements are summarized. They illustrate two important points. Comparing the 600°C and 700°C data, a strong temperature dependence of the crack growth resistance is apparent. If the rim temperature of a gas turbine discs were to be increased by 100°C, an acceleration of the crack growth rate by more than one order of magnitude would result. It is also evident that crack propagation is very fast at moderate stress intensities. For $K=20 \text{ MPa}\sqrt{\text{m}}$ the crack advance is about 5 mm per hour at 700°C. In other words, a hold time of 12 minutes would be sufficient to propagate the crack by one millimeter. No incubation time for crack growth was observed. Also included in Fig. 3 is a data point from /12/ which is in good agreement with the measurements presented here. Both observations clearly demonstrate the need for improved material performance especially if component temperatures are to be further increased.

In addition, CSR tests were performed. It is known that this type of test is a sensitive means to establish the resistance of Ni-base superalloys against SAGBO /12/, because two important conditions are met for the SAGBO mechanism to take place: (i) compared to long time creep tests, a relatively high tensile stress is built up which promotes stress assisted grain boundary oxidation; (ii) compared to common tensile tests, the test duration is long enough for oxygen diffusion to occur. A further advantage of CSR testing is that it is easy to compare virgin with surface modified material.

In Fig. 4, the test results are summarized for unmodified and boronized samples. The environmental attack is reflected in poor ductility values of the unmodified specimen below 1% (see also Table 3) compared to a room temperature ductility of approx. 20%. Prior to fracture, the tensile stress drops sharply within one hour (total test duration: 20 h) from approx. 800 MPa to less than 300 MPa indicating a continuous reduction of the load carrying cross section by creep crack growth. Hence, about 95% of the lifetime is consumed by crack initiation.

Table 3: Yield strength $R_{p0.2}$, time to fracture t_f and plastic fracture elongation ϵ_f obtained after CSR testing at $T = 600^\circ\text{C}$ and $d\epsilon/dt = 5 \cdot 10^{-4} \text{ h}^{-1}$.

Specimen No.	Treatment	$R_{p0.2}$ [MPa]	t_f [h]	ϵ_f [%]
1	unboronized	820	22.2	0.55
2	unboronized	790	20.5	0.42
3	boronized	780	76.6	3.3
4	boronized	790	78.8	3.6

Also plotted in Fig. 4 are results for the boronized samples exhibiting drastically improved ductility values. The life extension by about a factor four clearly stems from the surface modified zone which is capable of protecting the base material from environmental attack. Interestingly, a similar stress drop within the last hour of the tests is noted as with the unmodified material. At this point, the surface zone must have been damaged to such an extent that environmentally assisted crack growth of the unprotected base metal could take place as discussed above.

Under LCF loading (Fig. 5) the situation is less clear. While the boronized samples containing a hard boride layer (group B) are inferior to the unmodified material (group A), a significant life extension is noted for the boronized samples with removed boride layer (group C). This demonstrates on the one hand the detrimental effect of the boride layer as site for early crack initiation. The fact that the cyclic life of group C is significantly longer than that of group A shows, on the other hand, that SAGBO is playing a role even under LCF loading conditions and that significant life extension can be gained through the proposed surface modification provided the outer boride layer is avoided or removed.

5. FRACTOGRAPHY

In Fig. 6 the fracture surfaces after CSR-testing of unmodified material are shown. The intergranular fracture mode clearly shows that grain boundaries are the weakest link in the microstructure under the test conditions selected here, which is in line with the view that SAGBO is the cause for accelerated crack propagation. Fracture surfaces of the creep crack growth specimen show exactly the same brittle, intergranular fracture morphology independent of the applied stress intensity factor.

In contrast, a markedly different fracture morphology is observed for the boronized samples (Fig. 7). Within a surface zone of approx. 150 μm , a ductile, transgranular fracture mode is apparent which is followed by intergranular fracture as discussed above. According to Fig. 2, the depth of the ductile fracture zone corresponds well with the depth of the boron enriched zone. The results show that boron is effective in preventing grain boundary embrittlement at elevated temperatures and that concentrations of approx. 100 ppm are sufficient to cause this effect. It may be speculated that occupation of interstitial grain boundary sites by boron hinders oxygen diffusion along grain boundaries thus grain boundary weakening is prevented.

In the transgranular fracture zone two different surface structures are distinguishable. Directly behind the boride layer the fracture appearance is featureless. Shear lips are not visible. According to Fig. 2, this area is correlated to relatively high boron concentrations in excess of about 500 ppm. In the following area, shear lips and a honeycomb-like structure appear indicating a more ductile fracture mode. This zone is

related to the matrix volume having only a slight boron enrichment. Also visible in Fig. 7 is the outer boride layer of approx. 35 μm thickness which fractures brittle due to its hardness.

A typical fracture surface after LCF testing is shown in Fig. 8. Compared with Figs. 6,7, a mixed fracture mode is noted. In the areas exhibiting transcrystalline fracture, striations are visible. These differences are a consequence of the cyclic loading and the shorter test duration compared to the CSR-tests. However, the presence of areas with intercrystalline fracture demonstrates that SAGBO still plays a role under LCF loading. Hence, it is logical that an improved cyclic lifetime was observed for group C test specimen compared to group A specimen.

6. CONCLUSION

The results of the mechanical tests and the metallographic investigations reveal two important points. First, it is confirmed that boron effectively protects grain boundaries against SAGBO. Small quantities of about 100 ppm appear to be sufficient to cause this effect. Secondly, it shows that modification of the grain boundary chemistry in a relatively narrow surface layer is a viable means to extend the lifetime of Ni-base disc alloys at elevated temperatures. Under uniaxial loading, relatively large plastic strains of several percent are needed before the boron enriched matrix zone is damaged to such an extent that oxygen can penetrate the unmodified material. At that point, however, oxygen accelerated creep crack propagation commences as in the unmodified material leading to rapid failure of the specimen. Because the outer boride layer fails in a brittle fashion upon loading, it does not protect against the environment and is, therefore, not responsible for the beneficial effect observed here.

Also under fatigue loading significant life extension can be expected, especially when extended hold times are involved. However, under these loading conditions special care must be taken to avoid the outer boride layer, for example by chemical or mechanical removal. A probably more practical solution is the selection of processing parameters such that the boride layer is avoided or dissolved during diffusion heat treatment. Options are to lower the boronizing time and temperature, reduce the boron activity of the powder pack or increase temperature and time of the diffusion cycle. These possibilities are currently under further investigation.

ACKNOWLEDGEMENT

The authors would like to thank Daniel H. Yates of INCO Alloys International Inc. (USA) and ABB Power Generation Ltd. for providing IN706 test material and Dr. H.-J. Hunger from Elektroschmelzwerk Kempten, Werk Greifath (Germany) for boronizing the samples.

REFERENCES

- /1/ J.P. Pedron and A. Pineau, *Mater. Sci. Engr.* **56**, 143 (1982).
- /2/ K. Sadananda and P. Shahinian, *Metal Science* **15**, 425 (1981).
- /3/ R. Molins, J.-C. Chassaigne and E. Andrieu, in "Superalloys 718, 625, 706 and various derivatives, E.A. Loria (eds.), TMS, 655 (1997).
- /4/ E. Andrieu, G. Hochstetter, R. Molins and A. Pineau, in "Superalloys 718, 625, 706 and various derivatives, E.A. Loria (eds.), TMS, 619 (1994).
- /5/ D.A. Woodford and R.H. Bricknell, *Met. Trans.* **12A**, 1467 (1981).
- /6/ S. Floreen, *Met. Trans.* **6A**, 1741 (1975).
- /7/ A.F. Koul, P. Au, N. Bellinger, R. Thamburaj, W. Wallace and J.-DP. Immarigeon, in "Superalloys 1988", S. Reichman et al (eds.), TMS, 3 (1988).
- /8/ D.P. Mourer, E. Raymond, S. Ganesh and J. Hyzak, in "Superalloys 1996", p. 637, The Minerals, Metals & Materials Society, Warrendale (1996).
- /9/ D.F. Smith and J.S. Smith, in "Physical Metallurgy of Controlled Expansion Invar-Type Alloys", KC. Russell and D.F. Smith (eds.), TMS, 253 (1990).
- /10/ S. Floreen and J.M. Davidson, *Met. Trans.* **14A**, 895 (1983).
- /11/ J. Rösler and S. Müller, European Patent Application, EP 97/03728.
- /12/ G. Härkegard, W. Balbach, K. Stärk and J. Rösler, in "Superalloys 718, 625, 706 and various derivatives," E.A. Loria (ed.), p. 425, The Minerals, Metals & Materials Society, Warrendale (1997).
- /13/ H.-J. Hunger and G. Trute, *Heat Treatment of Metals* **21**, 31 (1994).
- /14/ H.-J. Hunger, *Mat. Sci. Forum* **163**, 341 (1994).
- /15/ J. Rösler and S. Müller, to be published

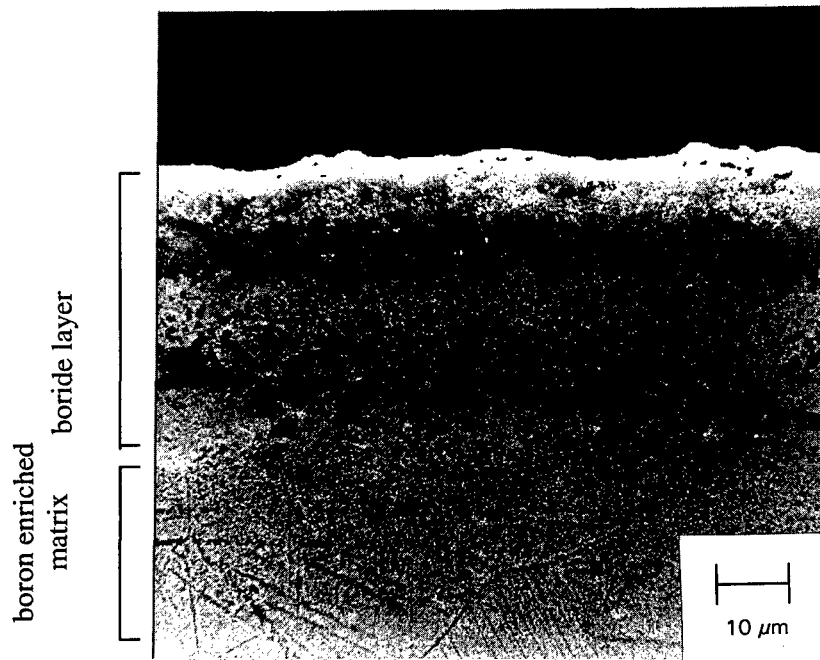


Fig. 1: Microstructure of the modified surface zone after boronizing and diffusion heat treatment (SEM - secondary electron image).

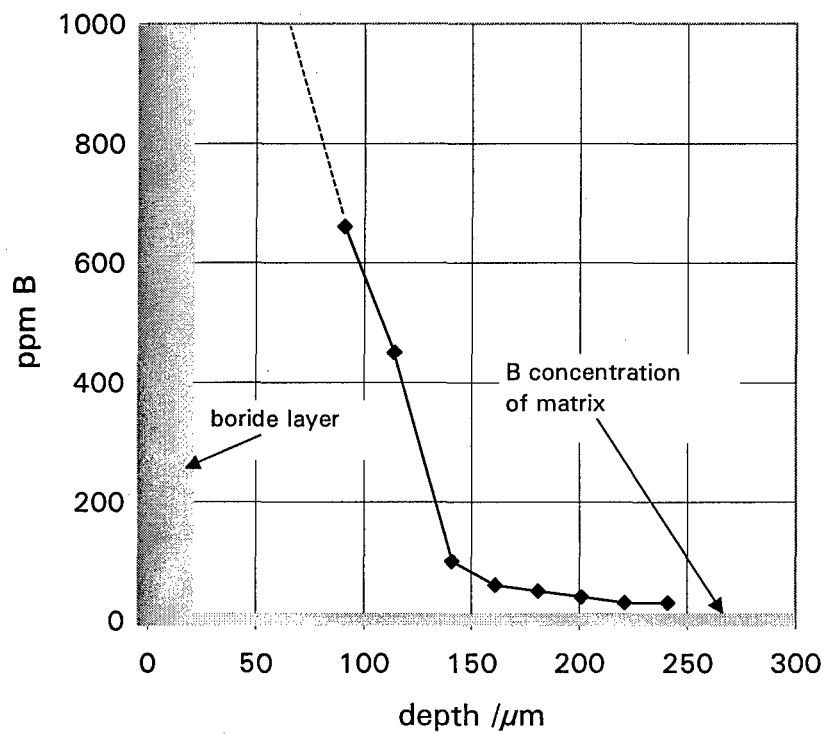


Fig. 2: Boron diffusion profiles behind the boride layer after diffusion heat treatment as measured by GDOS.

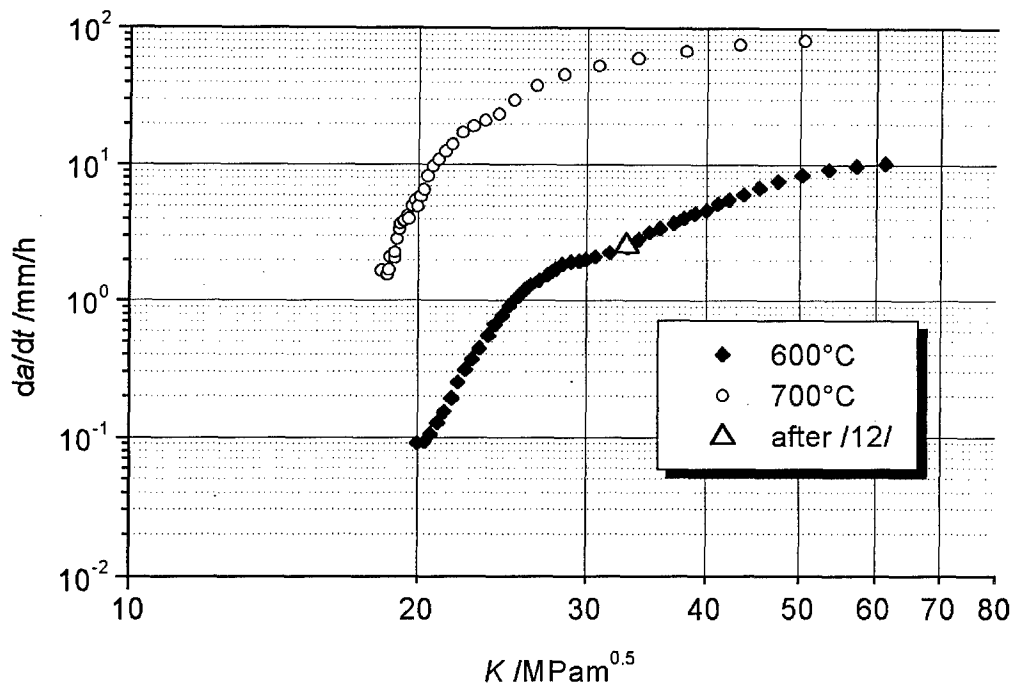


Fig 3: Creep crack growth rates of 1" CT specimen at 600 and 700°C.

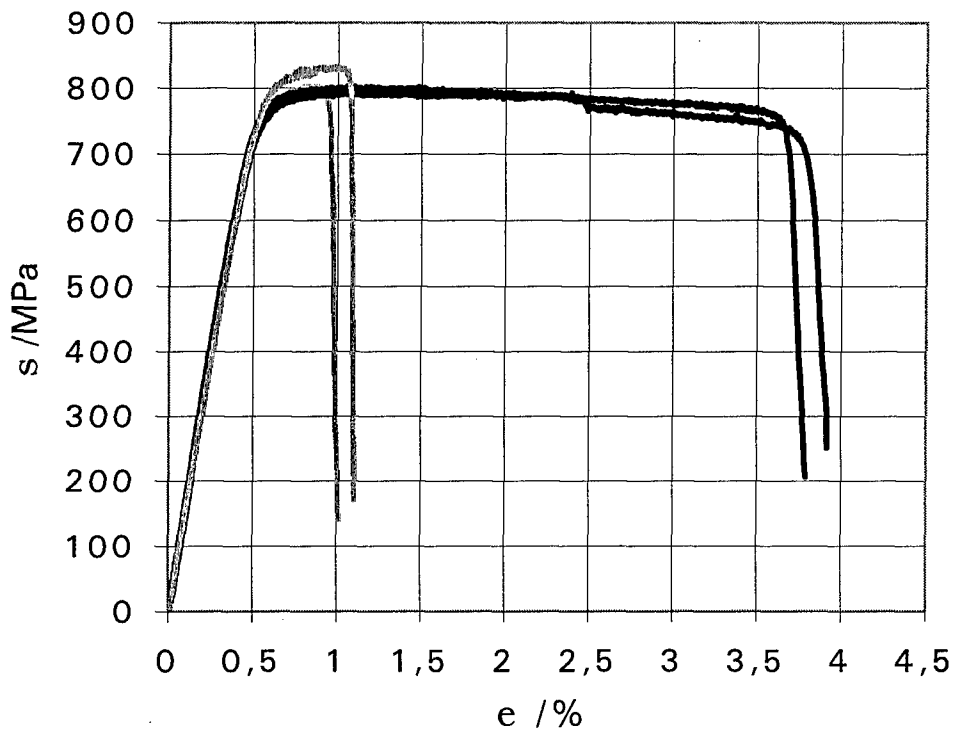


Fig. 4: Stress-strain diagram of the constant strain rate tests (grey curves: unmodified specimen, black curves: boronized specimen).

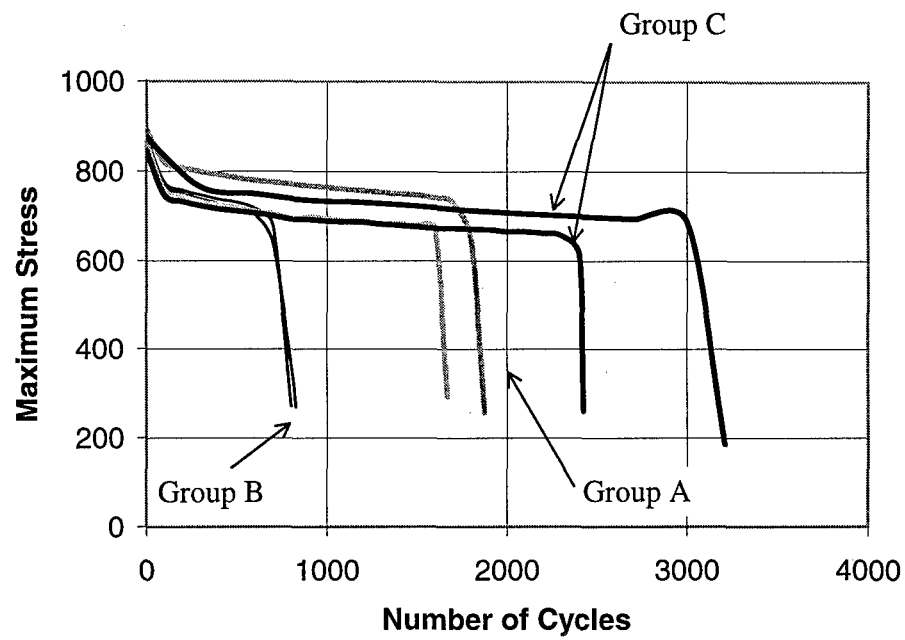


Fig. 5: Maximum stress measured vs. number of cycles for the different material conditions as shown in Table 2).

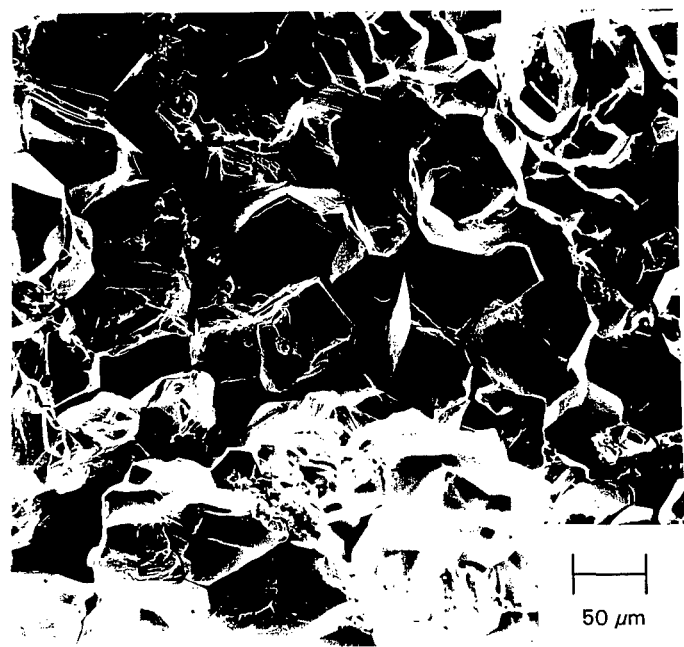


Fig. 6: Intergranular fracture surface after constant strain rate testing (SEM).

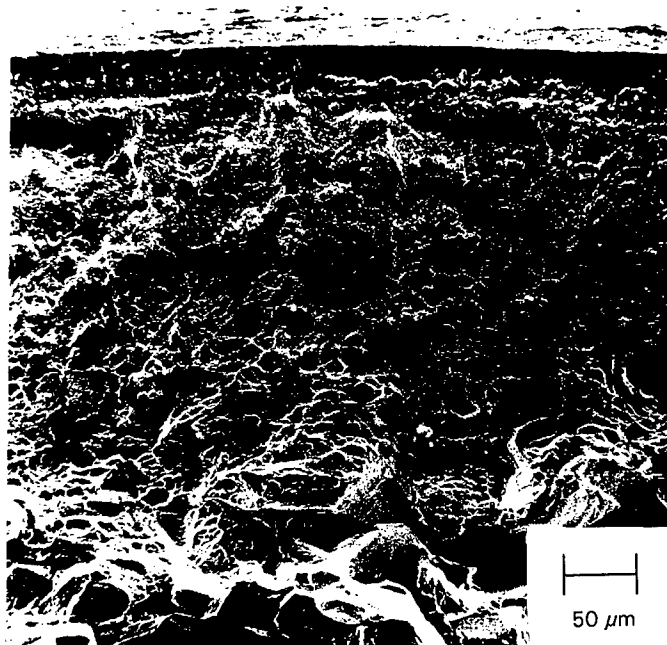


Fig. 7: Fracture surface of a boronized specimen after constant strain rate testing (SEM).

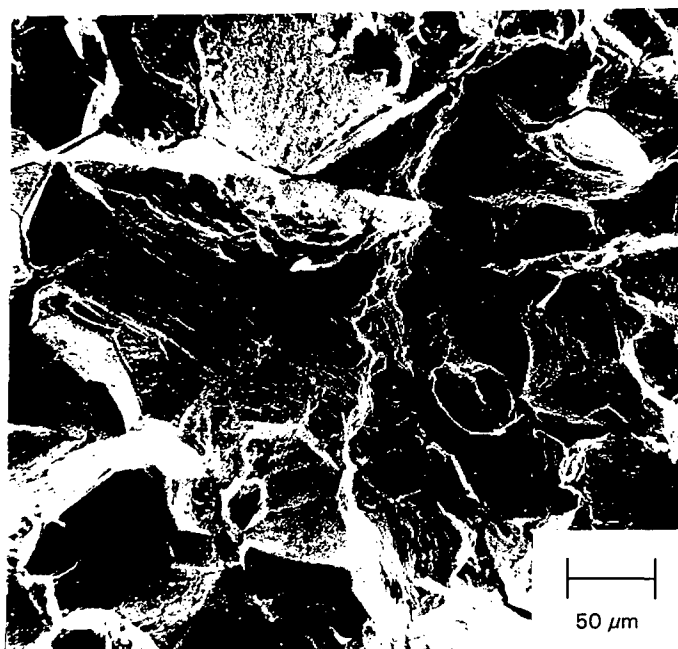


Fig 8: Fracture surface after LCF testing. A mixed fracture mode and striations are visible (SEM).

TBC AND OTHER SURFACE COATINGS; BENEFITS AND LIFING PROCEDURES

D L Shaw
Rolls Royce plc
P.O. Box 3, Filton
Bristol BS34 7QE, UK

SUMMARY

For the past two decades, thermal barrier coatings have offered the promise of increased turbine capability in terms of increased temperature or reduced cooling flows. They have also held out the promise of life extension to existing hot end components by offering simple solutions to localised cooling problems. These goals have remained tantalisingly unattainable. That their potential is now within reach, is largely a result of the development of successful lifing methodologies. These lifing methodologies have identified the significant design parameters and enabled the development of process parameters that have ensured the survival of the coating for acceptable life attainment on both new and refurbished components.

The lifing methodologies have highlighted the significance of the bond coat in ensuring coating integrity in terms of cracking, spallation and cyclic behaviour.

INTRODUCTION

This paper describes the methodologies developed for TBC lifing at Rolls Royce plc, and their validation against engine demonstrator programmes which have been the basis of qualification for service usage. Prediction of cracking made before engine running have proved to be 95% accurate on HP turbine rotor blades.

Thermal barrier coatings, (TBCs) have been around for many years, waiting to be used to provide an initial design capability, or an extension of existing operational capability.

On occasions, they have worked very successfully and a significant improvement in hot end life has been achieved. On other occasions they have not worked nearly as well, and only minor, if any, improvement has been seen.

In some instances, the coating has failed through some unforeseen phenomenon. Indeed, it has not been unusual for the coating to crack or spall during the application process or when the components are in stores awaiting fitment.

The introduction of TBCs as a recognised and reliable design capability has not been helped by the multiplicity of coating systems, including bond coats and ceramic layer coatings that have abounded.

Initially a 'scatter gun' approach was used as manufacturers sought to cash in the advantages that were so tantalisingly on offer.

Not only has there been a wide variety of combinations and proportions of constituent elements for bond and barrier coatings, but the means of application and the process parameters employed have been manifold.

This 'haphazard' approach to TBC process has compounded the difficulty in establishing a coherent approach to development and usage with any degree of certainty of a significant result.

Very often the reason for failure or lack of success, either during the coating process or in engine operation, has not been understood. Attempts to remedy defects have often resulted in other failure modes being activated. The result was that success in one application was not transferable to other applications with any degree of certainty.

This has meant that to qualify a particular TBC system on a particular component in a particular operating environment has require an extensive programme of coating determination. This has to be followed by laboratory testing and finally engine service trials.

These programmes have offered no prior guarantee of success, and, the more successful the coating system proved to be, the longer the testing required to fully demonstrate it. It would take even longer to be able to claim across the board the life improvements demonstrated by a single test.

The key to understanding, and therefore being able to predict, both process and operational capabilities has come about with the understanding of the failure modes and mechanisms associated with a TBC system. This understanding will need to encompass the way that it is produced and the constituents that it may have.

TBC DEVELOPMENT

Before understanding the failure modes and mechanisms of TBC systems, it is necessary to realise what it is that constitutes a TBC system, and

the process and compositional options that are generally available.

A thermal barrier coating system basically consists of one or more coating layers whose main purpose is to protect the substrate material from the main gas stream temperature. This it does by acting as a low thermal conductivity layer, reducing the substrate temperature during steady state operation. In order for this to be effective, there must be a temperature gradient set up between the hotter gas washed surface and the inner cooler substrate surface. This is usually brought about by the use of cooling air directed across the inner substrate surface during steady state operation as shown in figure 1. During transient operation the thermal inertia of the thermal barrier coating system itself can significantly improve the life of an uncooled component by reducing the thermal gradients that would otherwise be there.

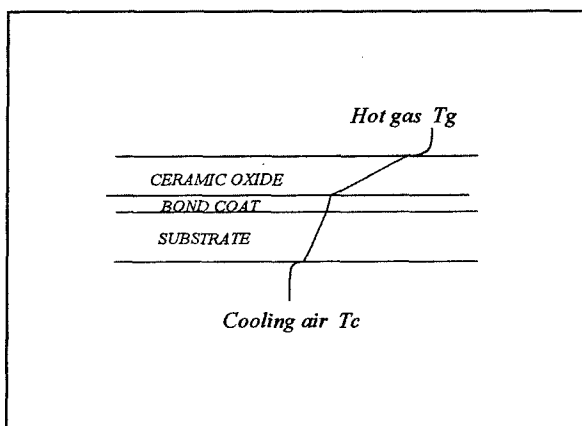


Figure 1. Temperature distribution

Whichever effect is required, the insulating outer layer is invariably a ceramic oxide. Many such oxides have been used in the past, but industry has largely standardised on an eight per cent Yttria partially stabilised Zirconia. There are two main production process routes, air plasma spray and physical vapour deposition. Air plasma spray coatings can be applied in a variety of ways, directly in air (APS), surrounded by an Argon shroud (ASPS) or in a low pressure vacuum chamber (LPPS). It is not the purpose of this paper to compare or promote the virtues of particular systems, nor is it the intention to give an exhaustive review of every coating system. Rather, it is intended to give some indication of the diversity that exists and general problems that the main coating systems bring.

Physical vapour deposition and air plasma spray coating systems produce substantially different morphologies, both of which are shown in a stylised form in figure 2.

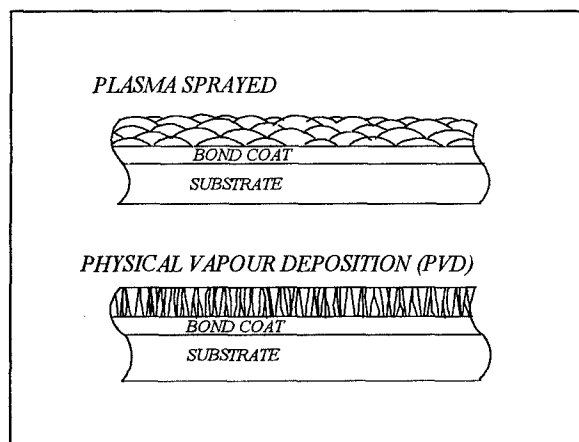


Figure 2. TBC coating morphology

The air plasma spray systems are produced by splattering 'blobs' of plasma from the spray gun onto the surface in a succession of passes, building up the thickness to achieve the required thermal gradient. The morphology of the physical vapour deposition coating is significantly different from the APS system resulting in a columnar structure, growing up from the bond coat surface. Since the columns have little lateral adhesion, it is more easy for the gas to penetrate to the surface and cause oxidation at the interface. Additionally, these pathways result in a higher conductive material, and therefore lower temperature gradients for a given thickness. Conversely, the structure provides better adhesion to the substrate, having a chemical bond, rather than the physical bond of the sprayed systems. Each system then has its advantages and disadvantages, both technical and economic, the details of which are again beyond the scope of this paper.

What both types of coating do have in common, is that they are to a greater or lesser extent porous, and would allow hot gasses to permeate to the surface of the substrate surface. Another characteristic that they have in common is that neither coating provides adequate adhesion when applied directly to the substrate. In order to improve adhesion, and at the same time to counteract the oxidation from the permeated gasses, a bond coat layer is invariably applied between the substrate and the ceramic layer.

The use of bond coats introduces yet more variables into the system. This, in part, emphasises the difficulties in attaining a position of understanding that enables prediction of the behaviour of thermal barrier systems and allows assessment of its suitability to perform a given duty.

Bond coat application is normally through the air plasma spray route, although physical vapour deposition does offer an alternative, but at a price.

Bond coat composition however is infinitely more varied than that of the ceramic top coats, and it is fair to say that this is the area in which most development work is currently directed.

Generally, the options commercially available, (and again this is by no means intended to be an exhaustive list), fall into the general categories of overlays, diffusion coatings, and more recently, thin metallic layers.

MCrAlX overlays offer a wide range of material composition each of which contain Chromium (Cr) and Aluminium (Al). 'M' denotes one or more metallic element, commonly Cobalt (Co), Nickel (Ni) or Iron (Fe), and 'X' represents one or more of the rare earth elements such as Yttrium (Y) or Thorium (Th). The overlays can also be enhanced with additives such as Platinum (Pt), Tantalum (Ta) or oxide dispersion strengthening (ODS) elements.

The simplest form of diffusion coating is pack aluminising, although this is rarely used on its own as a bond coat, and for environmental reasons is being rapidly superseded by the vapour aluminising route. The most common of the diffusion coatings is Platinum aluminising, in which the pack aluminising process is preceded by an electrolytic Platinum deposition which acts as a diffusion barrier.

Of the single metallic deposited coatings Platinum is again the most common element in general use and development, although both Chromium and Palladium have not been overlooked.

Whichever thermal barrier coating system is finally chosen or specified, the component behaviour will have been significantly changed from that of a bare or environmentally protective coated material. Several additional and different potential failure modes and mechanisms will have been introduced, whilst some of the traditional failure modes will have had their failure mechanisms modified.

FAILURE OF THERMAL BARRIER SYSTEMS

It is the identification of the failure modes and understanding the behaviour of the failure mechanisms with time that has allowed thermal barrier coating systems to be qualified for life extension on engine components, without the need to fully demonstrate each component and application in an engine test. Indeed, with the life extension that is potentially possible with thermal barrier coatings, it would not always be practicable to fully demonstrate their capabilities in a single engine test. Furthermore, accelerated engine testing can produce erroneous results.

It has therefore become imperative to understand these failure modes and their effect on component lives, in order to be able to predict with confidence

what the life of a hot end component will be when subjected to a particular environment through a particular mission profile.

It is also essential that any engine testing that is intended to be used to demonstrate a life or life extension through acceleration of the failure mechanisms does so in a controlled and predictable manner. It is important that it does so without introducing additional failure mechanisms or disproportionately exercising other failure mechanisms that would give a false indication of the coating capability.

For example, a bench engine test was set up in the past to reproduce cracking seen on a hot gas path component in service. The test cycle was accelerated by raising the operating temperature, a technique that had often been used with success on previous occasions. In this case however, strain range was the driving criterion, not the temperature per se. Increasing the operating temperature of the test had the effect of reducing the driving strain range of the element by increasing the compressive thermal fraction. Understanding of the failure mechanism and the lifing methodology demonstrated that the cracking could be reproduced by increasing the temperature overshoot in the cycle. The cracking was engendered during the transient phase in the cycle, not at the maximum condition.

Any hot gas path component will suffer from certain failure or damage mechanisms, one or more of which will be life limiting. It is the intention of the Designer to exploit these failure mechanisms to the full. He has to ensure that their life limits fall outside the service life requirements, at least with a certain degree of probability, in order to optimise cooling flow and engine efficiency requirements.

The most common failure modes seen in uncoated components are creep, thermo mechanical fatigue, oxidation, hot corrosion and erosion. These can occur either separately or in combination. High cycle fatigue is designed out of the engine running range in all the dominant modes.

The addition of a single environmental protection coating will extend the component life if the predominant failure mode is oxidation or hot corrosion. However, it does not reduce the number of potential failure modes. It does instead introduce an additional component to the thermo mechanical failure mode in that it affects the structural integrity during cycling. This can have an effect of promoting thermo mechanical fatigue, for instance on single crystal materials by exploiting slip band interfaces. These failure mechanisms will also be present in a bond coat of a thermal barrier system in the same way.

Addition of the ceramic oxide top coat to the bond coat will further modify the behaviour of the ceramic and bond coat failure mechanisms. In addition, it will introduce new criteria of failure such as spalling of the thermal barrier coating. It can modify existing mechanisms leading to premature thermo mechanical failure of the component.

It is not the intention of this paper to explore the substrate failure modes, since they have been the subject of several conferences on their own. Suffice to say that an understanding of the bare component behaviour is essential in order to understand and extend the life of a component under the failure mechanisms within the thermal barrier system. This understanding will be assumed when considering the thermal barrier coating failure modes and mechanisms.

Coating integrity cracking

During the coating process, and after the bond coat has been applied, a high temperature heat treatment is performed so as to promote diffusion and adhesion. In cooling down from these temperatures, a residual strain is imposed in the coating. This is a result of the bond coat exhibiting an apparent increase in ductility above the brittle/ductile transition temperature that is brought about by creep. At temperatures higher than the ductile/brittle transition temperature, figure 3, the bond coat is unable to carry any appreciable load, or transmit strains through from the substrate to the ceramic coating layer.

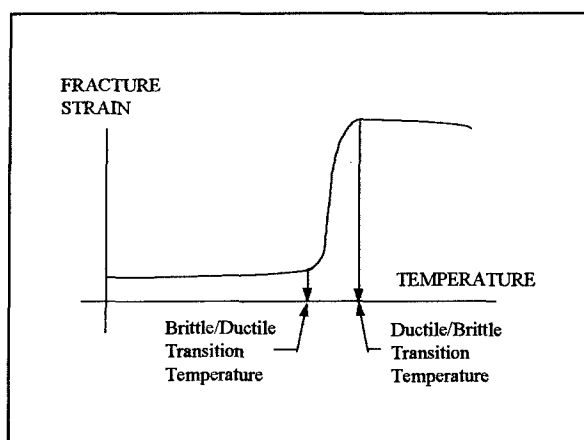


Figure 3. Transition temperatures

When the bond coat temperature is reduced below the ductile/brittle transition temperature (and certainly below the brittle/ductile transition temperature), it is able to carry a load again. It then is able to take on and transmit strains from the substrate to the ceramic.

The strain/temperature cycle in the bond coat will then be similar to that shown in figure 4.

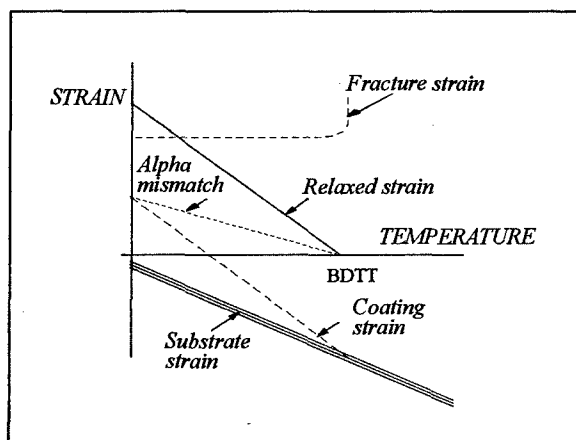


Figure 4. Bond coat coating strains

The bond coat will take on and transfer the component substrate strains to the ceramic. It will generate within itself thermal mismatch strains caused by its intimate contact with the component. These are due to the difference in expansion, or contraction rates of the bond coat and the substrate materials.

The thermal expansion mismatch strains and the substrate strains transferred to the bond coat will be additive in the bond coat. The thermal mismatch strain will reduce to zero at the ductile/brittle transition temperature of the bond coat.

Over a short period of time during cycling through the ductile/brittle transition temperature, the bond coat strains will creep relax. The contribution due to the substrate loading will also drop to zero. There will be no strain or load transmitted to the bond coat at temperatures at or above the ductile/brittle transition temperature. This creep relaxation at the ductile/brittle transition temperature will mean that the combined component substrate and thermal strains below the brittle/ductile transition temperature will also relax. In the example shown in figure 3, this will result in a large relaxed strain range in the bond coat at room temperature.

Integrity cracking will occur at any point at which the strain induced in the bond coat exceeds its fracture strain at the relevant temperature. This fracture strain is roughly constant up to the brittle/ductile transition temperature, increases sharply between the two transition temperatures until it reaches a very high but essentially constant value above the ductile/brittle transition temperature.

Any cracking that occurs will therefore take place at a temperature close to room temperature and, certainly, below the brittle/ductile transition temperature of the bond coat.

The direction of the substrate strain/temperature loop as it varies with time during an engine cycle will have an important bearing on the residual strain in the bond coat at room temperature. This will affect its propensity to crack. In general, clockwise loops will be more likely to crack than anticlockwise loops.

The mechanism described above explains why diffusion coatings can survive and be in some circumstances be less liable to crack than overlay coatings. Whilst overlay coatings generally have higher fracture strains than diffusion coatings, they also have residual thermal expansion mismatch strains that are predominately tensile. Diffusion coatings have mostly compressive residual strains. It is here that the direction of the strain temperature loop is of great significance and can easily alter the ranking of the two types of coating.

The strains that are taken on by the bond coat will be transferred to the ceramic coat at temperatures below the bond coat ductile/brittle transition temperature. Ceramic layer brittle/ductile and ductile/brittle transition temperatures are considerably higher than those of the bond coat. Future developments may produce ceramic layers with values that fall below values of the bond coat. If so, a similar creep relaxation would have to be applied to the ceramic layer to determine the strain level in the ceramic layer.

Figure 5 demonstrates how the ceramic layer will take on the bond coat strains and will also add a mismatch strain due to the difference in expansion rates between the ceramic and the bond coat. This mismatch strain is invariably compressive, resulting in predominately compressive relaxed strains in the ceramic layer.

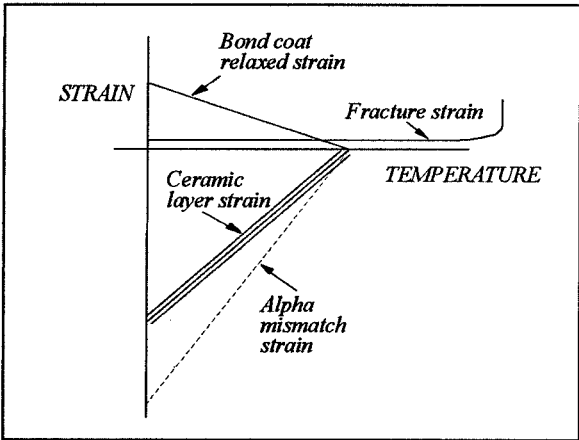


Figure 5. Ceramic layer coating strains

Any propensity to exceed the fracture strain of the ceramic layer will then generally occur at or around the brittle/ductile transition temperature. If the bond coat temperature had not exceeded its brittle/ductile

transition temperature during cycling, there would not have been any stress relaxation. This would then have yielded higher residual strains in the ceramic at those lower temperatures. A designer needs to consider the merits of applying thermal barrier coatings where it will reduce the bond coat temperatures below its transition temperature. An alternative may be to reduce cooling flow locally to increase these temperatures.

Cracking generated only within the bond coat could result in crack propagation into the substrate or into the ceramic layer or into both. The likelihood that this will occur will depend upon the stress/strain field surrounding the crack at the substrate or ceramic interfaces with the bond coat. If the field is compressive, then the crack will generally not propagate, whereas if it is tensile, then it will. If the crack propagates into the substrate, then it can significantly reduce the thermo mechanical life of the component. If it propagates into the ceramic layer, then it can ease gas penetration and increase the rate of oxidation.

Similarly, integrity cracking originating in the ceramic layer can propagate through the bond coat, and ultimately into the substrate. This will again reduce the component thermo mechanical fatigue life.

A third scenario shows the crack originating in either the bond coat or the ceramic layer and propagating along either of the interfaces, parallel to the component surface, as shown in figure 6.

A simple model prediction can be made of the propensity to cracking and the likelihood of

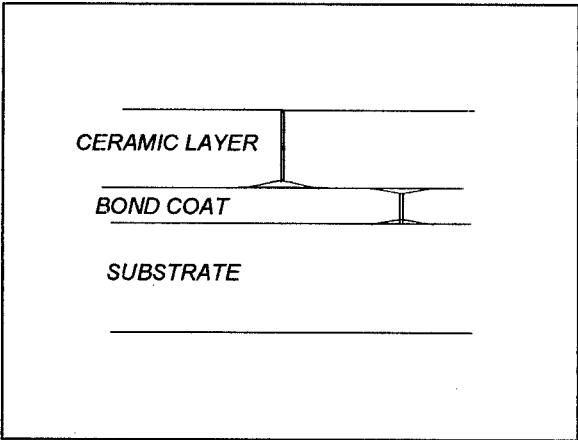


Figure 6. Interface crack propagation

propagation. This can be done at the design phase when selecting the coating for the component.

Thermo mechanical cracking

During normal service operation, a number of thermal cycles will be performed. In a rotor blade, for

instance, this will mean that mechanical and thermal strains will be cycled at the same time as the temperature is cycled. This combined cycling will eventually cause fatigue failure to occur, and this phenomenon is what is referred to as thermo mechanical fatigue.

Each element of a bare component will be cycled through its own unique thermo mechanical fatigue cycle. The nature of the strain/temperature loop will depend on the local temperature and strain variation throughout the engine cycle. There is theoretically an infinity of loops through which an individual element of a component can be cycled, and each will have its own effect on life. It is by predicting these loops, their shapes and directions that the life of an uncoated component can be predicted.

When the component has been coated, then the thermo mechanical behaviour of the coating layers themselves will effect the time to failure of the component.

In the previous section on integrity cracking, an explanation was given of the strain/temperature loops generated within the coating layers themselves due to a combination of thermal mismatch strains and transferred substrate strains. These loops form the cycle through which the particular coating will cycle whilst the substrate is performing its own local strain/temperature loop.

When considering integrity cracking, we were concerned with exceeding of the fracture strain of each layer causing cracking. In thermo mechanical fatigue cracking, we are concerned with the value of the strain range in each layer element, even though the maximum strain may not have been high enough to cause fracture.

Depending on whether we are considering the bond coat or ceramic layer, the strain/temperature loop can be determined. In each case the temperature range of interest will be that between zero and the ductile/brittle transition temperature. The strain range will be the relaxed strain range in the layer element. As the substrate cycles through one strain range, the coating element adjacent to it will cycle through a significantly different strain/temperature cycle. The life at which failure of the coating will occur can be determined from specimen generated strain temperature failure data.

SPALLING OF THE CERAMIC LAYER

Design considerations

Predominately, as we saw from the coating integrity cracking analysis, the ceramic coating layer is in considerable in-plane compressive strain at room temperature. In regions remote from the edges and corners, crack growth is mainly associated with

coating buckling. This is itself a function of the curvature of the component.

Convex surface curvature produces tensile stresses perpendicular to the surface interface. This effect is enhanced by the surface roughness at the interfaces, which determines the local stresses across the interface.

In PVD coatings, the ceramic to metal interfaces are smooth compared to an APS system, which depends for its adhesion on the mechanical key at the surfaces. Thus the contribution of surface roughness to residual stress normal to the surface is small in PVD coatings compared to APS systems.

IN APS systems, Cristinacce has shown that tensile elastic deformation in the ceramic layer close to the bond coat at high temperature, together with subsequent stress relaxation, can increase the residual in plane compressive stress that contributes to spallation due to buckling.

Oxidation of the bond coat

The permeability of the ceramic layer will allow oxidising agents to penetrate through to the bond coat interface. The rate of penetration is determined by partial pressure, so the rate of oxidation is considerably less than it would be if the ceramic layer were not there.

However, it has been shown both in burner rigs and in engine testing that the level of oxide growth required to cause delamination of the ceramic layer is very low.

Generally, spalling is not seen at high temperature, and it is only during the cycling down through the ductile/brittle transition temperature that it occurs.

Spallation of the ceramic coating is induced by thermal mismatch strains during cycling. At areas where oxidation has occurred, the ceramic layer is free to expand and contract as the temperature cycles. Surrounding areas that have not oxidised are constrained in their movement by the behaviour of the bond coat. Thus a lateral strain is set up in the ceramic layer between the attached and oxidised areas during cycling. This is sufficient to cause cracking in the ceramic layer at the interface between the oxidised and non-oxidised areas. This then completes the cracking around the oxidised layer which will spall.

In PVD coatings the cracking in the ceramic layer is perpendicular to the surface and the resulting 'crater' has steep sided walls perpendicular to the surface. However, the APS system has some through thickness strength parallel to the surface. The cracking in this case will not be directly perpendicular

to the surface but will result in an angled fracture front as shown in figure 7.

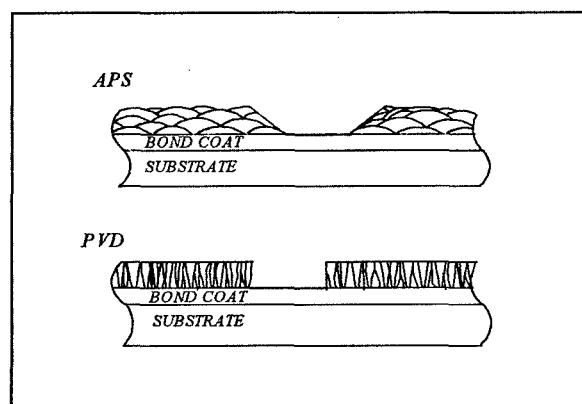


Figure 7. Fracture surfaces

The effect of sintering

The natural state of ceramics is to be fully sintered, and much work has been done in the ceramic industry in reducing temperatures at which a ceramic becomes fully sintered. To be effective as a thermally resistant layer, however a ceramic needs to be in a state that induces maximum thermal resistance with maximum strain compliance. In ceramics, the unsintered state most closely optimises those requirements, and this is the state in which ceramic layers of a thermal barrier system are produced. However, with time at temperature, and under a stress field, the gas washed surface of the ceramic layer will attain its sintered state. In this state, the rate of heat conduction increases, resulting in higher ceramic/bond coat interface temperatures and increased rates of oxidation. At the same time the sintered outer layer of the ceramic will have a reduced fracture strain, and modified thermal expansion properties. This change in state will therefore increase the propensity to crack, as well as increasing the rate of bond coat oxidation. Either effect will considerably reduce the life of the thermal barrier coating.

To this end, in designing a thermal barrier coating for life extension, it is essential to limit the gas washed surface temperature. If the intent is to extend the life of a component and reduce the substrate surface temperature by the use of a thermal barrier coating, that extended life will itself be limited by the surface temperature of the ceramic layer. Thus it may be necessary to also modify the local cooling system.

DEMONSTRATION OF CAPABILITY

In order to demonstrate the capability and underlying methodology for thermal barrier life and behaviour, a number of engine demonstrator programmes have been undertaken in collaboration with MOD. Among the aims of these demonstrator programmes was the prediction of the behaviour of thermal barrier coatings in aggressive endurance running conditions.

In one instance, in the XG40 life assessment programme, the hot gas component had been coated with a thermal barrier after the design had been completed. In other words, the thermal barrier coating was intended as a life extension demonstration, rather than a demonstration of the life of a component that had been designed to run with thermal barrier coating.

In this demonstrator programme, coating integrity cracking was predicted to occur in the bond coat in ten separate positions around the airfoil. Subsequent to the test, cracking was seen in nine of those positions, and also in one position where cracking had not been predicted.

Similarly cracking was predicted to occur in twenty positions where cracking was subsequently seen, and eight positions that failed to show cracking after engine running. In addition, cracking was seen at four positions where no cracking had been predicted. Of the eight predicted cracks that failed to occur, seven were explained after a temperature reassessment. This showed that the region of the component in which these cracks had been predicted had attained higher temperatures than predicted. These higher temperatures had taken the bond coat beyond its brittle/ductile transition temperature, and the subsequent stress relaxation had prevented cracks from occurring in the ceramic coating.

Of the predictions, and subsequent engine running cracks, seven of the cracks occurred in both bond coat and ceramic layer. Only three were restricted to the bond coat, whilst thirteen cracks occurred in the ceramic layer only.

Of the four cracks that were predicted during the intensity crack analysis, two were identified as having a thermo mechanical fatigue initiation. The other two were associated with micro cracking that had been induced during a laser drilling process.

A second high temperature demonstration unit designated HTDU4X was used to investigate spalling of the ceramic layer of the thermal barrier coating that had occurred after oxidation of the bond coat. In this case, the component was designed to carry a thermal barrier coating, and the oxidation and spalling had not been predicted or expected in advance. The spalling was the result of higher than predicted temperatures brought about by an inadequate design feature that restricted the cooling flow. The degree of oxidation was subsequently calculated from more accurate assessment of the design feature effects, and shown to be in agreement with design algorithms.

RECOMMENDATIONS

Life extension brought about by the addition of thermal barrier coatings is difficult to demonstrate

through material approval testing, or engine testing designed to accelerate the damage mechanisms. There is a very real danger of not exploiting the correct failure mechanisms, and thereby deriving a misleading result, particularly when rainbow sets of coatings are to be evaluated.

The preferential route is that of understanding the failure mechanisms associated with the use of thermal barrier coating. The next step is to understand, before the coating system is applied, the effect that thermal barrier coatings can have on the existing failure modes of components.

This paper has set out to describe these failure

modes and mechanisms and has indicated that they can be accurately predicted, if the material data is available.

With this capability, it is possible to predict what will happen to a component during life extension as well as during any accelerated engine test.

ACKNOWLEDGEMENT

The author would like to acknowledge the support of the Turbine Systems life team at Rolls-Royce plc, and in particular acknowledge the finite element analyses of TBC systems, carried out by N S A Cristinacce.

The views and ideas presented in this paper are attributable to the author, and do not necessarily represent Rolls-Royce procedure

Enabling Technologies For Turbine Component Life Extension

J. Liburdi

Liburdi Engineering Limited
400 Highway #6 North
Dundas, Ontario L9H 7K4
Canada

SUMMARY

The evolution in materials and turbine design has resulted in the parallel development of advanced equipment and processes capable of manufacturing and repairing the critical engine components. Modern, vision based automated welding systems are now essential for precise, low heat welding of crack sensitive alloys, while unique powder metallurgy processes such as LPM™ allow repairs to be engineered for higher localized strength or better wear properties such as abrasive tips. Significant changes have also occurred in the stripping and coating processes with the introduction of sophisticated vapour based technologies that are beyond the reach of smaller repair facilities. The availability and costs associated with these enabling technologies, along with the difficulty in obtaining approvals, will serve to further consolidate the industry and restrict the sources for advanced component repairs.

INTRODUCTION

The successful implementation of any turbine component repair or life extension program requires a multi-disciplinary understanding of the materials, design and processing technologies that are critical to the proper function of the component. This is especially important for more advanced jet engines that operate at higher temperatures and rely on sophisticated cooling, aerodynamics, materials and coatings for optimum performance and life. These engines often operate with reduced sealing clearances and design margins compared to the older generation of engines and therefore require more modern technologies for the repair of critical components.

In addition to knowledge of the original design and manufacture of the components, a detailed understanding of the metallurgical and physical changes that occur during operation and re-manufacturing processes such as chemical stripping, brazing, welding, machining, heat treatment and coating is required to develop technologies for advanced component repair. In the balance of this paper, the importance and use of these enabling technologies are described with reference to both compressor and hot section turbine components.

METALLURGICAL AND DESIGN EXPERIENCE

A basic understanding of the operation, temperatures, stresses and materials encountered in a jet engine design is an essential prerequisite for anyone involved in the development and implementation of repair schemes. Several references [1] [2] [3] and specialty seminars [4] provide a broad appreciation of problems encountered with components from various parts of the engine.

The compressor section, for example, operates at comparatively low temperatures, but the airfoils are prone to physical damage due to impact, erosion, corrosion and tip rubs [5] which result in significant losses in performance and increases in specific fuel consumption. Compressor airfoils and seals are routinely restored by welding, using both manual and automated processes. Corrosion and erosion resistant coatings are also applied to protect the surfaces and extend their life [6].

By contrast, the turbine section, with its high temperatures, intricate cooling schemes, advanced superalloys and coatings, presents unique metallurgical challenges and requires the most advanced technology to refurbish the components. The airfoils, which are manufactured using conventional equiaxed or advanced directional or single crystal casting technologies, are often coated internally and externally with complex oxidation resistant and thermal barrier coatings that make their repair difficult and expensive.

The life of the hot section components is typically limited by the aging reactions that occur in the microstructure of the alloy (Figure 1) [7], as well as the depletion and loss of coating protection on the surface of the airfoil and in cooling passages (Figures 2 and 3). Increased seal clearance is also a common problem due to the oxidation, erosion and rubbing of seal surfaces such as blade tips (Figure 4). These phenomena must be effectively addressed and reversed as part of a successful refurbishment scheme. Following is a brief description of some of the processes used to repair and re-manufacture critical components.

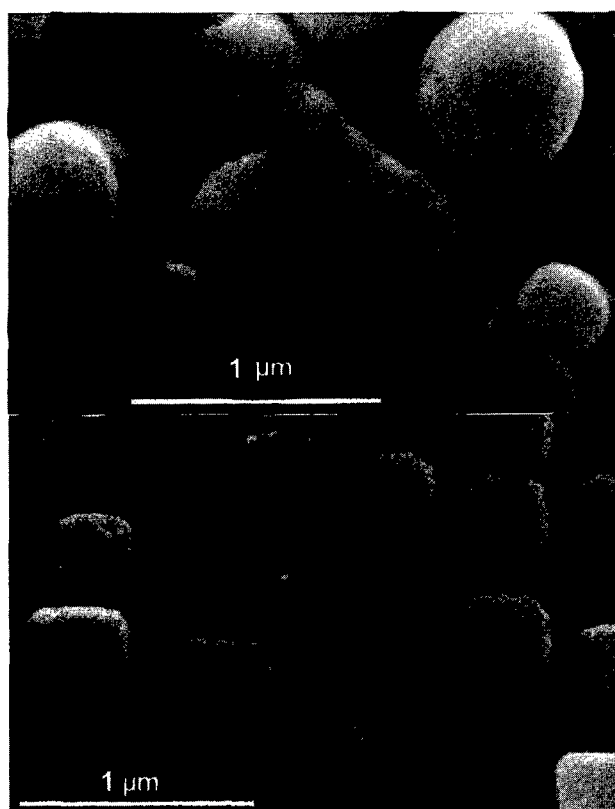


Figure 1 - A comparison of the microstructure in the hotter airfoil (top) and cooler root (bottom) of an HP blade manufactured from MarM002 nickel-based superalloy. The high metal temperatures in hot regions of turbine blades lead to growth and agglomeration of the originally cubic γ' particles and associated degradation in mechanical properties in nickel based superalloys.



Figure 2 - Cross section through a region of a turbine blade in which the protective NiCoCrAlY coating has suffered depletion of the dark band of aluminum-rich β phase through oxidation and interdiffusion with the alloy. The depletion has rendered the coating ineffective at preventing base metal oxidation in areas where the β is fully depleted (arrow), resulting in the formation of a region of internally oxidized base metal.



Figure 3 - Photomicrograph showing oxidation on a blade cooling passage (arrow) which had not been protected with an oxidation resistant coating.



Figure 5 - Photomicrograph of pits formed through dissolution of γ' eutectic colonies at the surface of a directionally solidified superalloy (arrows).

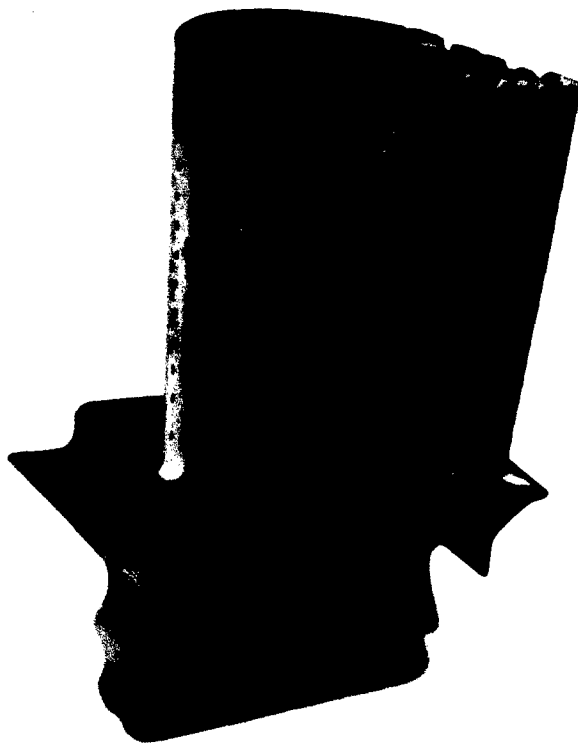


Figure 4 - High pressure turbine blades commonly lose material at the blade tip through oxidation and thermal mechanical fatigue cracking.

MANUFACTURING PROCESSES

Chemical Stripping

For most coated airfoils, it is essential that the coating be removed prior to any solution heat treatment in order to prevent excessive diffusion and rumpling of the surface. The acid solutions used to dissolve the aluminum rich phases in the coating are very aggressive. To prevent intergranular attack of the base material or dissolution of Ni_3Al (γ') eutectic islands in some of the newer high strength superalloys (Figure 5), the solutions must be buffered and carefully controlled.

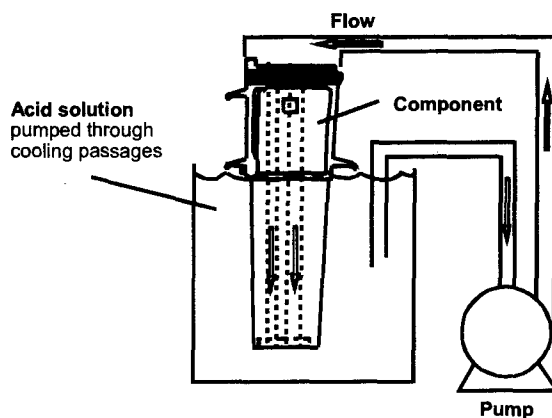


Figure 6 - Schematic of a stripping process for removing coating from external surfaces and internal passages in turbine blades.

A modern chemical stripping process (Figure 6) must be able to flow the hot solution in a controlled manner through the internal cooling passages, in order to remove any internal coatings while simultaneously stripping the thicker external coatings. Special care must be taken to prevent chemical attack on the critical blade root surfaces and inside internal cavities. An experienced technical staff is required to safely operate and maintain such advanced stripping facilities.

Automated Welding

The manufacture of components with higher strength superalloys, combined with the need for stronger, more oxidation resistant filler alloys have significantly increased the difficulty of performing weld repairs. This has resulted in the development of advanced Laser and Plasma systems capable of welding most compressor and turbine components. Automated Welding Systems consistently apply weld metal using extremely low heat input to minimize the effect on the base alloy.

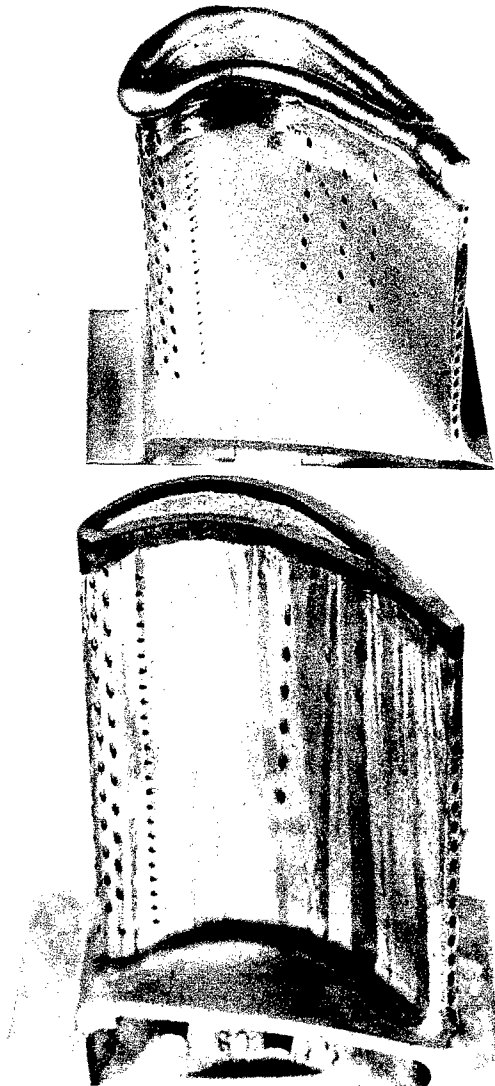


Figure 7 - Tip repair of an HPT blade manufactured from a DS superalloy by vision-assisted automated plasma arc welding with an oxidation resistant nickel-based filler alloy. (Top: As - welded, Bottom: After machining and heat treatment)

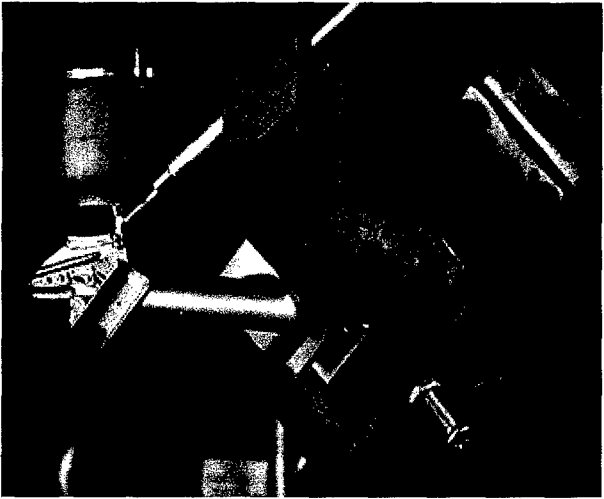


Figure 8 - Weld repair of a shrouded blade with nickel alloy filler on non-contact faces for oxidation resistance and a cobalt hard-facing material on the contact faces using an automated PAW system.

Fully automated welding systems are now used to restore the tips on high pressure turbine blades, as shown in Figure 7, and for hard facing the contact surfaces on new and worn shrouded blades (Figure 8). Compressor blades and vanes (Figure 9) are routinely restored using this advanced technology, taking advantage of the improved productivity and quality that can be achieved compared to manual welding. Larger components, such as disk labyrinth seals, are welded using the automatic Dabber™ process shown in Figure 10, in order

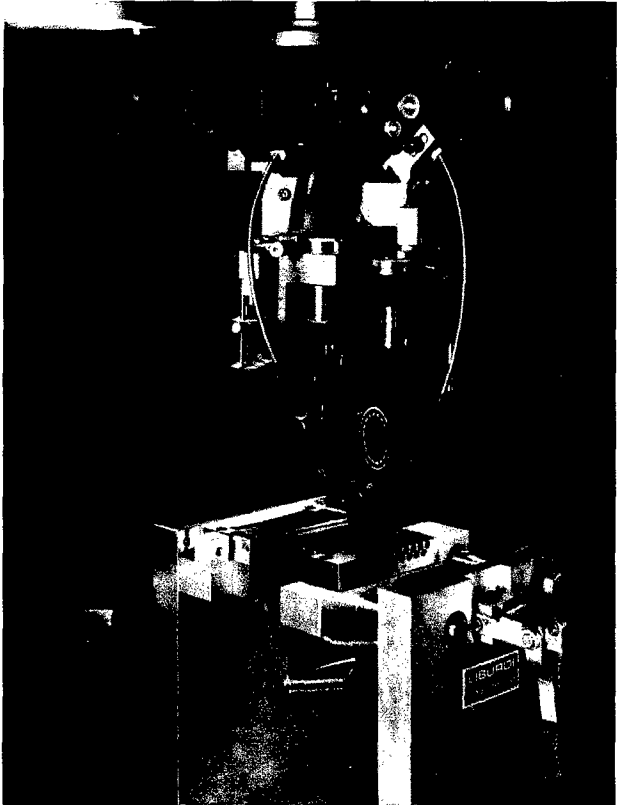


Figure 9 - An automated plasma arc welding system is used to restore a rubbed tip on a compressor blade with matching filler material..



Figure 10 - Precision seal repair welds (arrows) made using the automatic Dabber™ welding system.

to achieve the high quality and accurate stacking of the weld beads on such thin edges. The improved quality resulting from the automation of the welding process has not only provided better reliability, but has also extended the range of components that can be economically repaired.

Advances in the technology related to the power supplies have expanded the options beyond the traditional Gas Tungsten Arc Welding (GTAW) process to include Laser and Plasma Arc Welding (PAW) processes. The higher power density provided by the Laser is ideal for cutting, drilling and autogenous fusion of thin sheet metal components such as the cooling can inserts used inside vane cavities. The softer, bell-shaped arc produced by the latest Micro-Plasma units [10] can be precisely controlled down to 0.1 Amp for minimum heat input to provide a more cost effective solution for most blade and vane welding applications. The plasma welding process can also be modified, as illustrated in Figure 11, to provide pulsing of the arc current level and cyclic reverse polarity to cathodically clean the surface and weld pool. In practice, the wave form is fully customized for specific applications. This Variable Polarity feature, which is widely used in Aerospace welding of aluminum pressure vessels [11], has been successfully used since 1992 to weld the most difficult superalloys and to improve the tolerance of the weld pool to surface contaminants such as residual coatings on turbine airfoils.

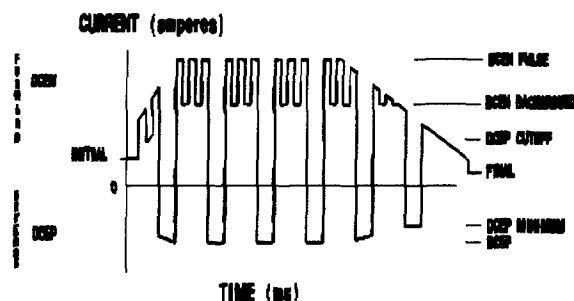


Figure 11 - Current cycle produced by a variable polarity power supply. The use of current pulses in the straight (DCEN) direction helps control weld pool shape, while pulses in the reverse direction provide a cleaning action. The power supplies also allow current to be sloped up and down in a controlled manner

Advanced Brazing

Traditional diffusion braze processes, such as Activated Diffusion Healing™ (ADH) by General Electric and TurboFix™ by Pratt & Whitney, have been widely used in the aero industry to repair cracks in vanes. These processes rely on Fluoride or Hydrogen cleaning to remove oxides from crack surfaces so that the braze can wet and infiltrate the crack surfaces by capillary forces. Adequate cleaning cannot be always achieved in production parts and, as a result, the quality and performance of the repairs tend to be inconsistent [12].

The Liburdi Powder Metallurgy (LPM™) process [13] was designed as a hybrid, wide gap process that allows the defects to be mechanically removed in a manner similar to welding (Figure 12) and then repaired using a powder metallurgy putty of matching or custom composition, to achieve the desired mechanical and metallurgical properties [14][15][16]. The resultant metallurgical bond, shown in Figure 13 exhibits excellent fusion to the base metal, as well as no evidence of prior powder particles and microstructure. The LPM™ process has been successfully used in industrial blade and vane repairs since 1987 and FAA approved since 1995 for several Allison T56 and 250 components as a superior replacement to previous braze and weld repairs. Recently, the process has been qualified by OEM's for closing core pin holes on new blade castings, as well as for forming abrasive tips on single crystal blade tips (Figure 14).

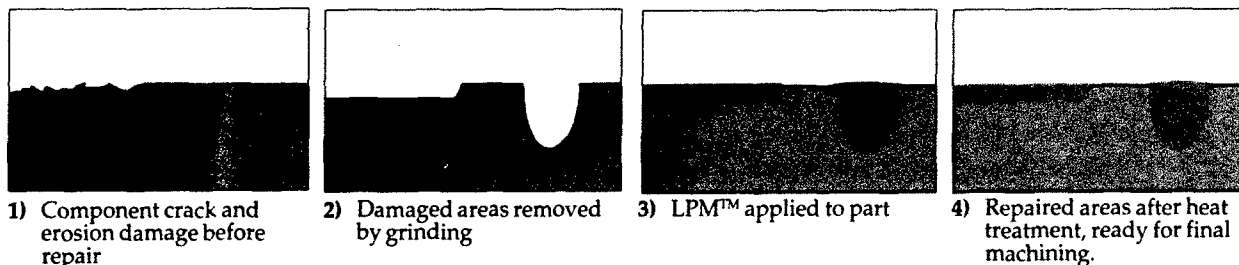


Figure 12 - Schematic illustration of the steps involved in the LPM™ repair process.

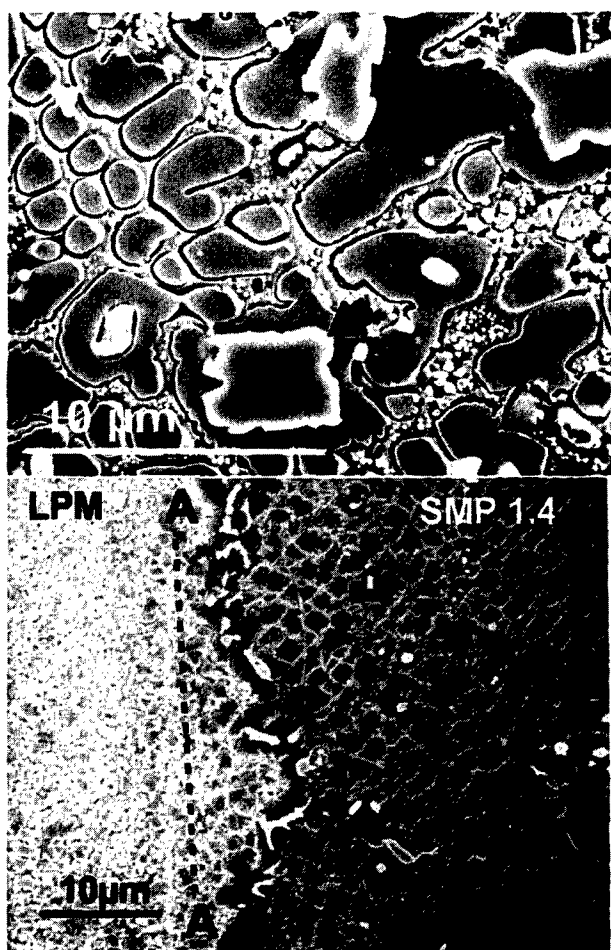


Figure 13 - Micrographs showing the microstructure of an LPM™ joint in SMP 1.4 single crystal alloy. The interface (bottom, A-A) is well-bonded and the microstructure in the joint (top) consists of γ' in an austenite matrix with dispersed borides (arrow).

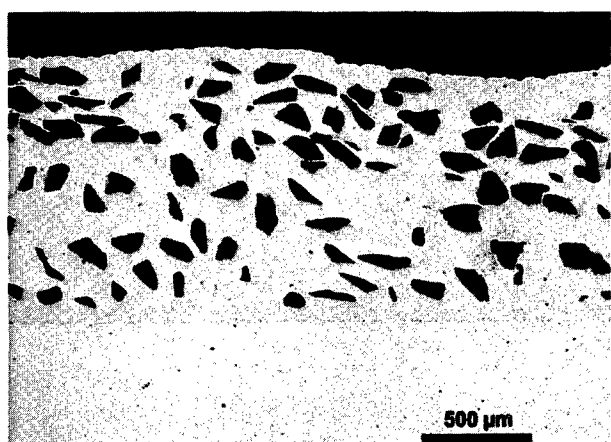


Figure 14 - Cross section through an abrasive blade tip manufactured by depositing LPM™ material containing ceramic particles.

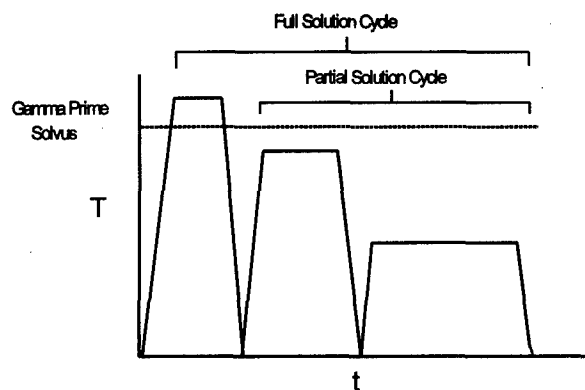


Figure 15 - Comparison of heat treatments incorporating a full solution cycle where the γ' particles are completely dissolved and a partial solution cycle in which not all of the γ' particles go into solution.

Rejuvenation Heat Treatments

Vacuum heat treatments are traditionally used during the repair process to restore the microstructure, improve weldability, apply brazes and diffuse coatings. Significant metallurgical knowledge and experience are required to tailor the heat treatment steps, graphically illustrated in Figure 15, to the superalloy being processed. This ensures that the creep, fatigue and aging damage incurred during service are reversed as much as possible, and that the correct microstructure and mechanical properties are produced after all welding and coating steps have been completed.

Aero-engine component repairs will often specify a lower temperature for the solution treatment which does not fully restore the γ' in the microstructure and results in a part life repair [7]. Where possible, blades and vanes should be exposed to a full high temperature heat treatment with the addition of a Hot Isostatic Pressure (HIP) cycle to fully dissolve and recondition the microstructure and heal any creep and fatigue damage accumulated during service. Heat treatment cycles also result in a thermal etching effect, which serves to expose any tight cracks and strain age cracking in welds (Figure 16). This improves the quality of the inspection and thus increases the reliability of the component in service.

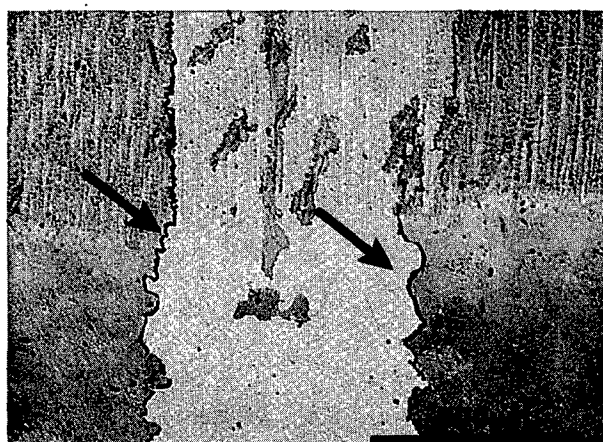


Figure 16 - Micro-cracks formed during post-weld heat treatment on the tip of a HP blade manufactured from DS Rene 142 alloy.

Coating Protection

The hot section blades and vanes in advanced engines rely on surface coatings to enhance the oxidation resistance of the base alloy and to provide a thermal barrier to insulate the cooled core against the high gas path temperatures. At the end of the repair process, these coatings must be re-applied using technology and equipment similar to that used in the original manufacture of the components.

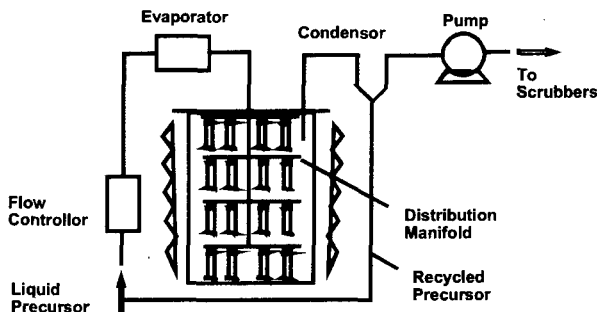


Figure 17 - Schematic illustration of a low temperature CVD coating process that can apply aluminide coatings uniformly to the surfaces of turbine blade cooling passages and airfoils.

The traditional pack aluminide processes and coatings such as Codep^{TM(GE)} are being replaced by significantly more expensive enhanced aluminides, MCrAlY and TBC coatings applied by Chemical Vapour Deposition (CVD) (Figure 17), Low Pressure Plasma Spray (LPPS), High Velocity Oxy Fuel Spray (HVOF) and Electron Beam Physical Vapour Deposition (EBPVD) technologies, which are beyond the reach of most repair facilities. The availability of these coating facilities and technology licenses will restrict the number of vendors capable of performing hot section repairs on the more advanced engines.

CERTIFICATION OF PROCESSES

The development and approval process for new aero repair schemes can be arduous and lengthy if engine testing is required. In many applications, where an incremental improvement in a repair process is being implemented, a reduced qualification testing procedure is adequate.

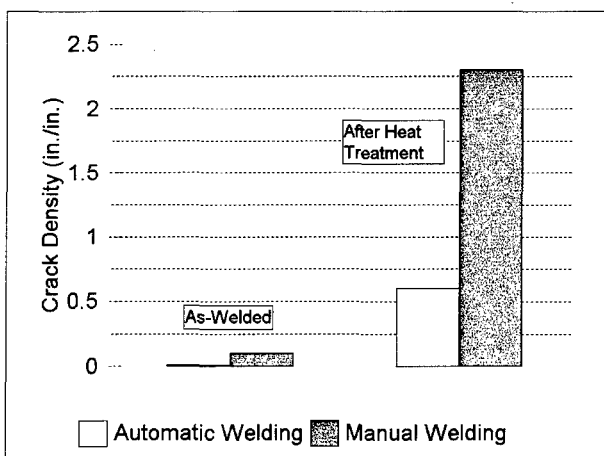


Figure 18 - Incidence of cracking in IN738 alloy showing the influence of automation and post weld heat treatment [17].

The existing repair procedure for a component, will define the limits of the repair, the materials and practices to be used, and the quality and testing requirements. When substituting a new process such as automated welding to replace an older manual operation, the substitution can be approved by demonstrating that the new process is capable of meeting or exceeding the metallurgical and quality requirements for the repair. This procedure is similar to qualifying a new welder or operator and can be done quickly without the need for expensive rig and engine testing. As illustrated in Figure 18, the quality and consistency of automated welds is significantly better than that of conventional manual welds which results in higher yields in the repair and improved reliability in service.

Coating substitutions will often require greater scrutiny and laboratory or rig testing to ensure that the correct structure and service behaviour is obtained. For example, a CVD aluminide coating can be fairly readily qualified to replace an older pack cementation coating of equivalent chemistry and microstructure; however, a plasma sprayed TBC coating may not be used to replace an EBPVD coating with the same chemistry but differing microstructure.

CONCLUSION

The ever increasing complexity of components in advanced turbine designs has stimulated a corresponding evaluation of new technologies and processes capable of providing higher strength and more reliable repairs. The manual welding operation has been replaced by sophisticated Vision based automated welding systems, while older pack coating processes have given way to advanced chemical and physical vapour coating technologies capable of infiltrating serpentine cooling passages or producing unique microstructural features. The cost and availability of these enabling technologies is beyond the reach of smaller repair facilities and will likely lead to a consolidation of the industry and greater control by the engine manufacturers.

REFERENCES

1. "The Jet Engine, 5th Edition", Rolls Royce, 1996 (ISBN 0-9902-12123-5).
2. Cohen, H., Rogers, G. F. C., Saravanamutto, H. I. H., "Gas Turbine Theory, 3rd Edition", Harlow, England, Longman Scientific & Technical, 1987 (ISBN 0-582-30359-X).
3. Sims, C. T., Stoloff, N. S. and Hagel, W. C., "Superalloys II", New York, USA, John Wiley & Sons, 1987 (ISBN 0-471-01147-9).
4. Liburdi, J. and Lowden, P., "The Turbine Materials Course", Dundas, Canada, Liburdi Engineering Limited, 1998.
5. Nagy, D. R., Parameswaran, V.R., MacLeod, J.D. and Immariageon, J.P., "Protective Coatings for Compressor Gas Path Components," AGARD 83rd Symposium of the Propulsion and Energetics Panel, Rotterdam, The Netherlands, April, 1994, Paper 27.
6. "T56 Compressor Airfoil Coating Datasheet", Allison Engine Company, 1997, Datasheet GTP-6378.

7. Liburdi, J. and Lowden, P., "*Observations on the Life and Overhaul Requirements of Aeroderivative Engines on Base Load Industrial Applications*", ASME Gas Turbine Conference and Exhibition, Anaheim, California, May-June, 1987 (ASME Paper 87-GT-105).
8. Lowden, P., Pilcher, C. and Liburdi, J., "*Integrated Weld Automation for Gas Turbine Blades*", ASME Gas Turbine Conference and Exhibition, Orlando, FL, June 3-6, 1991 (ASME Paper 91-GT-159).
9. Pilcher, C., Liburdi, J., Berger, C. and Iovene M., "*Laser and Micro-plasma Welding of Single Crystal Blades - Advantages of Total Process Control*", ASME Turbo Expo 93, Cincinnati, Ohio (ASME Paper 93-GT-367).
10. "Pulsweld - 50/100 Amp MICRO GTAW/PAW Power Sources", Liburdi Pulsweld Corporation, 1996.
11. Nunes, A. C., et al, "*Variable Polarity Plasma Welding on the Space Shuttle External Tank*", Welding J., September, 1984, pp.27-34.
12. Brauny, P., Hammerschmidt, M. and Malik, M., "*Repair of Air-Cooled Turbine Vanes of High Performance Aircraft Engines - Problems and Experience*", Mat. Sci. and Tech., August, 1985, v. 1, pp. 719-727.
13. Liburdi, J., Lowden, P. and Ellison, K., "*Powder Metallurgy Repair Technique*", U.S. Patent No. 5,156,321.
14. Ellison, K.A., Lowden, P. and Liburdi, J., "*Powder Metallurgy Repair of Turbine Components*", International Gas Turbine and Aeroengine Congress and Exposition, Cologne, Germany, June 1-4, 1992 (ASME Paper 92-GT-312).
15. Liburdi, J., Ellison, K. A., Chitty, J. and Nevin, D., "*Novel Approaches to the Repair of Vane Segments*", ASME Turbo Expo 93, Cincinnati, Ohio (ASME Paper 93-GT-230).
16. Ellison, K.A., Liburdi, J. and Stover, J. T., "*Low Cycle Fatigue Properties of LPM™ Wide-Gap Repair Joint in Inconel 738*" in "*Superalloys 1996*", Warrendale, USA, TMS, 1996 (ISBN 0-87339-352-X), pp. 763-771.
17. Liburdi, J., Lowden, P. and Pilcher, C., "*Automated Welding of Turbine Blades*" Trans. ASME, J. of Eng. for Gas Turbines and Power, v. 112, October 1990, pp. 550-554.

DEVELOPMENT OF A QUALIFICATION METHODOLOGY FOR ADVANCED GAS TURBINE ENGINE REPAIRS/REWORKS

P.C. Patnaik
R. Thamburaj
Advanced Materials and Energy Systems(AMES)
Orenda Aerospace Corporation
Suite 608
Gloucester, Ontario, K1J 9L8 Canada

Summary

In this paper, the engine and component qualification test requirements with specific application to component repairs/reworks of Civilian and US military specifications and standards for turboshaft, turboprop, turbofan and turbojet engines have been reviewed and a methodology developed.

Having identified that repairs were feasible and cost beneficial, a review of civil and military airworthiness guidance was conducted in order to identify a process that would ensure that a high state of airworthiness was maintained and which would easily translate to civil requirements.

Failure mode, effects and criticality analysis, as a reliability analysis tool, for Gas Turbines has been developed for component repairs/reworks. As part of the development of a FMECA engineering tool, a specific procedure has been developed for performing FMECA on various type of gas turbines, including turbojet, turbofan, turboshaft and turboprop engines.

According to the specification established by Orenda and GasTOPS (the sub-contractor), the developed software contains the following important features:

- (i) System definition with iconic display,
- (ii) Complete FMEA capable to use either hardware or functional approach or a combination of both,
- (iii) Complete CA capability with either qualitative or quantitative method and,
- (iv) FMECA report format to help the users to generate a complete FMECA report.

The software is a generic FMECA tool for the applications to various types of aircraft engine systems, including turbojet, turbofan, turboshaft turboprop and etc. The test of the software has been carried out by both GasTOPS and Orenda using a set of F404 data.

In terms of a Qualification Methodology Development, coupon, component and full scale engine testing are required by all standards to show compliance with the structural integrity and durability requirements (e.g. low cycle fatigue, high cycle fatigue, creep, vibration, containment) for gas path structural components under different environmental operating conditions.

An Engine Repair Structural Integrity Program (ERSIP) Standard was proposed which is an integral part of the Qualification Methodology for engine component repairs. The ERSIP Standard incorporates the damage tolerance concept as required in MIL-STD-1783 (USAF-Engine Structural Integrity Program (ENSIP)). The ERSIP Standard establishes the repair development and repair qualification tests to ensure structural integrity and performance throughout the repair life cycle.

The generic component test specifications relating to the types of repairs and reworks carried out on the F404-GE-400 engine have

been established. The test specifications include the following tests:

1. Hardness Testing
2. Ballistic Impact Testing
3. Rub Testing of Shrouds and Blades
4. Water Flow Testing
5. Natural Frequency Impact Testing
6. Natural Frequency Vibration Testing
7. Erosion Testing
8. Corrosion Testing
9. Dynamic Resonance and High Cycle Fatigue Testing
10. Whirligig Testing
11. Spin Pit Testing
12. Air Flow Testing

The objective of AMET is the elimination of engine operating conditions which do not contribute, in a significant way, to the damage accumulation on critical components, notably compressor and turbine discs and blades, as well as combustors.

It is important to tailor an AMET to the intended aircraft mission and to the component(s) under test, in order to address all stresses that are likely to be encountered in the field. Components that are sensitive to total engine operating time, such as bearings and accessory parts, may have to be tested separately in laboratory bearing, bushing or dwell test rigs. It may be stated that no single AMET will fully evaluate an entire engine.

Judging from the literature, most AMET testing is carried out with new engine models during the development stage, rather than on upgraded engines or refurbished components. No references were found regarding AMET testing for repaired engine components.

A generalised procedure for the development of an AMET cycle was developed for the CF-18 engine to qualify component repairs/reworks.

1 INTRODUCTION

Modern gas turbine engines for military aircraft applications cost several millions of dollars with annual expenditures on new spare parts in excess of \$50,000 per engine. The majority of this cost is attributed to the replacement of expensive turbine hot section components. In addition, the repair and overhaul costs can alone exceed \$100,000 per engine excluding the spare parts costs.

It is well established that approximately 30% of the Life Cycle Cost (LCC) of an aircraft can be attributed to the engines that power the aircraft and that overhaul by repair/rework rather than replacement of component would contribute a significant cost benefit. However, repaired/reworked components must be must be qualified for airworthiness prior to their use in service. This is because the repairs/reworks may alter dimensions, change vibration characteristics and affect component mechanical

properties. The purpose of establishing a repair/rework qualification methodology is therefore to ascertain that a redesigned/repaired/reworked piece of hardware meets the airworthiness requirement before it is implemented in service.

The modern gas turbine engine is a highly sophisticated device involving many components and materials. It is virtually impossible to predict the exact conditions which these parts will be subjected to in the operational environment starting from a wide range of atmospheric temperature and pressure conditions, flight speeds, load settings, sand, dust, corrosive environments and transient acceleration and deceleration rates with a variety of fuels. Internal engine conditions change as a function of these variables, and the designer is faced with hundreds of combinations of possible operating conditions and a variety of failure modes (Fig. 1 and Table 1). The repair/rework designer must make the best decision using past experience, design and analytical methods, computer simulations and extensive coupon, rig and engine testing. A Qualification Methodology is as important to the case of component repair/rework/design change as it is to the task of the original design, since every type of repair/rework/design change while healing the type of degradation has the potential of introducing a new type of fault or defect.

The qualification of flight critical, high cost rotating components has not been undertaken outside of the Original Equipment Manufacturer (OEM) domain in the past. Design proprietary information, full scale test facility development and operational costs, and the costs of qualifying these repairs have precluded operator instigated repair process development. Previous DND (Department of National Defence Canada) technology base collaborative investments with Orenda and the National Research Council (NRC) have established the knowledge and resource base for Canada to now pursue this technologically challenging venture. This paper will begin by briefly describing the cases where qualification is necessary and then lead to the development of a methodology. The qualification tests for design changes may vary depending on the failure modes and acceptable technical risk from very simple tests to complex ones.

2 TYPES OF DESIGN CHANGES / REWORKS

The types of design changes/reworks addressed here are associated with material changes, process changes, weld repair, braze repair and application of advanced protective coatings. Some specific examples are given below for illustration purpose.

(i) Material Property Upgrades

Material property upgrades are required in cases where higher strength or higher fracture toughness, lower weight, higher corrosion resistance or resistance to fire is required as illustrated in Table 2.

(ii) Compositional Changes

Changes in alloy material or composition may be encountered with heat to heat variation in material (change of supplier, variations in processing conditions), change of welding filler rod composition for improved weldability and modified base material composition for improved fabricability and mechanical properties as shown in Table 3.

(iii) Processing Changes Which Alter Microstructure

Changes in processes such as heat treatment cycles can have a significant impact on the microstructure of a component and

consequently affect its mechanical properties. Various types of processing changes, which could alter microstructure in a beneficial way, are given in Table 4.

Other types of design changes that may require qualification are as follows.

- (iv) Specialty Material Changes
- (v) Coating/Surface Modification
- (vi) Heat treatment
- (vii) Simultaneous Application of Heat and Pressure
- (viii) Weld Repair
- (ix) Changes in Machining Process
- (x) Changes in Component Design
- (xi) Braze Repair
- (xii) Life Extension
- (xiii) Manufacturing Defects
- (xiv) Unique Environments
- (xv) Engine Specific Repairs

It is also important to note that more than one of the design changes listed in the above may be applied to a component. For example, a component could be braze repaired, Hot Isostatic Pressed (HIP'ed) and subsequently coated and each one of these changes can produce effects that interact with another and produce a complex combination of requirements for qualification.

This large complex database makes it necessary to have a computer based system that can assess the criticality of the failure modes arising from the design changes to be attempted on the component which is addressed in the next section.

3 DESIGN CHANGE/REPAIR/REWORK QUALIFICATION METHODOLOGIES FOR GAS TURBINE ENGINES

The development of a methodology for the airworthiness verification of gas turbine component repairs or reworks has been prepared in the following manner:

3.1 Preliminary Technology and Economic Feasibility Studies

Prior to initiation of the qualification of repair/rework in a gas turbine engine as a target of opportunity, component failure and rejection rates at all levels of maintenance, repair and overhaul were analysed. Components that offered potential for significant cost savings were identified along with the technology needs for repair.

3.2 Regulatory Agency Review

Having identified that repairs were feasible and cost beneficial, a review of civil and military airworthiness guidance was conducted in order to identify a process that would ensure that a high state of airworthiness was maintained and which would easily translate to civil requirements.

3.3 Qualification Methodology

The process and personnel required to certify a repair to a gas turbine engine component must be specified and a process audit trail defined. The rationale and approach developed for the Qualification Methodology for DND Gas Turbine repairs is described below.

3.4 Failure Mode Effects and Criticality Analysis (FMECA)

This element of the Qualification Methodology is of value to fleet repair analysis as well as for repair redesign purposes and will serve as a stand-alone tool for Gas Turbine Engine's Life Cycle Materiel managers (LCMM). The FMECA is a computerised aid that leads design authorities for aerospace equipment through the types of failures that can occur on each component, identifies the probability of those failures, and suggests the possible consequences of failure.

4 QUALIFICATION METHODOLOGY DESCRIPTION

The qualification methodology describes how to design and certify a repair as being airworthy following a systematic and responsible procedure. To do so, the methodology must address such issues as repair design, life analysis, verification testing, and personnel qualification requirements. The qualification methodology is applicable to aero-gas turbines, and must be valid for flight critical and non-critical components. The Qualification Methodology for Gas Turbine Repair/Rework is comprised of the following components:

- a. Failure Mode, Effects and Criticality Analysis (FMECA) Methodology
- b. Coupon Level Testing Methodology
- c. Component Rig Testing Methodology
- d. Engine Testing;
- e. Design Change Approval.

Depending upon the criticality of the component and repair/rework, (c) and (d) can be eliminated.

To manage the development and qualification of repairs, an Engine Repair Structural Integrity Program (ERSIP) is proposed as part of the qualification methodology. ERSIP modifies and extends the limits of MIL-STD-1783 (USAF) Engine Structural Integrity Program using a damage tolerance based life cycle management philosophy. This approach has been taken as repairs will correct damage incurred during service due to conditions which will continue to impact on the repaired component when returned to service. In practice, after the original design, verification and type approval process, engine components are introduced to service with an appropriate life cycle management philosophy - scheduled, which can be either hourly or cyclic based, or on-condition maintenance. Additional considerations for damage tolerant operations can be applied to either life management approach. When damage to an engine component is observed, the FMECA will be used to establish the criticality of the event by identifying the failure mode and its effects on engine and aircraft operation. Further, a Reparability and Cost Benefit Analysis (RCBA) will determine whether the component should be repaired or replaced. If a repair decision is made, ERSIP will be applied to establish repair development and verification requirements to assure structural integrity for the repaired component. Through the DND approval procedure, the repaired component will be returned to service with an appropriate life cycle management procedure in place. Clearly, this generic program will be applicable to every engine in the Canadian Forces (CF) inventory.

4.1 Failure Mode Effects and Criticality Analysis (FMECA)

Failure Mode Effects and Criticality Analysis (FMECA) is a method of reliability analysis intended to examine the potential failure modes within a system and its equipment and to determine the effects on equipment and system performance in order to establish priorities for remedial action. The FMECA consists of two separate analyses, The Failure Modes and Effects Analysis (FMEA) and the Criticality Analysis (CA). FMEA is usually a qualitative analysis of the failure modes of hardware; however, it does not exclude factors of human or software error. The Criticality Analysis combines the concepts of severity of consequences of failure and the rate or probability of occurrence of a failure within a specified time period. The CA can either be conducted in a qualitative or quantitative manner dependant on the quality and availability of failure data. The FMECA will attempt to:

- a. Determine the effects of each failure mode on system performance;
- b. Provide data for developing Fault Tree Analysis (FTA) and reliability block diagram models;
- c. Provide a basis for identifying root failure causes and developing corrective action;
- d. Facilitate the development of design alternatives for improved reliability repairs;
- e. Aid in developing test methods and troubleshooting techniques; and
- f. Provide a foundation for qualitative reliability, maintainability, safety and logistics analysis.

The input to the FMECA is a series of component failure rate data obtained from various sources such as R&O contractor, field, OEM tests, CIP data, user data from USN, USAF and DND and data from the regulatory agencies such as FAA, Transport Canada Aviation, BAA and JAA.

It should be noted that a FMECA can be used at the initial design stage, as well as during the life cycle of a component. Its purposes are to: highlight single point failures which require immediate action, rank failures according to severity classification of the failure effect on mission success and personal/equipment safety, provide estimates of critical failure rates, and to identify reliability/safety critical components requiring special management approaches.

To complete the FMECA required for the gas turbine component repair/rework qualification program, hardware test requirements should be identified for the repairs on the engine components. An example of introducing a new protective coating to an uncoated HPT nozzle in a gas turbine is given below.

a) **Potential Failure Modes:**

- Thermal fatigue cracking
- Coating deterioration and spalling
- Oxidation, corrosion and erosion
- Over heat

b) **Possible Failure Causes:**

- High thermal stress levels mainly due to engine start up and shutdown
- Oxidation, corrosion and erosion produced by the hot gas
- Failure or improper functioning of the cooling system

c) **Typical Tests, Inspections and Examinations:**

- Dimensional inspection
- Metallurgical examination
- Cooling path tests: air flow, pressure or water flow
- Burner rig test
- Engine test

4.2 **Coupon & Rig Level Testing Methodology**

The Qualification Methodology Development program involves the identification of coupon test requirements for qualification of engine component life extension schemes prior to engine testing. The coupon test requirements were generic in nature, identifying where possible an alternative means for initial screening of repair or rework schemes. An example of fretting fatigue coupon testing is given in Figure 2 and a burner rig component testing in Figure 3.

The repair/rework included, but not be limited to the following:

- Protective coatings applied to hot or cold section rotating and non-rotating components.
- Weld repairs of fan and compressor blades and vane segments.
- Weld or braze repair of turbine nozzle segments or turbine blades.
- Rejuvenation of components by various means including Hot Isostatic Pressing (HIPing).
- Life extension of rotating and non-rotating, flight and non-flight critical, components.

A review of Society of Automotive Engineers (SAE), Aerospace Information Reports by SAE (AIR), Aerospace Material Specifications by SAE (AMS), Aerospace Recommended Practices by SAE (ARP), Aerospace Standards by SAE (AS), American Society for Non-Destructive Testing (ASNT), American Society for Testing and Materials (ASTM), American Welding Society (AWS), British Standards (BS) and European Standards (EN) specifications on materials, processing, inspections and testing that are relevant to the repairs/reworks has been conducted. Some examples are provided.

4.3 **Requirements for Coupon Level Testing of Protective Coatings Applied to Hot and Cold Section Rotating and Non-Rotating Components**

4.3.1 *Coupon Test Materials*

Wherever possible, and if the component dimensions permit the machining of suitable coupons, every attempt should be made to

machine the coupon test specimens from repaired parts. If not, then the coupon test specimens should be machined from the same materials as those used to manufacture the fan and compressor blades or vanes that are to be repaired. The requirements for composition, form, mechanical properties and heat treatments of coupon test materials should be as per Aerospace Material Specifications (AMS) and/or engine manufacturer's material specifications (EMMS).

4.3.2 *Coating Processes*

Specifications for conventional coating processes, such as plasma spraying, physical vapour deposition, plating or chemical treatments have been published by SAE, AWS and other societies. The specifications for special coating processes may be obtained from the engine manufacturer or coating vendors. A detailed list of specifications relevant to different coating processes (including plating and chemical treatments) has been compiled elsewhere.

4.3.3 *Coupon Level Testing of Coated Components*

Coupon testing should be conducted to verify the effectiveness of the protective coating. The coating properties and the effects of the coating process on substrate properties must also be examined. Coupon testing for cold and hot section coatings will be described separately because the test requirements for the two are different.

4.3.4 *Typical Tests for Evaluating General Coating Properties*

- (1) Coating Adhesion Strength Test
- (2) Coating Microhardness Test
- (3) Coating Ductility Test
- (4) Ductile to brittle transition temperature (DBTT) Test

4.3.5 *Typical Tests for Evaluating the Effects of Coating on Substrate Properties*

- (1) Tensile or Low Cycle Fatigue Test
- (2) Fracture Toughness Test
- (3) High Cycle Fatigue Test
- (4) Thermal-Mechanical Fatigue Test
- (5) Fatigue Crack Growth Rate Test
- (6) Creep Test

4.3.6 *Testing of Cold Section Coatings*

Coatings are applied to cold section components to improve their durability, such as erosion resistance and fretting resistance. For all cold section coatings, coupon tests are required for evaluating the coating quality and the effects of the coating processes on the mechanical properties of the substrate. In addition, coupon level tests are required for verifying the protection provided by the coating.

4.3.6.1 *Erosion Resistant Coatings*

These types of coatings are developed to improve the erosion resistance of the components without sacrificing their corrosion resistance. To verify the coating's effectiveness against erosion, coupon level erosion tests and corrosion tests must be conducted as described below:

- (i) Erosion Test
- (ii) Corrosion Test

4.3.6.2 Fretting Fatigue Resistant Coatings

These types of coatings are developed to improve the fretting fatigue resistance of engine components. To *verify* the coating's effectiveness, coupon level fretting fatigue, Figure 2, and corrosion tests must be conducted.

- (i) Fretting Fatigue Test
- (ii) Corrosion Test

4.3.7 Testing of Hot Section Coatings

Coatings are applied to hot section components to increase their temperature tolerance (such as thermal barrier coatings), or to improve their oxidation and/or hot corrosion resistance in aggressive operating environments. For all hot section coatings, coupon tests must be conducted for evaluating the coating quality and the effects of the coating processes on the mechanical properties of the substrate. In addition, coupon tests are required for verifying the level of protection provided by the coating.

4.3.7.1 Oxidation and Hot Corrosion Resistant Coatings

These types of coatings are developed to improve the oxidation and/or hot corrosion resistance of the hot section components. To verify the coating's effectiveness against oxidation and hot corrosion, coupon level oxidation and hot corrosion tests must be conducted as described below:

- (i) Oxidation Test
- (ii) Hot Corrosion Test

4.3.7.2 Thermal Barrier Coatings

These types of coatings are developed to improve the temperature tolerance of the hot section components. To verify the coating's effectiveness in improving temperature tolerance, coupon level thermal conductivity, oxidation, hot corrosion and thermal fatigue burner-rig tests are required.

- (i) Thermal Conductivity Test
- (ii) Oxidation Test
- (iii) Hot Corrosion Test
- (iv) Thermal Fatigue

4.4 Development of Accelerated Mission Testing Methodology

4.4.1 General Definition

Any form of Accelerated (Simulated) Mission Endurance Tests (AMET or ASMET) serves two functions: it reduces the test time and increases safety considerations when compared to on wing testing. In essence, AMETs eliminate or reduce the engine operation phases which contribute very little to the stressing of a part investigated. Conversely, an Accelerated Mission Test (AMT) must contain all the damaging elements in service that result in particular failure modes.

Accelerated mission endurance testing has been accepted, in general, by every major engine manufacturer as an important tool for testing whole engines, Figure 4, and/or their components, in a cost and time effective manner.

4.4.2 Elements of Accelerated Mission Endurance Testing

It is absolutely essential that the AMET be tailored to (a) the component(s) under investigation and (b) the mission(s) of the engine. If several parts are involved, and if the projected missions

are many fold, the AMET may become rather complex. The layout of an AMT must be carefully designed to simulate real-life operating conditions, for example: (a) the complete cooling down of disk bores, representative of an overnight shutdown, (b) the hold times at idle, which establish the bore-to-rim thermal gradients that affect the low cycle fatigue (LCF) life of the hot disks and (c) the throttle acceleration rates which should match those in the aircraft. The purpose of the AMET is to subject the complete engine to all failure modes relevant to the test requirements.

In general, the following categorisation can be made: high cycle fatigue (resonance) and thermal distress can be accelerated by sustained high power running, while low cycle fatigue (LCF), mechanical wear, and thermal distress can also be accelerated by increased start-stop, cycle operation. Thermal fatigue is accelerated by increased throttle cycles during each test run. High cycle fatigue (HCF) is accelerated by operating the engine at specific speeds to excite the required vibratory modes.

Low cycle fatigue is such an important distress mode that sophisticated means have been designed and built to subject components specifically to this failure mode. Generally, AMTs are concentrated on hot end components because of the higher temperatures and stresses to which they are exposed and because their times between overhaul (TBOs) are shorter than those of the less-stressed cold end parts. The exceptions are compressor components affected by LCF due to centrifugal stress and pressure cycling. Hot parts, on the other hand, are subject to thermal stress cycling, creep, and stress rupture, in combination with mechanical stresses.

In designing an AMT, the inlet air temperature, as a function of the season, may have to be taken into account, as it may affect the turbine inlet temperature (TIT). This cautionary note only applies for engines not controlled by a fixed maximum TIT.

4.4.3 Mission Data Gathering

The major missions typically flown by military combat aircraft are: air combat, intercept, air to surface attack, functional check, ground test, navigational, anti-submarine warfare, training, search-and-rescue (SAR). Each of these missions subjects the engine(s) to a particular usage profile, each of which will consume engine life at varying rates. For modern state-of-the-art aircraft, the mission flown is automatically recorded by the on-board mission computer and stored on a cassette tape. This information is downloaded after each flight, to provide a permanent record of all events during the flight.

This information includes engine data such as rotor speed(s), exhaust gas temperature (EGT), power lever angle (PLA), etc. In addition, some mission computers calculate cycle counts or life usage indices (LUI). For older generation aircraft, in-flight data is not recorded, and thus the only information available is the log entries from the pilot. This information has very little detail other than the type of mission flown (generic), and the number of flying hours.

Mission data is generally gathered by the squadron analysis group, and reports are forwarded to a central data registry. In some cases the information is catalogued or managed by private contractors on behalf of the Department of Defence.

4.4.4 Mission Mix Assessment

The mission mix is obtained by studying the mission profiles for a particular type of aircraft in the fleet to determine the percentage of time over which each mission type has been flown. A survey of multiple aircraft from different squadrons is used to determine the fleet average mission mix. To determine the mission mix, a mission analysis is required to evaluate the type of mission, the percentage of use for each mission, and the severity of each mission. Once the mission mix is known, a composite mission profile can be developed by applying the percentage of each mission applicable to a combined mission.

4.4.5 Determination of the Engine Duty Cycle

The engine duty cycle replicates the field engine operation for engine parameters such as speeds, temperatures and pressures for various altitudes and Mach numbers with activation of the anti-ice valves, bleed air, and horsepower extraction. For the development of an AMT cycle, the engine duty cycle is obtained from the mission profile data. If exact engine data are available from the on-board computer, then a realistic profile of engine parameters is plotted to illustrate the actual duty cycle as shown in Figure 5. If pilot observations are the only data available, then a generic engine duty cycle will be used for each mission.

4.4.6 Design Duty Cycle Development

In essence, AMET's eliminate, or reduce, the engine operation phases which contribute very little to the stressing of a part investigated. Conversely, an AMET must contain all the damaging elements in service that drive the particular failure modes.

The design duty cycle is developed from the missions mix and the engine duty cycle to determine the thermal and strain response of the engine components. To develop the cycle, the sequence of events, the range, dwell time, quantity of cycles, and inlet conditions must be known. The AMT cycle is usually obtained by removing or shortening the dwell time at part-power settings or removing the partial throttle movements from the engine duty cycle, as shown in Figure 5.

4.4.7 Generalised AMET Requirements

The basic requirement of any AMET is to ensure that the design duty cycle contains all the damaging events that drive the particular failure modes of interest. Secondly, it must adequately simulate the mission mix, and finally, it should eliminate the non-damaging events to provide the test time compression factor. To reduce the test time, increased turbine inlet temperatures are sometimes used.

It is generally accepted that no single accelerated endurance test schedule will completely evaluate an entire engine. All damaging conditions are not fully simulated during AMET testing, such as parts like bearings and accessory components that are sensitive to total engine run time, flight manoeuvre loads, and installation effects, such as external pressure and vibratory-induced loads. Particularly bearing distress, which is very much a function of manoeuvre loads encountered in flight, cannot easily be simulated through ground tests.

There are risks in interpreting AMET test data: Deterioration may be achieved in one engine part but not in others, or it may be exaggerated in one vis-à-vis others. This situation may lead to confusing and misleading results.

Where flight conditions would affect the engine or component durability, testing in an altitude facility, or in flight, may be necessary.

While it has been acknowledged that AMET testing yields significant saving in engine test time, a test program may still comprise many cycles and several hundred running hours.

4.4.8 Procedures for the Development of an AMET Cycle

The procedures outlined below are for the development of an AMT to test the durability of repaired parts in a fully qualified production engine that has a known service history.

- a) Determine the potential failure modes for the parts that are being tested. This information comes from the service history of the parts.
- b) Determine the mission mix for the engine under test, and acquire the mission profile(s) or preferably the engine duty cycle(s).
- c) Remove non-damaging segments of the engine duty cycle(s) to form the design duty cycle(s). For example, if the primary failure mode is creep damage, remove all throttle cycles and increase dwell time at high power settings. If thermal fatigue is the concern, increase idle-max throttle movements and remove partial throttle settings. Warm-up, cool-down and idle dwell times should be of a sufficient duration to simulate thermal relaxation behaviour within the components.
- d) Combine the design duty cycle(s) together in proportion to the mission mix to arrive at the composite profile. The final step is to determine the shutdown time between cycles. Typically 20-30 minutes is chosen to allow the core temperature to drop down below 200 F. This constitutes the final AMT cycle.

4.5 Methodology for Design Change Approvals

A schematic of the methodology is presented in Figure 6 with each step detailed in the following sections.

4.5.1 Application

The initial application must be made in writing by the DND Design Approval Organization (DAO) in a manner approved by DND. This application should include a brief description of the repair or modification. If at all possible, the application for approval should be accompanied by the preliminary data package.

4.5.2 Initial Data Review

In order to expedite the approval process, the initial application to DND for repair or modification design approval should be accompanied by data describing the nature of the repair or modification, the proposed certification standard(s), the criticality of the component(s) affected, and any proposed testing requirements.

4.5.3 Identify Certification Standard(s)

All aeronautical products are designed to a certain standard of airworthiness. Military equipment may be designed to a standard written specifically for a given mission, while equipment originally certified for civilian use would have been certified to the applicable civilian airworthiness standards.

In order to maintain the same level of performance, reliability, and safety, it is essential that any modifications and repairs be carried out to the standard the original product was certified to.

The applicable standard of airworthiness must therefore be chosen as the first step in any modification or repair approval.

4.5.3.1 *Applicable Military Standards*

Military standards for engine certification may include, but not be limited to the following:

MIL-STD-8593
MIL-E-005007
MIL-STD-1529.

Other military standards may be applicable depending on the type of engine.

4.5.3.2 *Applicable Civilian Airworthiness Standards*

Many engines in Canadian Forces can also be found in the civilian market. Common ones include the General Electric CF-34 and Avco Lycoming ALF-502 turboprops on the Canadair Challenger aircraft, the PT-6 family of turboprops, the JT-3C turboprops on the Boeing CC-137 aircraft, etc.

Applicable civilian airworthiness standards for engine design include the following:

CAR-13 (obsolete, superseded by FAR-33, but still applicable to old engines)
FAR-33
JAR-E (European standards)

The basis to which an engine was approved is called the Certification Basis or Approval Basis, and can be found in the applicable Engine Type Approval (Transport Canada document), or Type Certificate Data Sheets (U.S. Federal Aviation Administration (FAA) document).

4.5.4 *Design Compliance Program*

Once the applicable airworthiness standard(s) has been identified, the affected paragraphs should be presented by the DND-DAO as items requiring a demonstration of compliance for the particular modification or repair in question. The compliance program, or compliance checklist, should be reviewed for completeness with respect to the paragraphs and items affected.

Method of demonstrating compliance, whether analysis or test, or design, etc., should be reviewed in conjunction with the FMECA Qualification and Test Qualification Methodologies below.

4.5.5 *Failure Modes & Effects Criticality Analysis (FMECA)*

For any proposed modification or repair to an engine or component therein, a Failure Modes Effects Criticality Analysis is required to assess and identify component criticality and to initially define subsequent hardware test requirements.

4.5.5.1 *Coupon/Rig Test Requirement*

Evaluation by the FMECA should have identified the detailed coupon and rig test requirements necessary for the proposed engine modification or repair. Any coupon and rig testing should normally be completed prior to any engine block or Accelerated Engine Testing (AET), unless such testing is deemed unnecessary.

4.5.5.2 *Accelerated Engine Test or Block Test Requirements*

Where Accelerated Engine Test or Block Testing has been identified as required by the FMECA, the test parameters, test mission cycles, and test plan as proposed by the applicant should be reviewed for its validity and appropriateness for the engine type in question. The final test requirements should be agreed upon between the DND-DAO and the DND technical office prior to proceeding with the test program. This is to avoid unnecessary testing and having to repeat tests.

4.5.6 *Test Witnessing*

All testing as identified above are to be witnessed by either a Delegated Engineer from the DAO, or by a DND technical representative.

4.5.7 *Final Data Review and Design Compliance Program*

Upon completion of all necessary engineering substantiation the final Design Compliance Program should be signed off by all Designated Engineers (DE's) involved. All compliance items should be signed off as approved by the DAO (where authority has been delegated to the DAO), or recommended for final DND approval where the item is not delegated to the DAO. The applicable military standards and/or civilian airworthiness standards should be referenced in the compliance document.

All related test and analysis reports, and any other related documents for the modification or repair, should be referenced from the compliance program.

4.5.8 *Final Reports*

All reports associated with the modification & repair in question should be submitted for DND review and records prior to the issuance of the final approval. The following is a list of reports that could be required with a modification or repair program:

- (a) Analysis Reports
 - (i) FMECA
 - (ii) Stress, Vibration, Thermal, etc.
- (b) Test Reports
 - (i) Coupon / Rig Test results
 - (ii) AET Results

4.5.9 *Issuance of DND Approval on Modification or Repair Design*

Once all documentation has been reviewed, and compliance program signed off with all items being approved, either by the DND-DAO and/or by DND, an approval may be issued by DND on the subject modification or repair through a "Certification Management Plan".

5 CONCLUDING REMARKS

The development of a methodology for repair/rework/design change of gas turbine engines and the required airworthiness certification has been completed.

This methodology has addressed an organized engineering approach for engine structural repairs or material protection/rejuvenation through analysis and qualification, and for life cycle management of repaired gas turbine engines through an ERSIP.

The goal of ERSIP is to ensure structural safety, durability, reduced life cycle cost and increase service readiness of a repaired engine.

As part of the repair/rework qualification methodology the developed computerized FMECA tool has provided an insight to develop coupon and component rig tests which simulate these failure modes with the closest possible service condition. A failure methodology was developed for designing an engine block test cycle from the actual mission of a CF-18 aircraft and the EBT was utilized to certify the developed repair/rework. An important step in the post-certification is the plan to introduce the certified repairs/reworks into service. This was developed in conjunction with DND airworthiness authority through a "Certificate Management Plan". The design change methodology existing in the civil engine industry was reviewed and elements were incorporated into the certification management plan (CMP).

6 ACKNOWLEDGEMENTS

The authors gratefully acknowledge the Canadian Department of National Defence who have provided the opportunity for this technology to be developed and grown within Canada. As well, significant contributions were provided by the staff at the Institute for Aerospace Research at the National Research Council of Canada and the Orenda staff of the Advance Materials and

Energy Systems group who were involved in all aspects of this work.

7 REFERENCES

1) Qualification Methodology Development for Advanced Gas Turbine Repair/Reworks, Contract deliverable produced by Orenda for DND, 1995.

2) D. Fuleki, J. Dyer, P. Azar, P. Li, P.C. Patnaik and Captain R. Dhaliwal, "Qualification Testing of Component Repairs for the Canadian Forces F404-GE-400", Proceedings of the Propulsion Symposium, Canadian Aeronautics and space institute, 1998.

3) R.G. Andrews, D. Fuleki, J. Dyer, P.C. Patnaik, J.D. MacLeod and Captain S. MacDonald "Accelerated Engine Block Test Cycle Development for the Canadian Forces F404-GE-400 Engine Component Repair Qualification Program", Proceedings of the Propulsion Symposium, Canadian Aeronautics and space institute, 1997.

4) Capt. K.M. Jaansalu, R.R. Hastings and P.C. Patnaik, "Advanced gas turbine repairs and airworthiness certification", Proceedings of the Propulsion Symposium, Canadian Aeronautics and space institute, 1996.

TABLE 1 FAILURE MODES IN GAS TURBINE COMPONENTS

COMPONENT		FAILURE MODE	
		Primary	Secondary
Fan	Blades	Low Cycle Fatigue; High Cycle Fatigue (resonant vibration); Bird Strike; Foreign Object Damage Burst; Low Cycle Fatigue	Erosion Corrosion
	Discs		High Cycle Fatigue
Compressor	Blades	High Frequency Fatigue (resonant vibration); Foreign Object Damage; Engine Object Damage Burst; Low Cycle Fatigue	Erosion Corrosion
	Discs		High Cycle Fatigue
Combustors	Liner	Thermal Fatigue; Overheating	
Turbines	Blades	Thermal Fatigue; High Cycle Frequency Fatigue (resonant vibration); Tip rub/wear; Creep rupture Low Cycle Fatigue aggravated by thermal gradients; Burst	Engine Object Damage
	Discs		High Cycle Fatigue; Creep; Corrosion
	Nozzle Vanes	Hot Corrosion; Thermal Fatigue; Coating Distress; Overheating; Creep Deflection	Distortion Engine Object Damage
Low Pressure Shafts		Low Cycle Fatigue; Whirling	Creep (Hot End)
High Pressure Shafts		Creep (Hot End); Whirling; Low Cycle Fatigue	
Engine Casings		Corrosion	Blade Containment
Flanges		Low Cycle Fatigue	
Bearing Supports		Low Cycle Fatigue; Creep	

TABLE 2 MATERIAL PROPERTY UPGRADES

Types of Change	From	To	COMPONENTS TO BE ADDRESSED
Material Property Upgrade	Lower Strength	Higher Strength	Discs, Blades, Lever Arms, Hook Bolts, Shafts, Gears
	Lower Corrosion Resistance	Higher Corrosion Resistance	Discs, Blades, Casings, Shafts, Gears, Bearing Components
	Lower Impact Strength, Fracture Toughness	Higher Impact Strength, Fracture Toughness	Blades, Bearing Components, Casings, Shafts
	Lower Crack Growth Resistance	Higher Crack Growth Resistance	Discs, Blades, Shafts
	Higher Fire Retardant Properties	Lower Fire Retardant Properties	Casings (e.g. Titanium to Steel Casings)
	Upgrade of materials to newer specialty alloys offering low thermal expansion, high strength and oxidation resistance (e.g. Haynes alloy 242)	Upgrade of materials to newer specialty alloys offering low thermal expansion, high strength and oxidation resistance (e.g. Haynes alloy 242)	Seal Rings, Containment Rings, Duct Segments, Casings, Fasteners

TABLE 3 COMPOSITIONAL CHANGES

Types of Change	From	To	Components To Be Addressed
Alloy Composition	a. Changes in wt % content of (i) Aluminium (ii) Titanium (iii) Boron (iv) Silicon (v) Carbon		Weld fabricated, weld repaired components.
	b. Trace Element Content		
Alloy Material	a. Nickel Base Alloy	Cobalt Base Alloy	Turbine Blades, Vanes
			Afterburner sheet metal components, e.g. from Hastelloy X to Hayness 188

TABLE 4 PROCESSING CHANGES

Type of Change	From	To	COMPONENTS TO BE ADDRESSED
Microstructural	Polycrystalline	Directionally Solidified	Turbine Blades, Vanes
	Directionally Solidified	Monocrystal	Turbine Blades, Vanes
	Conventionally Forged	Dual Property	Discs
	Conventionally Forged	Investment Cast	Blades, Blisks
	Fabricated	One-Piece Investment Cast	Front Frames, Exhaust Frames
	Investment Cast	Powder Processed (Extruded)	Turbine Vanes
	Conventionally Forged	Powder Processed (HIP) (HIP & Isothermal Forge)	Turbine Cooling Plates Discs, Cooling Plates
	Precipitation Hardened	Oxide Dispersion Strengthened	Braze Repaired Components, eg. Turbine Vanes, Nozzles

FIGURE 1 TYPICAL FAILURE MODES FOR A TURBOFAN ENGINE

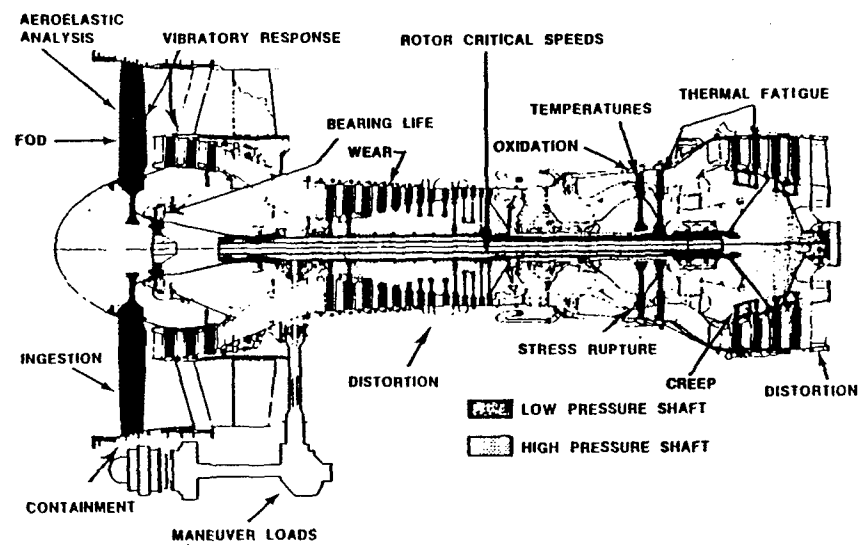


FIGURE 2 EXAMPLE OF COUPON LEVEL TESTING (FRETTING FATIGUE)

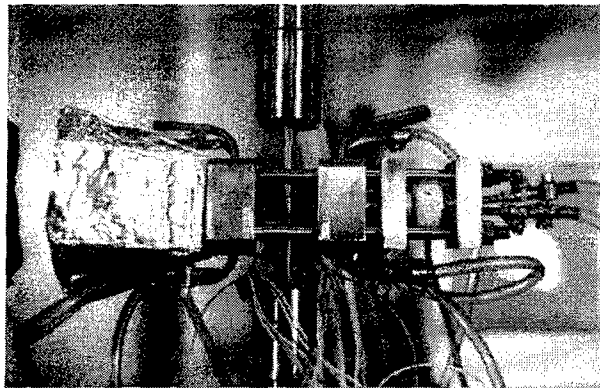


FIGURE 3 EXAMPLE OF COMPONENT TESTING (BURNER RIG)



FIGURE 4 EXAMPLE OF ENGINE TESTING (F404-GE-400)

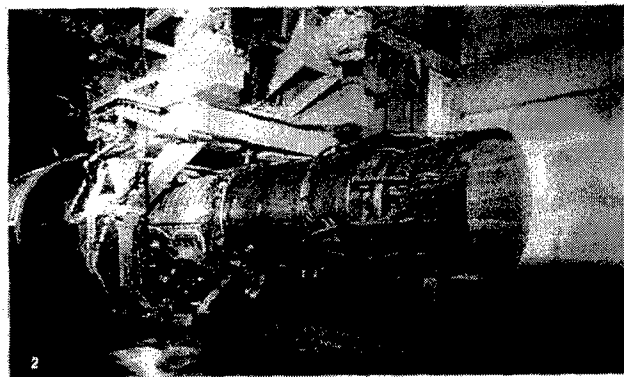


FIGURE 5 AMT CYCLE DEVELOPMENT

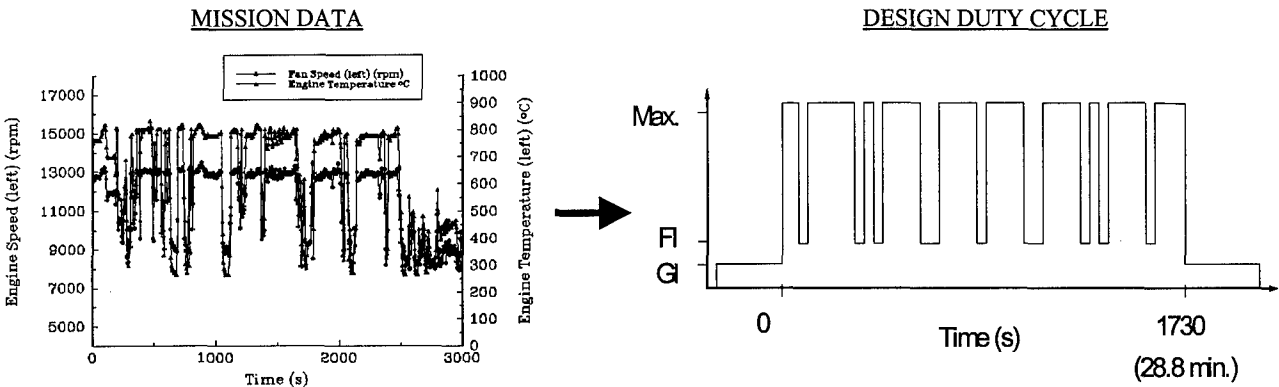
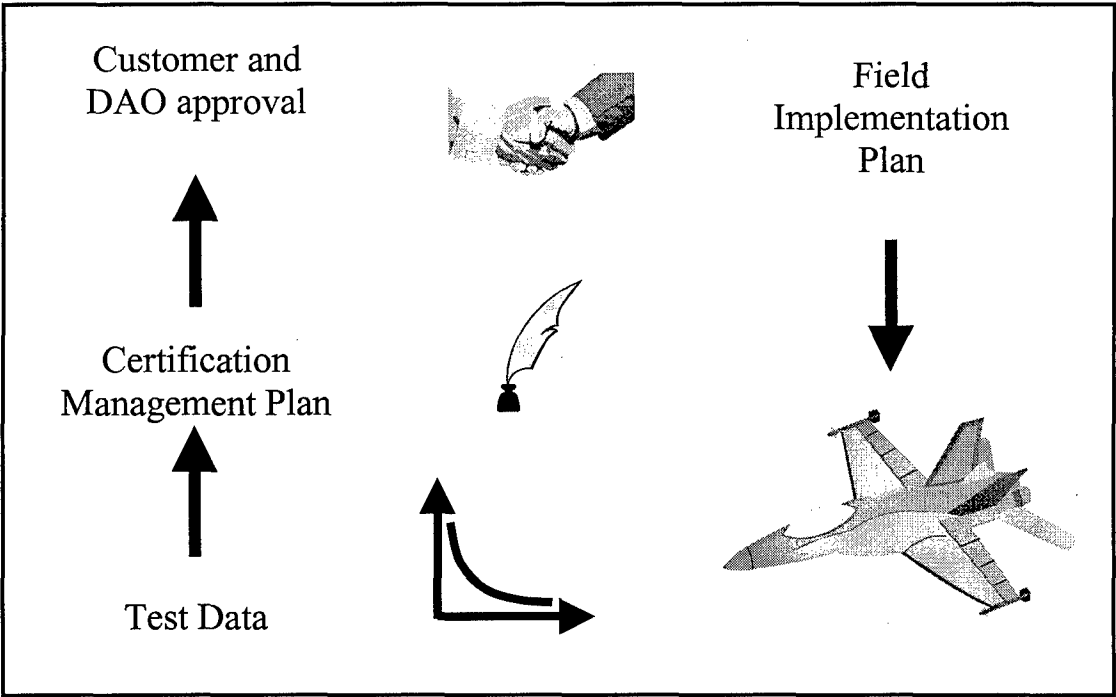


FIGURE 6 FIELD IMPLEMENTATION



Advanced Recontouring Process for Compressor Blades

M. Panten

Lufthansa Technik AG

Weg beim Jäger 193

22335 Hamburg

H. Hönen

Institut für Strahlantriebe und Turboarbeitsmaschinen

Aachen University of Technology (RWTH Aachen)

Templergraben 55

52062 Aachen

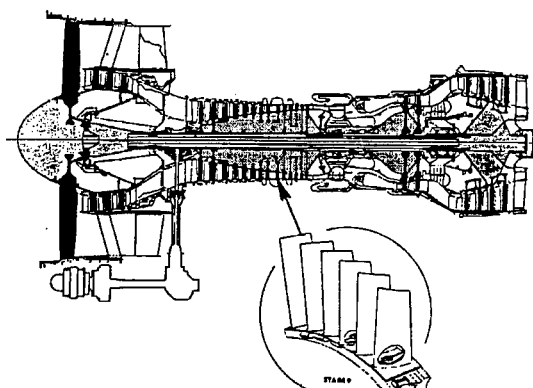
Germany

1. SUMMARY

The paper deals with the re-contouring of the leading edges contours of compressor airfoils by application of a new developed method for the profile definition. Lufthansa Technik AG and the Institute of Jet Propulsion and Turbomachinery, Aachen University of Technology have developed the "Advanced Recontouring Process" (ARP) which is an automated inspection and grinding process to produce defined and airflow optimised leading edge profiles with high reproducibility.

2. INTRODUCTION

The core engine of modern jet propulsion systems has an essential influence on the total engine performance. An important core engine module is the high pressure compressor.



Substantial performance factors here are the tip-clearance and the aerodynamic airfoil quality. During flight, the compressor airfoils are subject to wear and tear on the leading edge and blade tips mainly through erosion. This causes a shortening of the blade length as well as the chord length, thus causing a deformation of the leading edge profile. This results in a deterioration of the engine efficiency performance level and reduced stall margin.

During overhaul, airfoils should be restored to a quality as near as possible to the original condition. Appropriate repairs are made on the compressor blades and vanes of GE and CFMI engines (i.e. CF6 and CFM56 family). Leading edge blending is part of an essential working step. This occurs today by smoothing out on a wheel grinding station. However, in using this procedure, neither a desired contour

nor a sufficiently reproducible contour can be met. This results in product quality deterioration and, consequently, in airfoil performance loss. In order to obtain satisfactory compressor performance, the chord length limit often is restricted. This in turn means an increase in the yearly costs for spare parts material procurement.

In order to obtain an optimal air flow a precise working on the blade leading edge became necessary. The development of an appropriate process, the "Advanced Recontouring Process", was the answer.

3. REASONS FOR THE DEVELOPMENT OF THE ARP

3.1 AERODYNAMIC ASPECTS

Due to the erosion in the leading edge region the chord length of the profiles becomes reduced. This causes two problems. First the leading edge angle is decreased so that an increasing incidence angle ($\Delta\alpha$) and a shift of the stagnation point will occur (Fig. 2).

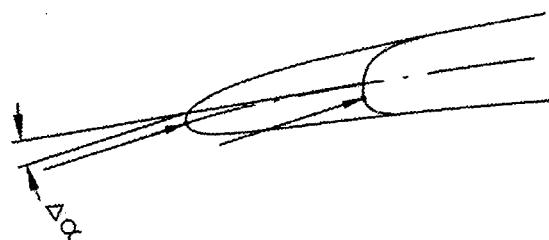


Fig. 2: Aerodynamic effects due to chord length reduction

Secondly, the aerodynamic load of the reduced profile has to be elevated in order to meet the original flow conditions of the blading. Both effects increase the risk of flow separation with high aerodynamic losses. Therefore, the problem of designing a new leading edge cannot only be reduced to a remake of the original one at a new position. It has to take into account the changed geometry and aerodynamic conditions in order to improve the performance of the redesigned blades.

3.2 HARDWARE ASPECTS

As already mentioned in the introduction, the L/E profile will change due to erosion during operation and also in the framework of engine overhaul by manual smoothing. To get an idea of the difference in comparison to a new part profile, the L/E profiles of statistical lots of worn blades were measured and evaluated as well as those of conventional

manually smoothed. The following pictures show typical L/E contours of rotor blades (Fig. 3a & 3b).

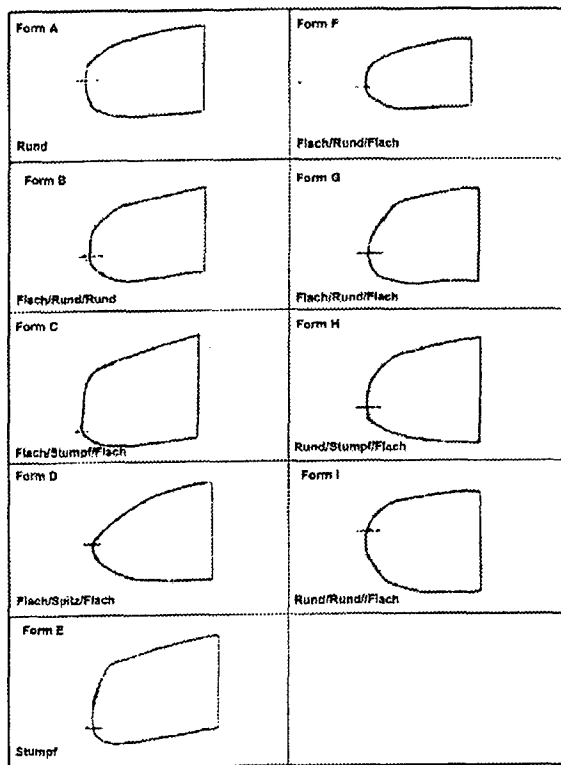


Fig. 3a: Different leading edge contours of worn blades

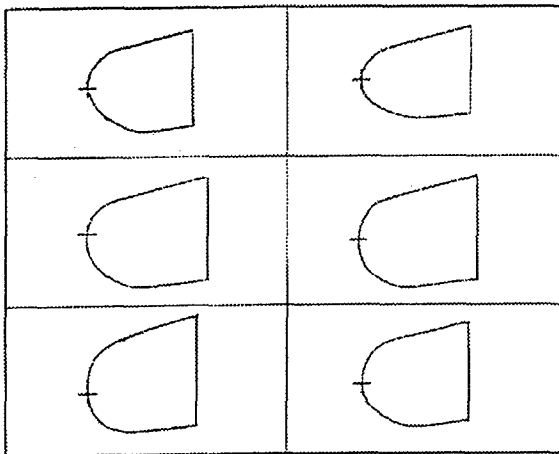


Fig. 3b: Different leading edge contours of manually smoothed blades

The L/E profile of a new part serves for comparison (Fig. 4).



Fig. 4: Leading edge contour of a new part blade

The deformation of L/E profiles leads to a variation of airflow conditions which deviate significantly from the

OEM designed one. The airflow quality deterioration could be proved by numerical simulation.

3.3 ECONOMICAL ASPECTS

To guarantee a sufficient overall compressor performance, even when using recycled blades, today's standard procedure is to offset chord length scrap limit against profile performance loss. Therefore, a scrap limit is applied which is above the shop manual (SM) limit and results in an unnecessary high scrap rate.

By using airfoil hardware which almost meets the originally designed flow conditions, several savings can be achieved:

- Improvement of overall compressor-/engine-performance leads to fuel savings (i.e. ~ 6.50 DM/EFH for CF6-50).
- SM limit of chord length can be applied as scrap limit. Full material exploitation provides at least one additional run.
- As a result of the improved airflow behaviour, erosion is reduced and consequently also the speed of L/E profile deformation. The mean time between overhauls will increase.

4. TOOLS FOR THE DEVELOPMENT OF THE ARP PROCESS

The quality of the working result is an important basis for the aerodynamic behaviour in the blade row. Therefore, geometric measurements of several manually recontoured blades were taken. A great variation in leading edge contours could be found. For a better understanding of the influence on the flow field around these blades, flow calculations were performed. The necessary boundary conditions were taken from the design flow data at the rotor inlet and outlet provided by the jet engine manufacturer. The calculation results demonstrated that a great number of worn blades produced quite poor flow conditions. However, since the whole variety of recontoured blade geometries is combined in one blading, a reliable overall performance can be provided. This investigation shows that a suitable monitoring scheme is necessary as a basis for high quality recontouring results.

This problem is even more important for the ARP. A precondition for the automatic production of recontoured blades is the exact definition of the target geometry for the grinding machine. Based on these data the manufacturing process produces leading edge contours with a high level of similarity. By this the performance of the whole blade row is already fixed with the definition of the target contour. In the worst case a wrong profile design could lead to extremely bad flow conditions in the bladings so that the performance of the whole compressor would be influenced. Therefore, a suitable method has to be applied to acquire reliable results of the flow behaviour of the recontoured blades.

Experimental investigations in a wind tunnel could provide detailed information about the flow field around one blade or the whole blading. In the case of a new part profile or a worn blade this would be a suitable way. However, the definition of the new leading edge contours for the worn blades is an iterative process with a great number of parameter variations. The time taken for the experimental effort involved would become unacceptable. Therefore, a suitable calculation method had to be applied in order to check the influence of the newly designed leading edge contours on the blade flow field.

In particular, the flow conditions in the front section of the blades are of great interest for a comparison of the recontouring results. The velocity and pressure distribution profiles as well as occurring flow separation should be visualised.

Since the numerical investigations for the recontouring are performed in a parameter variation, the time effort had to be minimised. The erosion of the blades occurs mainly in the upper third of the span. In order to provide a representative target contour for the manufacturing process, the calculations are performed for a radius at 10 % below the tip. A comparison of the results from a 3D and a 2D Navier Stokes calculation showed a reasonable agreement. Therefore, a 2D-Navier Stokes code has been chosen for the calculations.

The main interest in the analysis of the results is the comparison of the changes of the flow conditions due to variations of the leading edge contour. Therefore, a detailed resolution of the flow field especially in this region is very important. The quality of the results is directly based on the quality of the calculation grid. In this case an O-grid has been chosen for an optimal fitting of the grid elements to the leading edge profiles. Figure 5 shows the shape of the grid and the distribution of the calculation knots. The size is 201 x 33 knots.

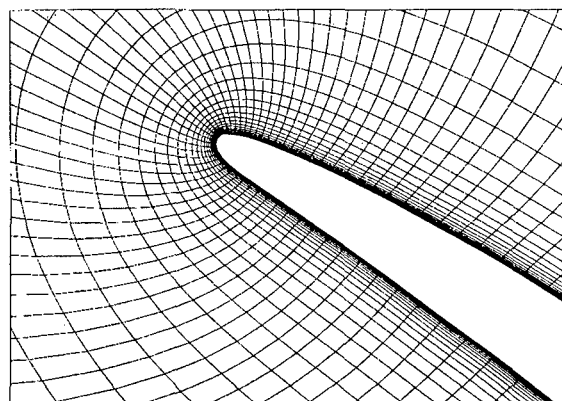


Fig. 5: Except of an O-grid fitted to the L/E contour

5. REALIZATION OF THE ARP

From the theoretical point of view each worn blade ought to be treated individually. That means that for each blade an individual target contour and an appropriate machining program for the grinding robot ought to be developed just in time during the overhaul process. This process is not realisable, however, for two main reasons:

- A closed algorithm for the determination of the target contours is not available.
- An automatic dynamic programming of a precision grinding machine for working the individual airfoil profiles may be realisable from the technical side, but from the economic point of view an invest in such an expensive and complex equipment is not sensible.

This led to the search for an easy and tolerant machining process (90%-solution). A procedure similar to that which has already been applied in new part production meets the requirements. The airfoils are machined on a grinding

station with a smooth grinding wheel handled by an appropriately programmed robot. Airfoil profiles with similarly worn contours show nearly identical shapes after having passed through this procedure. Therefore it was possible to categorise the large number of differently worn contours into 2 - 3 clusters per compressor stage. In the framework of airfoil overhaul they get inspected by a specially designed, computer-controlled inspection system, which measures the airfoil geometry according to defined criteria and selects them amongst other things into those clusters. The following machining of the L/E is then achieved with a grinding machining program which is appropriate to the specific target contour of the compressor stage.

6. DEVELOPMENT OF SUITABLE TARGET CONTOURS

The aim of the ARP-profile developing process is the definition of redesigned profiles with a high performance in combination with low profile losses. In order to meet this aim a reference base had to be established. The criteria are the flow parameters based on the design data of the manufacturer of the engine and the new parts themselves. The flow conditions around the ARP profiles should be in good agreement with those parameters.

For a judgement of the quality of the newly defined leading edge profiles several parameters had to be taken into account. One main problem is the behaviour of the ARP profiled bladings in the frame of the neighbouring bladings of the multistage compressor. Therefore, the flow parameters have to be kept in a defined range in comparison with the design values. First of all, the pressure rise as well as the turning angle of the ARP designed blading must be in agreement with the design. This causes comparable velocity and pressure distributions around the profiles. In addition the profile lift is calculated for a comparison with the original data of the new part profiles.

In a first step the contour of the remaining profile has to be checked. The criteria for the design of the new contour are the chord length, the profile thickness in the working area and the leading edge angle. By these parameters the maximum dimensions and the direction of the newly designed leading edges are fixed. In a second step different target contours are designed considering the above mentioned parameters. Possible geometric shapes are circles, ellipses, parabola or hyperbolas. The new L/E contours have to be checked concerning the transition to the remaining profile. At this position both contours must provide the same surface angle.

The profile data in the front part of the profiles are replaced by the geometric data of the suitable contours. Now the calculation grid can be fitted to each of the redesigned profiles and the flow calculation performed. The results are compared to those of the new part calculation. The aim of this procedure is the definition of a redesigned contour which provides a flow behaviour close to that of the new parts. By changing the construction parameters the shape of the new contours can be altered and the flow field optimised.

7. RESULTS OF CONTOUR DEFINITION

The first investigations were performed by calculating the flow behaviour of blades with L/E contours of different geometric shapes. The chosen geometric shapes were circles, ellipses, parabolas, and hyperbolas. Figure 6 shows

the arrangement of the new leading edge contours inside the remaining profiles.



Fig. 6: ARP L/E contour fitted into the remaining profile

The hyperbola type has the largest number of variation parameters. A redesign for the leading edges has been carried out based on several worn rotor blades of the 5th compressor stage. The calculated flow data of each constructed profile were compared with the design data of the engine manufacturer. The hyperbola construction showed very good results. Figures 7a and 7b show the calculated pressure distribution around the profile in comparison with a new part profile.

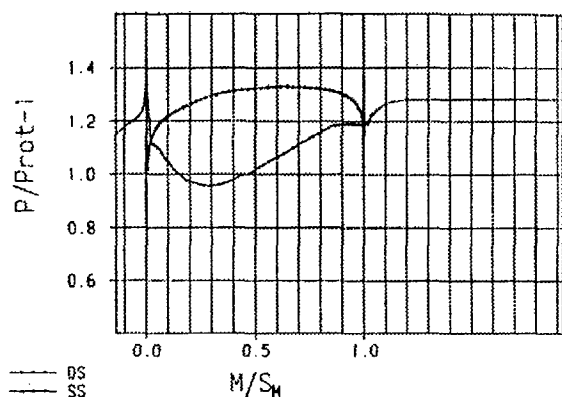


Fig. 7a: Pressure distribution around the OEM design profile

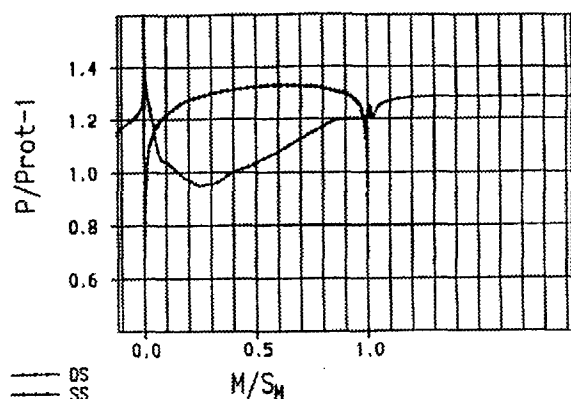


Fig. 7b: Pressure distribution around the ARP target profile (hyperbola construction)

However, for a good fitting of the new geometric form inside the remaining profile, a wide area of machining, up to 1/3 of the chord length, has to be accepted (see fig. 6). This involves a higher degree of abrasion, consequently the manufacturing process becomes ineffective. Furthermore, not sufficient material remains to allow application of more than two or three overhaul/recontouring procedures. Considering this, a minimised abrasion has to be aspired as an additional condition for the definition of the new leading edge contours.

For the further investigations the machining area was limited to 10 - 15 % of the chord length. With this limitation the parabola and the hyperbola were no longer suitable as new contours. It was impossible to find a parameter set which covers the above defined conditions. The activities were concentrated on optimisation of the elliptical leading edge contour. By redefining the construction method, the performance of the newly generated blade contour could be further improved. The method has been approved for a large number of worn blades of the 5th and 7th stage rotors. The good results of the flow calculations provide the basis for the application of this method to the whole compressor. Figures 8a and 8b show the pressure distributions of a new part blade in comparison with a redesigned blade of the 11th stage.

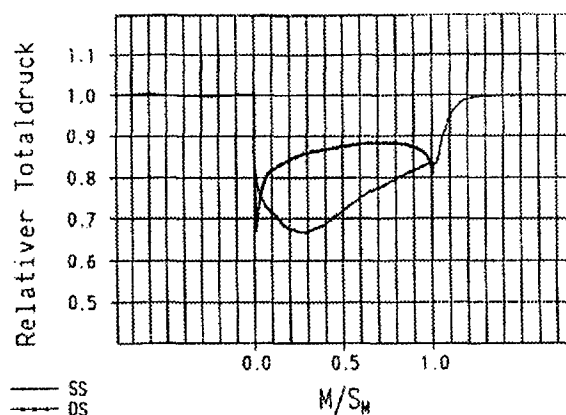


Fig. 8a: Pressure distribution around the OEM design profile

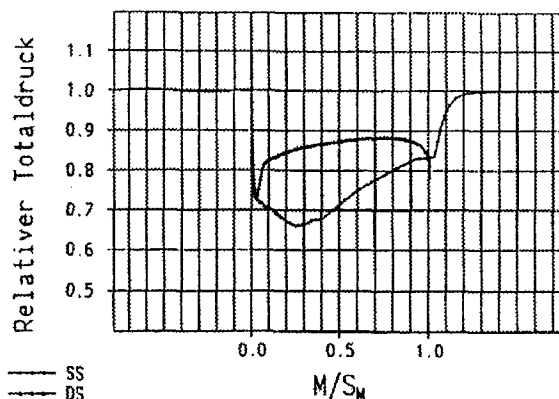


Fig. 8b: Pressure distribution around the ARP target profile (elliptical construction)

8. LEADING EDGE MACHINING PROCESS - RESULTS

The machining process described in chapter 6 is used to realise L/E profiles with the contour characteristics of the specific target profiles. The correlation between target and recontoured profiles is not 100% exact but it is a very good approximation. Statistical checks applied on test series have shown that approx. 95% of all blades treated with the ARP are nearly identical to the specific target contour. The quality of the remaining 5% was similar to the conventionally smoothed blades or better.

The following both pictures illustrate the airflow performance of a worn blade (HPC rotor CF6-50, Stg. 5) and of the same blade after passing through the ARP machining process. The improvement is clearly visible when comparing the corresponding relative pressure distribution diagrams (Fig. 9a & 9b). It is obvious that the flow separation on the pressure side (pressure collapse) has been nearly eliminated after application of the ARP.

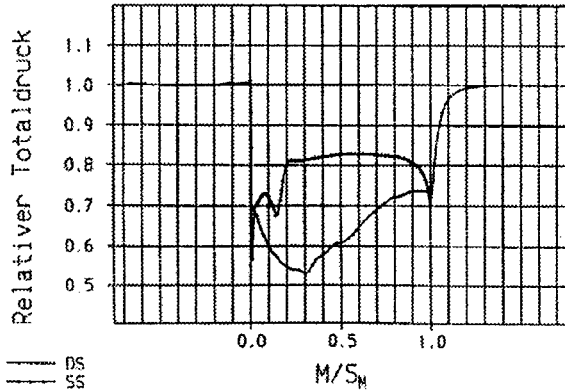


Fig. 9a: Calculated pressure distribution for a worn blade

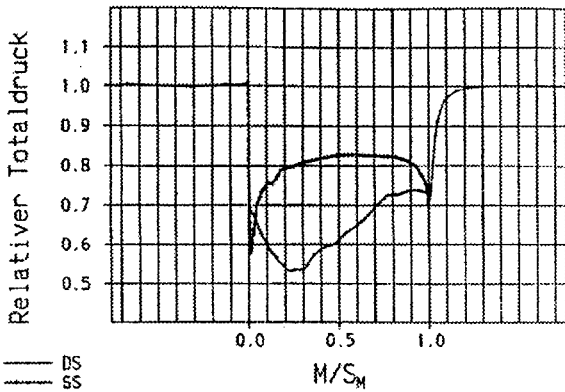


Fig. 9a: Calculated pressure distribution for the same blade after the ARP machining process

9. CONCLUSIONS

A new method for the re-machining of the leading edges of compressor airfoils has been developed. This method provides an improved airfoil aerodynamic compared to conventionally overhauled profiles. The resulting overall performance of the compressor could be increased to approach as closely as possible to the original design performance of the engine manufacturer.

The economical consequences for the operator are fuel savings due to an increased compressor efficiency, reduced technical operating costs due to extended on-wing times, and reduced spare part costs due to a better use of the airfoil material.

Repair developments to fit customer needs

Daniel Burlon
CFM56 Product Support,
Manager, Turbomachinery
Snecma-Services Melun-Montereau
77019 Melun Cedex

Introduction

This presentation describes the repair development process from identification of repair needs to repaired parts installed on an engine. The key factors in this process will be identified and economical inputs will be highlighted. The presentation will show how and why Snecma-Services involves his customers in identification of repair need and in evaluation process. This process is called : Top Repair Program.

Repair development process

After reminding the repair goals, identification of repair need, repair evaluation, repair substantiation and repair development, which are the main steps of the repair development process, the development process will be described. After the presentation shows when a repair substantiation must be requested. The conclusion of the first part outlines the economical inputs to be taken into consideration by a repair source before offering a new repair.

Some words about "Repair"

The goal of a repair is to restore initial part properties. Main properties are the functionality and the mechanical resistance. So, before to develop a new repair, the root causes for part deterioration have to be understood. The common deterioration causes are erosion, oxidation or corrosion, fretting, wear, thermal deformation... Fixes to correct part deterioration have to be identified and evaluated. If they appear to be efficient, they must be incorporated through modifications which are not classified as a repair.

Repair need identification

Identification of repair need are done all along the engine life. It starts during design. In an engine development program the design schemes include part reparability as a major item. Previous model experience is also used. All developed repairs on previous models are analyzed and the development decided when the deterioration causes are expected to be similar on both models. All common parts (Same part number) can be repaired using a Rep (Repair page in the Engine Shop Manual) from any engine model. If a Rep is available for a part number fitted on a given engine model, the Rep must be introduced into this engine shop manual.

Experience from development is providing a lot of inputs for identification of repair. Parts from factory test engines are inspected to demonstrate the engine and the part behavior in order to understand deterioration

modes. Then corrective actions are identified and developed. If no corrective action is suitable to avoid part deterioration, a repair is identified and developed

Later in-service experience will be used. Obviously, factory tests do not reflect exactly field experience. So, in-service experience is carefully collected to identify deterioration causes and develop fixes and/or repair. This experience is collected by several ways, shop finding reports, which are provided by on-site representatives, customer questions and Top Repair Programs, which will be presented later in this presentation. All these inputs are analyzed, and each time a repair need is identified, an evaluation is performed and a solution is defined. The solution can be a repair or any other solution if it fits customer needs.

Repair evaluation

When repair need is identified a evaluation must be performed. This evaluation must find the adequate technology and the process to perform the repair. Expected benefit life after repair must be evaluated. The repair substantiation program has to be defined, after that development and substantiation costs will be evaluated. The customer cost of the repair must be evaluated, versus expected benefit and the cost of a new part. Finally, the decision to develop the repair or to provide the customers with alternative solutions is taken.

Repair substantiation

The goal of the repair substantiation is to demonstrate that the repair will restore initial geometrical and mechanical properties. Geometrical dimension are affected by wear and deformation mainly. Mechanical properties are affected by heat treatment, welding, plasma spray but also by diffusion between basic material and coating.

Repair substantiation program will define and perform the laboratory test to check that mechanical properties are not too much affected by the repair process. The key process and inspections to be performed to insure the repair quality have to be identified. If needed, an engine factory test or an in service evaluation will be defined and performed in order to validate the repair.

Repair development

The repair development start with the design and the realization of the tooling. The repair is performed on the first parts in using as much as possible "production conditions". Then all tests and inspections required by the substantiation program are conducted. The results are evaluated and corrective actions decided, if needed.

Finally the Repair document is issued and introduced into the shop manual.

Proprietary process

Some specific parts or repairs may request Proprietary processes, which bring better properties or better reliability than standard processes. Most common proprietary processes are coating and brazing

Proprietary Process example

Proprietary Process example



Source and Services Proprietary Data Unsubstantiated Disclosure Prohibited

Page 1

The process used to repair cracks in airfoil inner/outer platform surfaces on LPT nozzles segment is Recharge Brazure Diffusion. This process is a proprietary process developed by Snecma. To be substantiated each shop has to demonstrate its capability to refill the cracks and that the diffusion fulfills Snecma requirements.

Critical repair

In some cases repair quality is insured by the process itself and cannot be checked only during final inspection. So for this repair Snecma-Services requests shops to define precisely their own processes, to check the repair quality through destructive inspections then shops must follow exactly the approved processes. Fan blade patching or major case rebuilt are examples of critical repairs.

Critical Repair example



Source and Services Proprietary Data Unsubstantiated Disclosure Prohibited

Page 1

Repair source substantiation

Snecma-Services requests the shops to be substantiated when they wish to perform Proprietary or Critical repair on CFM56 engines. To be substantiated, a shop must

have access to the proprietary processes from the owner of the proprietary process. The owner of the proprietary can be the original engine manufacturer or an independent company. The substantiation process starts with the definition of the substantiation plan, which must prove that the implemented repair process will provide requested quality level. Usually Snecma-Services provides guidelines to define substantiation plan. The shop must perform the substantiation program and Snecma-Services reviews the results before pronouncing the substantiation.

Conclusion

Snecma-Services goal is to provide a repair source for all repairs and if possible more sources. Repair shops must take into consideration market size, investment cost and expected benefits before implementing any repair process.

Top repair program

The goal of the Top Repair Program is to identify customer needs in a data driven approach. The top repair program will help the customers and Snecma-Services to identify and prioritize repair needs. This program will work only if customers provide inputs.

Top Repair Program Overview

The main steps of the top repair program are input data, Snecma-Services analysis, feedback to the customers and data exchanges between Customers and Snecma-Services.

Needed input data

Basically inputs are the number of parts waiting for a repair on shelves. However, some other details will be useful as part identification including Part Number, Serial Number, Time since new, cycles since new. An accurate description of the defects helps to understand the root cause of the deterioration and to define a fix or a repair. Snecma-Services adds customer inputs to prioritize the repairs. The cost of the part is a key element to prioritize the repair. Parts expected to need a repair in the coming months will be taken into consideration to prioritize the repair development program.

Snecma-Services analysis

Every time the product support engineering receives new data they are analyzed, the Top Repair Program data base is updated by adding the new parts on shelves and all requests are reevaluated. Afterwards the repair programs are sorted.

The repair program are sorted versus of the total value of parts waiting on shelves in the different shops. So, even if a customer has one part only, other customers might have one or several, so when they reports their parts on shelves to Snecma-Service, Snecma-Services adds all requests. When the total value of part on shelves reach the amount of \$75.000 the repair program is launched in priority A. If the amount does not reach \$75.000 but if

the fallout rate is expected to be high enough to reach this value the repair program is launched in priority "B". If the amount does not reach this value and it is not expected to reach it, the repair need is recorded as priority "C" and the program not launched.

Snecma-Services feedback to the customers

Snecma-Services provides the status on all repairs in process, priority "A" & "B". The customer participating to the Top Repair Program are periodical informed on each request repair development program target date and technical information when the request is answered by a repair. Periodicity is agreed between Customer and Snecma-Services. If the request is not answered by a repair, alternate solutions are evaluated.

Conclusion

The Top Repair Program provides better visibility on repair programs to customers and Snecma-Services. It helps customers and Snecma-Services to better forecast repair and spare part needs. The Top Repair Program helps Snecma-Services to fit customer needs. Customer inputs make the Top Repair Program a key process on Snecma-Services repair programs.

Fracture Mechanics Evaluation of Weld Repaired Seal Teeth for Life Extension of Aircraft Gas Turbine Engine Components

P. A. Domas

GE Aircraft Engines

One Neumann Way, M/Z K105
Cincinnati, OH 45215-1988, USA

1. SUMMARY

Typical aircraft gas turbine engine rotating air seals incorporate radial protruding, knife-like, circumferential seal teeth at the outer diameter that intrude into a surrounding abradable shroud, forming a seal to unwanted air passage. The thin teeth are susceptible to wear in operation and nicks and dents during assembly and disassembly for overhaul. It is economically desirable to be able to repair such worn or damaged seals for return to service. A potential repair process is to grind down the tip of a damaged tooth, rebuild it with overlaid layers of similar alloy weld metal and machine the built up material back to final shape. A complication is that the welded material may contain porosity or other microstructural features that can act as surface or subsurface fatigue crack initiation sites and limit the cyclic life capability of a repaired tooth.

This paper discusses an experimental fatigue test program and associated test specimen and component fracture mechanics analyses conducted to assess the viability of a seal tooth weld repair process. The role of simulated component fatigue testing, nondestructive evaluation, fatigue and residual life prediction, and design trade studies in determination of life extension plans is discussed. Complications and issues that arise and potential means of addressing these are emphasized.

2. INTRODUCTION

Figure 1 depicts a typical gas turbine engine circumferential air seal tooth configuration that could be considered for repair. Such seals are used in components manufactured from various alloys (e.g. Rene'95, Ti-17, IN718). Several base material - weld filler material combinations are feasible and have been evaluated. The phase of the

development program discussed here assessed Ti-17 base material welded with Ti-6Al-4V filler.

Among the first steps in this effort was the generation of a cause and effect diagram as outlined in Section 3. This and other "Six Sigma" tools^{1,2} proved useful in identifying potential risks to meeting the desired goal of a viable repair compatible with component life extension objectives.

One concern identified was potential inadequate low cycle fatigue (LCF) life due to possible imperfections in the weld repair material. To assess this a fatigue test program was conducted (Section 4).

The testing identified porosity and other microstructural and manufacturing related imperfections as likely limitations to repair applications with this alloy combination. A fracture mechanics analysis of the specimens (Section 4.2) proved useful in understanding the test results and in guiding selection of lower risk applications (Section 5.0).

This program offers experience of possible use in developing life management and extension methodologies as discussed in Section 6.

3. CAUSE AND EFFECT ASSESSMENT

As part of the program planning a cause and effect or fishbone diagram similar to that in Figure 2 was generated by a cross functional Design, Repair, Materials and Life Management Engineering team. The defect was defined as "failure to meet non-repaired part usage capability" and potential causes that might contribute to that outcome were brainstormed. Among the key concerns was the possibility of imperfections in the built up weld material or at the weld metal - parent metal

interface, serving as initiation sites for LCF cracks. A risk abatement identified for assessing this potential was to conduct a laboratory LCF test program on weld repaired seal teeth. The objective was to test samples simulative of typical component geometry (and the associated challenges for the weld repair procedure). The samples were prepared using materials, tools, methods and personnel as representative of planned production as could be obtained.

4. LCF TEST PROGRAM

Simulated seal tooth specimens, as shown in Figure 3 were cyclic fatigue tested in axial load control, $R \sim 0.05$, 20-30 cpm, 600F (316C) at several stress levels. The specimens were symmetric with three teeth per side. Tooth geometry and spacing were typical of component seal configurations. Specimen blanks were excised from Ti-17 (beta) forgings by wire electro-discharge machining and the teeth milled into the blanks. Some specimens were tested without repair to establish a baseline. Some specimens had the tooth tips initially machined off, were repair welded using Ti-6Al-4V filler material to rebuild the tooth height, and then were final machined to nominal configuration. The induction heated samples were cycled to failure (separation). [Initial attempts to detect crack initiation using extensometers were abandoned because of lack of sensitivity in this complex geometry sample.] Some tests failed due to causes extraneous to the test and some tests were purposely discontinued.

4.1 Test Results

Figure 4 is a graph of alternating stress versus cycles to failure showing the results of the seal tooth tests for four sets of conditions:

- Baseline (non-repaired)
- Weld repaired and tested as welded
- Repaired, heat treated and tested, and
- Repaired, alternative heat treated and tested.

Also shown for reference are cylindrical (smooth) bar, low stress ground and polished, load controlled Ti-17 specimen results. Points for tests stopped before failure or failing from extraneous causes are flagged with an arrow.

Some general observations from these data were:

- Simulated seal tooth specimens, even without repair, had lower LCF life than standard round bars
- There was large scatter in repaired sample lives
- Weld repair sample LCF life was lower than non repaired samples
- Post weld heat treatments did not improve the repaired sample results.

Fractographic examination of the failed welded samples, such as in the one example shown in Figure 5, revealed typical crack initiation occurring in the weld metal region from various imperfections including porosity, large microstructural features (e.g. grain facets) and laps left during the machining.

4.2 Fracture Mechanics Analysis

The metallographic evidence of failure from weld imperfections led to conducting a simplified fracture mechanics (FM) analysis. The pore sizes at the initiation site of four samples at several stress levels were measured and modeled in an FM analysis as a buried circular crack in a thin plate approximating the tooth geometry. The predicted residual life is compared to the test results in Figure 6. In one case the life was very well predicted. However, in the other three cases the prediction was approximately half of the observed cycles to failure. Weld metal crack growth rate variability, FM model approximations, potential nucleation cycles required to transition the imperfection to a sharp crack, and stress redistribution as the cracks propagate are some potential causes for this typical under prediction.

These same model predictions are shown as the solid line in Figure 4. Despite model shortcomings, the FM model predictions tend to lower bound the weld repaired data and are consistent with a large life reduction potential under some conditions

4.3 Test Program Conclusions

It was concluded that the repaired specimens could be life limited by cyclic crack growth from included porosity and other metallurgical or mechanical imperfections. The presence of these imperfections introduces a probabilistic aspect to the expected component behavior. The LCF life capability depends upon the presence and severity

of these imperfections and can lead to significantly increased scatter. The statistical aspects have a twofold importance: a) the allowable design stress levels for repaired teeth should reflect potential imperfection size (and behavior) variation; b) the assessment of the applicability of the repair process is influenced by the degree of variability. That is, the process may be good on average, but excessive variability could preclude general use. Implications include, for example:

- Necessity to include determination of an imperfection size distribution or at least a determination of the largest possible imperfection size in assessing repair viability
- Inclusion of FM analyses (with starting crack sizes representative of the imperfection size distribution) in repaired component LCF life assessment
- The need to better characterize the amount of nucleation time associated with some imperfections, or to default to an often pessimistic FM prediction based on imperfections size alone.

5. APPLICATION SENSITIVITY ANALYSIS

Recognizing the susceptibility to tooth damage and the behavior of the Ti-64 repaired Ti-17 specimen testing, an analytic sensitivity study was undertaken to assess the suitability of selected engine component seal teeth to weld repair. A simple single edge notch, uniform stress, constant temperature, thin flat sheet, $R=0$, FM model was used. Design analysis operating loads and temperatures for each specific tooth rack were input to the model with an assumed initial crack depth of 0.005" (0.127 mm). Residual lives were calculated for titanium and nickel base alloy teeth from the fan through the turbine for various engines. Results are summarized on graphs of relative mean stress versus relative residual life in Figures 7 and 8 for nickel and titanium teeth respectively. [The stress scales are normalized by an arbitrary high end mean stress value and the residual life scales by the specified minimum life requirement for the component.] Obviously repair of more highly stressed teeth provides less margin to life requirements than repair of teeth operating at lower stress (or temperature). There are a significant

number of teeth, particularly in the nickel alloy, that have substantial predicted residual life capability from a 0.005" deep initial imperfection. These teeth are more likely candidates for repair than the others.

Another potentially useful result from these analyses is shown in Figure 9. The FM model predicted relative critical crack sizes for the various teeth are plotted for several component alloys and compared to the planned depth (below the tip) of the weld repair. "Nickel alloy 2" teeth have comparatively short critical sizes confined to the repaired material zone. Any envisioned nondestructive evaluation (NDE) methods would need to be capable of detecting cracks smaller than these sizes and recognize the further challenges presented by the cast material structure of the weld material. "Nickel alloy 1" teeth have comparatively large critical sizes in some applications and would likely be better suited to inspection and perhaps more amenable to several alternate NDE methods.

It is clear that many other factors, such as: weld material integrity (e.g. contrasts in nickel weld filler to titanium weld filler failure modes), susceptibility to damage (e.g. exposure to foreign or domestic object damage (FOD/DOD)), consequence of failure, accessibility, inspectability and component life cycle cost enter into candidate tooth selection. The FM analysis provided a physical behavior motivated, quantitative measure of repair potential that assisted in program planning decisions.

6. OBSERVATIONS

Some observations from this program are potentially useful in establishing best practices for developing life extension schemes.

It is clearly essential to validate proposed life extension methodologies through testing that confirms ability to achieve the ultimate requirement, namely component life. While theoretical and analytical arguments can be compelling, in general there are sufficient unknowns to warrant confirmation of assumptions and understandings through test. These unknowns can be identified through risk assessment, failure modes and effects, and root cause types of exercises.

Testing programs introduce their own complications. In the present example the non-standard test sample was expensive to make, difficult to analyze (complex geometry) and provided test results that were sometimes difficult to interpret (e.g. load versus strain control, non-uniform material properties through the cross section). Never-the-less, a combination of analysis and metallurgical evaluation in conjunction with recognition of the limitations of the sample provided key insight into likely repaired component behavior. This guided selection of appropriate Design analysis tools and helped assess production and field NDE needs.

It is prudent to consider all of the potential product lines that might be affected by implementing a particular scheme. Again with reference to the tooth repair project, certain combinations of component alloy, tooth location, engine usage, and repair process offer a high likelihood of success. Other combinations were assessed as having low probability of resulting in adequate life extension.

As is often the case, when dealing with problems relating to component life exhaustion and rejuvenation, fracture mechanics provides a highly useful tool in understanding observed behavior and forecasting component life.

7. CLOSING

The test program, results and analyses presented here do not represent state-of-the-art innovations or advancements. In fact some of the early testing was concluded in the late 1970's. Rather, the retrospective review of a perhaps industry typical component life extension type of program is offered as a vehicle for identifying and discussing some of the issues arising in such an undertaking. These were mentioned in Section 6.

In addition, planning tools such as cause and effect diagrams, Product Trees and Pareto diagrams being more widely promoted through quality and reliability initiatives across various industries including the aircraft engine industry^{3,4} are useful to ferret out potential technology and program risks to be abated.

Finally, this example highlights the increasingly recognized, but always present, process variability and the need to quantitatively characterize process

capability in terms of desired margins and specification limits.

The term "6-sigma" is increasingly being used to describe quality and reliability initiatives across various industries^{1,2} including the gas turbine engine industry^{3,4}. In simple terms the concept utilizes data collection and statistical data analysis to quantitatively establish process capability and margins in relation to specification limits. Most often this type of quality measurement is discussed in connection with manufacturing issues such as tolerances or scrap rates. However, the concepts are potentially useful in assessing "design margins" or other possible engineering measures of component robustness.

8. ACKNOWLEDGMENTS

Several GE Aircraft Engine teams contributed to the results discussed by the author. The contributions of S. Schnure, E. Strable, C. Sasser, W. Wagner, H. Lynch and A. Coles in planning and conducting the initial work and subsequent additional testing and extension to evaluate weld material crack growth rate and the influence of post repair heat treatment by W. Ross are gratefully acknowledged.

9. REFERENCES

1. Harry, Mikel, J., "The Vision of Six Sigma: A Roadmap for Breakthrough", 4th Ed., Sigma Publishing Co., Phoenix, 1994.
2. Squires, T., and Clingerman, D., "Six Sigma and Robustness", presented at Second Annual Workshop on the Application of Probabilistic Methods to Gas Turbine Engines, Dayton, OH, 8-9 October, 1996.
3. Welch, John, F., Jr., "GE Quality 2000: A Dream with A Plan", Presented at the GE Company 1996 Annual Meeting, Charlottesville, Virginia, April 24, 1996.
4. Welch, John, F., Jr. "Jack Welch's Encore - How GE's chairman is remaking his company again", Business Week, Oct. 21, 1996.

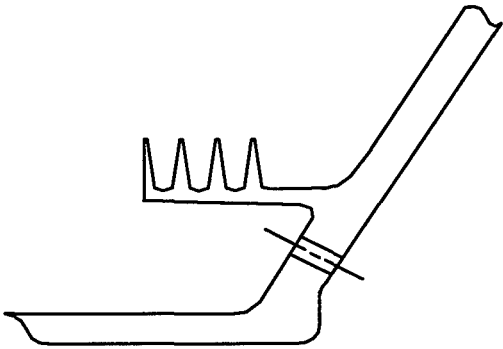


Figure 1: Schematic of typical engine rotating seal teeth configuration.

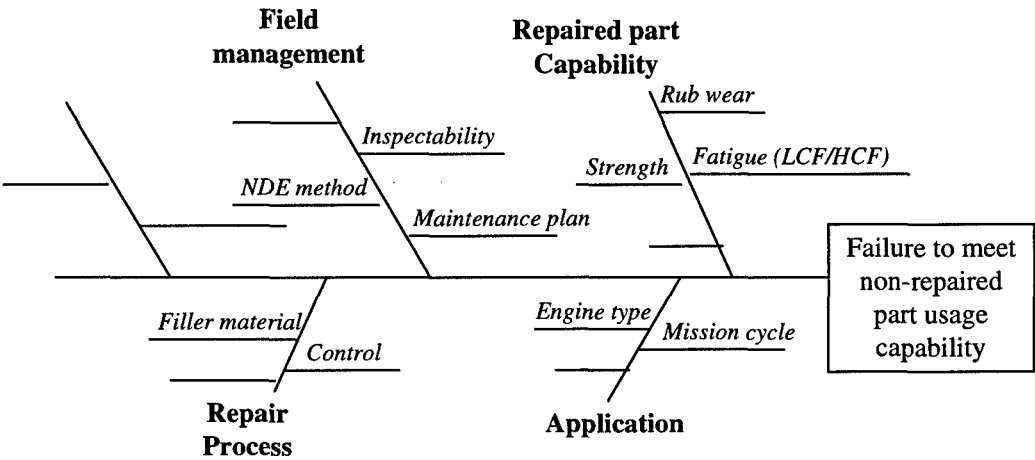


Figure 2: Cause and effect (fishbone) diagram.

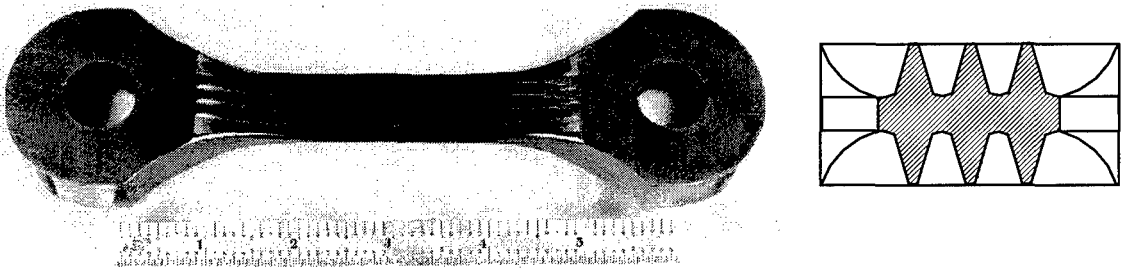


Figure 3: Simulated Ti-17 seal tooth LCF specimen.

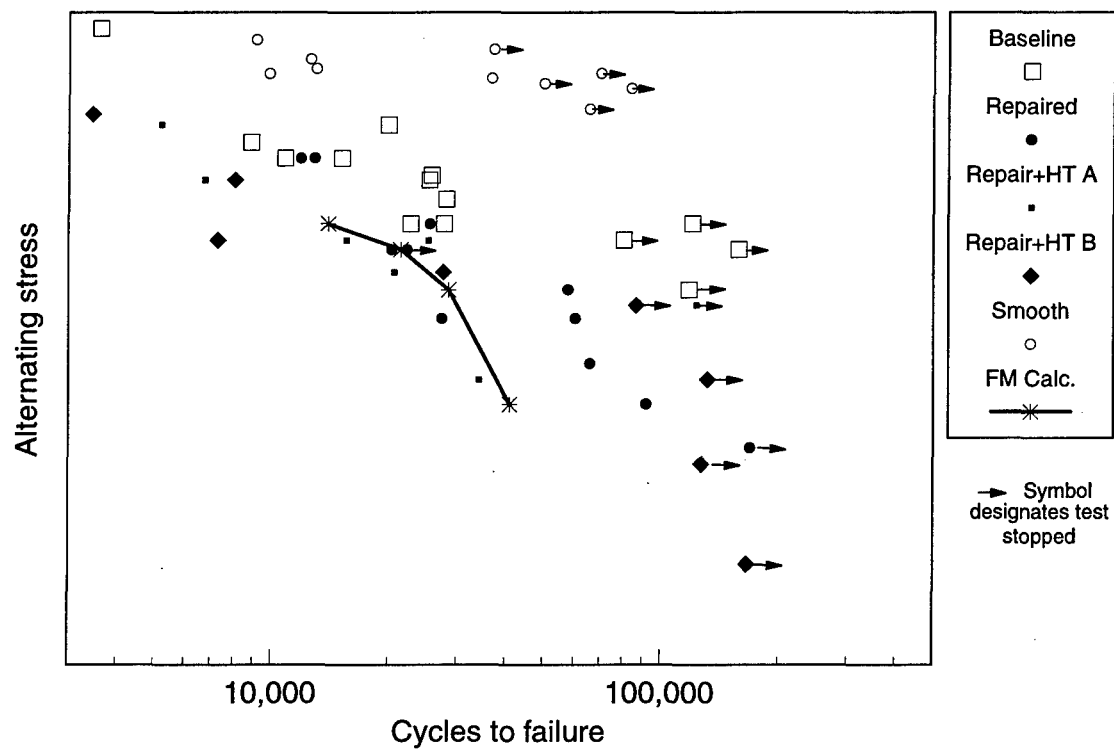


Figure 4: Simulated seal tooth low cycle fatigue test results.

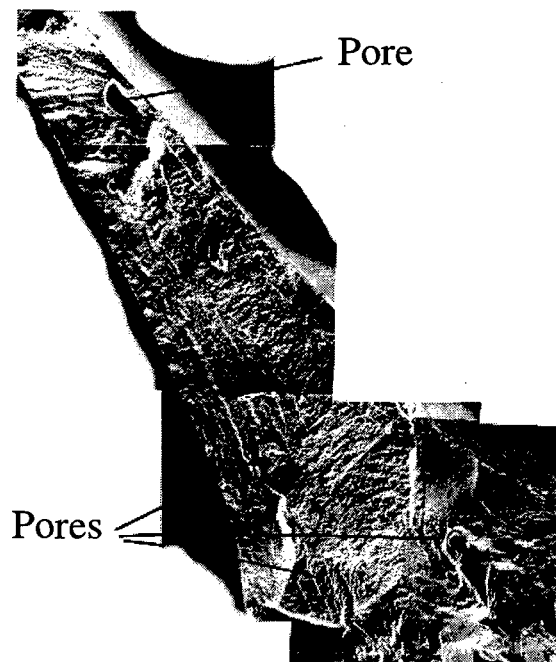


Figure 5: Fractograph showing pores at fatigue crack initiation sites

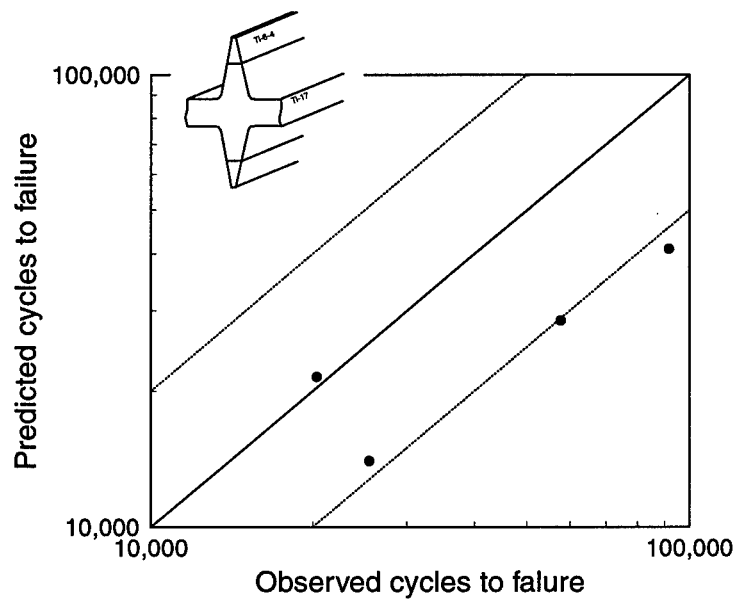


Figure 6: Fracture mechanics predictions for selected weld repaired test samples.

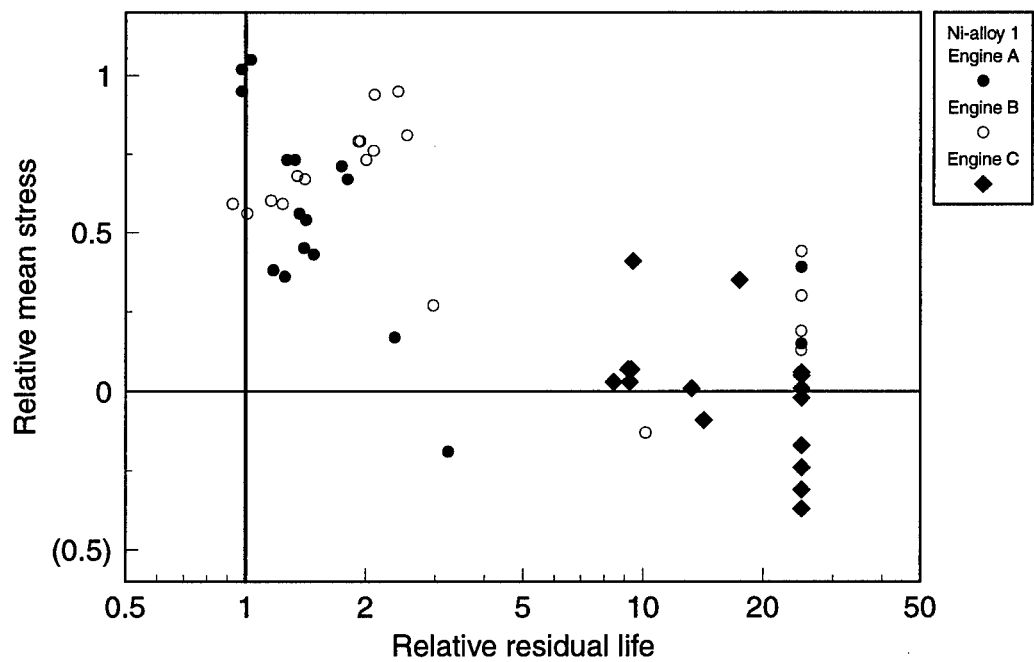


Figure 7: Relative residual life versus relative stress for nickel alloy seal teeth.

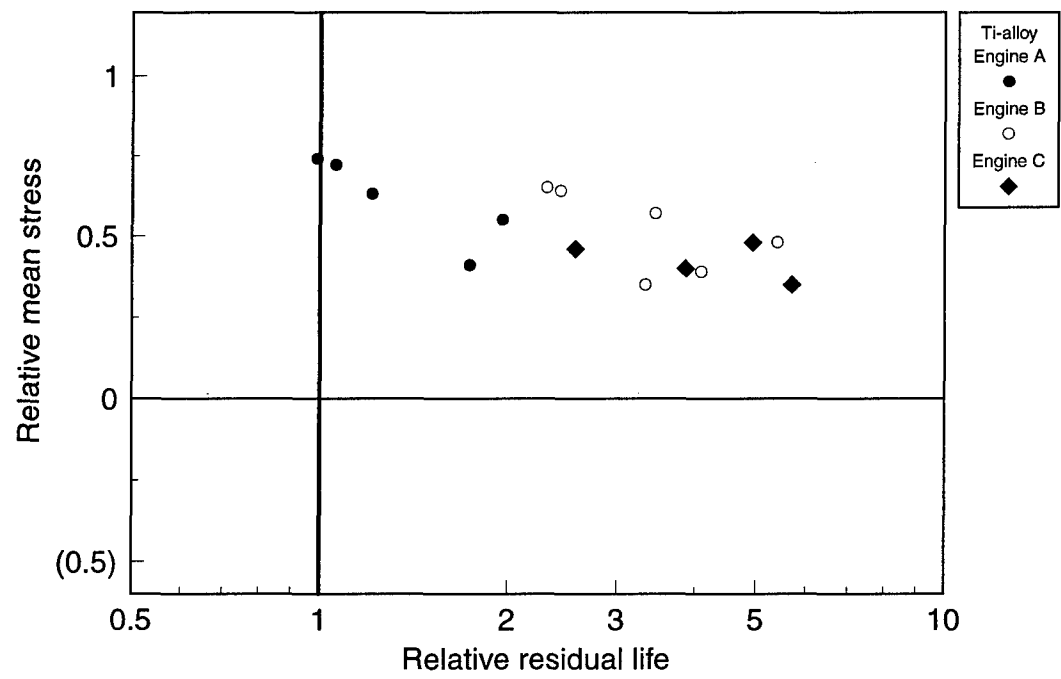


Figure 8: Relative residual life versus relative stress for titanium alloy seal teeth.

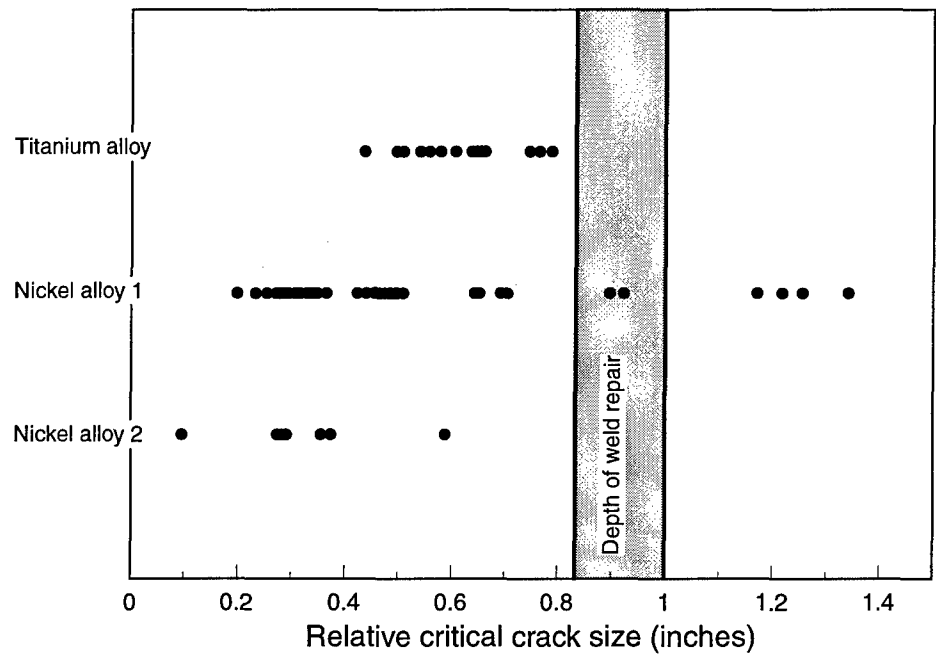


Figure 9: Relative critical crack sizes for various engine seal teeth.

PROPELLER BARREL CAM LIFE EXTENSION

Kedar Tandon
Brent Junkin
Wayne Thomas

STANDARD AERO LTD.
33 Allen Dyne Road
Winnipeg, Manitoba, Canada R3H 1A1

SUMMARY

Overhaul inspection instructions and acceptance criteria provided by the OEM are sometimes not adequate to assess the suitability of the part for continued service. Propeller barrel cams with helical cam tracks were found to have pitting on the surface, which caused the inspectors to reject them. An engineering analysis of the wear surface using scanning electron microscope (SEM) and metallographic techniques was performed. Based on this analysis, the inspection data, (including techniques and interpretation) was re-evaluated. The careful evaluation of the service degradation damage resulted in an improvement of inspection methods and guidance material. The reject rate of the cams was dramatically reduced and thus their life was safely extended.

1. INTRODUCTION

During the overhaul process of propeller assemblies, many helical cams were noted to have degradation of the wear track. Inspectors observed many small pits in the track (Figure 1) and quarantined a number of cams. They considered these pits as corrosion pits. The Overhaul Manual cam track inspection procedure did not allow the presence of "any pits which were irregular in shape and have sharp edges and/or jagged bottoms, such as those which might be caused by corrosion or spalling". Local reworking to blend pits in the cam tracks was also not permitted.

The manual does allow the presence of pits, which are shallow (no deeper than 0.010 inch) and round bottomed, such as those which might be caused by denting of the surface.

The inspection process was very subjective, and the inspectors did not have any comparative criteria on which to judge the size and depth of pits for accepting or rejecting the cams. Thus the reject rate for the cams was high.

2. EXPERIMENTAL PROCEDURE:

The following tasks were undertaken in this investigation:

- Visual and Scanning Electron Microscope (SEM) examination of wear tracks/pits

- Surface profilometry of wear tracks
- Metallurgical characterisation of cams and rollers
- Polishing and subsequent examination of wear tracks/pits
- CMM of wear track to assess loss in thickness due to polishing

3. RESULTS AND DISCUSSION

Visual and SEM examination:

One of the cams was sectioned for further examination of the wear surfaces on five of its helical cam tracks. The tracks exhibited typical metal to metal wear patterns with many small pits and micro-scratches. Low magnification views of pits in the wear surface are shown in Figures 2a and 2b. These give some indication of pits size but do not show details of the edges or the depth of pits.

Several pits in the wear surfaces of the cam were further examined under a SEM. Two of these pits have been marked by arrows in Figures 2a and 2b. Enlarged views of pits in the tracks are shown in Figures 3 and 4, which clearly show the edge and the bottom of pits. Pits are shallow and do not appear to be caused by corrosion. Instead their features are consistent with damage caused by spalling. It should be noted that spalling of material on a micro scale is a normal outcome during extended metal to metal lubricated wear (Ref.1).

Views of other areas on the wear track exhibiting scratches and pits are shown in Figures 5 and 6. It is clear that these pits are very shallow and don't have sharp edges. Most of them have originated from the micro-spalling process which results from sub-surface micro-cracking generated due to cyclic stresses. The debris being trapped between the roller and the cam normally creates numerous scratches and small pits on the wear surface. It should be further noted that none of the pits show any cracks originating from them and that no cracks propagate from the pits into the matrix.

A view of the roller wear surface is shown in Figure 7 which shows very little spalling or scratching of the wear surface. These rollers are typically replaced during the overhaul of the Propeller Assembly.

Surface Profilometry of wear tracks:

Although SEM micrographs give a good perception of depth of pits and scratches on the wear surface, it is not possible to quantitatively measure the depth. By determining the surface profile of the track using a profilometer, one can measure the roughness of the surface as well as the depth of pits. Therefore, a profilometer was used to scan the wear track and typical profiles are shown in Figure 8. Maximum depth of pits was measured to be 0.002 inch. Typical Ra and Rq (RMS) values of the wear track, in micro-inches, are also noted in Figure 8 (24 and 32 μ ins respectively).

Metallurgical analysis of cams and rollers

A sectioned piece of the cam wear track was mounted, polished and etched to reveal its micro-structure. The wear track of the cam was found to have been induction hardened to a depth of 0.125-0.250 inch, Figure 9a. The base material is tempered martensite containing a few inclusions, Figure 9b. Hardness values of the hardened track surface and the interior matrix were measured as HRC 56 and HRC 42 respectively. An analysis conducted using the energy dispersive system (EDS) attachment on the SEM indicated the chemical composition of the cam to be AISI 4300 series steel (most likely 4340); the carbon content of the alloy couldn't be determined by EDS.

A piece from the roller was, mounted, polished and etched. Figure 10 shows the micro-structure of the matrix which is tempered martensite and contains some inclusions. The hardness of the roller was measured to be HRC 61, and there was no surface hardening present on the rollers. Chemical composition of the roller as determined by EDS conforms to AISI 52100 steel; again, the carbon content couldn't be determined.

It is well known that the presence of non-metallic inclusions just below the wear surface facilitates the spalling or de-lamination process, and some of the pits seen on the wear surface of cam tracks may have originated by this phenomenon.

Polishing of wear track:

The overhaul manual does not allow any blending or repair of pits on the wear track. Polishing of the worn surface would be non-invasive, and remove small pits and scratches. Therefore, wear surfaces on two of the cam tracks were manually polished using 600 grit emery paper for about 15 minutes. This removed the traces of the wear except for a few pits which were still visible. The polished surface of the two wear tracks was viewed under the SEM, with a significant improvement surface quality; see Figure 11a and 11b. Most of the wear scratches and small pits were removed, and the pit size, (shown in Figures 3 and 4) area and depth was reduced. The edges of pits also became smoother as a result of the polishing process, see Figures 12 and 13.

Surface profiles across the polished wear track were also taken and, as shown in Figure 14, the surface has become significantly smoother (compare this with the profile in Figure 8). The Ra was reduced to 13 μ ins. And the Rq to 18 μ ins. The pit depth was slightly reduced.

Polishing of the wear track also made it easier to inspect for pits, since most of the debris, scratches and small pits were removed during this process.

CMM measurements of the polished wear track:

One of the concerns related to the polishing of the wear track is that of the loss of material from the surface, which may adversely affect the tolerance between the roller and the cam. Therefore, CMM mapping of the surface was performed on a cam wear track before and after polishing. Maximum loss in thickness on the wear track was found to be 0.0003 inch. Therefore, polishing of the wear track should have an insignificant effect on the cam/roller fit and their function.

Improved Inspection & Training Methods:

Using only the manual as a guide, inspectors were originally using a 10x magnifier in making critical decisions on the acceptability of the cams. Training consisted of OJT by other inspectors "familiar" with the cams and thus, included a very subjective interpretation of both the manual information and what they were actually observing on the cam surfaces. This resulted in a high rejection rate.

With the completion of the wear analysis we were able to formulate a scientific, knowledge based acceptance criteria with which to inspect the cams. A significant effort was made to make the inspections easier to perform and to train the inspectors in the techniques and interpretation of results. The rejection rate was dramatically reduced. This was accomplished by:

1. Improving inspection equipment by purchasing inspection scopes suitable to the job.
2. Making available "comparator blocks" which contained known, quantified, imperfections.
3. Modifying the inspection process by allowing limited polishing of the cam surface.
4. Improving the inspector's confidence in their decision by educating them on the mechanisms of wear and corrosion of the cams.
5. Holding training sessions with the inspectors showing them how to use the tools provided and interpret their findings.

4. CONCLUSIONS:

The following conclusions can be drawn from this investigation/development work:

- Most of the pitting observed on wear tracks has not originated from corrosive actions as originally interpreted by the inspectors. Rather, pits have features of micro-spalling which is the normal process of metal/metal wear.
- The pits examined do not have sharp edges or deep crevices. The pits were shallow, less than 0.002 inch deep, and showed no evidence of generating cracks in the matrix of the cam.
- Polishing the wear track with a 600 emery paper removes most of the scratches and small pits caused by the wear process, and significantly improves the quality of the surface. The size of pits- width and depth is also reduced. This should improve the wear life/performance of cams.
- Polishing of the wear surface results in a much cleaner surface where pits or defects can be easily observed and inspected.
- Proper training of the inspectors in the use of new inspection tools and in the interpretation of the findings as a result of this study has resulted in a dramatic decrease in rejection rate.
- Engineering analysis of the OEM overhaul inspection requirements combined with sound metallurgical analysis was required to ensure that effective inspection practices were put in place.

REFERENCES:

1. ASM Handbook, Vol 18, "Friction and Wear of Rolling-Element Bearings" pp 499-514, 1992, ASM International, Ohio, USA



Figure 1. View of a typical wear damage on a Cam

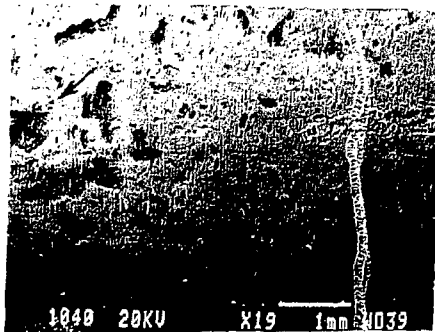
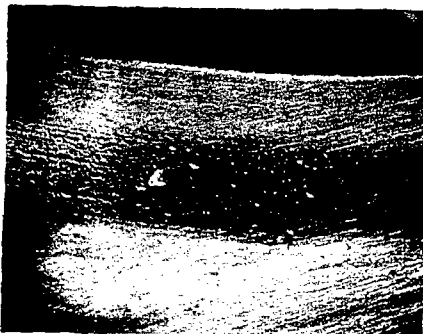


Figure 2a. View of pits on the wear surface of track 1B, stereo micrograph, 2X; b. SEM micrograph of a cluster of pits on the wear surface of the cam track. The vertical scratch has been intentionally marked



Figure 3. An enlarged view of the pit in Fig. 2a



Figure 4. An enlarged view of the pit marked in Fig. 2b



Figure 5. View of a spot on the wear surface of track 1B



Figure 6. View of an area on track 1B where micro-cracks are visible.

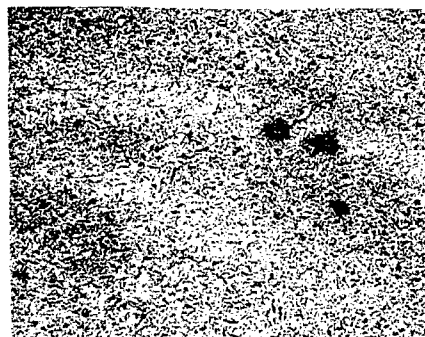


Figure 9a. Induction hardened zone of the cam wear surface

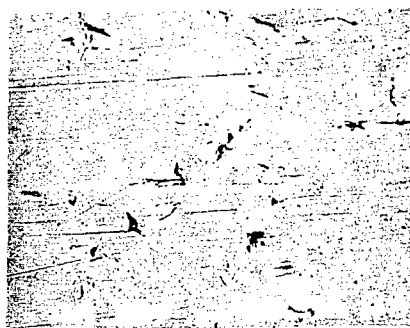


Figure 7. View of the roller wear surface



Figure 9b. Interior matrix of the cam, 200X

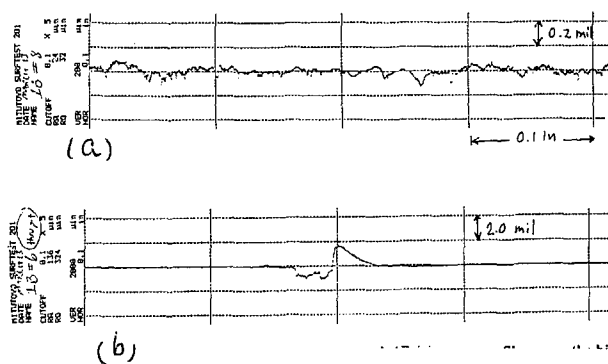


Figure 8. Typical wear profile across the wear track 1B, (a); wear profile across the big pit in Figure 3, (b).

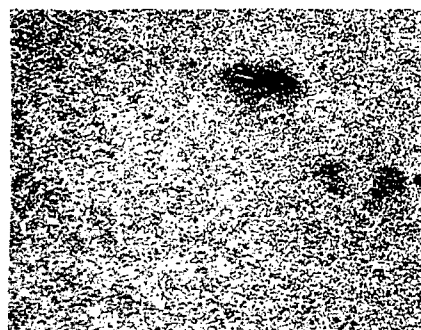


Figure 10. Microstructure of the roller matrix, 200X



Figure 11a. Polished surface of the wear track 1B. The pit is same as shown in Fig.3

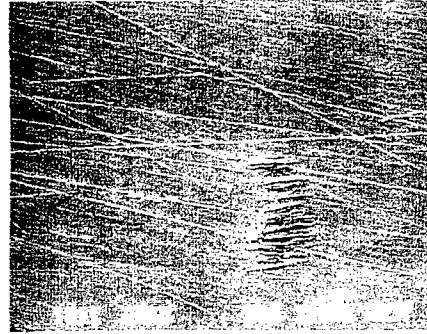


Figure 13. Another area on the wear track 3b

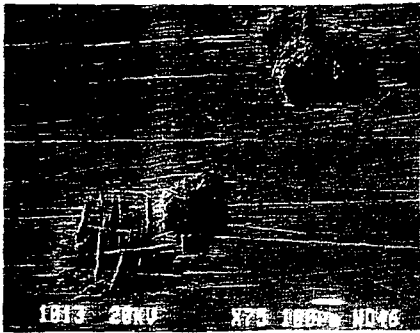


Figure 11b. Polished surface of the wear track 3B. Spot is same as in Figure 4.

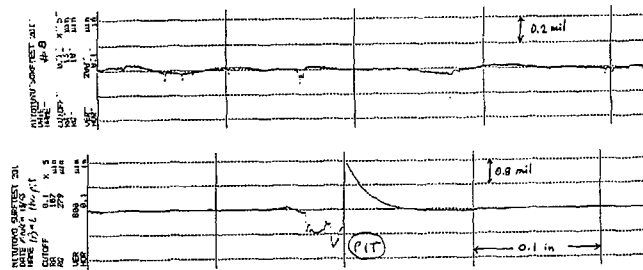


Figure 14. Surface profiles across the polished wear track 1B. Compare with the profiles (at same locations) in Fig.8



Figure 12. Polished surface of wear track 3B, same spot as in Fig.2b.

The Development of Life Extension Methods for Fracture Critical Aero-Engine Components

A.D.Boyd-Lee
G.F.Harrison

Defence Evaluation and Research Agency, Farnborough,
Hampshire, GU14 OLX, UK

1.1 List of symbols

	given that
Π	product of a series of terms
β	reference cycles consumed per efh
K	stress intensity
σ	population standard deviation
a or d	crack radius or depth
Ar	declared safe service life (reference cycles)
c	Paris rate constant
efh	engine flying hours
Fr	alias for LTFC (reference cycles)
Gr	crack propagation life (reference cycles)
GM	geometric mean
J	rank number
LTFC	life-to-first-crack (a first crack being defined as having a 0.38mm radius)
m	Paris exponent
n	sample size
N	fatigue life (reference cycles)
p(x)	probability of event x
PD(x)	probability density function w.r.t. x
S	combined safety factor

1.2 Subscripts and superscripts

'	implies a change of variable
-	refers to non-finite value
95%	95% confidence estimate
μ	refers to geometric mean value
+3 σ	refers to +3 σ value
-3 σ	refers to -3 σ value, ie. 1/750 quantile
b	refers to burst distribution
com	from component testing
eff	refers to effective stress cycle
hi	refers to effective max. stress level
i	refers to LTFC value
lo	refers to effective min. stress level
mat	from materials characterisation
max	refers to max. load
min	refers to min. load
p	refers to crack propagation value
ref	refers to reference load conditions
res	refers to residual stress
s	refers to sampling distribution for the component test results
test	refers to test load conditions

2 Summary

Service experience and the rapid advancement of understanding frequently prompt revisions of the declared service lives for aeroengine components. Downward revisions can occur because:

- 1) ex-service disc tests show that engine operation is harder on components than was estimated at design;
- 2) in-service cracks, catastrophic failures, and ex-service testing show that some failure mechanisms differ from those identified at design;
- 3) improvements to service usage models has resulted in more conservative exchange rates;
- 4) refined analyses for some components show the operating stresses are higher than those estimated at design; and
- 5) some component design modifications cause a change in a life limiting critical area, etc.

From whatever cause, the imposition of service life reductions often results in unexpected component life expiries. The resulting costs of grounding the aircraft and of engine removal can be many times greater than the component replacement costs. Thus, demand for life extensions is usually aimed at life reduced parts.

Three life extension methods developed to meet this need are presented. Firstly, methods of life extension for crack tolerant component designs are outlined. Secondly, a robust statistical method for exploitation of non-finite results is demonstrated to provide significant life extensions. (A non-finite result is associated with a test stopped before reaching the desired component dysfunction point). Finally, in view of the importance of risk assessment modelling in the more critical cases, the derivation of a risk of fatigue failure model is presented.

In this paper, the life-to-first-crack concept and the '2/3 dysfunction' criterion are used as standard 'reference lives' or 'stakes in the ground' relative to which life extensions are measured.

3 Life-to-first-crack (LTFC)

For a large proportion of civil and military aeroengine discs, their current declared service lives are calculated using the life-to-first-crack methodology. In this approach, it is assumed components enter service defect free and they are rejected before the appearance of a fatigue initiated 'engineering crack' (>0.38mm radius)¹.

Under current UK Military Defence Standards (Def. Stan. 00971)² and European Civil Joint Airworthiness Requirements (JAR-E)³, service lives are declared on the basis of testing full size engine discs in a spin-rig test facility, under stresses and temperatures similar to those applying in service. With tests costing in the region of £100,000, the number of available test results rarely exceeds 5. The Lifting Regulations define the procedure to be used in interpretation of these results and in calculation of the declared safe service lives. In the procedure, it is assumed that for all conventional aeroengine materials (with a single failure mode), fatigue lives (for identical load conditions) are distributed according to a lognormal density function. Long experience has shown the engineering assumption that the ratio of the lives at the $\pm 3\sigma$ points is less than 6, has wide application to aeroengine disc materials.

The certification regulations require that the calculated safe cyclic life is then declared at a suitably remote point on the life-to-first-crack distribution, specified as the 1/750 quantile (-3σ). Given the assumed scatter factor of not more than 6, the life corresponding to the lower 1/750 quantile is a factor of $\sqrt{6} = 2.449$ below the geometric mean (GM) reference life-to-first-crack obtained from the sample.

In recognition that component test sampling error affects the safety level inherent in the calculation of a safe service life, it is also required that the life be evaluated to 95% confidence (with respect to estimation of the geometric mean (GM) life of the population failure distribution to which the sample belongs). This confidence interval can be shown to correspond to a factor in life of

$$6^{\left(\frac{1.645}{6\sqrt{n}}\right)} \quad (1)$$

where 95% corresponds to 1.645 standard deviations. It can be seen that expression 1 is an increasing function with respect to decreasing sample size. In summary, a declared safe service life 100% Ar is calculated by formulae of the type

$$Ar = \frac{\sqrt[n]{\prod_{j=1}^n N_j}}{2.449 \times 6^{\left(\frac{1.645}{6\sqrt{n}}\right)}} \quad (2)$$

where N_i , $i=1, \dots, n$ are the individual LTFC test results. The two quantities on the denominator of equation 2 are called 'safety factors'. In general, any factor by which a life is divided to obtain a more conservative value is called a safety factor.

An additional safety feature is that at entry into service of a new design, a release life of only 50% of this value is approved. When the lead disc reaches this life, it is

withdrawn for spin testing, whilst the other discs are allowed to remain in service for up to 75%Ar. The ex-service disc test result is added to the sample and the component life revised accordingly. After a second ex-service disc test, the remaining discs are allowed in service for the full 100%Ar. Consequently, at the stage where component life extensions are sought, the full Ar has often been declared.

4 '2/3 dysfunction'

In the LTFC approach, it is assumed that an acceptable but variable margin of safety is given by defining an 'engineering crack' as having a 0.38mm radius. However, the crack radius that gives a constant factor of safety is both geometry and material dependent.

In the UK, this has led to an improved approach, still based on the assumption that components are defect free on entry into service, but now the 'engineering crack' is replaced by a set fraction of '2/3 of the total life to dysfunction', that is, the life before the onset of rapid crack growth¹. The value of 2/3 was chosen because for many materials and disc designs, the crack size at '2/3 failure' is approximately equal to the value of 0.38mm defined in the LTFC method. (From a total of about 80 results covering nickel, steel and titanium discs, DERA found the average ratio of life-to-first-crack to burst life is equal to 0.72).

The constant ratio between the 2/3 dysfunction life and the burst life ensures a more consistent margin of safety. Moreover, in very high strength disc alloys the critical crack size for the onset of rapid crack growth can be smaller than the 0.38mm radius 'engineering crack' size. Therefore, the 2/3 dysfunction principle enables these alloys to be exploited safely. Having been in use in the UK for some time, the '2/3 dysfunction' safety factor is now seeing wider application within Europe.

Both theoretical analyses and experimental test programmes have shown that relative to an identical major loading sequence, minor cycles are relatively more damaging during potential crack propagation than during the LTFC. Throughout the paper, we consider a typical case $\beta_p/\beta_i=2.5$, where β_p is the exchange rate for crack propagation and β_i is the exchange rate for the LTFC. For those components whose LTFC and life-to-2/3-dysfunction are equal, the propagation life in hours is 50%/2.5=20% of the LTFC. That is, the '2/3 dysfunction' safety factor is then equal to 1.2. It follows that the combined safety factor S for a component that has reached 'efh' engine flying hours is equal to

$$S = 1.2 \times 2.449 \times 6^{\left(\frac{1.645}{6\sqrt{n}}\right)} \times \frac{Ar}{efh \times \beta_i} \quad (3)$$

5 Life extension of crack tolerant components

Crack tolerant components have significantly longer crack propagation lives than 50% of their LTFC's. This can occur if the critical area(s) of the component is surrounded by a rapidly decreasing stress field. An example, is the vent hole critical area of the disc shown schematically in figure 1, with stresses at peak load shown in figure 2.

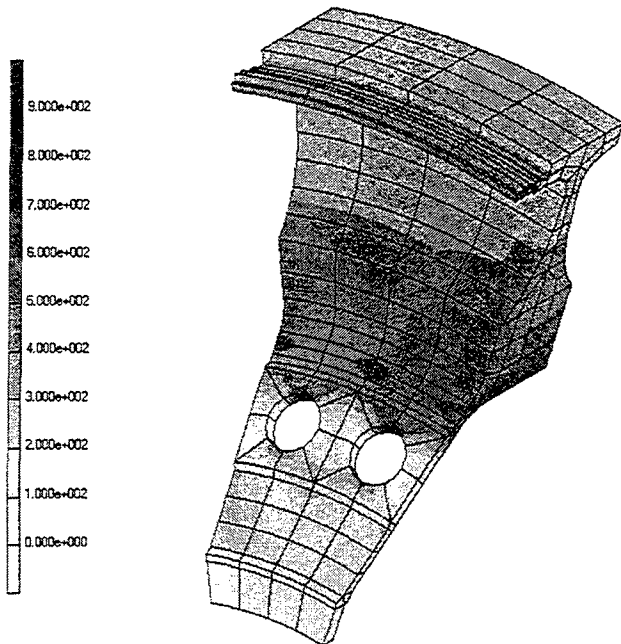


Figure 1. Example disc with vent holes

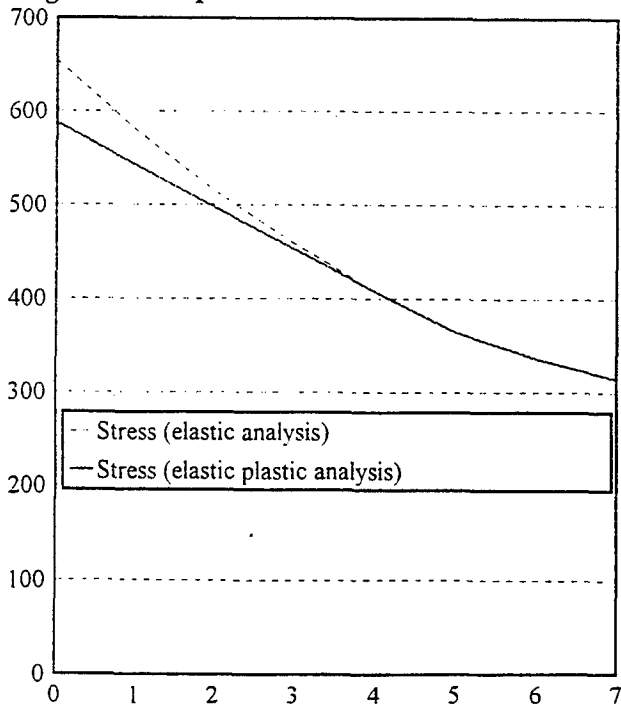


Figure 2. Variation of peak stress with distance from surface of vent hole shown in figure 1.

Crack tolerant components can be life extended beyond 100% Ar, without compromising risk levels associated with conventional failure locations. However, to ensure a consistent level of safety, the useable crack growth life must have an associated 'never exceed 2/3 dysfunction' margin of safety. A safe life can be calculated as follows.

D = safe growth life (reference cycles),
 Fr = LTFC (reference cycles),
 Gr = propagation life (reference cycles),
 $2/3$ dysfunction = $2/3(Fr+Gr)$ and given that $\beta_p/\beta_i=2.5$,

$$D = (2/3 \text{ dysfunction}) - Fr = \frac{2}{3} Gr - \frac{1}{3} Fr \quad (4)$$

$$\begin{aligned} \therefore \text{Total safe life (efh)} &= \frac{Fr}{\beta_i} + \frac{\frac{2}{3} Gr - \frac{1}{3} Fr}{2.5 \beta_i} \quad (5) \\ &= \frac{13 Fr}{15 \beta_i} + \frac{4 Gr}{15 \beta_i} \end{aligned}$$

$$\begin{aligned} \& \% \text{ life increase (efh)} &= \frac{\frac{4 Gr}{15 \beta_i} - \frac{2 Fr}{15 \beta_i}}{\frac{Fr}{\beta_i}} \times 100 \quad (6) \\ &= \frac{4Gr - 2Fr}{15Fr} \times 100 \end{aligned}$$

It can be seen, a life extension is given when $Gr > 0.5Fr$.

In conventional damage tolerance procedures, the release life equates to 50% of the mean propagation life. That is, it would typically require 4 inspections prior to achieving the safe service life. Considering LCF crack growth data for components show scatter factors of 4 between $\pm 3\sigma$ (ie. 2 between mean and -3σ), it is imperative that NDI inspection techniques can reliably detect cracks of 0.38mm radius, even under the penalties of machined component surface finish, possible surface treatments and compressive residual stresses induced via shot peening or local yielding at stress concentration features.

6 Crack tolerance and non-linear fracture mechanics

Most test discs are loaded at overspeed relative to service operating conditions, to reduce the high disc spin rig operating costs. Due to overspeed or material softening under cyclic loading, there can occur local plastic deformation in some components. On load removal, compressive residual stresses form to accommodate the plastic deformation.

Linear-elastic fracture mechanics should not be applied to such cases, because the engine reference cycle would

be underestimated, and a non-conservative estimate of the component's life capability would result. For such components, a safe life assessment methodology is required such as that summarised in figure 3. The symbols are defined at the beginning of the paper. Apart from basic component testing practice, the procedure has two features:

Firstly, a full elastic-plastic stress analysis is carried out (boxes 1-3). The residual stresses resulting from plastic deformation are included in the calculation of the magnitudes of the stress cycles for both test and engine service reference conditions (box 3).

Secondly, to predict crack growth life within the plastic volume, direct calculation of the stress intensity range ΔK may not be adequate. Instead, for the disc lifing test, the calculated stress intensities at specific depths are adjusted via a geometry correction factor to the stress intensities calculated for a simple laboratory test specimen experiencing similar crack growth rates. The identified geometry correction factor is then applied to all subsequent loading life calculations, such as, for engine reference conditions. That is, the method combines the values given by stress modelling (boxes 1-3), component testing (boxes 6 and 8) and materials characterisation (box 4), via a geometry function $g(a)$ selected to satisfy

$$\Delta K(a) = g(a) \cdot \Delta \sigma(a) \quad (7)$$

where 'a' is the crack radius or depth and $\Delta K(a)$ is an effective stress intensity range for the component. Re-expressing equation 7 in terms of da/dN gives,

$$\left(\frac{da}{dN} \right) = \left[\frac{\left(\frac{da}{dN} \right)_{\mu}^{test}}{\Delta \sigma_{test}^m(a)} \right] \cdot \Delta \sigma^m(a) \quad (8)$$

The square bracketed argument in equation 8 is effectively a calibration term which comes from the component testing and stress modelling - thus, it is not expressed in terms of ΔK . The ' $\Delta \sigma^m(a)$ ' is a Paris based 'overstress term' which accounts for the deviation of the stress (of interest) from the calibration stress. When the overstress is close to unity, predictions based on equation 8 should be sufficiently accurate. At higher deviations from the calibration stress, a more complex term for the effect of deviation from the calibration stress may be required.

Equations 7 and 8 predict conventional fatigue. In high temperature critical areas, creep and environment enhanced fatigue may occur, in which case other formulae would be used.

7 Non-finite component test results

7.1 Introduction

Many of the declared safe-service lives for fracture-critical components are calculated from results of fatigue tests that are stopped before an 'engineering crack' had been detected. Results of this kind are called 'non-finite'. Non-finite results can also arise due to a change of failure location within a component following:

- 1) calculation of a more detailed stress analysis; or
- 2) if service cracks occur in different location(s) to that assumed to be the critical area at original assessment; or
- 3) as a result of component design modifications, etc.

Current lifing regulations were originally derived to accept only finite results. In the past, this has caused non-finite results to be either rejected unnecessarily or accepted overconservatively assuming 'failure on the next load cycle'.

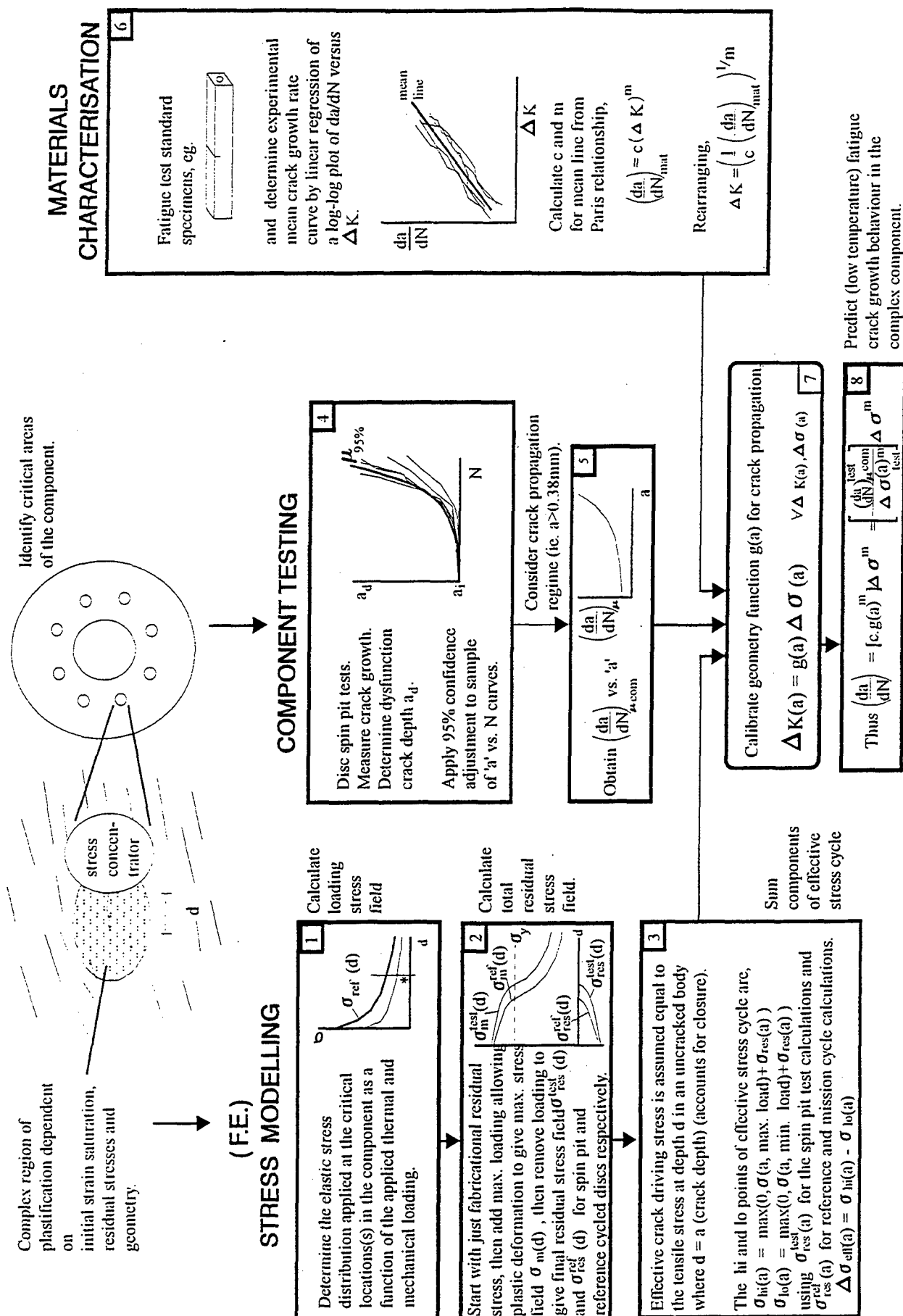
Under such an approach, for example, a sample of 5 non-finite results each of 10000 cycles, would have been treated as 5 finite values of 10001 cycles. A service life of $10001/(2.449 \times 1.246) = 3277$ cycles would therefore have been obtained using equation 2. But it is improbable all 5 components would fail at 10001 cycles.

Methods to solve this problem are explained. Initially, because of their continued use, two somewhat crude approaches and their limitations are discussed. This is followed by discussion of a recently developed statistically robust model

7.2 Selection of a favourable sub-sample

One approach to obtain a safe life increase, is to ignore unfavourable non-finite results and assume 'failure on next cycle' for the other non-finite results. In general, this method is conservative, since non-finite values do not indicate that the corresponding finite values are low. But, it is almost always overconservative because: of rejection of significant non-finite results, and the 'failure on next cycle' assumption is overused.

For example, given a sample of non-finite results of 10,000, 10,000 and 8222 cycles, a safe life of 2879 cycles is given by equation 2. The 8222 cycles result would be ignored because a marginally higher life of 2885 cycles would be obtained. However, after an advanced analysis is presented in section 7.4, a better estimate of the safe service life based on this sample will be calculated.



7.3 Rank order and plot

Another approximate method is to rank order the results and plot them on cumulative probability paper. A 50% confidence estimate of the median of the population life distribution can then be read off the graph. This method has some merit for mixed finite and non-finite results.

Quite apart from the slight inaccuracy of probability paper, it is not always possible to rank order a mixture of finite and non-finite results. For example, the rank order of a non-finite result of 10,000 cycles and a finite result of 12,000 cycles is indeterminate.

For a sample of finite results a very good approximate of the median rank is given by the formula⁴

$$\text{median rank} = \frac{J - 0.3}{n + 0.4} \quad (9)$$

The median rank is defined as the median (ie. 50% confidence) estimate of the quantile (ie. probability point on the respective distribution) of the result, given the result's rank J . 'n' is the sample size. When there are non-finite results in the sample, Bompas-Smith⁴ suggests formula 9 should be modified to:

$$\text{median rank}(J) = \frac{\kappa(J) - 0.3}{n + 0.4} \quad (10)$$

$$\kappa(J) = \kappa(J-1) + \frac{n - \kappa(J-1)}{\xi} \quad \& \quad (11)$$

$$\kappa(1) = 1 \quad (12)$$

where median rank(J) is an estimate of the rank order of the J 'th failure. ξ is the number of results with a life greater than or equal to that of the J 'th finite result

Analysis of this second method shows that it is better than the 'favourable sub-sample method', but has been shown to be in error by up to 20%.

7.4 Improved statistical approach

In the improved statistical approach, no significant results are rejected and no crude assumptions are made about the sample's rank order.

It is then found that analysis of an entirely non-finite sample involves $n-1$ statistical degrees of freedom, whereas analysis of any other sample involves 'n' degrees of freedom. Thus, different confidence intervals have to be applied to these two sample types. In this paper we present just the analysis for non-finite results, since this illustrates the basis of the methodology that has been developed. This analysis is also restricted to

cases where the respective life-to-first-crack distribution is lognormal with a known conservative scatter factor.

As for finite results, the geometric mean (GM) of the population life-to-first-crack distribution is estimated to 95% confidence. And again, as for finite results, once this value is obtained, it is divided by the $1/750$ (-3σ) safety factor to give a value for the required safe-service life A_r (cycles).

The 95% confidence estimate of the GM is the value that the true GM stands a 95% chance of exceeding. To identify the required confidence interval, consider the likelihood of obtaining a non-finite result at N_i^- cycles given a certain value of the GM (see figure 4).

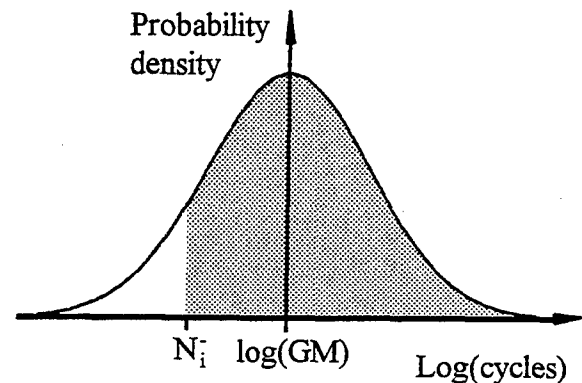


Figure 4 analysis of a non-finite result belonging to a life-to-first-crack distribution

The minus superscript indicates that the value is non-finite. The x-axis (cycles) has a log-scale, so that the life-to-first crack (LTFC) distribution is transformed to a normal function. Then the likelihood of obtaining a non-finite result at N cycles is represented by the shaded area. Now there is a 95% chance that the defined likelihood lies within the interval 0.05 to 1, assuming the result lies at a random number of standard deviations away from the GM. Therefore, given the value of N_i^- , a 95% confidence estimate of GM can be obtained when the equation 13 is satisfied.

$$p(\text{the result is non-finite}) = 0.05 \quad (13)$$

As the sample size is equal to one, this confidence test leads to the same formula as if the result were finite. This is an indication of the conservatism of the confidence test so defined. Where the sample size is greater than unity the confidence test generalises to

$$\prod_{j=1}^n p(\text{result } J \text{ is non-finite}) = 0.05 \quad (14)$$

That is, the probability of all results in the sample being non-finite is equal to the product of the probabilities of the individual results in the sample being non-finite. As for a sample of size one, a confidence interval on GM is chosen such that the probability of obtaining the sample

ranges between 1 and 0.05. The 95% confidence estimate of the GM is then taken as the minimum (ie. conservative) value of the GM over the defined confidence interval.

General analysis shows that equation 14 embodies a failure-on-next-cycle assumption for at most one of the non-finite results and therefore its conservatism is clear. It is slightly overconservative because the odds of just one of the non-finite results reaching dysfunction on the next cycle are normally lower than 50/50. However, in general, removal of this slight overconservatism is complex and it does not result in a significant life increase. At best, removal of this overconservatism might involve hypotheses that assume that first non-finite result to become finite would lie at the most unfavourable position on the sampling distribution. Thus, any life gains would only be up to a few percent (ie. probably negligible compared to other living uncertainties).

It remains to substitute equations of the failure distribution into equation 14. Firstly, a change of variable is defined by equations 15 and 16.

$$N_J^- = \frac{1}{\sigma'_i} \log \left(\frac{N_J^-}{N_\mu} \right) \quad J = 1, 2, \dots, n \quad (15)$$

$$\sigma'_i = \frac{1}{6} \log \left(\frac{N_{+3\sigma}}{N_{-3\sigma}} \right) \quad (16)$$

where N_μ is the population geometric mean life. Even though its value is indeterminate, it is a fixed value. N_J^- is the non-finite value associated with test result J. The purpose of this change of variable is illustrated by fig. 5.

It can be seen that the 'log' term transforms the lognormal distribution to a normal distribution. Division by N_μ has the effect of placing the origin at the population GM. The σ' term rescales the axes so that they are in units of standard deviations. $N_{+3\sigma}$ and $N_{-3\sigma}$ refer to the $\pm 3\sigma$ points on the untransformed distribution. In forged disc lifing, for example a conservative value of $N_{+3\sigma}/N_{-3\sigma}=6$ is frequently assumed. For a random test result, therefore, the failure distribution in the transformed co-ordinates satisfies

$$\begin{aligned} P(N' < a) &= \int_{-\infty}^a \frac{1}{\sqrt{2\pi}} \cdot \exp \left(-\frac{x^2}{2} \right) dx \\ &= \text{normal}(a) \end{aligned} \quad (17)$$

Substituting equation 17 into equation 14 gives

$$\prod_{J=1}^n [1 - \text{normal}(N_J^-)] = 0.05 \quad (18)$$

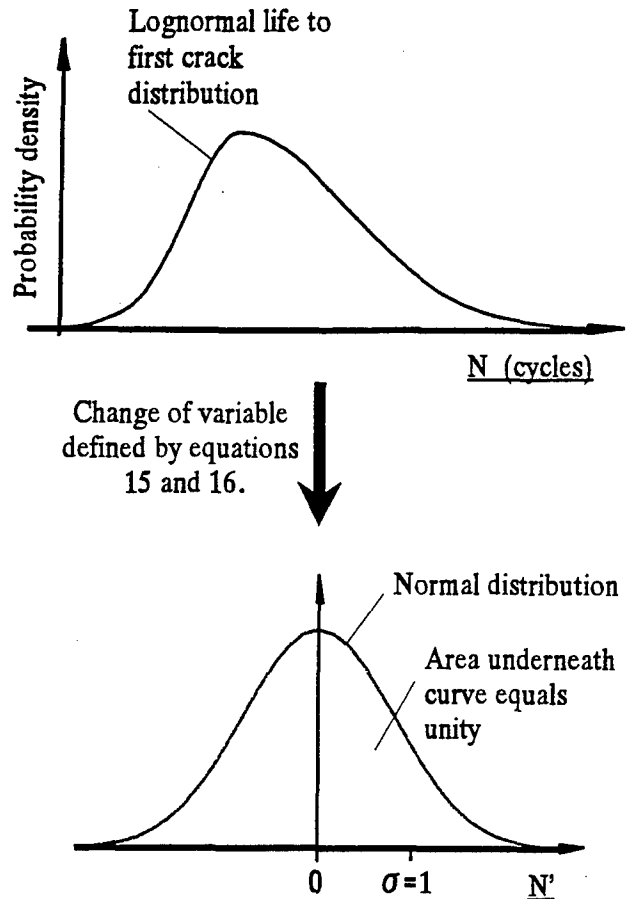


Figure 5. Effects of the change of variable defined by equations 15 and 16.

On removing the change of variable originally applied by equations 15,16, the following result is obtained:

$$\prod_{J=1}^n \left[1 - \text{normal} \left(\frac{\log \left(\frac{N_J^-}{N_\mu^{95\%}} \right)}{\frac{1}{6} \log \left(\frac{N_{+3\sigma}}{N_{-3\sigma}} \right)} \right) \right] = 0.05 \quad (19)$$

The $N_\mu^{95\%}$ value given by equation 19 is a 95% confidence estimate of the geometric mean of the population fatigue life distribution. Equation 19, is solved by substitution of the known values and iteration until the equation is satisfied, to give the value of $N_\mu^{95\%}$.

Once this value has been established, safety factors can be applied. For example, to apply a safety factor that not more than 1/750 components reach the defined dysfunction point, the following formula would be used.

$$Ar = N_{-3\sigma}^{95\%} = \frac{N_\mu^{95\%}}{\sqrt{\frac{N_{+3\sigma}}{N_{-3\sigma}}}} \quad (20)$$

Going back to the example of 5 non-finite results of 10,000 cycles and with an assumed scatter factor $N_{+3\sigma}/N_{-3\sigma}$ of 6, substitution in equation 19 gives $N_{\mu}^{95} = 10374$ cycles and substitution of this value in equation 20 gives an Ar value of 4235 cycles. Thus the percentage safe life increase for this component given by equations 19 and 20 is equal to $(4235 - 3277)/3277 \times 100\% = 29\%$.

Returning to the example given in section 7.2, the improved analysis procedures (equations 19 and 20) using all 3 results gives a safe life of 3492 cycles, that is 21% higher.

The percentage life increases given by the above two examples are fairly typical, although in service applications, the life extensions given have ranged between 5% and 50%.

8 Simplified risk model

As discussed earlier, situations have arisen where component life reductions have caused large numbers of mature age engines to suddenly have life expired parts. In such cases, although components should be rejected before their safe service lives have expired, strict application of this rule could have grounded significant portions of several fleets of military aircraft.

Allowing specified components to operate at slightly higher risk for short specified periods, may give life increases beyond Ar, which may largely alleviate these situations. It can buy the lead time required to obtain spares and to replace the lifex parts.

As formulated, current lifing procedures cannot be used to estimate risk because they use 'safety factors' which hide the actual risk. To get an appropriate estimate of the risk of fatigue failure, all of the generally applied safety factors have to be replaced by robust statistical modelling of the respective sources of component life uncertainty.

DERA's latest model achieves this capability, however, representation of service usage aspects can involve more complexity than is appropriate for covering within a single paper. To aim for relevance to a wider audience, the core of the model is presented below, but excluding the service usage modelling detail.

Also, although risk models do not have to use safety factors, risk estimates are usually required at given percentages over the respective declared safe-service life Ar. For these reasons, the risk equations given below include terms that relate to the safety factors supporting an 'Ar' value.

To simplify the derivation, the following change of variable is used

$$N' = \log(N) \quad (21)$$

and so the combined safety factor S (given by equation 3) is transformed to S', where

$$S' = \log(S) \quad (22)$$

The risk/efh is defined as the rate of increase of probability of failure with respect to engine flying hours. It is also easier to express the risk in terms of the rate of increase of the transformed variable $\delta S'$, than in terms of $\delta(\text{efh})$ and so the following partial derivative is used:

$$\begin{aligned} \text{risk} / \text{efh} &= \frac{\partial \{p(\text{fail})\}}{\partial \{\text{efh}\}} = \frac{\partial \{p(\text{fail})\}}{\partial S'} \cdot \frac{\partial S'}{\partial \{\text{efh}\}} \\ &= \frac{\partial \{p(\text{fail})\}}{\partial S'} \cdot \frac{1}{\text{efh}} \end{aligned} \quad (23)$$

If there existed an infinite sample of component tests results, there would be no sampling error. The location of the component life relative to the geometric mean of the burst distribution would then be precisely determined as shown in figure 6. Therefore, the risk/efh would simply be equal to the shaded area in figure 6.

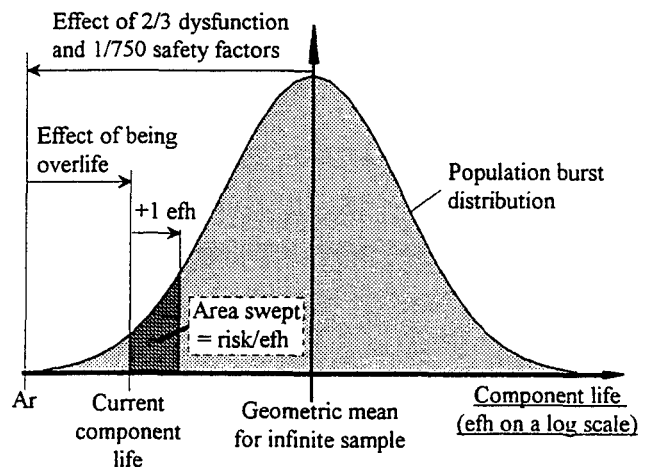


Figure 6. Illustration of how the risk model works in the simple case where the geometric mean of the population burst distribution is known.

In practice most component test samples are small. As discussed, the form and scatter of the burst distribution are identified. Therefore the sampling error is equal to the difference between the sample geometric mean GM and the population GM.

To account for the sampling error x' , the risk/efh is equal to the integral of the risk/efh given the location x'

of the sample mean on the sampling distribution times the probability of the sample mean being located at x' on the sampling distribution (see figure 7). That is,

$$\begin{aligned} \frac{\partial \{p(\text{fail})\}}{\partial S'} &= \int \partial \{p(\text{fail})\} / \partial S' | x' \cdot PD_s(x') \cdot \partial x' \\ &= \int PD_b(x'-S') \cdot PD_s(x') \cdot \partial x' \end{aligned} \quad (24)$$

To solve equation 24, it is necessary to obtain the expressions for the two To solve equ probability density functions PD_b and PD_s for the burst and sampling distributions respectively.

When the scatter factors for LTFC and crack propagation are assumed conservatively to be equal to 6 and 4 respectively, a typical scatter factor used for the corresponding burst distribution is 5. (A value lower than 6 is appropriate since it is less likely that below average crack propagation life will combine with below average LTFC). A value of 5 shall be assumed in the following derivation. The standard deviation of the burst distribution (in the transformed co-ordinates) is given by equation 16. That is,

$$\sigma_b' = \frac{\ln 5}{6} \quad (25)$$

The standard deviation of the transformed sampling distribution of the GM of an LTFC sample is equal to the standard deviation of the transformed population LTFC distribution times the reciprocal of the square root of the sample size. As discussed, the transformation is defined by equations 15 and 16. Therefore,

$$\sigma_s' = \frac{\ln 6}{6\sqrt{n}} \quad (26)$$

Both the sampling and burst distributions are assumed to be lognormal. Due to the change of variable specified by equation 21, they are transformed to normal distributions. The location of the component relative to the mean of the sampling distribution is simply x' (see figure 7) and thus the expression for $PD_s(x')$ is

$$PD_s(x') = \frac{1}{\sqrt{2\pi}} \cdot \frac{1}{\sigma_s'} \cdot \exp\left(-\frac{1}{2} \left[\frac{x'}{\sigma_s'}\right]^2\right) \quad (27)$$

The location of the component relative to the GM of the burst distribution is equal to $(x'-S')$ and the expression for $PD_b(x'-S')$ is

$$PD_b(x'-S') = \frac{1}{\sqrt{2\pi}} \cdot \frac{1}{\sigma_b'} \cdot \exp\left(-\frac{1}{2} \left[\frac{x'-S'}{\sigma_b'}\right]^2\right) \quad (28)$$

Substitution of equations 27 and 28 into equation 24 and evaluation of the integral (between $\pm\infty$) gives the following expression

(29)

$$\frac{\partial \{p(\text{fail})\}}{\partial S'} = \frac{1}{\sqrt{2\pi}} \cdot \frac{1}{\sqrt{\sigma_b'^2 + \sigma_s'^2}} \cdot \exp\left[\frac{-S'^2}{2} \left(\frac{1}{\sigma_b'^2 + \sigma_s'^2}\right)\right]$$

Equation 29 is of a type typical for summation of two random errors each belonging to a normal distribution. Substitution of equations 21, 22, 25 and 26 into equation 29 gives the following solution for the risk/efh

(30)

$$\begin{aligned} \frac{\partial(\text{risk})}{\partial(\text{efh})} &= \frac{1.5}{\text{efh}} \sqrt{\frac{n}{n+1239}} \times \\ &\exp\left[-6.949 \left(\frac{n}{n+1239}\right) \left(\ln\left(\frac{\text{efh}}{Ar \times \beta_i}\right) - 1.0782 - \frac{0.49094}{\sqrt{n}}\right)^2\right] \end{aligned}$$

where equation 30 represents the risk/efh experienced by an individual component at a life of 'efh' where 'n' is the component test sample size

To illustrate the methodology, suppose a component has a declared safe service life of 10,000 cycles, based on a test sample of 3 and that the life-to-first-crack reference cycle exchange rate is 2. Then, for a component at full life (100% Ar) substitution of values into equation 30 gives an estimated risk/efh of $2.8e-8$. Note that to convert from efh to 'Ar', the LTFC is simply divided by the exchange rate β_i .

Suppose next, that the declared safe service life of the component type were reduced by 20% to 8000 cycles. Then such a component at its original life of 10,000 cycles would experience a higher risk ($2.1e-7/\text{efh}$), i.e., if, an additional risk of $1.8e-7/\text{efh}$ is deemed acceptable for a limited period (ie. $2.1e-7-2.8e-8$), then the life extension of 25% would be available to the component.

Having established equation 30, it is straightforward to derive related formulae applicable for other scatter factors or for damage tolerance terms.

9 Conclusions

Calculation of the safe service life, A_r , is discussed. Life extension beyond the values given by this method is sometimes possible, and 3 opportunities for so doing have been described in the paper. It has been shown that

- 1) Exploitation of the full safe-service-life capability of crack-tolerant components can give safe life increases of up to 20% in engine flying hours over those associated with conventional safe life procedures.
- 2) Exploitation of non-finite fatigue test results can give safe life extensions in engine flying hours of 20% on average, as illustrated by the examples. (The benefit is an increasing function with respect to both the number and significance of the non-finite results in the sample).
- 3) Service operation to lives beyond A_r , may be possible with little compromise of safety. The life increase available is dependent on the level of risk deemed acceptable in the circumstances. The risk model developed in the paper illustrates that short term life increases of up to 20% are sometimes at the price of less than an order-of-magnitude increase in risk/efh.

10 References

- 1) 'Life assessment of fracture critical aeroengine parts', G.F. Harrison, Int. Conference, Sheffield 97
- 2) UK Military Defence Standards Def. Stan. 00-971 General Specification for Aircraft Gas Turbine Engines, 1986.
- 3) Joint (European) Airworthiness Requirements-Engines, (JAR-E), Civil Aviation Authority, 1986.
- 4) 'Mechanical Survival', J.H. Bompas-Smith, 1973, Ed. Mc. Graw-Hill, Maidenhead, Berkshire, England.

© Crown Copyright 1998/DERA
Published with the permission of HMSO

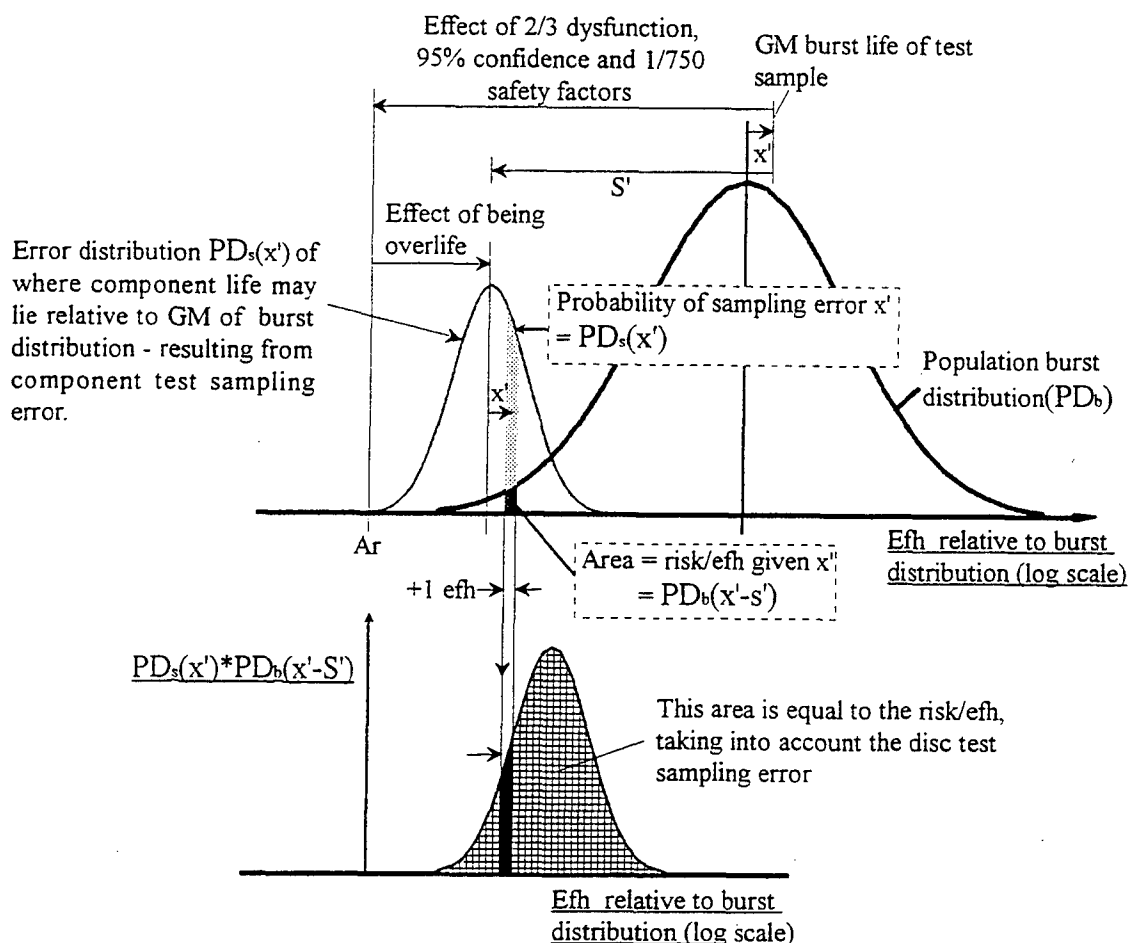


Figure 7. Illustration of how the disc test sampling error is accounted for in the risk model

Critical Parts' Life Extension Based on Fracture Mechanics

Peter Blüml and Jürgen Broede
MTU Motoren- und Turbinen-Union München GmbH
Dept. TPMR and TPMM
P.O. Box 50 06 40
80 976 Munich
Germany

1. SUMMARY

The classical method for fracture critical parts lifing is the safe life approach, where 'safe life' in fact means safe crack initiation life. In many cases, the released life of a critical part can be extended if the lifing concept is supplemented with the safe crack propagation life approach. In particular, if the life limiting area of a part possesses substantial damage tolerance capability, the possible parts' life extension will be significant.

The underlying safety criteria and the statistical treatment of the test results for both the approaches are equivalent, but for prediction of the crack propagation life the application of fracture mechanics methods and the knowledge of material crack growth behaviour are necessary. Crack growth is directly related to the stress intensity factor. The stress intensity factor itself depends on the currently applied stress field (which in turn depends on mechanical and thermal loading), the geometry of the component, and the current shape of the crack front. Load and crack front shape vary with time. Two methods are discussed how the stress intensity factor can be obtained, namely experimentally from crack growth tests of the real component or analytically from 3D finite element calculations.

Service life of an aero engine component is determined by its released life and its life consumption caused by operational usage. Therefore, it is important to monitor the operational usage either by on-board monitoring devices or by the application of adequate cyclic exchange rates (β -factors). Experience gained with the RB199 IP compressor and IP turbine (where this safe crack propagation life approach is utilised) shows that crack propagation β -factors are by a factor of 2 - 3 higher than crack initiation β -factors. Nevertheless, the achieved life extension in terms of engine flying hours is about 40%.

2. INTRODUCTION

Fracture critical parts in aero engines undergo cyclic loading under operational usage. This cyclic loading causes cyclic fatigue at highly stressed critical areas, what leads to initiation and propagation of cracks. For most of the fracture critical parts, fatigue is the life limiting damage mechanism. The life limit is directly related to the presence of a fatigue crack or to a predetermined stage of its propagation. Fatigue life of a part is defined as a number of cycles (with a given stress range at given temperature conditions) that the life limiting critical area is able to endure until a crack with specified properties has developed.

The way, how the fatigue life of a fracture critical aero engine part shall be established, is laid down in lifing procedures.

They specify the basic lifing concept and details of the methods and criteria to be used. Particularly for military applications, the lifing procedures are part of project related specifications. Although the general ideas of the lifing concepts are the same, one can observe some development. One of the most important improvements of the recent past is, that parts originally lifed to safe (crack initiation) life may now take advantage of life extension into the safe crack propagation regime.

3. SAFE CRACK INITIATION LIFE - THE CLASSICAL APPROACH

The concept of safe crack initiation life can be considered as the classical lifing approach for critical parts in aero engines. The basic idea of this concept is that

- a new part is free of defects
- a defect (in this case a fatigue crack) is generated in service
- the part's life is expired, when the defect has been created

The criterion for 'existence' of a crack is that the crack has been initiated and grown to a certain depth. A commonly used value for this crack depth is 0.4 mm. This criterion is a little arbitrary, although sensibly based on long experience.

Figure 1 illustrates the safe crack initiation life. The axes represent the number of cycles N and the corresponding crack depth a . The point of dysfunction identifies one of the criteria defined in para 4. The number of cycles to dysfunction is denoted N_{dys} . The crack initiation life N_i describes the number of cycles to a crack depth of 0.4 mm.

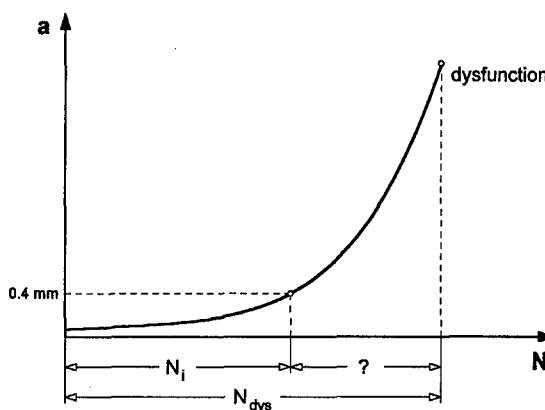


Figure 1: Safe Crack Initiation Life

The safe crack initiation life is established as the number of cycles to reach an accepted statistical probability for the

existence of a crack with that depth. The statistical probability takes into account that material strength exhibits some scatter. And for the weakest individual of the parts' population, the structural integrity must be ensured. Generally accepted statistical probabilities for that weakest part are in the range of 1 out of 750 to 1 out of 1000.

Parts lifed under this concept are not inspected if the crack is present when they are retired, and due to the nature of this concept only the fewest of them would contain one. Nevertheless, re-use of the parts beyond the safe life - as defined above - is not considered.

The criterion of this concept - namely the existence of a crack - does not mean that the part will fail immediately when the crack depth is exceeded. Some safety margin to the final part failure will remain. However, the concept cannot provide a measure for the real safety of the critical part, since it is unable to predict a value for the failure margin. In most of the applications there will be sufficient margin for a crack to grow to part dysfunction, but it is also possible that the dysfunction life is very close to the crack initiation life. In such very rare cases the crack initiation life cannot be considered as really safe.

4. SAFE CRACK PROPAGATION LIFE - THE APPROACH FOR LIFE EXTENSION

The concept of safe crack propagation life is more suitable to exploit the life potential of a fracture critical part. This concept is also known as damage tolerance concept.

The concept is based on the idea that

- the part contains an initial defect at the beginning of the crack propagation phase (where the defect behaves like a crack of a certain depth)
- the crack propagates under service loading
- the part's life is expired when the crack enters the phase of part dysfunction

Part dysfunction may include a number of different criteria, for example

- unstable crack growth under basic operational loading
- onset of continuous crack propagation due to superimposed vibratory stresses (i.e. if high frequency stress levels exceed the crack growth threshold)
- loss of overspeed capability (i.e. a crack depth where overspeed conditions could cause spontaneous failure)
- unacceptable out-of-balance conditions

In contrast to the crack initiation criterion, the dysfunction criterion really determines the end of the part's life. This enables us to define a measurable safety margin. Thus, the part will be retired when a certain portion of the number of cycles to dysfunction have been accumulated. In most of our recent projects, this portion was two third.

The number of cycles to dysfunction encompasses both the crack initiation and the crack propagation phase. The safety factor of two third will be applied to the total number of cycles, i.e. the number of cycles necessary to generate the crack and to grow it to the dysfunction criterion.

Figure 2 illustrates the safe crack propagation life in an a vs N diagram. The point of dysfunction is given by one of the above criteria. N_{dys} is the number of cycles to dysfunction, whereas N_i represents the number of cycles to crack initiation

($a = 0.4$ mm) and N_p the period of crack propagation from $a = 0.4$ mm onwards to $2/3$ of N_{dys} .

The safe crack propagation life is established as $2/3$ of the number of cycles to reach an accepted statistical probability for the presence of the applicable dysfunction condition. The statistical probability takes into account that material strength and crack growth properties exhibit some scatter. For the weakest individual of the part's population, the structural integrity must be ensured. Generally accepted statistical probabilities for that weakest part are in the range of 1 out of 750 to 1 out of 1000.

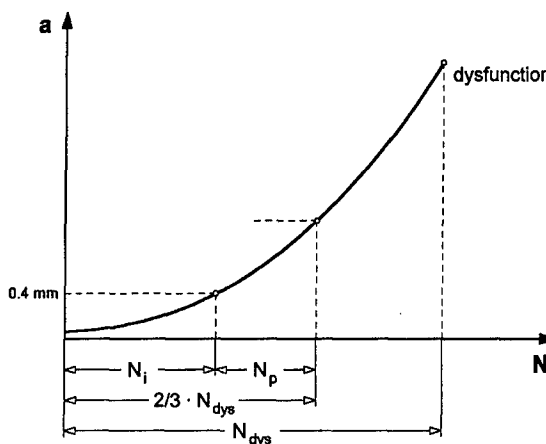


Figure 2: Safe Crack Propagation Life

Parts lifed under the safe crack propagation lifing concept are not inspected if the crack is present when they are retired. Re-use of the parts beyond the safe crack propagation life is not considered, although most of the parts will not contain a crack grown to the depth which is correlated with the dysfunction criterion.

There are a number of examples where the crack growth period has about half as many cycles as the crack initiation period. In those cases, two third of the dysfunction life equals to the crack initiation life. Thus, there cannot be taken much benefit from the application of the crack propagation life concept. Typical representatives for such conditions are bore areas of discs. But there are other critical areas, e.g. holes in flanges, arms and cones as well as rim areas of discs, which exhibit significant damage tolerance capability. For these areas, utilisation of the crack growth phase can significantly extend the part's fatigue life.

Both the discussed concepts have a lot of commonality. They both define the part's life in terms of multiples of the reference cycle (where the reference cycle defines the most damaging combination of two stress-temperature conditions in the design mission) and they use the same statistical criteria. Additionally, it is common to both that they do not care whether the assumed cracks are really present or grown to the assumed depth. This does not mean that, if cracks were found in the course of part's inspection, these observations would be ignored. Of course, each deviation from the predicted behaviour would be thoroughly investigated.

5. LIFE PREDICTION PROCESS

The basis of the life prediction process for both these concepts is the same, but in the details there are many differences.

A flowchart showing the life prediction process is given in

Figure 3.

The life prediction process starts from the design mission. The design mission is normally defined in the engine specification. It provides the required thrust and power as a function of time.

The engine design must also be given. This includes the detailed geometry of the components and the specification of the materials used. The kind of manufacturing processes should be taken into account, too.

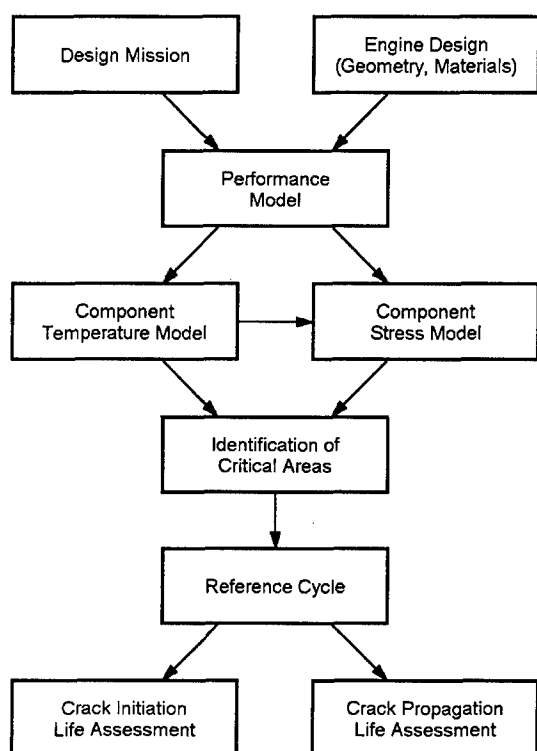


Figure 3: Life Prediction Process

In a first step, from thrust and power requirements there are engine performance parameters derived. They define for each point of the design mission the temperatures and pressures in the main gas stream, the spool speeds and shaft loads and torque. Additionally, the cooling air flows, temperatures and pressures in the secondary air system are determined.

In a second step, these performance and cooling system parameters are used as boundary conditions for the calculation of transient temperature distributions in the engine components. Finite element programs are used for this job. Of particular interest are the engine rotor systems which contain the majority of the fracture critical parts. Since the rotating parts are axi-symmetric, a 2D analysis is usually sufficient.

The third step is concerned with the mechanical analysis. Stresses and strains are calculated taking into account

- centrifugal stresses due to part rotation
- thermal stresses induced by temperature gradients
- stresses from pressure differences, shaft forces and torque
- manoeuvring stresses resulting from g- and gyro-loads
- assembly stresses

For these calculations, finite element codes are employed as well. Again for most of the features it is sufficient to use 2D

axi-symmetric models. Disturbances of the axi-symmetry (e.g. holes, scallops) are treated with stress concentration factors. For the determination of the stress concentration factors, there are frequently 3D detail analyses performed. Based on the stress analysis, the critical areas of the engine parts can be identified. Critical areas are those areas which carry the highest stresses and therefore are expected to determine the fatigue life of the part.

The second and third step together provide stress-temperature histories at the critical areas over the entire design mission. The stress-temperature histories are analysed with respect to their cyclic content. The most damaging cycle is identified and declared as the reference cycle for the considered critical area.

For most of the critical areas, the concept of safe crack initiation life is employed. Under this concept, the number of reference cycles needs to be predicted, which the critical area can undergo until a fatigue crack will have been generated and grown to the predicted depth of 0.4 mm. Material SN-curves are used which describe the relationship between applied stress (i.e. cyclic stress with a range between zero and applied stress; short: zero-max stress) and the corresponding number of cycles to crack initiation. If the reference cycle is not a zero-max cycle, then an equivalent zero-max cycle is determined, taking into account the mean stress effect. The SN-curve depends also on the temperature (i.e. for the same stress range but different temperatures, there are different numbers of cycles predicted). It is common practice that those curves are provided as design lines, what means that the relevant safety factors have been already included.

For critical areas where the life is extended into the safe crack growth regime, additionally the safe crack propagation life needs to be predicted. This calls for the application of fracture mechanics procedures. Typically, the methods of linear elastic fracture mechanics are used. Two elements are important

- the stress intensity factor (SIF) as fracture mechanics parameter and
- the crack propagation law (i.e. the crack propagation rate as a function of the SIF range)

The time history of the stress intensity factor must be calculated for each of the investigated critical areas. The stress intensity factor depends on the stress field around the critical area and the current shape of the crack.

The crack shape is given by the crack surface (which in many cases may be considered as a plane) and the crack front. For reliable predictions of the crack development it is necessary to consider the crack as a whole. In particular, it should be noticed that the stress intensity factor varies along the crack front, so that the crack growth velocity is different at different points of the crack front.

The development of a crack can be simulated with finite element calculations in combination with an appropriate crack growth law. A 3D FE model of the considered engine part is necessary. The crack surface and the crack front are introduced into this model. Details of the applied technique have been already published [1 - 3].

The procedure starts with an initial crack. The initial crack shape is either taken from test experience with real parts or simply assumed as a half or quarter elliptical front at a plane perpendicular to the direction of the maximum principal stress. The exact shape of the initial crack is not so important as the crack will develop into a balanced shape anyway.

For the part containing this initial crack, the stress intensity factor along the crack front is calculated. All relevant loads contributing to the stress field around the critical area are included. With the stress intensity factor and the crack propagation law, the crack growth increment at each point of the crack front is calculated and a new crack shape predicted. Since the crack develops slowly, the stress intensity factor will not change significantly during a small number of cycles. Thus the crack growth for a number of cycles can be computed with the same stress intensity factor distribution. But when the grown crack is distinctly different from the original one, a new SIF calculation becomes necessary. This process (calculation of the SIF, determination of the according crack growth rate and prediction of the new crack shape) is repeated several times building up a complete crack growth history over the number of applied cycles. This crack growth history ranges from an initial crack (which is usually smaller than or equal to that for the crack initiation criterion) to the onset of unstable crack growth.

Now, one can choose a path at the crack surface from the point where the crack has originated into the depth of the part. Along this path the crack depth is measured. For this path, a relationship between the crack depth and the corresponding stress intensity factor can be established. Dividing the stress intensity factor by the stress present at the critical area itself, defines a so called geometry function. This geometry function provides the relationship between the stress at the critical area and the stress intensity factor at the crack front for each value of the crack depth and enables us to calculate the time history of the stress intensity factor from the time history of the stress at the critical area including the effect of increasing crack depth.

For this procedure it is assumed that the stress fields around the critical area are proportional for all load cases of the mission. In fact, this is not the case. But the error is considered negligible as long as the stress intensity factors for the higher stress levels are modelled correctly. Deviations for sub-cycle stress intensity factor ranges are acceptable as their contribution to the overall damage is small. However, if it turns out that the inaccuracy becomes intolerable, an additional influencing parameter (e.g. the stress gradient) needs to be incorporated into the geometry function.

Currently only a correction for residual stresses is made. The basic idea for this correction is that during the first load cycles some local plastification occurs, what causes some redistribution of the stress fields. This redistribution is accounted for by an additional additive term in the formula for the stress intensity factor calculation.

The crack propagation life can be established by integration of the crack propagation rate from the initial crack depth (i.e. 0.4 mm) to the criterion of dysfunction under reference cycle loading. For this process it should be noticed that the crack growth law usually describes the average crack growth rate. Since the safe crack propagation life is required, an additional scatter factor needs to be applied. Based on statistical considerations, a scatter of 2 can be derived (assuming a 4:1 ratio between $+3\sigma$ and -3σ value of a log-normal distribution in life, which is typical for crack growth scatter). This factor is in addition to the 2/3 safety margin defined as part of the concept of safe crack propagation life.

6. LIFE VERIFICATION PROCESS

The expected predicted safe cyclic crack initiation life for a

critical area of a fracture critical part is verified by cyclic testing. In the case of a rotating disc or drum, this test consists of cyclic spinning.

A flowchart showing the life verification process is given in Figure 4.

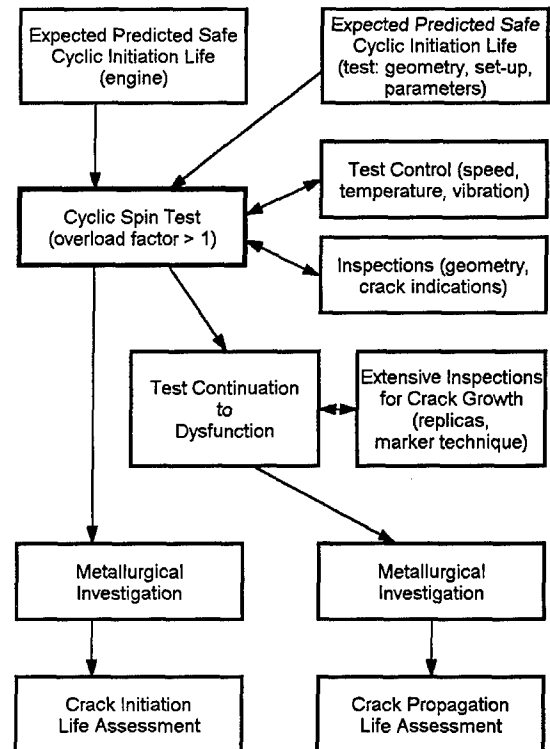


Figure 4: Life Verification Process

In many cases, the LCF life of most of the critical areas of a compressor or turbine disc - there are typically bore, web, bolt hole and rim slot - can be demonstrated within one test. The aim of the test is to verify the initiation life of the life limiting critical area. In most cases finite results, i.e. initiation life with a technical crack size of 0.4 mm depth, are thus only gained for one or two critical areas, whereas the others stay non-finite, i.e. without crack indication.

The test parameters chosen are such, that the reference cycle is covered for the critical area to be demonstrated. This means in detail that the temperature is very close to the maximum peak (stress and temperature) of the mission. The speed is adjusted to produce a small overload - compared to engine conditions. Correction of temperatures - test relative to engine - is done by rationing Young's modulus or ultimate tensile strength. An equivalent life is then calculated taking into account overload and the statistical model to be used for the project (see para 3).

The test result must state the Mean First Crack Line (i.e. the average relationship between stress and number of cycles to produce a technical crack) as it is a typical one.

Tests are performed on horizontal or vertical spin pits in atmosphere or nearly vacuum - whatever is best for the specific test or available. Temperature and speed are monitored continuously during the complete test and vibration measurements ensure the safe testing. Regularly non-destructive inspections i.e. visual, dye penetrant, magnetic particle, or eddy current are carried out to indicate unexpected

early cracking. To ensure that the technical crack size of 0.4 mm depth is reached, most test candidates are spun till cracks have a length of several mm.

In most cases, the tests produce several cracks. After testing, the most severe cracks are broken up and the cyclic crack initiation life is demonstrated by striation counting.

The test results gained over many years showed in some cases a remarkable life extension potential.

For example the cooling air hole in the cone of the RB199 IPC is a damage tolerant critical area. With this component our methodology for crack propagation life usage was developed. Due to the specific design, cyclic spin tests can be carried out till dysfunction is reached - which means here a crack length of 30 to 40 mm (see Figure 5). The scatter in the crack propagation behaviour is shown in Figure 6. On this basis the application of reduced scatter factors - compared to the initiation phase - could be justified (see para 5).

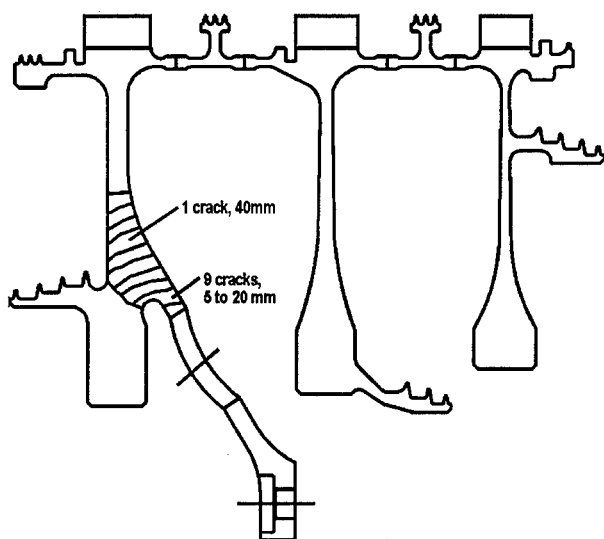


Figure 5: Crack Propagation at IPC Rotor Venting Hole

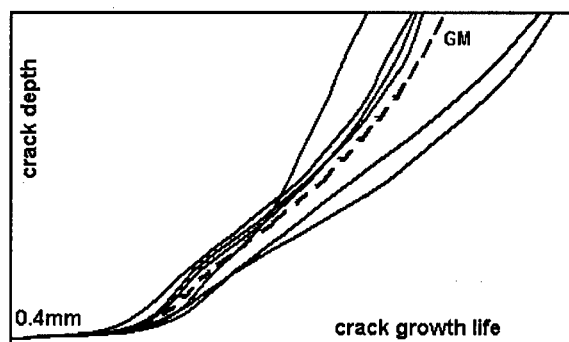


Figure 6: Scatter in Crack Propagation Behaviour

For other components (e.g. the RB199 IPT disc) it was necessary to verify the safe cyclic crack propagation life with a special crack growth test.

The rim slot bottom and the locking plate slot (the two leading areas of the RB199 IPT disc) were pre-damaged by eroding. The artificial cracks were half circular shaped and had a depth

up to 0.3 mm. This procedure was necessary to avoid early cracking in the firtree serrations. To calibrate striation counting after test end and breaking up the cracks, the marker load technique was used [10]. Every 3000 test cycles the heating was switched off for 600 sub-cycles. The fractographic picture shows small sharp bands thus enabling the calibration of striation counting (see Figure 7). In addition, replicas were made at each inspection interval. The matching of the three methods: striation counting, marker cycles and replicas was excellent as can be seen in Figure 8. After each interval, the surface geometry of the crack (replica) was compared with the corresponding FE calculations. Figure 9 shows crack growth life versus crack dimension. The test result is in good agreement with the FE calculation. To avoid burst, the test was stopped before the crack grew to dysfunction size. The test cycles from 0.4 mm to test end were then counted from striations by correcting with our marker cycle results. Multiplying these test cycles by a life factor (see para 5 and [4]) leads to the mean crack propagation life in reference cycles. Applying a scatter factor as described in para 5 the minimum crack propagation life in reference cycles, i.e. the factored crack propagation life is derived.



Figure 7: Crack Fronts Made Visible by Marker Loads (at different stages of crack propagation), [10]

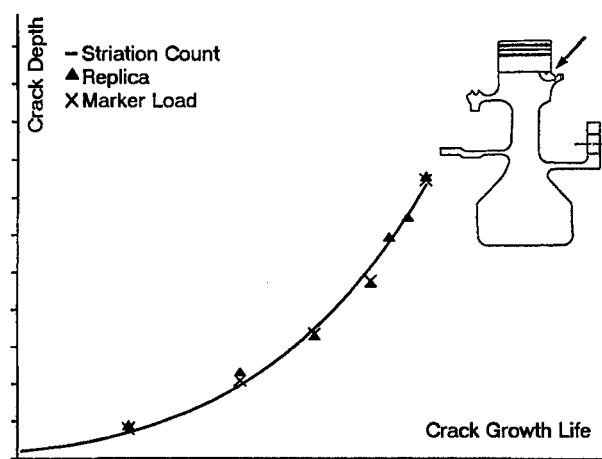


Figure 8: Comparison of Crack Monitoring Techniques

Above, there were two examples discussed. The first one (RB199 IPC cone hole) provided the experimental establishment of the geometry function. Furthermore, the

related test results gave evidence of the reduced scatter for crack propagation compared to crack initiation scatter. The second example (RB199 IPT disc) provided confirmation of the analytically predicted geometry function and the underlying crack propagation law.

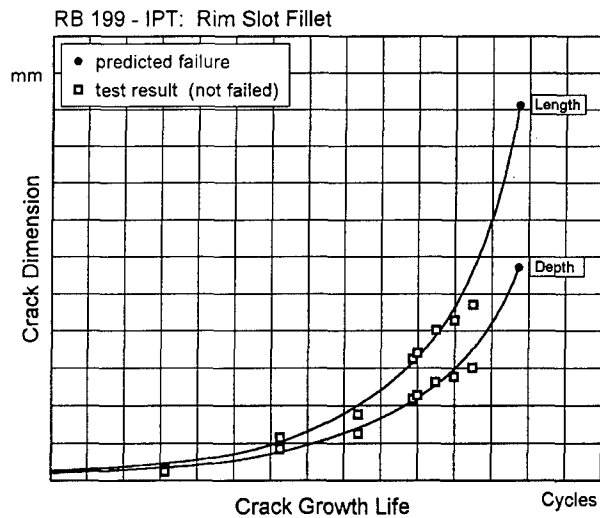


Figure 9: Comparison of Predicted and Observed Crack Propagation

The test results 'factored critical area cyclic crack initiation test life' (F_{ci}) and 'factored critical area cyclic crack propagation test life' (F_{cp}) were added and 2/3 hereof released as 'predicted total safe cyclic life'.

In order to support the life progression procedure in the crack propagation part, technical life reviews are conducted before the relevant critical part reaches the specified service life. Especially inspection results gained on a natural arising basis provide additional safety with this increased life usage method.

7. OPERATIONAL USAGE

How long an engine - especially its fracture critical parts - can be kept in service, depends on both the released life of the part and life consumption due to operational usage. Different methods for life usage monitoring have been established.

The traditional method is to count the engine flight time and to multiply it with a cyclic exchange rate. The cyclic exchange rate (also called β -factor) provides a relationship between the flight time and the life consumed at a critical area due to the according engine operation. But the correlation between flight time and cyclic life consumption is very weak. This means that conservatism needs to be incorporated into the β -factor, what in turn leads to overestimation of life consumption for most of the parts.

Better exploitation of the released life can be achieved with individual monitoring, where life consumption of each part is individually calculated based on actually measured engine parameters. A typical solution is the utilisation of an on-board life usage monitoring system. Examples for such systems were the subject of several presentations [5 - 9].

The question important in this context is, what are the differences in life consumption between life consumed in the crack initiation phase and life consumed in the crack propagation phase. Generally, the fatigue life consumption of a critical area is related to the cyclic content of the stress-

temperature history at this critical area for a given mission. The stress-temperature history consists of a main cycle and a number of sub-cycles. Life consumption of the main cycle can be expected similar to the reference cycle damage. This is true for both the crack initiation and the crack propagation phase. But for sub-cycles the situation is different. In the crack propagation regime, the sub-cycle consumes a higher portion of a reference cycle than in the crack initiation regime. This is due to the different slopes of SN-curve and crack propagation curve. Additionally, the crack propagation threshold is 'lower' than the endurance limit of the SN-curve, so that a number of sub-cycles which do not contribute in the crack initiation phase add their portion to the accumulated life consumption in the propagation phase.

Consequently, one can expect that mission life consumption (particularly if the mission contains many sub-cycles) is faster in the crack propagation regime. When thinking in terms of β -factors, one may expect significantly higher values for the crack growth phase than in the crack initiation phase.

Experience obtained with the IP compressor and IP turbine of the RB 199 engine shows that crack propagation β -factors may be a factor 2 - 3 higher than crack initiation β -factors. But one should be aware that these differences mainly depend on the sub-cycle content of the mission profile. So, these figures may be regarded as example or general hint, but do not serve as a rule for other applications.

The customer preferred units of life consumption are not cycles and β -factors but engine flying hours (EFH). To get this information, one has to divide the released life (in cycles) by the relevant β -factor. If only life in the crack initiation regime is released, this released life divided by the crack initiation β -factor yields the authorised service life in EFH. The situation becomes more complex if crack initiation and crack propagation life is released. In that case, the difference between crack initiation life and 2/3 of dysfunction life (in terms of cycles) needs to be divided by the crack propagation β -factor to result in authorised crack propagation life in EFH. The total life in EFH is then the sum of crack initiation and crack propagation life (in EFH).

The life extension beyond the safe crack initiation life in terms of EFH is a real measure for the benefit gained by the introduction of the safe crack propagation life concept. Life extension of about 40% (in EFH) could be achieved for the RB 199 IPC and IPT rotor.

8. CONCLUSION

Two methods - the 'safe crack initiation life approach' and the 'safe crack propagation life approach' - have been discussed. For prediction of the crack initiation life, the traditional methods of the elasticity theory are used together with a phenomenological damage rule. For the crack propagation life, additionally the methods of linear-elastic fracture mechanics in conjunction with an also phenomenological crack growth law are applied.

Common to both concepts is, that life is treated in terms of reference cycles. Verification procedures and statistical methods used are the same, too. This ensures that both concepts can be applied in parallel - and even in combination - with common appearance to the customer.

Utilisation of the crack propagation portion of a critical area's life potential can significantly extend the authorised life of an

aero engine part. Care should be taken, as not all critical areas exhibit remarkable damage tolerance capability. But in any case, assessment of the real safety margins is possible when crack development to dysfunction (what means in reality 2/3 of it) is considered.

9. REFERENCES

1. G. Dhondt, "Automatic 3-D Mode I Crack Propagation Calculations with Finite Elements", *Int. J. Numer. Meth. Engng.*, 41, 739-757 (1998)
2. G. Dhondt, "Cutting of a 3-D Finite Element Mesh for Automatic Mode I Crack Propagation Calculations", *Int. J. Numer. Meth. Engng.*, 42, 749-772 (1998)
3. G. Dhondt, "Automatic Three-Dimensional Cyclic Crack Propagation predictions with Finite Elements at the Design Stage of an Aircraft Engine", RTA/AVT Symposium "Design Principles and Methods for Aircraft Gas Turbine Engines", Toulouse, France, 11-15 May 1998
4. TU 346, "Lifing Procedure for the RB199 Group A Parts", (TURBO UNION private data)
5. J. Broede, "Engine Life Consumption Monitoring Program for RB199 Integrated in the On-Board Life Monitoring System", AGARD Conference Proceedings No 448, Quebec, 1988
6. K. Richter, "The On-Board Monitoring System of the MTR390 Engine", 17th International Symposium AIMS, Bonn, 1993
7. F. Hörl, K. Richter, "Monitoring the EJ200 Engine", 18th International Symposium AIMS, Stuttgart, 1995
8. J. Broede, "Design and Service Experience of Engine Life Usage Monitoring Systems", 5th European Propulsion Forum, Pisa, 1995
9. J. Broede, H. Pfoertner, "OLMOS in GAF MRCA Tornado - 10 Years of Experience with On-Board Life Usage Monitoring", 33rd AIAA/ASME/SAE/ASEE Joint Propulsion Conference & Exhibit, Seattle, 1997
10. G. König and M. Mandjik, "Evaluation of the Cyclic Life of a Turbine Disc by Marker Loads", MTUM-N96ELB-0013 (MTU Proprietary Report), 1996

DAMAGE TOLERANCE AND RELIABILITY OF TURBINE ENGINE COMPONENTS

Christos C. Chamis

Senior Aerospace Scientist
NASA Lewis Research Center
Cleveland, Ohio 44135, U.S.A.

1. ABSTRACT

A formal method is described to quantify structural damage tolerance and reliability in the presence of multitude of uncertainties in turbine engine components. The method is based at the materials behavior level where primitive variables with their respective scatters are used to describe that behavior. Computational simulation is then used to propagate those uncertainties to the structural scale where damage tolerance and reliability are usually specified. Several sample cases are described to illustrate the effectiveness, versatility, and maturity of the method. Typical results from these methods demonstrate that the methods are mature and that they can be used for future strategic projections and planning to assure better, cheaper, faster products for competitive advantages in world markets. These results also indicate that the methods are suitable for predicting remaining life in aging or deteriorating structures.

2. INTRODUCTION

The pursuit of achieving and retaining competitive advantages in world markets necessarily leads to proactive drives for better-cheaper-faster products to market. This becomes even more important in the high-tech sector which includes aerospace vehicles. The awareness for conservation of natural resources also leads pro-actively to the reliable cost-effective useful-life extension of existing products. In the first case, it requires very effective use of available resources. In the second case, it requires formal methods to quantify the current strength of a specific structure/component and subsequent reliable evaluation of respective remaining strength. Both cases include a multitude of uncertainties. The first case includes uncertainties in new unproven methods for design and/or manufacturing as well as uncertainties associated with lack of sufficient data of new candidate materials. The second case is full of uncertainties from (1) unknown assumptions and conditions of the initial design, (2) records of environmental exposure, (3) material degradation of various factors, etc.

In scenarios of multitude of uncertainties described above, probabilistic methods offer formal approaches to quantify those uncertainties and their subsequent effects on material behavior, on service and on attendant reliabilities and risks. The objective of this article is to

describe one probabilistic method for evaluating structural damage tolerance and reliability from material behavior to service life and to retirement for cause. That probabilistic method (1) is based on formulations that describe the physics in terms of primitive variables and respective scatter ranges, at the lowest engineering manageable scale and, (2) relies on computational simulation methods to propagate those uncertainties from that elementary scale through all intermediate scales where metrics for structural damage tolerance and reliability are specified. The method has evolved over the past fifteen years and has matured sufficiently to evaluate structural damage tolerance and reliability under various scenarios (Refs. 1, 2, and 3). The method has several unique features. The two that are most useful to present results are: (1) quantifiable reliability in terms of cumulative distributions functions and, (2) sensitivity factors of the primitive variables that affect that reliability. The article first introduces the fundamental concept and computational simulation method by a simple example. This is followed by a brief description of the method and its attendant computer codes. Subsequently, several sample cases are discussed to: (1) illustrate the versatility of the method, (2) the large amounts of information it generates, (3) the relevance of the information and, (4) recommendations that are readily inferred for design, material development quality, certification, in-service health monitoring, retirement for cause and even recycling. The description is limited to typical results obtained and their respective interpretation. References are cited for specificities.

3. FUNDAMENTAL CONCEPT

It is instructive to describe some fundamental concepts of probabilistic structural analysis/design by using a simple example. The simple example for that purpose is the probabilistic evaluation of the tip displacement of cantilever beam loaded at the free-end as shown schematically at the top left of Figure 1. The equation (deterministic - model) for predicting the tip displacement is shown under the schematic. This equation describes the physics of the response sought and includes the fundamental parameters (primitive variables) that govern the tip displacement. For example P is the load, l is the length, E is the material stiffness, b is the width and t is the thickness. These primitive variables can also be grouped in three generic categories load (P), geometry (l , b , and t), material (E). Experience

has shown that if we make several cantilever specimens there will be a scatter of values for each of the primitive variables. The task, therefore, of probabilistic simulation is to account for the effects of that scatter on the displacement of the beam.

The task is considerably simplified when we recognize that (1) the tip displacement equation is the analogue of a physical testing machine and (2) the scatter in the primitive variable, P , l , b , t and E , can be assumed to be represented by simple and well known statistical distributions (Fig. 1, lower left). These distributions help us in two ways as will become evident subsequently. In order to evaluate the effects of the uncertainties of the primitive variables on the tip displacement, we proceed as follows: Step (1), we decide on the range of the scatter in each primitive variable. This range in practical cases is established from experience but for our simple example, we assume that scatter for the modulus is between 165 and 193 GPa (24 and 28 mpsi); for the length, between 48.3 and 53.4 cm (19 and 21 inch); for the width, between 2.41 and 2.67 cm (0.95 and 1.05 inch); for the thickness, 3.05 and 3.30 cm (1.20 and 1.30 inch); and for the load between 356 and 534N (80 and 120 lb.). It is important to note that the only test data we had were the mean values for the primitive variables. We assumed the range of the scatter. Note that the mean value for each primitive variable is where the vertical line, drawn from the peak of the respective distribution, intersects the horizontal line. Step (2), for each primitive variable in the equation we select randomly a value from within its respective scatter. Having the simple statistical distributions allows us to make non-biased random selections. For example the values selected randomly can be: 176 GPa (25.5 mpsi) for E , 52.8 cm (20.8 in) for l , 2.51 cm (0.99 in) for b , 3.23 cm (1.27 in) for t and 512N (115 lb.) for P . Step (3), We substitute these values in the equation and we get 0.193 cm (0.08 in) for the tip displacement. Step (4), Repeat Step 3 for different sets of primitive variable values until sufficient data have been accumulated to plot the probability distribution curve (Fig. 1, center-right). For example the mean value will be close to 0.165 cm (0.065 in). There is about 95% probability from the cumulative probabilistic curve (Fig. 1, center-right) that the tip displacement will be less than 0.193 cm (0.08 in) 95 of 100 trial calculations in Step (3).

When the data is generated in Step 4, as just described, it is called Direct Monte Carlo Simulation and generally requires a large number of simulations.

Methods/algorithms have been developed to generate the two probability graphs for the displacement with a relative few number of simulations. One such method is known as the Fast Probability Integration (FPI), [3]. That method was used to generate the probability curve (Fig. 1). Application of FPI requires input of mean value, scatter range and probability density function of the scatter for each participating primitive variable. As

was already mentioned, the probabilistic simulation can be performed with known mean values and judiciously assumed scatter ranges for the primitive variables.

A byproduct of the FPI is the sensitivity factors (Fig. 1, lower right). These factors quantify and order the sensitivity of the cumulative distribution function of the response variable to the uncertainty (scatter range) in the primitive variables. For our simple example, the load (primitive variable) has about the same effect on the tip displacement (response variable) as the geometry parameters (primitive variables) for low probability (less than 1 in 1000) while the thickness (primitive variable) dominates at high probabilities (greater than 999 in 1000). More about sensitivities in later sections. For application to structural components/systems the above procedure is generalized as follows:

- Step 1. Develop or use a deterministic model of the entire component/system with its boundary and load conditions and expected environmental conditions. In practical structural situations this would be mostly a finite element model.
- Step 2. Identify the primitive variables in the deterministic model. These will include material properties, fabrication process variables, structural parameters, loads, (including environment), boundary conditions, etc. In the case of composite structures use integrated composite mechanics to predict the composite properties starting with micromechanics and accounting for both fabrication and environmental effects.
- Step 3. Obtain/assume mean values, scatter range and probabilistic distribution for each primitive variable.
- Step 4. Perturb each primitive variable on either side of their respective means by a reasonable small amount usually up to about 10 percent (up to 20 percent may be used but with caution). Anything greater than 20% may be more of a shift or even multi-modal instead of reasonable scatter.
- Step 5. Conduct deterministic analyses with the values selected in Step. 4.
- Step 6. Repeat Steps 4 and 5 several times to generate sufficient information for FPI use.
- Step 7. Use FPI to generate the probability distribution functions for the desired responses, displacement, stress, frequency etc., as well as respective sensitivities at select probability levels.

The above generalized procedure is practical through computer codes as will be described subsequently. It is applicable to practically all disciplines as well as it is to structures described herein.

4. PROBABILISTIC SIMULATION OF COMPONENT/SYSTEM RELIABILITY

There are three essential parts in evaluating turbine engine component/system durability and reliability. These are: (1) probabilistic simulation of the loading conditions, (2) probabilistic simulation of the structural component including supports and, (3) probabilistic simulation of the material(s) behavior. Each of these parts must be defined by inputs of its respective deterministic model, primitive variables and their attendant scatter. The probabilistic simulation proceeds to evaluate a specific response and its attendant scatter. The evaluated response is then compared with the corresponding resistance to assess the probability of failure which can be used subsequently to evaluate component/system durability and reliability. A conceptual schematic of the procedure is shown in Figure 2. Shown in the figure are: (1) the three essential parts of component/system reliability simulation, (2) the structural response obtained, (3) the resistance evaluated, (4) probable damage (overlap of response scatter with resistance scatter), (5) info passed on for reliability and risk assessments and, (6) the institutions which participated to develop the requisite formalism of the concept and to implement it into an operational computational procedure (Ref. 1). A block diagram of the computer code logic is shown in Figure 3.

The schematics in Figures 2 and 3 succinctly summarize probabilistic structural performance assessment. The concept is relatively straight forward and perhaps appears simple. However, implementation in to a workable computer code requires knowledge of: (1) advanced structural mechanics, (2) efficient probabilistic algorithms, (3) material behavior, and (4) proficient and subtle computer programming techniques.

Note in Figure 3 that (1) uncertainties in the human factor and in the computer code can also be included, (2) inputs for required performance, component/system longevity and acceptable reliability and risk must be provided, and (3) the simulation provides information to probabilistically select verification tests to assure component/system certification with an acceptable reliability and affordable risk. All of these will be described later in the several sample cases.

Simple loading conditions can be input directly in the probabilistic structural analysis. Complex loading conditions require system specific computer codes. Those for the space shuttle main engine are simulated by the composite load spectra computer code (Ref. 2). Probabilistic structural analysis is performed by a

specialty computer code (Ref. 3). Suffice it to say that these computer codes exist, they are extensive and are described in those references which also include respective users' manuals

5. PROBABILISTIC SIMULATION OF MATERIAL BEHAVIOR

Probabilistic simulation of material behavior is relatively new. It was developed at Lewis Research Center and so far as the author knows is the only one of its kind. Since the impetus for this article is durability and reliability materials-based life-prediction is a very important part. Therefore, it is appropriate to describe the probabilistic material behavior models (PMBM) used in the simulation in some detail. The deterministic model evolved during the course of research for high temperature metal matrix composites (Ref. 4). Implementing the deterministic model for probabilistic simulations evolved from a research grant with the objective to formally describe uncertainties in material behavior (Ref. 5) for space shuttle main engine components.

Conceptually the model is based on the rather self-evident axiom that: "each material characteristic property, observed by conventional testing, constitutes a multi-dimensional surface". That surface is described by an attendant multi-dimensional vector where each component of the vector represents one observed, or assumed, effect on that material characteristic property. The surface is represented by a respective multi-factor model of product form. The product form is assumed to conveniently represent mutual interactions among the various factors. Each factor consists of four different variables/parameters as follows: (1) the factors terminal or final value, (2) the factors reference value, (3) the factors current value and (4) an exponent. The exponent is selected to represent continuous monatomic behavior so that the factor equals unity when the current value equals the reference value and approaches either zero or infinity (depending on the factors specific behavior) when the current value approached the final value. A schematic of the concept and the multi-factor interaction model MFIM is shown in Figure 4.

Probabilistic results from the model (Ref. 5) are shown in Figure 5. Shown in Figure 5 are cumulative distribution function curves for life-time strengths at three different temperatures. The curves shift to the left and their scatter range increases with increasing temperature as physically would be expected. A very important observation from these curves is that the MFIM can be used in conjunction with selective testing to substantially reduce the number of tests and amount of time required to characterize material behavior in complex environments. It can readily be deduced that the MFIM is not restricted to the use just described. It is generic - each factor can further be substructured to

another set of factors which may influence that factor - for example alloying elements, processing conditions, tolerances, assembly misfits, etc. Some comments on how it can be done are outlined in Reference 6 where its application to simulate the human factor effects in structural analyses is described. Another obvious use is for evaluating aging effects on material deterioration.

6. SELECT DEMONSTRATION CASES

6.1 Two Stage Rotor - This case is used to demonstrate one direct way to evaluate component/system reliability under multiple failure modes. A schematic of the rotor with summary of the results is shown in Figure 6. The details of this case are described in Reference 7. Herein we discuss the significance of the results and of the respective sensitivity factors. Four different failure modes were evaluated as noted in Figure 6. The survival probability of the rotor for each failure mode and the combination are determined from a special plot of survival probability versus remaining resistance. This plot graphically depicts the critical failure mode and the system failure mode. As can be seen, the critical failure mode is fracture at the rim in 10,000 cycles which coincides with the system failure mode. It is also seen that when the burst failure mode has 100 percent survival probability the system has only about 65 percent. In Table I the sensitivity factors which influence system failure are listed. On the left column the primitive variables included in the evaluations are listed. In the right column is the magnitude of each factor's contribution to the system probability of failure or reliability. These sensitivity magnitudes are part of the probabilistic simulation by using FPI and are evaluated simultaneously with the probability as was mentioned in the cantilever illustrative example.

The observations from Table I are: (1) the rotor speed is, by far, the most dominant, (2) the next one is the rotor density, (3) the third is the temperature of the rotor, (4) the other 11 factors have relatively negligible contributions. For example, critical parameters in damage tolerance evaluations (initial crack size A_0 , constants C in the fracture model, N_f and K_f) are insignificant in the rotor reliability assessment. The only critical material property is the rotor density. The recommendations for rotor material suppliers is to control the scatter of the density of the rotor materials and the thermal expansion coefficient. The recommendation for the rotor designers are to (1) assure that the rotor does not overspeed and (2) account for expected temperature spikes and avoid unexpected hot spots. The probabilistic evaluation of the rotor case illustrates how probabilistic results can be used to provide guide lines for material quality control and design considerations both of which are essential in product safety, reliability and reduced-cost.

6.2 Combustor Liner - The engine combustor liner to be described could be a part for supersonic aircraft engines. These liners are subjected mainly to thermal loads and some pressure both caused by the combustion process. A schematic of the liner with the finite element model is shown in Figure 7. The thermal loading profile is also shown. The details of this evaluation are described in Reference 8. Herein suffices it to say that the liner is assumed to be made from a cross-ply ceramic matrix composite. We, therefore, discuss probabilistic results obtained and interpretation/usage of these results for damage tolerance, reliability, and guidelines/recommendation for material selection deduced from the sensitivity factors. It is assumed that liner is designed for avoidance of vibration frequencies and buckling.

The cumulative distribution function of the first (lowest) vibration frequency is shown in Figure 8a. This frequency has a mean of 220 cycles per second ((CPS, Hertz) and a scatter range from 290 CPC to 350 CPS about 60 CPS. The sensitivity factors for two levels of probability are shown in Figure 8b. The following observations are evident from Figure 8b: (1) liner material density and shear modulus have significant effect on the liner frequency; (2) the liner thickness has the dominant effect and this effect is even more dominant at higher probability values; (3) the order of the sensitivity factors is the same at low and high probability values. This indicates that the probability of the frequency remain mostly linear throughout the scatter range.

The cumulative distribution function for buckling of the liner is shown in Figure 9a and the respective sensitivities are shown in Figure 9b. The mean value of the buckling pressure is six times that of the operating pressure or 60 psi. The attendant scatter range is from about 45 psi to 75 psi. The reliability of the liner for buckling is 100 percent with no risk. The factors that influence the buckling load most are liner thickness (geometry variable) thermal expansion coefficient (material variable) and thermal load (loading conditions of 2150 °F). The material moduli axial, hoop and shear have negligible effect. Note the order of the sensitivities remains the same for low and high probability values - which means that the buckling load probability is linear throughout the scatter range. Recommendations from these results are material supplier - control the thermal expansion coefficient. Designer: (1) control the temperature, (2) select the liner thickness to assure that it will survive at least 4.5 times the operating pressure and, (3) specify proof test pressures of at least 7.5 times the operating pressure to assure that the liner will buckle, in first test.

6.3 Space Shuttle Main Engine (SSME) High Pressure Blade - These blades are in the liquid hydrogen pump. They are relatively small, rotate at about 40,000 revolutions per minute and are subjected

cyclically to very cold and very high temperature (thermomechanical fatigue). Schematics of the blade airfoil with its respective operating loading conditions and finite element model are shown in Figure 10. The blade has relatively steep span-wise thermal and pressure gradients.

The cyclic temperature and load effects on the blade materials are simulated by the multi-factor interaction model (MFIM) described previously. The specific values for the various factors used are listed in Table II. Note that four factors were sufficient for that simulation. These were as follows: (1) the temperature dependence factor with an exponent of $\frac{1}{2}$; (2) the stress dependent factor with exponent n ; (3) the pressure cyclic load factor with exponent p ; and (4) the thermal cyclic load factor with exponent q . The temperature effects exponent was assumed to be a constant based on previous studies while the exponents n , p , and q , were assumed to have scatter as shown in Table II.

The damage propagation path caused by 100,000 fatigue cycles are shown in Figure 11 for two probability levels (1/100,000 and 2/10,000). Obviously the path with the highest probability will occur first. It is noted that several other paths are probable with probability levels between the two shown in Figure 11. However none was found with a higher probability than (2/10,000). The durability or damage tolerance of the blade in its operating environment can be simulated by using progressive structural fracture (Ref. 9). Results for the strain-energy release rate versus damage state are plotted in Figure 12. Two major points are worth noting in Figure 12: (1) the damage is stable and progresses rather slowly up to damage state 3; and (2) the damage progression increases very rapidly from damage state 3 to damage state 4. The plot in this figure displays several important aspects of structural durability and/or damage tolerance: (1) the blade is damage tolerant up to damage state 3; (2) with continuing operation the blade will fracture (disintegrate) just a trifle past damage state 4; (3) the safe design of the blade with 100 percent reliability is up to damage state 2; (4) the blade should be inspected for damage state 1 and damage state 2; (5) at damage state 2, the blade must be replaced (retired for cause) to assure safe operation of the SSME; (5) monitor in-service health based on changes in select blade responses (changes in vibration frequencies and vibration mode shapes for example) in order to infer damage state compared to blade inspection which is costly and time consuming.

The important message from the previous discussion is that an abundance of information is generated by probabilistic computational simulation that can be judiciously used from conceptual design to retirement for cause (from cradle to grave). Another important message is that comparable plots can be made for other

responses - for example blade material degradation due to oxidation or other causes.

The information from Figure 12 can be combined with costs for fabrication and costs (penalties) for failure. The results are shown in Figure 13 as log/log plots for probability of damage initiation versus number of cycles and for total cost versus fatigue cycles. Note that the cost increases very rapidly with fatigue cycles higher than 10,000. Interestingly the information in Figure 13 is really of the cascading type because it can also be used to generate information for benefits accrued by improving material strength, or controlling the quality of processing. Costs to improve structural reliability by decreasing - scatter are more beneficial than costs to increase strength for comparable probabilities in general (unpublished in-house results).

7. FAULT TREE SIMULATION FOR SYSTEM RELIABILITY

Systems usually fail by combinations of multiple failure modes. Multiple failure modes reliability is evaluated by formal combination of the probability of failure of each failure mode. Traditionally the formal method for combining those probabilities has been the fault tree simulation. A schematic depicting a set up for a fault tree simulation for the SSME high pressure blade is shown in Figure 14. Four different failure modes are included in the evaluation. The probability of failure for each failure mode are determined by probabilistic structural analysis. Their subsequent combination is accomplished by classical probability methods. The details are described in Reference 10. Herein we present some typical results and discuss their significance to how material behavior influence structural system reliability. The parameters (primitive variables) with their respective scatter standard deviation and assumed distributions included in the simulation are listed in Table III. Results obtained for the probability of failure of the system are shown in Figure 15. The probability for system failure from each individual failure mode is shown in Figure 15a together with the simulated correlation coefficients between the three different failure modes. It is seen in Figure 15a that the system will fail by creep because that failure mode has the highest probability of failure. It is also seen that the stress influences the vibration failure mode and the creep failure mode significantly, even though the system failure probability from stress only is relatively small compared to the other two. The sensitivity factors for system failure probability are shown in Figure 15b. The dominant factor is the direction solidification angle (the θ y) measured from the blade radial (spanwise) axis. The modulus and the Poisson's ratio have about the same influence, the rest of them have relatively negligible influence. Recommendations for material supplies and designers are comparable to those mentioned previously. Recommendations for the blade manufacturers and the

rotor assembler are to assure that the blade solidification direction line up with the blade span-wise axis. The important message from the previous discussion is that system reliability can be formally evaluated for multiple failure modes. The critical failure modes are identifiable and their respective dominant sensitivities are quantifiable.

It is important to mention that three different approaches were described for evaluating system reliabilities. The first is summarized in Figure 6 with its attendant discussion. The second is summarized in Figures 11 and 12 with their attendant discussions. The third is summarized in Figures 13 and 14 with their attendant discussions. The first and second methods are evaluated directly from the probabilistic structural/stress analysis while the third requires fault-tree evaluation in addition to probabilistic structural/stress analyses. The computer code described in Reference 3 was used for all three approaches.

8. CONCLUDING REMARKS

Description of probabilistic methods for structural damage tolerance and reliability from materials to service environments leads to the following concluding remarks:

1. Probabilistic methods via computational simulation are mature and credible to be adapted throughout the structural design practice. They provide quantifiable information that can be used to reduce costs product development, certification, and risk.
 2. These methods constitute a "virtual" statistical desktop laboratory applicable at all stages and for all aspects of the design, material selection and qualification, development, certification and service life cycles.
 3. Probabilistic methods rely on computational simulation results for decision making - especially in the preliminary design stages.
 4. Probabilistic methods can be used for future strategic projections and planning to assure better, cheaper, faster products for competitive advantages with acceptable reliability and quantifiable risk as well as to reliably evaluate the remaining life of existing products.
- ## 9. REFERENCES
1. Chamis, C.C: " Probabilistic Structural Analysis Methods for Space Propulsion System Components." Probabilistic Engineering Mechanics, 1987, Vol. 2, No. 2, pp. 100-110.
 2. Anonymous, "Composite Load Spectra for Select Space Propulsion Structural Components," Final Report, by Wo and J. F. Newell, NASA CR 194476, March 1994.
 3. Probabilistic Structural Analysis Methods (PSAM) for Select Space Propulsion Systems Components - II (6th Annual Report), by Southwest Research Institute, NASA CR-187200, November 1991.
 4. Chamis, C. C. and Hopkins, D. A.: " Thermoviscoplastic Nonlinear Constitutive Relationships for Structural Analysis of High Temperature Metal Matrix Composites." NASA TM 87291, November 1985.
 5. Scheidt Bast, C. C: "Probabilistic Material Strength Degradation Model for Inconel 718 Components Subjected to High Temperature, Mechanical Fatigue, Creep and Thermal Fatigue Effects, ." (by Univ. of Texas at S. Antonio), NASA CR 195284, March 1994.
 6. Chamis and S. N. Singhal: "Probabilistic Simulation of the Human Factor in Structural Reliability." Communications in RMSL Communications, Vol. 3, No. 1, January 1996, pp. 68-72.
 7. Mahadevan, S. and Chamis. C.C: "Structural System Reliability Under Multiple Failure Modes." AIAA/ASME/ASCE/AHS/ASC, 34th Structures, Structural Dynamics and Materials Conference, 1993, pp. 707-713.
 8. Pai, S.S., and Chamis, C.C: "Probabilistic Assessment of Combustor Liner Design." ASME International Gas Turbine and Aeroengine Congress and Exposition, Houston, Texas, June 1995, pp. 1-9.
 9. Chamis, C.C., Murthy, P.L.N., and Minnetyan L: "Progressive Fracture in Composite Structures." Published in Composite Materials, Fatigue and Fracture, 6th Vol. ASTM, STP 1285, 1997, pp. 70-84.
 10. Torng, T.Y, Wu, Y.-T and Millwater, H.R: "Structural System Reliability Calculation Using A Probabilistic Fault Tree Analysis Method." (Southwest Research Institute), AIAA/ASME/ASCE/AHS/ASC 33rd Structures, Structural Dynamics and Materials Conference, AIAA, 1992, pp. 1-11.

Table I
Rotor System Reliability Sensitivity Factors

Name	In u(i) Space
E_ROT	0.016011
E_RIN	-0.002698
ROTOR DENS	0.438499
RING DENS	-0.000386
SPEED	0.850827
TEMPE	0.170793
BURST	-0.011983
RINGY	0.073086
RK1C	-0.061872
AO	0.057976
C	0.133702
NI	-0.000008
Kt	0.060917
A_LCF	-0.005132
TOLER	0.0

Table II
Space Shuttle Main Engine: Multi-Factor Interaction Model Values Used in the Probabilistic Simulation of the Material Behavior

VARIABLE	DISTRIBUTION TYPE	MEAN	STANDARD DEVIATION	
			(VALUE)	(% OF MEAN)
T_F	NORMAL	2750 °F	51.4 °F	2.0
T_0	NORMAL	68 °F	2.04 °F	3.0
S_F	NORMAL	212.0 ksi	10.6 ksi	5.0
σ_0	CONSTANT	0	0	0
N_{MF}	LOGNORMAL	10^0	5×10^0	5.0
N_{MO}	LOGNORMAL	10^3	50	5.0
n	NORMAL	0.25		3.0
p	NORMAL	0.25		3.0
η	NORMAL	0.25		3.0

Table III
Primitive Variables Used in the Fault Tree Simulation for System Reliability

	Mean	Standard Deviation	Distribution	Bottom Event
Material Orientation θ_z	.05236°	0.067544	Normal	All
Material Orientation θ_y	-.03491°	0.067544	Normal	All
Material Orientation θ_x	.08727°	0.067544	Normal	All
Elastic Modulus E_s^*	18.36E6	.4595E6	Normal	All
Poisson's Ratio ν_s^*	.386	.00965	Normal	All
Shear Modulus G_s^*	18.63E6	.4657E6	Normal	All
Creep Equation Coefficient B_s	86.0	.086	Normal	Creep
Density ρ	.805E-3	.493E-5	Normal	Freq.

* Defined at Room Temperature

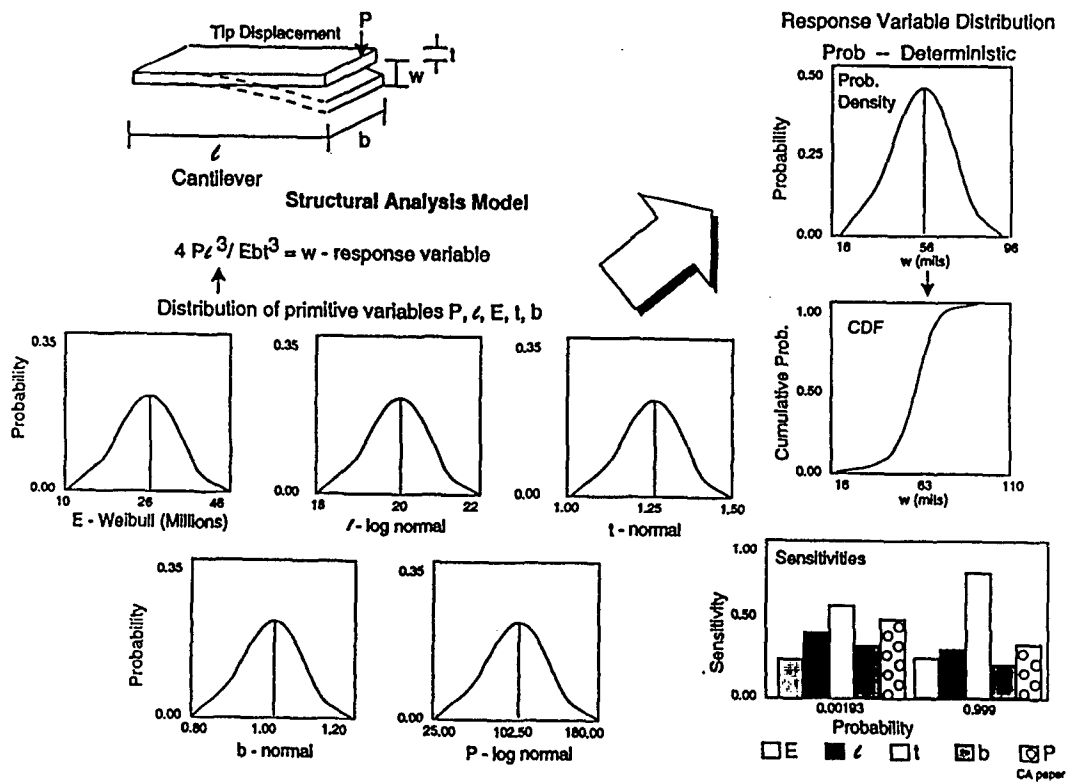


Figure 1 - Probabilistic structural analysis/response - illustrative examples.

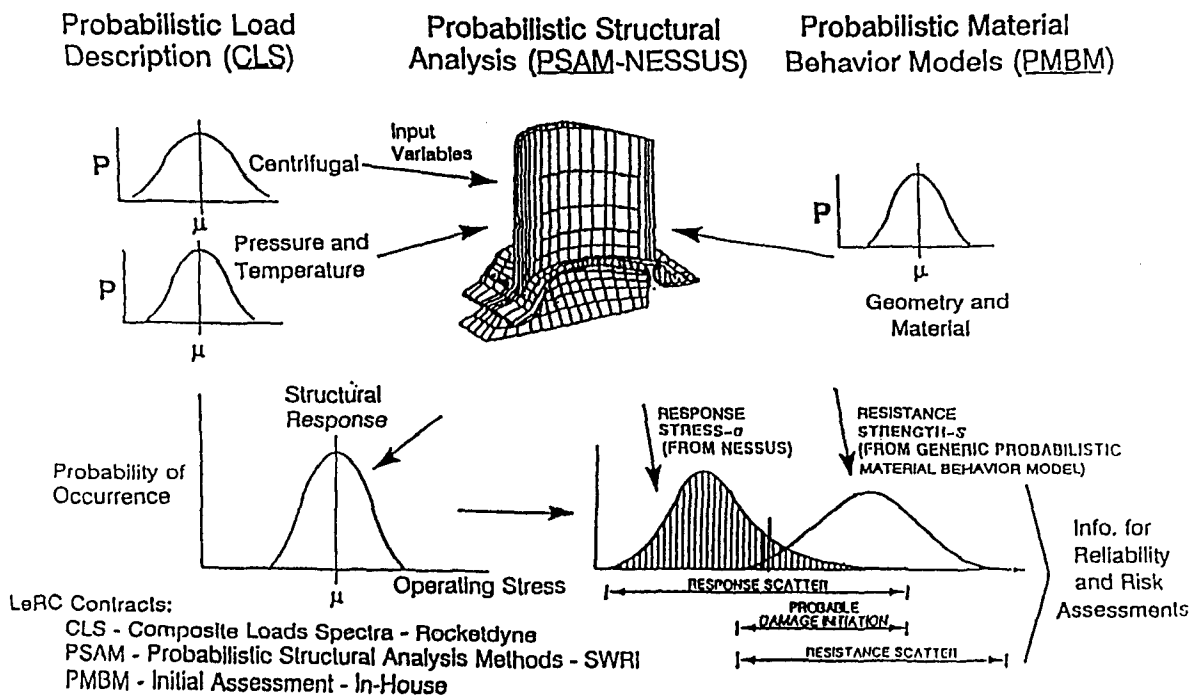


Figure 2 - Conceptual schematic of probabilistic structure/component reliability.

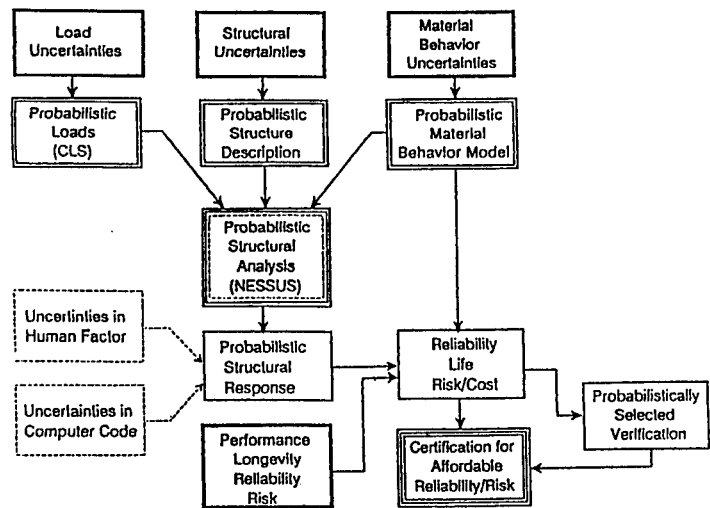


Figure 3 - Block diagram of probabilistic structural simulation for assured certification.

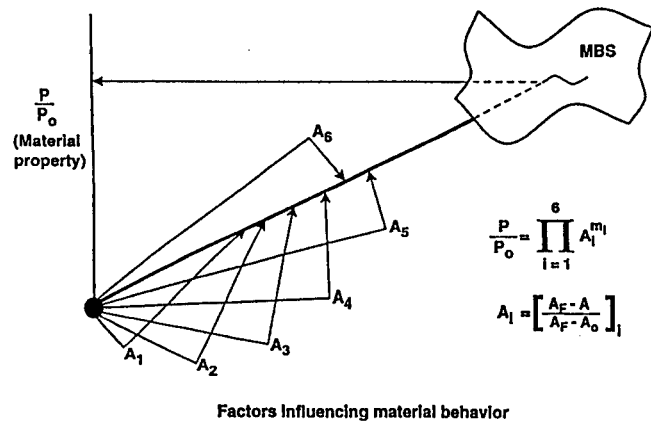


Figure 4 - Conceptual schematic of material behavior through a multi-factor interaction model (MFIM).

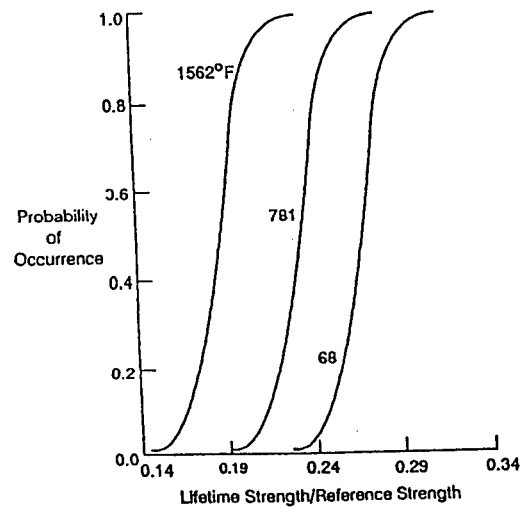


Figure 5 - PMBM-simulated lifetime strength for a nickel-based superalloy subjected to 3162 stress cycles and 100 hours of creep.

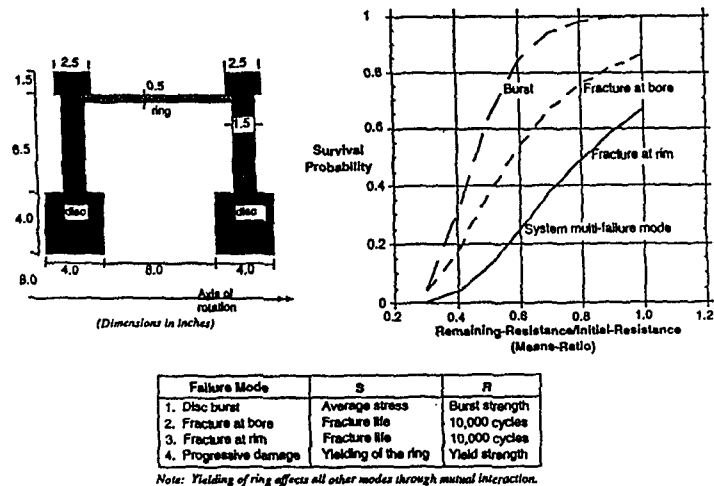


Figure 6 - Structural system reliability of a two-stage rotor with multiple failure modes.

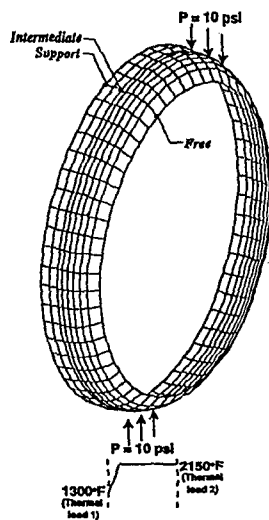


Figure 7 - Schematic of finite element model for an aircraft engine combustor liner.

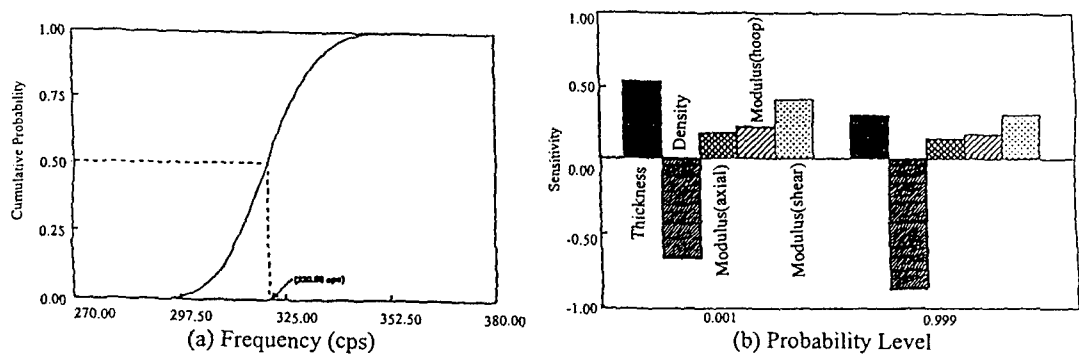


Figure 8 - Combustor liner probabilistic vibration frequency and sensitivities.

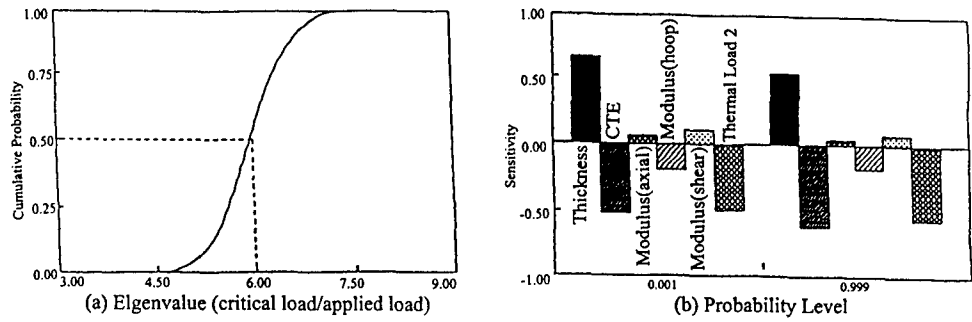


Figure 9 - Combustor liner probabilistic buckling and sensitivity.

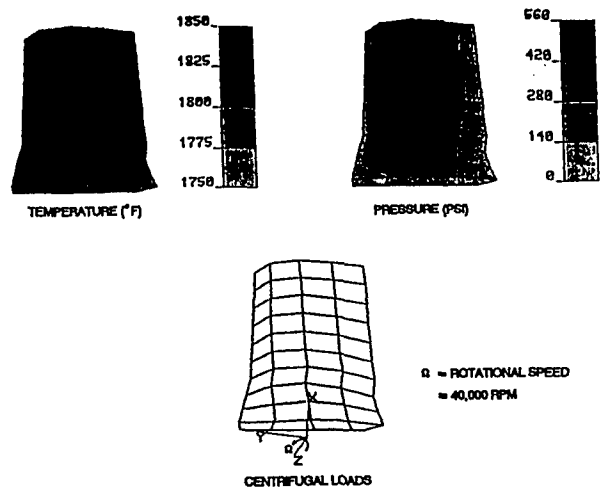


Figure 10 - Space shuttle main engine (SSME) blade - finite element model with thermo-mechanical loads.

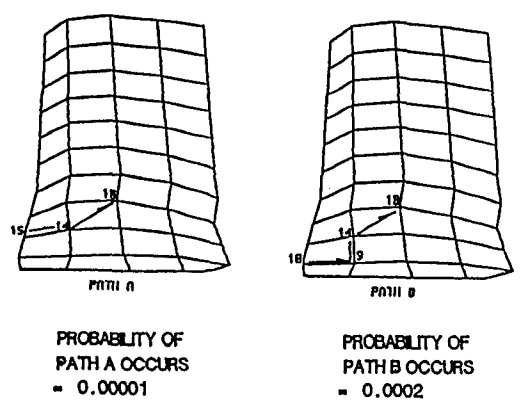


Figure 11 - Structural reliability of space shuttle main engine blade for 100,000 fatigue cycles - probable damage propagation paths to structural fracture.

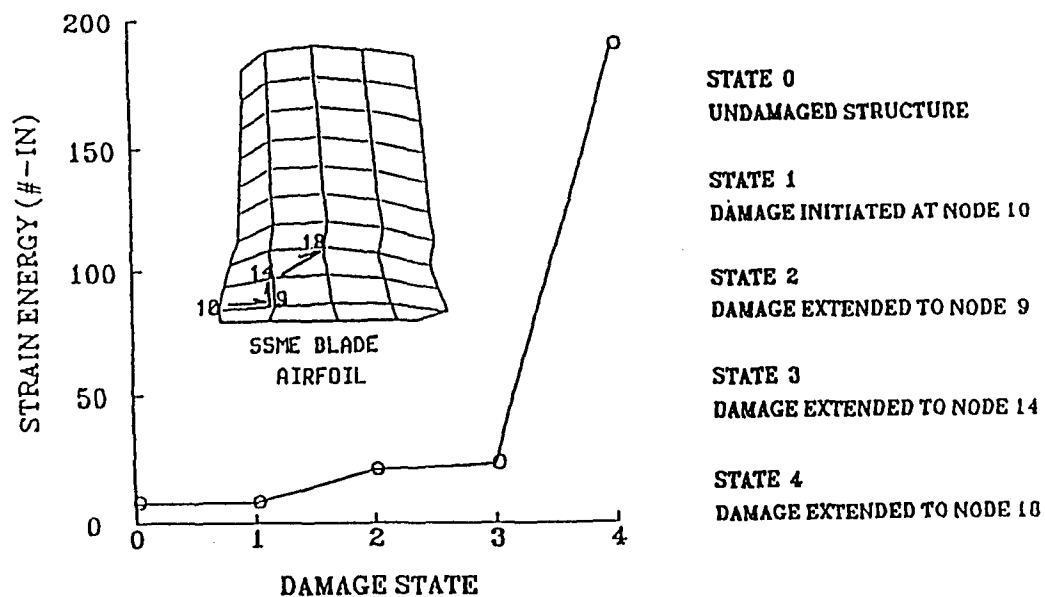


Figure 12 - Damage tolerance of space shuttle main engine blade along the most probable progressive damage path leading to structural fracture.

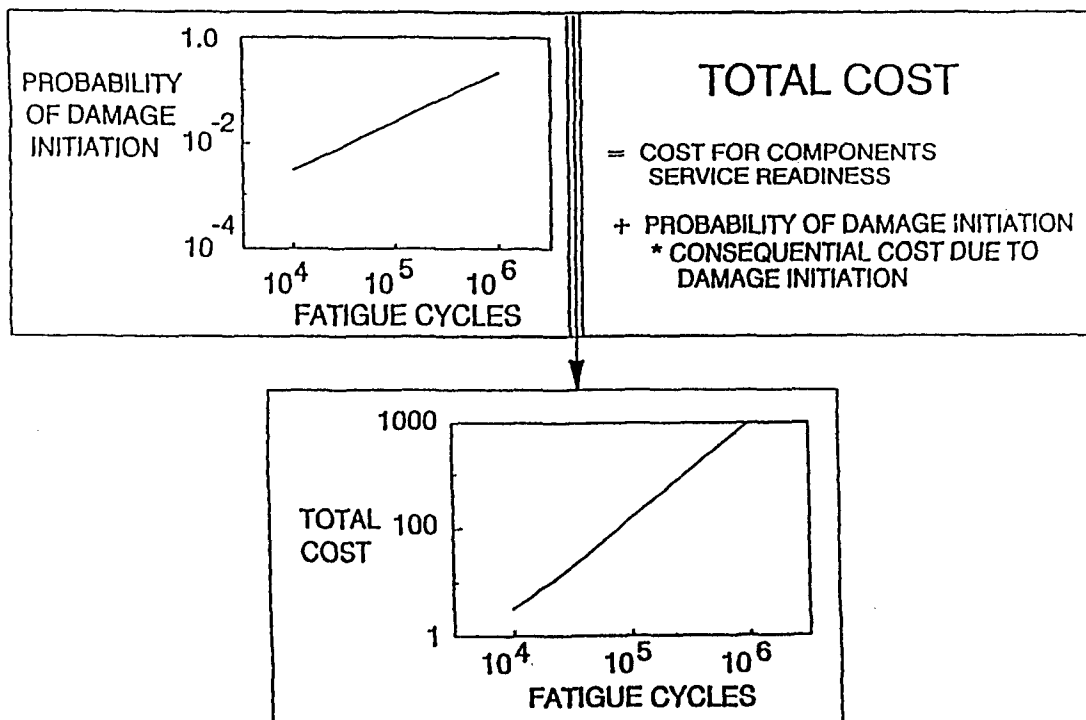


Figure 13 - Space shuttle main engine blade - probabilistic risk-cost assessment.

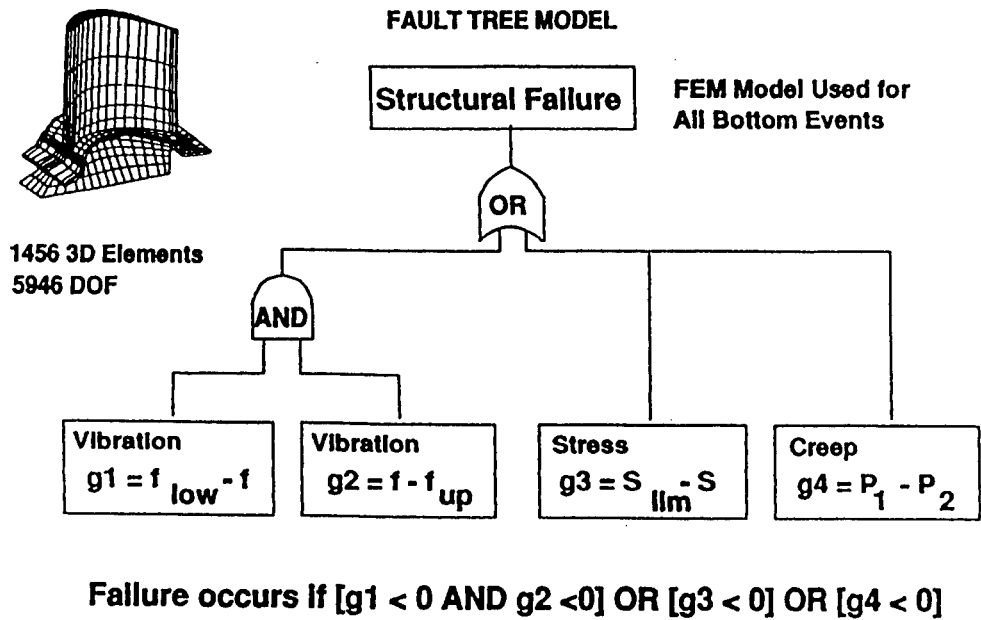


Figure 14 - System reliability by using fault tree simulation.

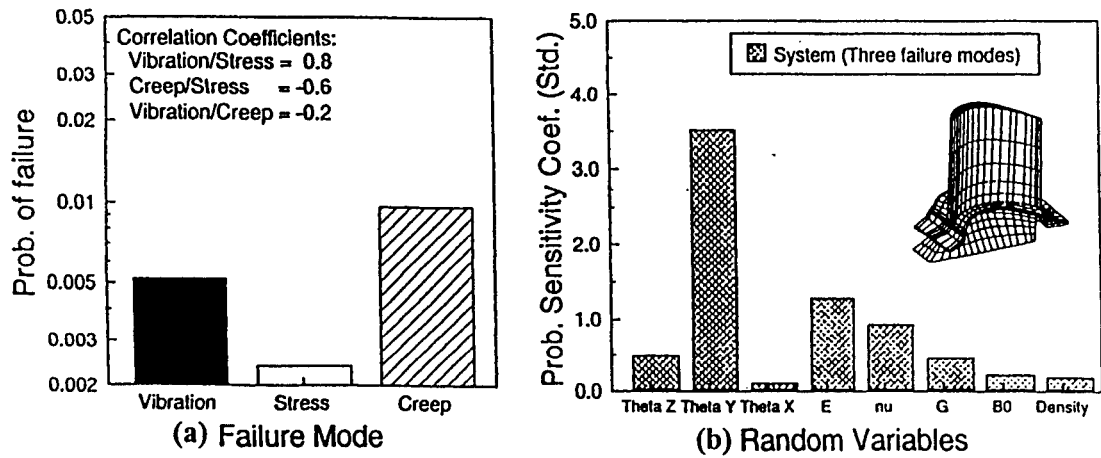


Figure 15 - System reliability - fault tree simulation and primitive variables sensitivities.

LIFE EXTENSION METHODOLOGY BASED ON CREEP-FATIGUE MODELS

By

C. Moura Branco and A. Sousa e Brito
Lisbon University of Technology (IST)
1096 Lisbon Codex, Portugal

and

J. Byrne
Department of Mechanical and Manufacturing Engineering
University of Portsmouth, Portsmouth PO1 3DJ, UK

ABSTRACT

The first part of this paper presents the results of a detailed study carried out in the nickel base superalloy IN718 used in turbine discs where fatigue and creep crack growth rate data (FCGR and CCGR) was obtained at 600°C in CT and CC specimens tested at different values of stress ratio and dwell time at maximum load (frequency). In the second part of the paper a presentation is made of creep-fatigue models, and also the results obtained with a computer program developed by the authors, which is able to make a comparison between the experimental data obtained for the FCGR in creep-fatigue situations and the equivalent results predicted by the models. This methodology can be directly used, with great advantages, in predictions of life extension in flawed components.

1. BACKGROUND

Fatigue is a continuous sub-critical degradation, consisting of initiation and propagation of a crack. The total fatigue life is the sum of the crack initiation life and the propagation life. However, modern defect-tolerant design approaches to fatigue are based on the premise that engineering structures are inherently flawed, i.e. that manufacturing defects are potentially present. The useful fatigue life is then the time or the number of cycles to propagate a dominant flaw of an assumed or measured initial size (or the largest undetected crack size estimated from the resolution of the non-destructive inspection), to a critical dimension (which may be detected by the fracture toughness, limit load, allowable strain or allowable compliance change). In the life management philosophy RFC (retirement for cause), for example, the components are subjected to periodic inspections, and are returned to service if no cracks larger than a specific size are detected. This requires the ability to detect cracks larger than a given detectable size with a high degree of reliability, the ability to predict crack growth rates accurately and to demonstrate that a crack of the detectable size or smaller will not grow to a catastrophic size during one inspection interval or during the lifetime. This methodology extends the life in existing components by retaining them in service until a crack has indeed been detected. According to this methodology, the study of the initiation can be avoided, and only the propagation life needs to be evaluated.

Life extension analysis is currently being applied in aircraft engines, and the turbine discs are one of the more critical parts where this approach is better suited. Hence, life extension methodologies, such as RFC, require the knowledge of the FCGR behaviour of the material in terms of its variation with several parameters, such as

- microstructure (grain size, intermetallics, heat treatment, etc)
- temperature
- residual stresses
- frequency
- environment
- stress ratio
- stress state
- load wave

The appropriate FCGR relationship should be used since the crack speed, da/dN or da/dt , can change considerably with the parameters referred above, as it will be described next. Later in the paper, the interaction effects between fatigue and creep will be presented.

The review will be concentrated on nickel base superalloys, used in turbine discs, and FCGR and creep data will be presented for the IN718 nickel base superalloys.

For nickel base superalloys, crack propagation under conditions of high temperature fatigue can be cycle dependent, time dependent or mixed. The occurrence of these crack propagation modes is related to micro mechanisms of damage acting at the crack front, which can be cyclic plastic deformation, oxidation and creep. Cycle dependent behaviour occurs when cyclic plastic deformation at the crack tip is the main mechanism producing crack propagation. In this case, the propagation is transgranular. However, propagation is accelerated by the presence of oxygen, which is attributed to: diffusion in slip bands ahead of the crack front, with local embrittlement, and to oxidation of crack surfaces, that inhibits their rewelding by unloading [1]. So, oxygen accelerates the cyclic plastic propagation. Time dependent behaviour occurs when oxidation and/or creep are the dominant mechanisms. In this case, the propagation is intergranular, because the grain boundaries act as preferential paths for diffusion, and oxidation and creep are diffusion-controlled mechanisms. In

mechanically processed nickel base superalloys, oxidation is dominant for temperatures up to 650°C [1,2]. For higher temperatures, intergranular propagation may be due to creep mechanisms, like cavitation and grain boundary sliding [3, 4]. In the mixed regime, both cyclic plastic deformation and time dependent mechanisms contribute to crack growth.

The parameters that control these micro mechanisms and propagation modes are: the loading (load range, cyclic stress ratio ($R = \sigma_{\min}/\sigma_{\max}$), wave shape and load history), material, geometry of the cracked component and environment (temperature and atmosphere). For nickel base superalloy materials at temperatures up to about 650°C, the stress intensity factor, K , appears to be the appropriate crack tip parameter to characterise crack growth behaviour under fatigue loads at elevated temperatures [5].

The decrease of frequency increases the duration of the loading cycle and, so, more time is available for creep and oxidation to occur. Also, the reduction in frequency leads to a proportional reduction in the density of the slip bands and, hence, more heterogeneous cyclic plastic deformation occurs. This increases the stress concentration at grain boundaries ahead of the crack front, and so the diffusion based mechanisms and creep oxidation [6]. Once again, there is an interaction between time dependent mechanisms and cyclic plastic deformation. If the frequency is high, cyclic plastic deformation is faster than creep and oxidation, and propagation is transgranular. For high frequencies, da/dN is independent of f , and so da/dt increases proportionally with f . For lower frequencies, in the time dependent regime, da/dt is constant, and so da/dN increases proportionally with cycle duration ($1/f$). The extrapolation of the cycle dependent regime line to time dependent frequencies gives lower crack growth rates, indicating that oxidation and creep are becoming dominant.

The increase in stress ratio contributes to creep effects, since the mean load increases and a creep threshold may be exceeded. So, an increase of R favours time dependent propagation. Additionally, crack closure effects explain the effect of R : the increase of R reduces crack closure, increasing effective ΔK and so crack growth rate. This effect is more pronounced in time dependent propagation, due to oxide particles and due to a high roughness associated with an intergranular propagation, especially with large grain size [7]. The effects of t_d at maximum load are dependent on temperature and of the frequency of the base cycle, f_c . It is known that, for temperatures between 500 and 700°C,

1. For frequencies, $f < f_{cm}$, there is an increase of da/dN with the dwell time, t_d , and intergranular fractures occur. f_{cm} is the transition frequency between the cyclic (transgranular) regime and the mixed regime where intergranular fractures start to appear.
2. If $f > f_{cm}$, da/dN is in the cyclic dependent regime, and both dwell time and frequency will not promote significant changes in the FCGR.

Sometimes, it is possible to define a second transition frequency, f_{mt} (low frequency and high dwell time), between the mixed and time dependent regimes where intergranular fractures occur.

For relatively high R values there is no crack closure, and the effect of R is explained by a change of creep mechanism.

In conclusion, for low R and high frequencies, the fatigue crack growth rate tends to be cycle dependent [8]. The transition frequency from transgranular to intergranular increases with R , because this promotes intergranular propagation [9]. Naturally, fatigue crack growth rates and transitions between regimes depend also on the other fatigue parameters, and not only on R and frequency. Also, if temperature is relatively low, propagation can be always transgranular, whatever the values of R or frequency.

The trapezoidal wave shape with a dwell time, t_d , at maximum load is representative of the loading pattern usually applied in turbine discs of aircraft engines. In this case, the effects on FCGR of the dwell time at high temperature are closely related with the effects caused by the frequency, as referred above. This problem has been widely studied in the literature [10-13]. Generally, the addition of a dwell time at maximum load in a fatigue cycle tends to increase the FCGR, da/dN , in the nickel base superalloys [14-15].

In particular, for the nickel base superalloy IN718, which is the base of this investigation, there is also a time dependent behaviour for high values of dwell time, t_d , at maximum load. The cyclic effects are negligible. However, there are certain conditions where the trend of increasing da/dN with the increase of t_d is not observed, in particular

- i) if the dwell time at maximum load is added to a fatigue cycle with low loads and low values of ΔK . In this case, the fatigue crack may stop [16, 17];
- ii) when the static loading is not applied at maximum load [18-21];
- iii) when certain heat treatments are used or the temperature is not sufficiently high to promote microstructural alterations in the material [12].

On the other hand, microstructural effects (like grain size), which apparently show a moderate influence on FCGR for pure cycle fatigue, seem to have a more significant effect with loading conditions with high temperatures and high dwell times at maximum load [22]. Some results have shown that da/dN increases when the grain size is reduced.

The dwell time at minimum load has also an effect on the FCGR behaviour. These effects can be summarised as follows:

- i) Low values of R and $K_{\min} < \Delta K_{th} \rightarrow da/dN$ increases with the increase of the dwell time;
- ii) Low and intermediate values of R and $K_{\min} < \Delta K_{th} \rightarrow da/dN$ will increase with the increase of the dwell time if intergranular fractures occur [18, 21];
- iii) Intermediate values of R and $K_{\min} < K_{th} \rightarrow da/dN$ tends to decrease with the increase of ΔK , and sometimes crack arrest may occur [18].

A detailed study of the effect of the wave shape may be found in [23].

An analysis of life extension is carried out, generally, in used components which have been subjected to thermal exposure, usually, for a significant amount of time. In this case, ageing effects may occur, and the FCGR properties might be different from those obtained in a new material, which did not enter into service. Hence, for a life extension analysis, FCGR data should ideally be obtained in specimens taken from used components which have been in service for the appropriate time until the life extension analysis starts. Scraped components could be used for this purpose, and an eventual degradation of properties with time can also be assessed. Limited work carried out in IN718 has shown a decrease on FCGR in specimens tested at 650°C, after having been exposed to this temperature only for 800 hours, in comparison with the FCGR values obtained in specimens which were not exposed to this treatment before being tested at the same temperature [24]. This difference in FCGR properties was attributed to microstructural modifications induced by ageing effects, increasing the strength to intergranular cracking.

2. CREEP-FATIGUE MODELS

2.1 Introduction

The basis of the life extension is to predict the safe residual fatigue or creep-fatigue life from a certain detected or assumed initial defect size, a_i , to a final or critical defect size, a_f . In terms of FCGR, this comes to

$$N_f = \int_{a_i}^{a_f} \frac{dN}{da} da \quad (1)$$

The crack speed, da/dN or da/dt can be given by different models who attempt to consider the creep fatigue loading pattern usually obtained in engine components with dwell times at maximum and minimum loading (Fig. 1). These models assume that the creep-fatigue crack growth rate is a superposition of the da/dN values in pure fatigue with the da/dN values in pure creep.

2.2 The Models

2.2.1 Basic Linear Model

This model [3] is given by the linear sum of the cyclic component with the time dependent term (based on the creep crack growth rate law (CCGR)). The equation is:

$$\frac{da}{dN} = \left(\frac{da}{dN} \right)_{\text{cyclic}} + \left(\frac{da}{dN} \right)_{\text{time}} \quad (2)$$

The cyclic component is given by the Paris law of the material. The time dependent component is obtained from the creep crack growth equation for the total time of the fatigue cycle (Fig. 1). Thus,

$$\frac{da}{dN} = C \Delta K^m + A \left(\frac{\Delta K}{1-R} \right)^n \times \frac{1}{f_T} \quad (3)$$

where

$$R = \frac{P_{\min}}{P_{\max}} = \frac{\sigma_{\min}}{\sigma_{\max}}$$

is the stress ratio, C , A , m and n are experimental constants for the fatigue and creep terms and f_T is the total frequency of the loading cycle (Fig. 1).

Note that, in the time dependent component, it is implicitly assumed that K is equal to K_{\max} during the entire cycle, which is not the case as corrected in the next model.

2.2.2 Gayda/Miner Model [16]

This model also gives a linear summation of the two components of the previous model but, in this case, the time dependent term is obtained by the integration, along the entire cycle, of the CCGR term.

Thus, this component will be given by

$$\left(\frac{da}{dN} \right)_{\text{time}} = \int \frac{da}{dt} dt = \int A K(t)^n dt$$

Since the stress intensity factor function is similar to the load function plotted in Fig. 1, and assuming that, during the cycle, there is no crack growth, comes

$$K(t) = \begin{cases} K_{\min} + 2f \Delta K t, & \text{for } 0 \leq t \leq \frac{1}{2f} \\ K_{\max}, & \text{for } \frac{1}{2f} \leq t \leq \frac{1}{2f} + t_D \\ K_{\max} - 2f \Delta K \left(t - \frac{1}{2f} - t_D \right), & \text{for } \frac{1}{2f} + t_D \leq t \leq \frac{1}{f} + t_D \\ K_{\min}, & \text{for } \frac{1}{f} + t_D \leq t \leq \frac{1}{f_T} \end{cases} \quad (4)$$

where

$$K_{\min} = Y \sigma_{\min} \sqrt{\pi a}; K_{\max} = Y \sigma_{\max} \sqrt{\pi a}; \Delta K = K_{\max} - K_{\min}$$

Therefore,

$$\begin{aligned} \int_0^{\frac{1}{2f}} AK(t)^n dt &= \int_0^{\frac{1}{2f}} AK(t)^n dt + AK_{\max}^n t_D + \\ &+ \int_{\frac{1}{f} + t_D}^{\frac{1}{f} + t_D} AK(t)^n dt + AK_{\min}^n t_m \end{aligned} \quad (5)$$

where t_m is the time at minimum load (Fig. 1). In this equation, the first and third terms are equal. Also

$$\begin{aligned} \int_0^{\frac{1}{2f}} AK(t)^n dt &= \frac{A}{(n+1)2f\Delta K} (K_{\max}^{n+1} - K_{\min}^{n+1}) = \\ &= A\Delta K^n \frac{(1-R^{n+1})}{2f(n+1)(1-R)^{n+1}} \end{aligned}$$

Hence, the FCGR given by this model is

$$\frac{da}{dN} = C\Delta K^m + A \left(\frac{\Delta K}{1-R} \right)^n \times \left[\frac{1-R^{n+1}}{f(n+1)(1-R)} + t_D + R^n t_m \right] \quad (6)$$

2.2.3 Nicholas and Ashbaugh Model

This model [8] uses the same assumptions as the previous model. The alteration is in the calculation of the integral for the loading cycle. In this case,

$$\int AK^n dt = \int AK(t)^n dt + AK_{\max}^n + AK_{\min}^n \quad (7)$$

Where, for the ramp loadings,

$$\int AK(t)^n dt = (1+\beta) \int_0^{\frac{1}{2f}} AK(t)^n dt$$

with

$$K(t) = K_{\min} + 2f\Delta K t, \quad \text{for } 0 \leq t \leq \frac{1}{2f}$$

and β an empirical parameter given by

$$\beta = \begin{cases} 1, & \text{for } \Delta K \leq \Delta K_0 \\ \exp\left(1 - \frac{\Delta K}{\Delta K_0}\right), & \text{for } \Delta K > \Delta K_0 \end{cases} \quad (8)$$

In this equation, ΔK_0 is the threshold value of the stress intensity factor.

The result given for the integrals in the two ramp loadings is only valid for symmetric load waves. Also, the result was based on the fact that the FCGR for low values of R , depends only on the frequency of the ramp [8]. The β parameter is arbitrary, since there is no experimental data available to predict its evolution, although it gives the total value given by the Gayda-Miner model for the two ramps of the loading cycle when $\Delta K \leq \Delta K_0$, since low ΔK values give high values of R with constant K_{\max} . For high ΔK values (low values of R), the unloading part is not so important.

The final result is given by

$$\frac{da}{dN} = C\Delta K^m + A \left(\frac{\Delta K}{1-R} \right)^n \times \left[\frac{(1+\beta)(1-R^{n+1})}{2f(n+1)(1-R)} + t_D + R^n t_m \right] \quad (9)$$

2.2.4 Weerassoriya model

The Weerassoriya model [25] is not based on the linear superposition of the cyclic and time dependent regimes. The creep-fatigue crack growth rate is given by

$$\frac{da}{dN} = \text{Max}\{F_c, F_m, F_t\} \quad (10)$$

where Max represents the maximum value of F_c , F_m and F_t .

F_c describes the material behaviour in the cyclic dependent regime where transgranular fractures occur and the FCGR is not frequency dependent. For F_c , the model proposes the Paris law with the Walker parameter [26]:

$$F_c = C\Delta K_{eff}^m \quad (11)$$

with

$$\Delta K_{eff} = K_{max}(1-R)^{m_1} = \Delta K(1-R)^{m_1-1} \quad (12)$$

and

$$m_1 = 0.725127 - 3.11247 \times 10^{-4} T \quad (13)$$

where T is the temperature in degrees Celsius, and m_1 the Walker exponent.

F_m is the FCGR function for the mixed regime, where a mix of intergranular and transgranular fractures occur. In this regime, there is a frequency dependence on FCGR, and the proposed equation for F_m is:

$$F_m = \frac{1}{f_t^\alpha} C\Delta K_{eff}^{m_1} \quad (14)$$

F_t is the total frequency of the loading cycle and α is the frequency exponent, $0 < \alpha < 1$.

F_t is the function of the material behaviour in the time dependent domain, with intergranular fractures. This equation is obtained simply by the integration, in one loading cycle, of the CCGR law. The result is similar to the time dependent term of the Gayda-Miner model but, since account was taken on the assumption that in a triangular load wave only the loading portion influences the da/dN values, the following equation was obtained:

$$F_t = A \left(\frac{\Delta K}{1-R} \right)^n \left[\frac{Y(1-R^{n+1})}{f(n+1)(1-R)} + t_D + R^n t_m \right] \quad (15)$$

with

$$Y = \begin{cases} 1, & \text{for } \Delta K < \Delta K_0 \\ 0.5, & \text{for } \Delta K \geq \Delta K_0 \end{cases} \quad (16)$$

Y is a parameter similar to the parameter β of the Nicholas and Ashbaugh model, but the extreme conditions are verified.

An analysis of the equations proposed in this section for F_c , F_m and F_t shows that, in this model, the transition frequency f_{cm} is constant and equal to 1Hz, which is not verified by the experimental data, as demonstrated in section (4).

2.2.5 Saxena model

This model [27] takes into account, also, the cyclic component of pure fatigue and the time dependent component. However, it defines a cutoff frequency for subtracting a portion to the time dependent term. This cutoff frequency tends to predict the time needed, during the fatigue cycle, for the intergranular cracking mechanisms to develop. This frequency was defined as the transition frequency between the mixed and time dependent components, f_{mt} .

The cyclic component in the Paris law $(da/dN) = C\Delta K^m$. The remaining component $(da/dN)_m$, mixed, depends on the value of f_{mt} and the value of time (given by $1/f_{mt}$). Thus, the equation for this term is:

$$\left(\frac{da}{dN} \right)_m = \int \frac{da}{dt} dt - \int_0^{1/f_{mt}} \frac{da}{dt} dt \quad (17)$$

where da/dN_m is the FCGR predicted for the mixed regime.

The integration of equation (17) gives:

$$\left(\frac{da}{dN} \right)_m = A\Delta K^n \left[\frac{\frac{2-R^{n+1}}{(1-R)^{n+1}} - \left(\frac{R}{1-R} + \frac{2f}{f_{mt}} \right)^{n+1}}{2f(n+1)} + \frac{t_D}{(1-R)^n} + \frac{R^n}{(1-R)^n} t_m \right], \text{ if } \frac{1}{f_{mt}} \leq \frac{1}{2f} \quad (18a)$$

$$\left(\frac{da}{dN} \right)_m = \frac{A\Delta K^n}{(1-R)^n} \left[\frac{1-R^{n+1}}{(1-R)^{n+1} 2f(n+1)} + t_D - \left(\frac{1}{f_{mt}} - \frac{1}{2f} \right) + R^n t_m \right], \text{ if } \frac{1}{2f} \leq \frac{1}{f_{mt}} \leq \frac{1}{2f} + t_D \quad (18b)$$

$$\left(\frac{da}{dN}\right) = A\Delta K^n \left[\frac{-R^{n+1}}{(1-R)^{n+1}2f(n+1)} + \frac{1}{2f(n+1)} \left(\frac{1}{1-R} - \right. \right. \\ \left. \left. -2f \left(\frac{1}{f_{mt}} - \frac{1}{2f} - t_D \right) \right)^{n+1} + \frac{R^n t_m}{(1-R)^n} \right],$$

$$\text{if } \frac{1}{2f} + t_D \leq \frac{1}{f_{mt}} \leq \frac{1}{f} + t_D \quad (18c)$$

$$\left(\frac{da}{dN}\right)_m = A\Delta K^n \frac{R^n}{(1-R)^n} \left[t_m - \left(\frac{1}{f_{mt}} - \frac{1}{f} - t_D \right) \right],$$

$$\text{if } \frac{1}{f} + t_D \leq \frac{1}{f_{mt}} \leq \frac{1}{f} + t_D + t_m = \frac{1}{f_t} \quad (18d) \\ \left(\frac{da}{dN}\right)_m = 0 \quad \text{if } \frac{1}{f_t} \leq \frac{1}{f_{mt}}$$

Finally, the equation of this model would be:

$$\left(\frac{da}{dN}\right) = C\Delta K^m + \left(\frac{da}{dN}\right)_m \quad (19)$$

where $(da/dN)_m$ is calculated from one of the equations (18a to 18e), depending on the values of f , f_{mt} and t_D .

3. EXPERIMENTAL DETAILS

3.1 Materials and Specimens

The material used in the creep and high temperature fatigue tests was Inconel 718, with the composition presented in Table 1.

Table 1

Chemical Composition (weight percentages)

Ni	Cr	Fe	Nb	Mo
52.7	18.928	16.814	5.208	3.162
Co	Cu	Si	Mn	Ta
0.301	0.106	0.148	0.099	0.014

Al	Ti	C
0.614	0.844	0.518

The alloy used was submitted to a conventional heat treatment: annealing – 1h at 935°C, followed by cooling in air; ageing – 8h at 720°C, followed by a decrease to 620°C with a rate of

38°C/h, during 8h at this temperature and by cooling in air down to room temperature.

The mechanical properties of Inconel 718 used are presented in Table 2, where σ_U is the ultimate tensile stress, σ_y is the 0.2% offset strain proof stress and ϵ_R is the % rupture strain. The Young's modulus at 600°C is 170000 MPa [28].

Table 2
Mechanical Properties of Inconel 718

Temperature (°C)	σ_U (MPa)	σ_y (MPa)	ϵ_R (%)
20	1420	1190	18
600	1270	1040	16.5
700	980	890	16

Specimens

One of the specimens used for the creep-fatigue and creep tests was corner crack (CC) specimens, with the geometry presented in Fig. 1. The cross section was 10x10mm square. A triangular corner notch, approximately 0.3mm length on each face, was machined in the middle section of the specimens (section A-A). The preparation of the specimens was:

- double vacuum melting: casting in vacuum by induction, followed by remelting in vacuum;
- forging at 1030°C with thermal-mechanical control;
- machining of turbine discs;
- conventional heat treatment of the discs
- machining of specimens extracted from segments of the discs;
- machining of the corner notch, using friction cutting.

The first four stages are the normal production route of turbine discs.

This geometry was used mainly because of the level of the bulk stress, defect size and defect shape, which are representative of gas turbine disc conditions.

The tests were performed in a universal servo hydraulic materials testing machine, with 100 kN maximum load capacity. A microcomputer connected to the controller of the machine was used to control the machine.

A few dwell tests were also carried out in CT specimens, but the results will not be presented here.

3.2 Test techniques

The direct current potential drop (DCPD) technique was used to monitor the propagation of the crack in the specimen.

ΔK was calculated from the PD values. For each value of PD, the crack length was first calculated using a calibration curve. The calibration curve was defined for each testing crack zone,

considering the initial and final values of crack length (measured on the crack surface after the test), and from the PD reading.

Finally, ΔK was calculated for each crack length, using Pickard's equation, which may be found in [28].

The constants of Paris law were obtained by a linear regression fit of a $\log(\Delta K)$ - $\log(da/dN)$ plot. At the beginning of the tests, transitory effects were normally observed. These points were omitted in the regression for the Paris law.

The parameters change with the frequency, stress ratio and ΔK . The values of R were 0.05, 0.5 and 0.8. A few specimens were also tested with negative values of R ($R = -0.25$ and -0.75). These results are not included in this paper, but are available in separate publications [29, 30].

3.2.1 EXPERIMENTAL DETAILS FOR THE CREEP TESTS

The dimensions and notch details of the CT specimens are given in Fig. 3. Prior to the creep crack growth tests, fatigue pre-cracking was carried out in two phases: first at RT and, afterwards, at the testing temperature. The load wave was triangular in shape, with a frequency of 5 Hz and maximum load ($R=0$) equal to the static load applied in the follow-on creep test.

A computer controlled servo-hydraulic test machine, with a maximum load capacity of ± 100 kN, was used for both the fatigue pre-cracking and static tests. Crack growth was monitored by a computer controlled pulsed DC potential drop system, directly linked to the control and software system of the testing machine. The reference specimen technique was also used, and calibration curves were used to convert dimensionless voltage ratios to crack lengths or cracked area. The calibration curves were obtained by optical measurements and checked against crack length values, measured on the fracture surfaces of the specimens after the creep tests, and obtained by fatigue marking. For that purpose, the creep test was interrupted twice, and two blocks of fatigue cycles were applied to obtain a 0.2 to 0.3 mm length fatigue crack. The maximum load of the fatigue cycles for marking was the same as the load of the static test. It was found that the difference in crack length values between the calibration curve and the fatigue marking at the fracture surface never exceeded 3%.

In the CT specimens, the stress intensity factor was computed with the appropriate equation in [28]. For the CC specimens, the Pickard equation was used.

4. PRESENTATION AND ANALYSIS OF THE RESULTS

4.1 Effect of frequency and dwell time, t_D

In Figs. 4 to 6, the effect of frequency can best be analysed [31, 32-34], since all other fatigue parameters are kept constant. For higher frequencies, the dominant damage mechanism at the crack tip is cyclic plastic deformation, and the propagation is transgranular. The fatigue crack growth rate is cycle dependent, and is independent of frequency. Fig. 7 is a scanning electronic microscope (SEM) photo of a cycle dependent propagation fracture surface.

For lower frequencies, the damage mechanisms are creep and/or oxidation. Inconel 718 is creep resistant at 600°C, and so the damage mechanism is presumed to be oxidation. In this case, the propagation is intergranular, because the grain boundaries act as preferential paths for diffusion of oxygen. Since the oxidation is time dependent, fatigue crack growth rate da/dN varies linearly with $1/f$. Fig. 8 is a SEM view of a time dependent propagation fracture surface. For intermediate frequencies, oxidation and cyclic plastic deformation are simultaneously responsible for crack propagation, and the crack propagation rates have intermediate values.

For $R=0.05$, the transition frequencies are: from cycle dependent to mixed regime $f_{cm}=0.1$ Hz, and from mixed regime to time dependent $f_{mt}=0.01$ Hz. Hence, the mixed crack propagation covers an order of magnitude of the frequency range. For $R=0.5$, the transition frequencies are: from cycle dependent to mixed regime, $f_{cm}=1$ Hz, and from mixed regime to time dependent, $f_{mt}=0.03$ Hz. For $R=0.8$, the transitions are not clearly defined, and additional tests are in progress [33, 34].

Fig. 9 shows the influence of stress ratio (R) in the three crack propagation regimes. The increase of da/dN with R is more pronounced for time dependent crack propagation, due to the existence of oxide particles on the crack surface and due to the higher roughness associated with an intergranular crack path. Also, the oxidation mechanism may be affected by the increase of mean stress.

The transitions from cycle dependent to mixed and from mixed to time dependent propagation are also affected by the change of R . The increase of R increases the average stress level, and so the diffusion assisted time dependent propagation is enhanced. So, the increase of R moves the transitions to higher frequencies, i.e. extends the time dependent propagation to higher frequencies, as shown in Fig. 9.

4.2 Creep data

The da/dt versus K plots are shown in Figs. 10. It is seen that for 600°C (Fig. 10), the data is grouped in four sets of results: the higher CCGR were for the CT specimens, the intermediate CCGR for the CC specimens with negligible incubation period

and the lower CCGR for the two CC specimens with a long incubation period. The best fit Paris law correlations are also plotted in the same Figure. The equations for 600°C were:

$$\frac{da}{dt} = 9.02 \times 10^{-11} K_{\max}^{2.26} \quad (20a)$$

$$\frac{da}{dt} = 5.15 \times 10^{-16} K^{4.57} \quad (20b)$$

For 700°C the equation da/dt ; K (Fig. 10) is:

$$\frac{da}{dt} = 5.13 \times 10^{-8} K^{1.26} \quad (20c)$$

In these equations, the units are $[m/s; MPa\sqrt{m}]$.

At 600°C there is an increase in slope from the CT data to the CC data. For these correlations, the points of the initial "tail" behaviour of the da/dt versus K results were not taken into account (Fig. 10).

The increase in temperature from 600°C to 700°C in the CT specimens produced an increase in CCGR of nearly one order of magnitude, although with a very close slope in the da/dt data (Fig. 10), suggesting a similar stress system operating at both temperatures.

The increase in the CCGR in the CT specimens, as against the CC specimens, is documented in the literature [3], and is due to the predominantly plane strain conditions prevailing in the CT specimens. Thus, a triaxial stress state is formed, and the acceleration of the crack is expected.

SEM fracture surface observations at 600°C are shown in Figs. 11 to 12 and refer to the same specimen at two values of K ; 50 and 80 $MPa\sqrt{m}$ respectively. The increase in K caused an increase in surface roughness due to the increase in both the quantity and depth of secondary cracks, and also the increase in the number of cavities. Both fracture surfaces show slip bands on the grains at approximately 45° with the crack propagation direction, from left to right. There are oxidation products in the grain boundaries and some grain boundary sliding, especially in Fig. 12, for $K=80 MPa\sqrt{m}$. Some second phase particles are visible, mostly in the grain boundaries which are not crossed by the crack.

4.3 Application of the creep-fatigue superposition models

A computer program called "DWELL" was developed to calculate da/dN in creep-fatigue, applying the equations presented before in 2 for the different creep-fatigue superposition models. This program runs in a PC, is interactive (user friendly) and takes as inputs all the parameters and

variables required by the models, which should be introduced by the user. The outputs of the program are the FCGR results predicted by the several models, presented in a tabular or graphical form, and compared with the appropriate experimental data introduced by the user.

Since all the resulting equations for the various models are available, i.e. it is possible to represent a dependent variable – da/dN – as an explicit function for all the other parameters, it was not necessary to use numerical methods. The crack speeds are, though, obtained, for each model, by their respective equations, given by the equations presented in 2 in the form of Paris type equation with constants C_m and q_m , which define the resulting (see 2) equation $da/dN = C_m \Delta K^{q_m}$ of the da/dN selected prediction model are obtained as follows:

$$q_m = \frac{\log_{10} \left[\frac{da}{dN} (\Delta K_f) \right] - \log_{10} \left[\frac{da}{dN} (\Delta K_i) \right]}{\log_{10} (\Delta K_f) - \log_{10} (\Delta K_i)}$$

$$C_m = \frac{\frac{da}{dN} (\Delta K_i)}{\Delta K_i^{q_m}}$$

The calculation of these constants is exclusively based on the values of the extreme points of the selected range of K values ($\Delta K = \Delta K_i$ and $\Delta K = \Delta K_f$).

The differences between the prediction model and the experimental data for creep-fatigue are given by:

$$\text{difference} = \left\{ \log_{10} \left[\left(\frac{da}{dN} \right)_{\text{theoretical}} \right] - \log_{10} \left[\left(\frac{da}{dN} \right)_{\text{exper.}} \right] \right\} \times 100$$

If, for example, $(da/dN)_{\text{exper.}} = 1 \times 10^{-6}$, with $(da/dN)_{\text{theoretical}} = 1 \times 10^{-5}$, one will obtain difference = 100% and, with $(da/dN)_{\text{theoretical}} = 1 \times 10^{-7}$ one would obtain difference = -100%.

The DWELL program was used to compare the values, predicted by all the 5 models, with the experimental results previously reported. All the tested cases refer to creep fatigue at 600°C, with the trapezoidal load type used in this work and characterised by:

ramp frequency – $f=0.5\text{Hz}$
time at minimum load – $t_m=1\text{s}$.

All the other variables, which define the conditions of each test – stress ratio and time v at maximum load, dwell time, (t_b) – as well as the equations of the respective experimental data, used in the various tests, can be found in [29,34].

The other data used in the program were:

- frequency exponent – $\alpha=0.34$

- Transition frequency from the mixed to the intergranular failure regime – $f_{mt}=0.015\text{Hz}$
(average between the values 0.01Hz and 0.02Hz)
- $\Delta K_0=8.0 \text{ MPam}^{1/2}$

In Figs. 13 to 16 the best fit experimental lines da/dN vs. ΔK are compared against the predicted lines given by the five models considered in section 2. For low values of R (Fig. 13), the predictions of the creep-fatigue models for the FCGR are generally close to the experimental data. However, for higher values of R (Fig. 14), these differences are close to one order of magnitude.

The Saxena model usually gave the lowest values of FCGR amongst the other models and, for short dwell times at maximum load, the differences are greater since, in this case, the time dependent component is not totally taken into account (with $f_{mt}=0.015 \text{ Hz}$ the time dependent term is not computed for $t_0 < 63.6\text{s}$). For the higher values of t_0 (Figs. 14 to 16), this model gives very close predictions in relation to the other ones. The Saxena model is in a way very much dependent on the assumed value of the "cut-off" frequency. The use of the frequency f_{mt} assumes that the time dependent term only starts at the end of the mixed fracture zone. Assuming that the time dependent term starts at the value of the transition frequency between the mixed and transgranular regimes, it is seen that the results obtained by this model, for low values of t_0 , will be higher and more close to the experimental values.

The remaining models (Gayda-Miner, Weerassoriya (35), Nicholas (36)) gave very close results, in some cases with negligible differences, specially for high dwell times since, in this case, the most important term is equal for all these models.

For the CT specimens (Figs. 13 and 14) it should be referred that, with the exception of the Weerassoriya model, the cyclic component is very small, ranging between 15% of the total for higher dwell times ($t_0=120\text{s}$ or 300s) and 5% for small values of t_0 . Another exception is the Saxena model which, for $t_0=1\text{s}$ ($f_t=0.25\text{Hz}$), gives 100% cyclic contribution, because $f_{mt} < f_t$.

In the CC specimens (Figs. 15 and 16), and for small values of the dwell time (Fig. 15), the cyclic component accounts for about 95% of the total FCGR. This component depends on the value of ΔK , decreasing with the increase of ΔK due to the fact that, usually, the exponent, n , of the time dependent term is higher than the exponent, m , of the cyclic dependent term. As the dwell time increases and, therefore, creep becomes more important, the influence of the cyclic component is diminishing (e.g, in Fig. 16, for $t_0=600\text{s}$; $R=0.05$ and $\Delta K=20.6 \text{ MPam}^{1/2}$, the percentage of the cyclic component is 14%).

The results obtained for high values of R (Fig. 14) have shown bigger differences between the experimental data and the predictions of the models for values of t_0 greater than 1s. The predictions were usually above the experimental data. Work is now in progress to assess the availability of the models for the data obtained in IN718 with negative stress ratios.

If, for the cyclic component of the models, the FCGR term is taken at room temperature, lower FCGR are obtained in the cases where the cyclic or mixed components are important, as it happens with the Weerassoriya model.

The results have shown that da/dN , in conditions of creep-fatigue, such as in the trapezoidal load wave assumed for turbine discs, can be safely taken as the sum of a cyclic dependent term with a time dependent term obtained in creep tests. Hence, for a life extension assessment, the residual life of the disc can be safely predicted using one of the creep-fatigue models presented in this paper, without the need for obtaining FCGR data in creep-fatigue tests with load waves with dwell times at maximum load. However, for higher values of R , the da/dN given by the superposition models can give excessive safety (Fig. 14) and, therefore, further work is required to check the accuracy of the models under these conditions, and also for negative values of R .

5. CONCLUSIONS

An adequate knowledge of the FCGR behaviour of the materials, in terms of its variation with frequency, stress ratio and temperature is required to apply life extension predictions. In nickel base superalloys, used for turbine discs, the results presented in this paper, and the data available in the literature, shows:

- (i) In terms of frequency, three regimes of crack propagation are obtained: time dependent, cycle dependent and mixed. These regimes are related to various damage mechanisms, responsible for crack propagation. For $R=0.05$, the transition frequencies were: from cycle dependent to mixed regime, $f_{cm}=0.1 \text{ Hz}$, and from mixed regime to time dependent $f_{mt}=0.01 \text{ Hz}$. For $R=0.5$, the transition frequencies are: from cycle dependent to mixed regime $f_{cm}=1 \text{ Hz}$, and from mixed regime to time dependent $f_{mt}=0.03 \text{ Hz}$;
- (ii) The increase of stress ratio gives an increase of cycle crack growth rate for the different regimes of crack growth. Possible explanations for this behaviour are reduced crack closure and/or an influence of mean stress. The effect of stress ratio is found to be greatest for time dependent propagation, suggesting that the intergranular crack growth mechanism (probably oxidation dominated) is influenced by mean stress;
- (iii) The influence of stress state is observed for time dependent crack propagation, producing a crack tunnelling effect. It may be related to a change of crack growth mechanism from time dependent to cycle dependent at the surface, or to an influence of stress state on intergranular crack growth.

For creep crack growth, and using the stress intensity factor, K , to characterise growth rate, slower rates are observed for the initially quarter circle cracks in the CC specimen than in the CT case, together with a greater degree of crack tunnelling. Also,

an increase in temperature for 600 to 700°C shows an expected increase in growth rate.

With the exception of the Saxena model, the other creep-fatigue models analysed in this paper have given very close predictions amongst themselves and also with the experimental data for low values of the stress ratio, and for a wide range of dwell times at maximum load (between 1 and 600s). For high values of stress ratio ($R > 0.5$), the predictions of FCGR given by the superposition models lie significantly above the experimental data, with differences ranging from a factor of 2 until one order of magnitude. However, with this result safe predictions can be made of the life in crack propagation under creep-fatigue conditions.

6. REFERENCES

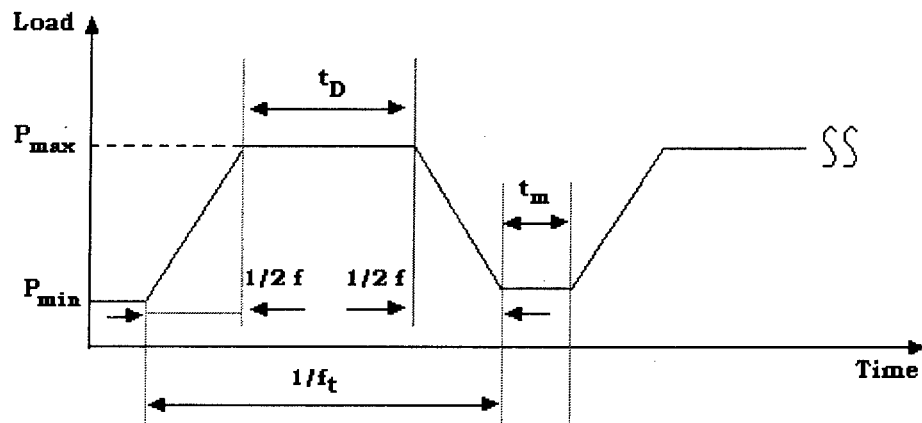
- (1) Gayda, J., Gabb, T.P. and Miner, R.V., "Fatigue Crack Propagation of Nickel-Base Superalloys at 650°C", Low Cycle Fatigue, ASTM STP 942, (Ed. H.D. Solomon, G.R. Halford, L.R. Kaisand and B.N. Leis), American Society for Testing and Materials, Philadelphia, pp.293-309, 1988.
- (2) Branco, C.M., Byrne, J. and Hodgkinson, V., "Elevated Temperature Fatigue in IN718 - a Review and Modelling", Paper nr. 6, NATO ASI Mechanical Behaviour of Materials at High Temperature, ed. Moura Branco, C., Ritchie, R., Sklenjicka, V., High Technology Series, 3/15, publ. Kluwer, The Netherlands, 1996, pp. 93-135.
- (3) Webster, G.A. and Ainsworth, R.A., "High Temperature Component Life Assessment", Ed. Chapman & Hall, U.K., 1994.
- (4) Pineau, A., "Defect Assessment Procedures in the Creep Range", Paper nr. 2, NATO ASI Mechanical Behaviour of Materials at High Temperature, Sesimbra, Portugal, September 1995, *ibid* (2).
- (5) A. Pineau, "Intergranular Creep-Fatigue Crack Growth in Ni-Base Alloys", Flow and Fracture at Elevated Temperatures, Ed. R. Raj, ASM Materials Sci. Div., Philadelphia, pp. 317-348, 1983.
- (6) Ghonem, H. and Zheng, D., "Frequency Interactions in High Temperature Fatigue Crack Growth in Superalloys", Metallurgical Transactions A, 23A, pp. 3067-3072, 1992.
- (7) Webster, G.A., "High Temperature Fatigue Crack Growth in Superalloy Blade Materials", Material Science and Technology, 3, pp. 716-725, September 1987.
- (8) Nicholas, T. and Ashbaugh, N.E., "Fatigue Crack Growth at High Load Ratios in the Time Dependent Regime", Fracture Mechanics, Nineteenth Symposium, ASTM STP 969 (Ed. T.A. Cruse), American Society for Testing and Materials, Philadelphia, pp. 800-817, 1988.
- (9) Nicholas, T., Weerasooriya, T. and Asbaugh, N.E., "A Model for Creep-Fatigue Interactions in Alloy 718", Fracture Mechanics: Sixteenth Symposium, ASTM STP 868, (Ed. M.F. Kanninen and A.T. Hooper), American Society for Testing and Materials, Philadelphia, pp. 167-180, 1985.
- (10) Lynch, S.P., Radtke, T.C., Wicks, B.J., Byrnes, R.T., "Fatigue crack growth in nickel based superalloys at 500-700°C. I-Waspalloy", Fat. Fract. Eng. Mat. Struct. (1994), pp. 297-311.
- (11) Ghonem, H., Nicholas, T. Pineau, A., "Elevated temperature fatigue crack growth in alloy 718 - Part II: effects of environment and material variables", Fat. Fract. Eng. Mat. Struct. (1993), pp. 577-590.
- (12) Lynch, S.P., Radtke, T.C., Wicks, B.J., Byrnes, R.T., "Fatigue crack growth in nickel based superalloys at 500-700°C. II-Direct aged alloy 718", Fat. Fract. Eng. Mat. Struct. (1994), pp.313-325.
- (13) Winstone, M.R., Nikbin, K.M., Webster, G.A., "Modes of failure under creep-fatigue loading of a nickel base superalloy", J. Mat. Sci. (1985), pp. 2471-2476.
- (14) Byrne, J., Hall, R., Grabowski, L., "Elevated temperature fatigue crack growth under dwell conditions in Waspalloy", Int. J. Fat., 19, 5, 1997, pp. 359-367.
- (15) Clavel, M. Pineau, A., "Frequency and wave form effects on the fatigue crack growth behaviour of alloy 718 at 298K and 823K", Metall. Trans., 9A (1978), pp. 471-480.
- (16) Gayda, J., Gabb, T.P., Miner, R.V., "Fatigue crack propagation of nickel base superalloys at 650°C in "Low Cycle Fatigue", ASTM STP942, Eds. H.D. Solomon, G.R. Halford, L.R. Kaisand and B.N. Leis, American Society for Testing and Materials, 1988, pp. 293-309.
- (17) Sadananda, K., Shahimian, P., "Hold time effects on high temperature fatigue crack growth in Udimet 700", J. Mat. Sci. (1978), pp. 2347-2357.
- (18) Shahimian, P., Sadananda, K., "Effects of stress ratio and hold time on fatigue crack growth in alloy 718", J. Eng. Mat. Tech., Trans. ASME (1979), pp. 101, 224-230.
- (19) Ghonem, H., Nicholas, T., Pineau, A., "Elevated temperature fatigue crack growth in alloy 718 - Part I: effects of mechanical variables", Fat. Fract. Eng. Mat. Struct. (1993), pp. 565-576.
- (20) Nicholas, T., Weerasooriya, T., "Hold time effects in elevated temperature fatigue crack propagation", Fract. Mech., 17th Volume, ASTM STP905, American Society for Testing and Materials, 1986, pp. 155-168.
- (21) Diboine, A., Pineau, A., "Creep crack initiation and growth in Inconel 718 alloy at 650°C", Fat. Fract. Eng. Mat. Struct., 1987, pp. 141-151.
- (22) James, L.A., Eng. Fract. Mech., Vol. 25, 1986, pp. 304-314.
- (23) Hodgkinson, V., "The effect of wave shape on fatigue crack growth in nickel base superalloys at elevated temperature", PhD thesis, Dep. of Mech. Engineering, University of Portsmouth, August 1997.
- (24) Zheng, D., Ghonem, H., "Influence of prolonged exposure on intergranular fatigue crack growth behaviour in alloy 718 at 650°C", Met. Trans, 23A, 1992, pp. 3169-3171.
- (25) Weerasooriya, T., "Effect of frequency on fatigue crack growth rate of IN718 at elevated temperature", in Fract. Mech., 19th Symposium, ASTM STP969, Ed. T.A. Cruse, American Society for Testing and Materials, Philadelphia, USA, 1988, pp. 907-923.

- (26) Walker, E.K., Report AFFDL TR 70-144, Air Force Flight Dynamics Laboratory, USA, available from the Department of Commerce, National Technical Information Service, Springfield, VA, USA, 22161 (1970), pp. 225-233.
- (27) Saxena, A., *Fat. Eng. Mat. Struct.* (1981), pp. 247-255.
- (28) Branco, C.M., "Fatigue behaviour of nickel base superalloys under dwell conditions", final report of AGARD Project P94, Support Program to Portugal, CEMUL/IST, Technical University of Lisbon, April 1995.
- (29) Baptista, J.C., "An analysis of the creep-fatigue behaviour at high temperature of the nickel base superalloy IN718" (in Portuguese), MSc thesis, Technical University of Lisbon, IST, June 1997.
- (30) Branco, C.M., Antunes, F.V., Byrne, J., "Influence of stress ratio and time at maximum load on the fatigue crack growth behaviour of IN718 at 600°C", *Proc. ECF 11, 11th European Conference on Fracture*, Ed.ESIS, Vol. II, 1997, pp. 1287-1293.
- (31) Branco, C.M., Byrne, J., "Fatigue Behaviour of nickel base superalloy IN718 at elevated temperature", *Mat. High. Temp.*, 1994, pp. 261-268.
- (32) Branco, C.M., Byrne, J., "Elevated temperature fatigue of IN718: effects of stress ratio and frequency", in "Thermal Mechanical Fatigue of aircraft engine materials", AGARD-CP-569, March 1996, Paris, France, paper 6-1, 6-12.
- (33) Branco, C.M., Baptista, J., Byrne, J., "Crack growth under constant sustained load at elevated temperature in IN718 superalloy", accepted for publication in *Materials at High Temperature*, 1998.
- (34) Antunes, F.V., "Influence of frequency, stress ratio and stress state on fatigue crack growth in nickel base superalloys at elevated temperature", PhD thesis, University of Portsmouth, UK, 1998.
- (35) Nicholas, T., Weerassoryia, T., Ashbaugh, N.E., "A model for creep-fatigue interactions in alloy 718", in *Fracture Mechanics, 16th Symposium*, ASTM STP868, 1995, pp. 165-180.
- (36) Nicholas, T., Mall, S., "Elevated temperature crack growth in aircraft engine materials", "Advances in fatigue lifetime predictive techniques", ASTM STP 1122, Eds. M.R. Mitchel and R.W. Landgraff, American Society for Testing and Materials, 1985, pp. 165-180.

ACKNOWLEDGEMENTS

This work was financed jointly by the former AGARD/SMP in the Support Program to Portugal, under Project P111 "Fracture mode transition and fatigue crack growth rates in nickel base superalloys", and also under the Project CCI Defesa 07/91 of the Ministry for National Defence of Portugal.

The specimens were provided by DERA, Farnborough, UK.



t_D – Time at maximum load; t_m – Time at minimum load; f – frequency; f_t – total frequency; P_{max} – maximum load; P_{min} – minimum load

Fig. 1 – Trapezoidal load wave.

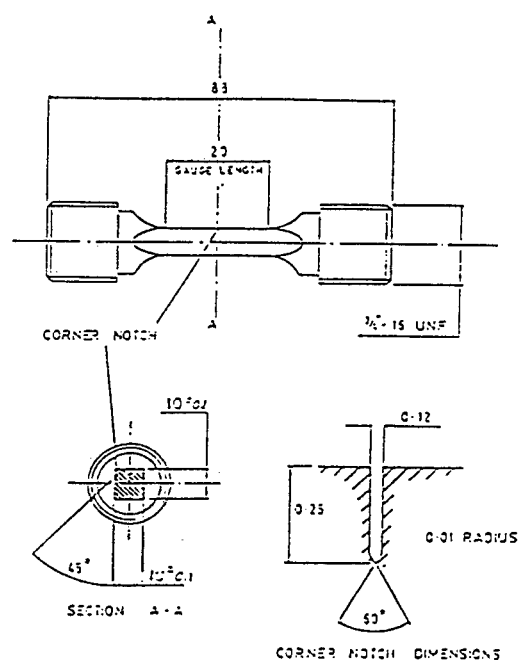


Fig. 2 – Corner Crack (CC) specimen.

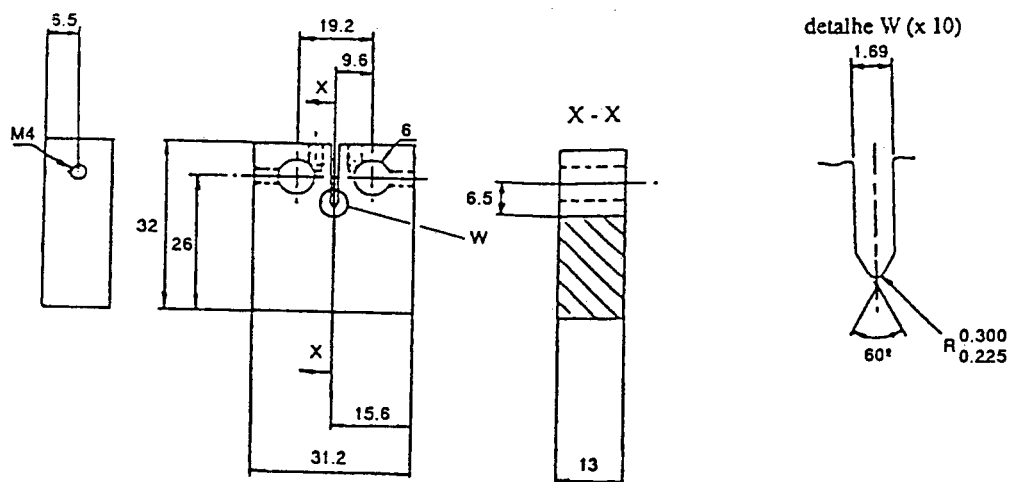


Fig. 3 – CT specimen geometry used for fatigue and creep tests.

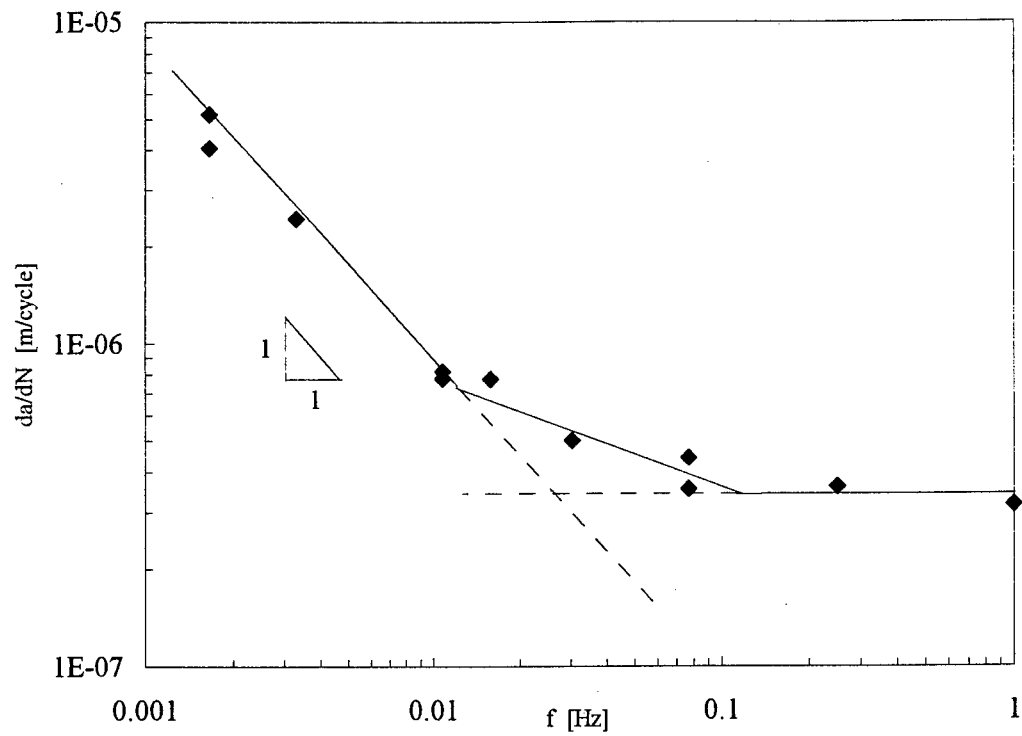


Fig. 4 – Effect of frequency at 600°C, for $R=0.05$ and $\Delta K=30 \text{ MPam}^{1/2}$. IN718.

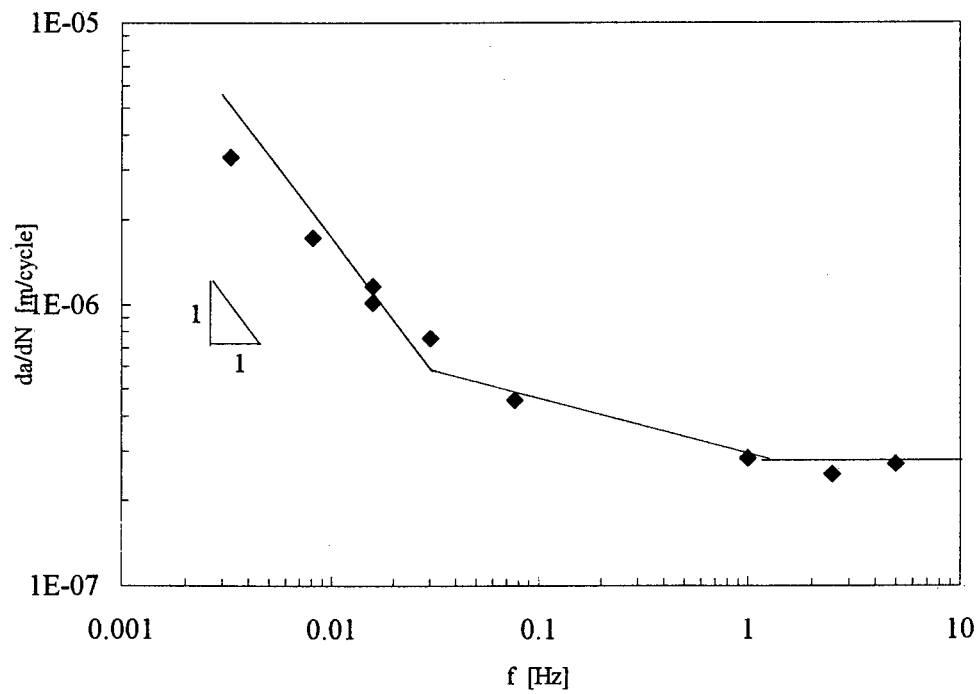


Fig. 5 – Effect of frequency at 600°C, for $R=0.5$ and $\Delta K=25 \text{ MPam}^{1/2}$. IN718.

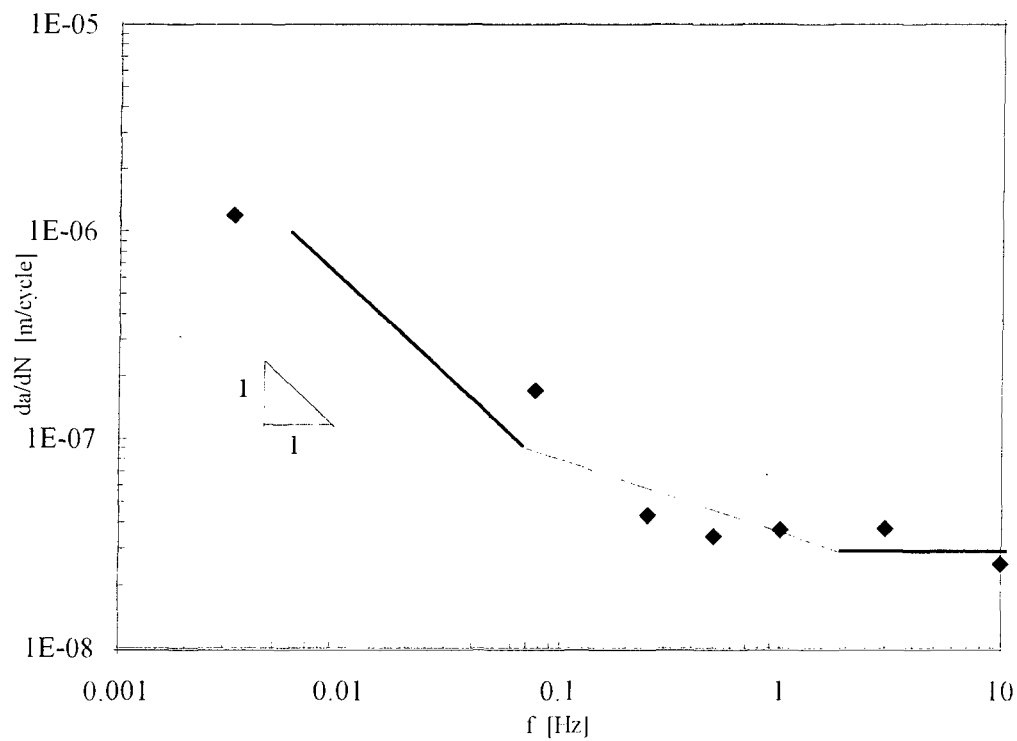


Fig. 6 - Effect of frequency at 600°C, for $R=0.8$ and $\Delta K=15 \text{ MPam}^{1/2}$. IN718.

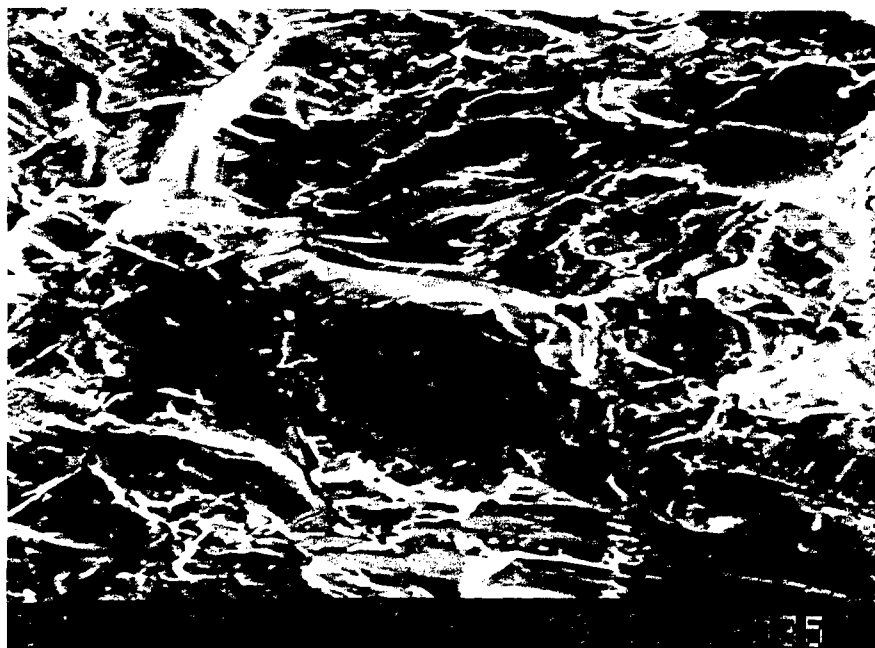


Fig. 7 - SEM photo for $T=600^\circ\text{C}$, $f=1\text{Hz}$, $R=0.5$, $\Delta K=17.5 \text{ MPam}^{1/2}$. Cycle dependent, transgranular crack growth. IN718.

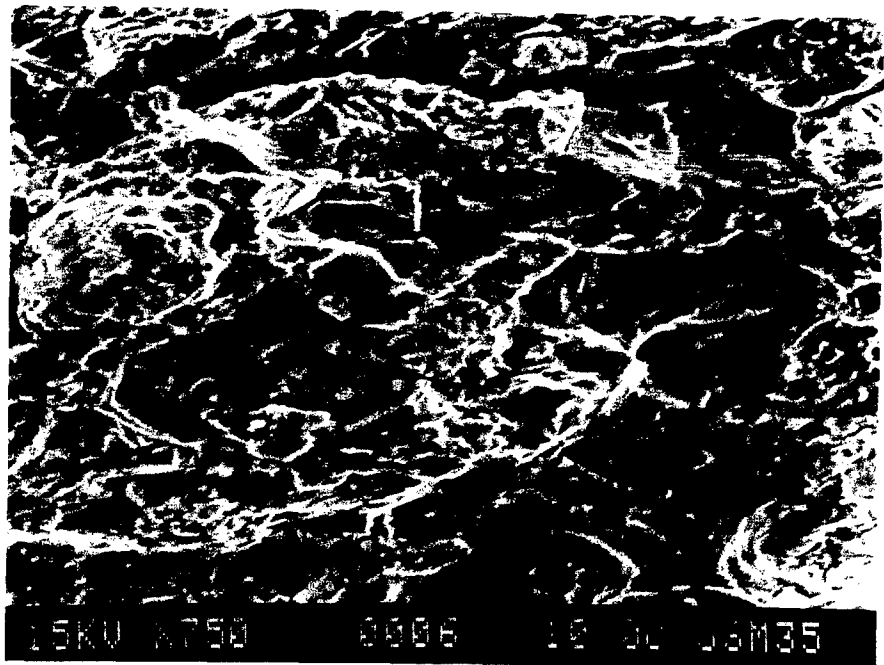


Fig. 8 – SEM photo for $T=600^{\circ}\text{C}$, $f=1/63\text{Hz}$, $R=0.5$, $\Delta K=34.5\text{ MPam}^{1/2}$. Cycle dependent, intergranular crack growth. IN718.

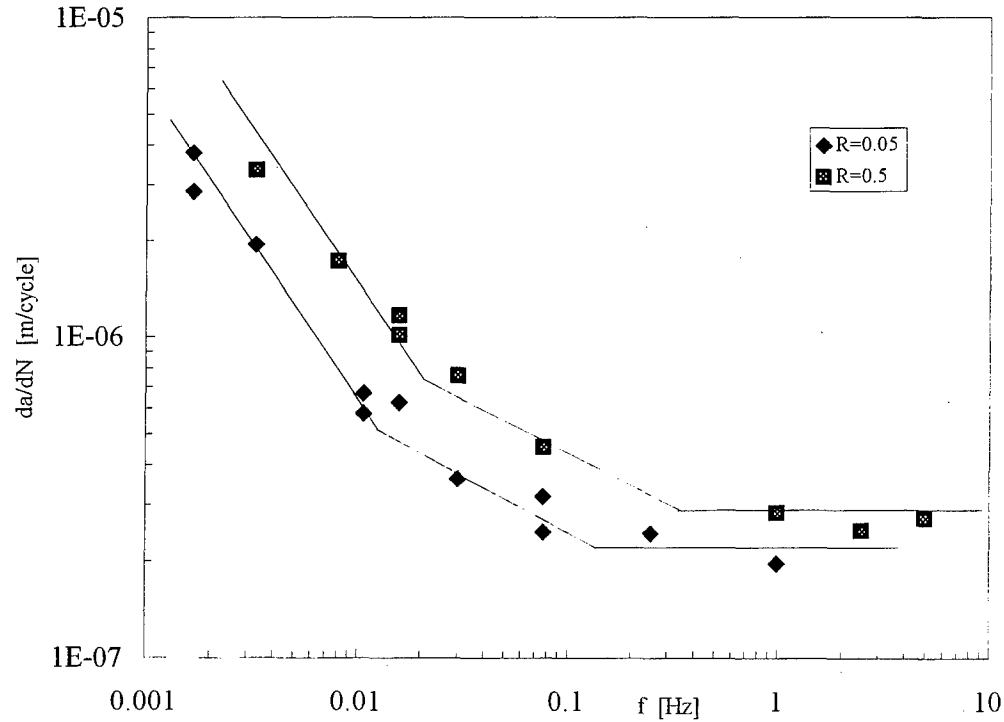


Fig. 9 – Effect of stress ratio. $\Delta K=25\text{ MPam}^{1/2}$. IN718.

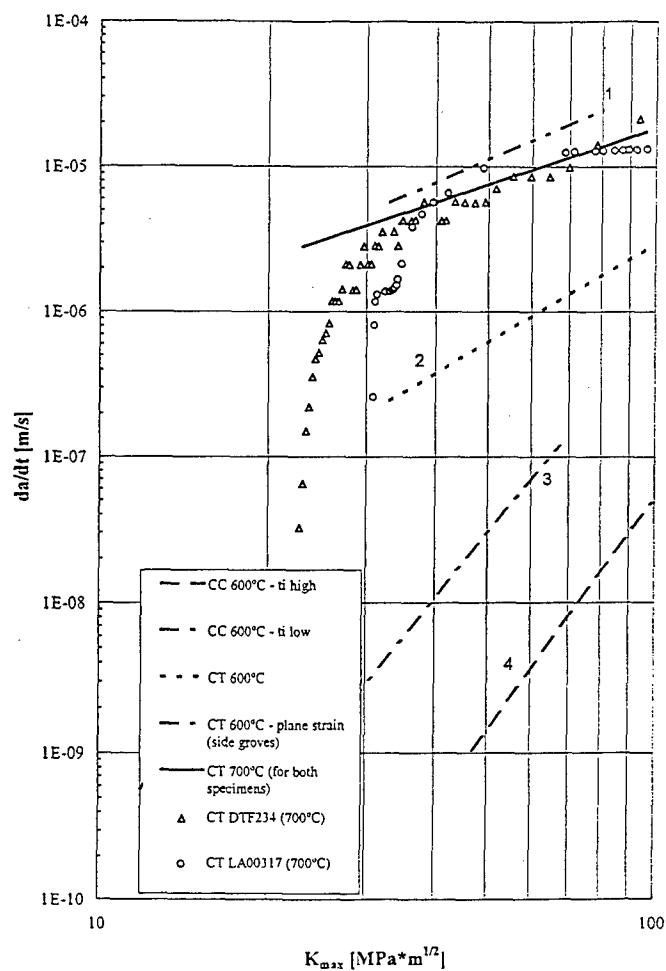


Fig. 10 – da/dt vs. K_{max} and best fit correlation line for 600 and 700°C.

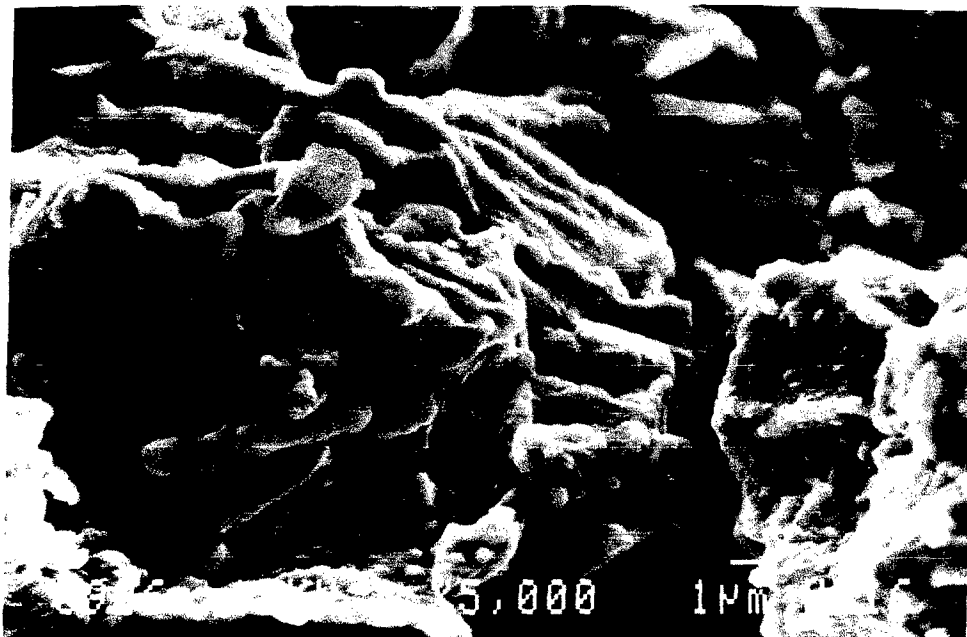


Fig. 11 – Creep intergranular crack. Crack propagation direction: top of left corner from bottom of right corner. IN718. 600°C. $K_{max}=50\text{MPa}\cdot\text{m}^{1/2}$.

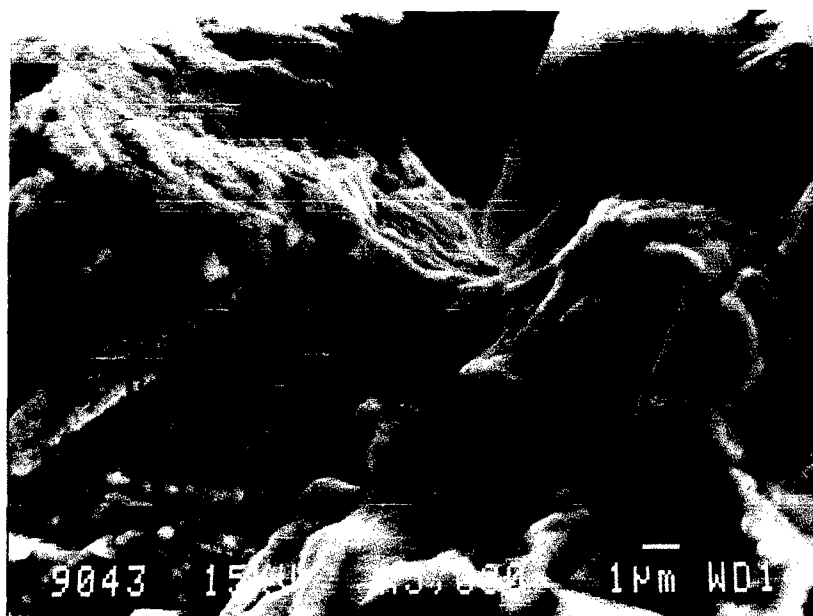


Fig. 12 - Creep intergranular crack. Crack propagation direction: top of left corner from bottom of right corner. IN718. 600°C. $K_{max}=80\text{MPam}^{1/2}$.

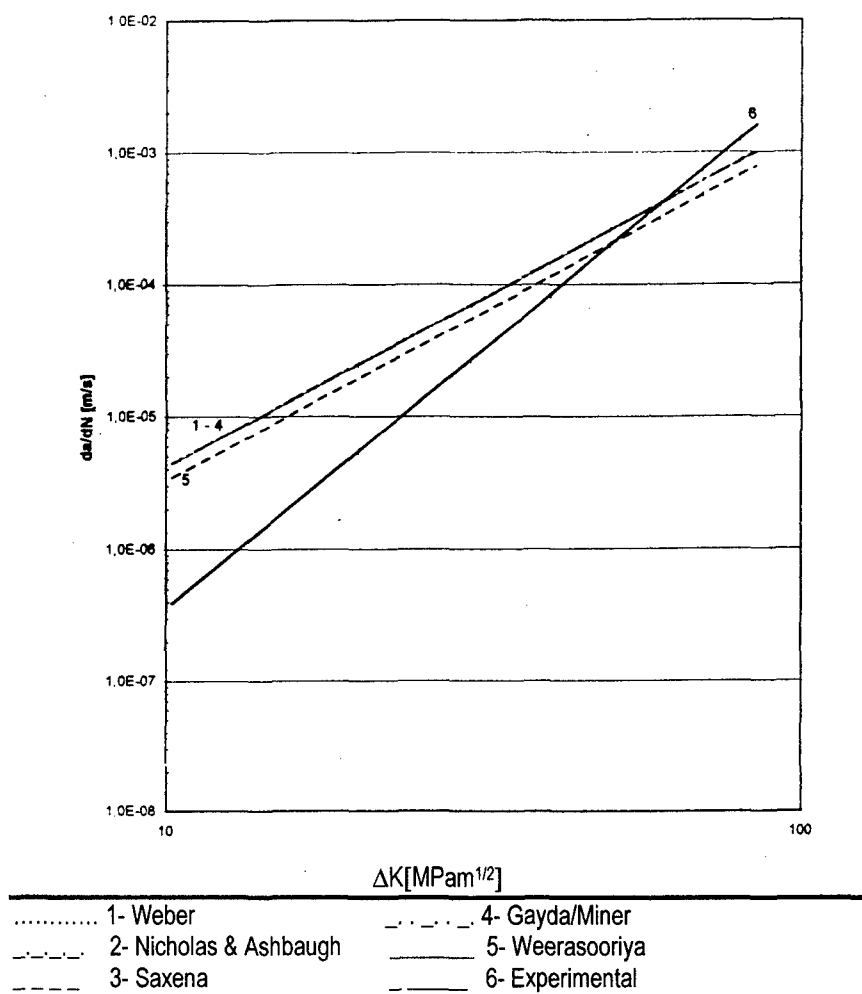


Fig. 13 - Prediction models for CT specimen ; $R=0.05$, $T_D=300\text{s}$ and $T=600^\circ\text{C}$.

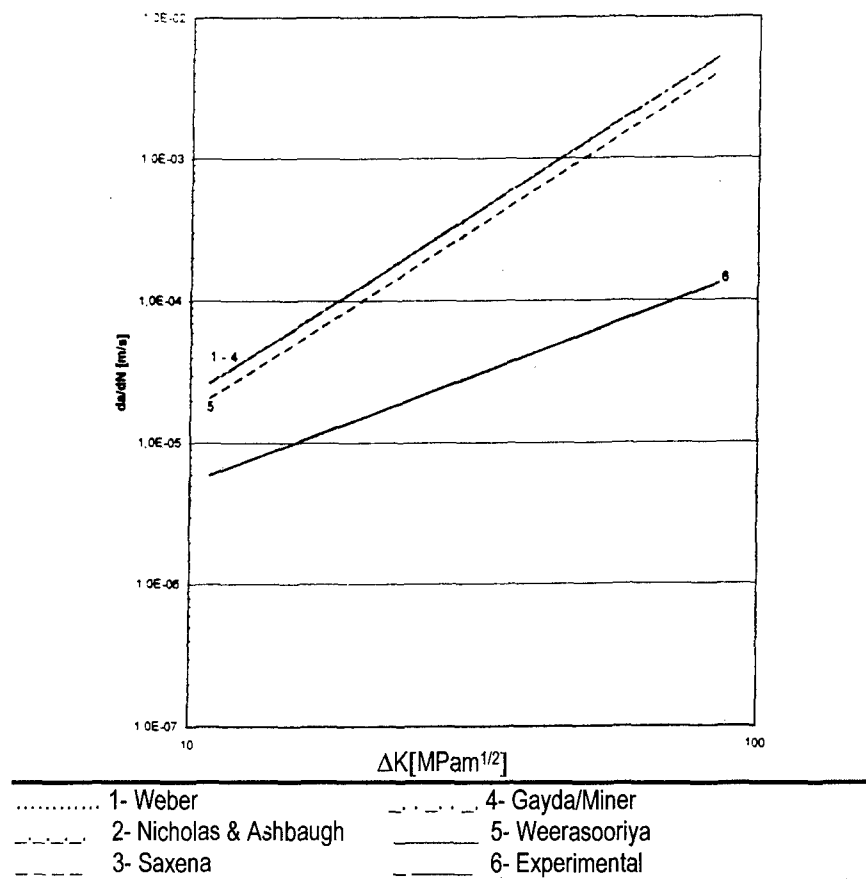


Fig. 14 - Prediction models for CT specimen ; $R=0.5$, $T_D=300s$ and $T=600^\circ C$.

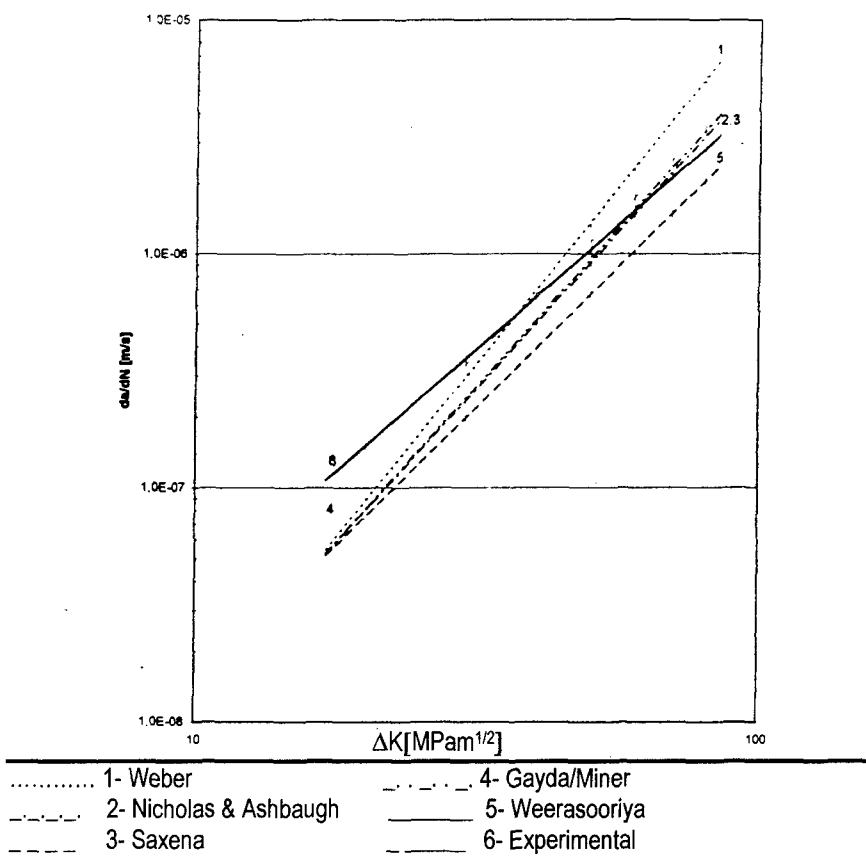


Fig. 15 - Prediction models for CC specimen ; $R=0.05$, $T_D=1s$ and $T=600^\circ C$.

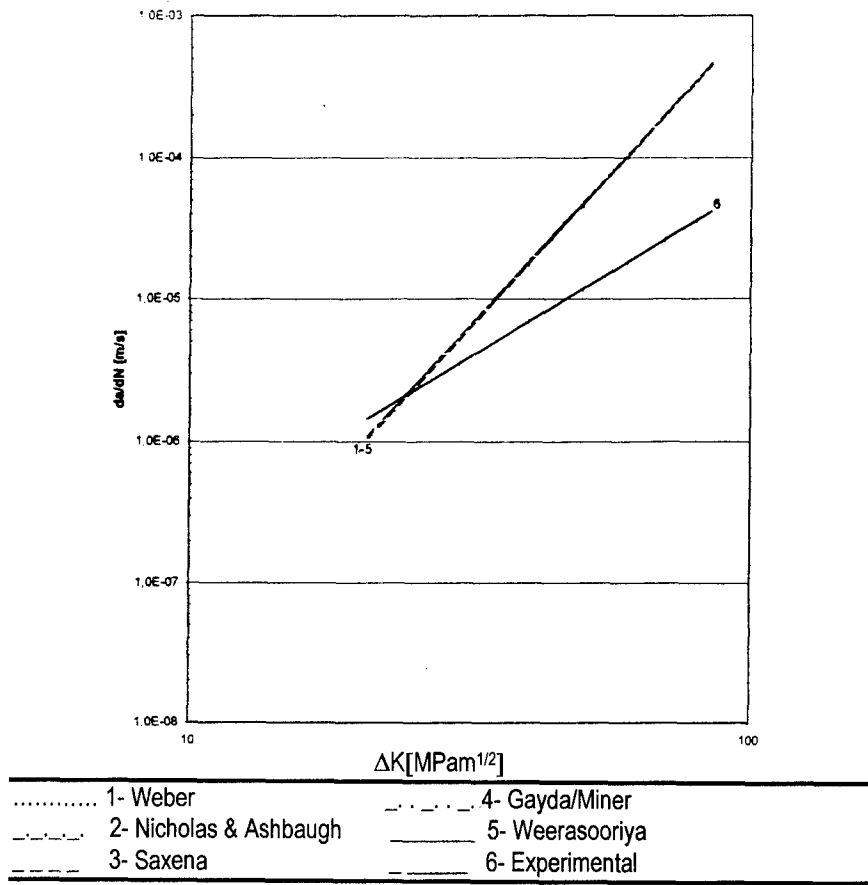


Fig. 16 - Prediction models for CC specimen ; $R=0.05$, $T_D=600s$ and $T=600^\circ C$.

REPORT DOCUMENTATION PAGE

1. Recipient's Reference	2. Originator's References RTO-MP-17 AC/323(AVT)TP/7	3. Further Reference ISBN 92-837-1012-6	4. Security Classification of Document UNCLASSIFIED/ UNLIMITED																				
5. Originator	Research and Technology Organization North Atlantic Treaty Organization BP 25, 7 rue Ancelle, F-92201 Neuilly-sur-Seine Cedex, France																						
6. Title	Qualification of Life Extension Schemes for Engine Components																						
7. Presented at/sponsored by	the Workshop of the RTO Applied Vehicle Technology Panel (AVT) – organised by the former AGARD Structures and Materials Panel – held in Corfu, Greece, 5-6 October 1998.																						
8. Author(s)/Editor(s) Multiple	9. Date March 1999																						
10. Author's/Editor's Address Multiple	11. Pages 172																						
12. Distribution Statement	There are no restrictions on the distribution of this document. Information about the availability of this and other RTO unclassified publications is given on the back cover.																						
13. Keywords/Descriptors	<table><tbody><tr><td>Aircraft engines</td><td>Reconditioning</td></tr><tr><td>Service life</td><td>Maintenance</td></tr><tr><td>Life cycle costs</td><td>Design</td></tr><tr><td>Defense economics</td><td>Safety engineering</td></tr><tr><td>Damage control</td><td>Tolerances (mechanics)</td></tr><tr><td>Durability</td><td>Fatigue (materials)</td></tr><tr><td>Performance</td><td>Cost effectiveness</td></tr><tr><td>Reliability</td><td>Benefit cost analysis</td></tr><tr><td>Materials replacement</td><td>Turbine components</td></tr><tr><td>Protective coatings</td><td></td></tr></tbody></table>			Aircraft engines	Reconditioning	Service life	Maintenance	Life cycle costs	Design	Defense economics	Safety engineering	Damage control	Tolerances (mechanics)	Durability	Fatigue (materials)	Performance	Cost effectiveness	Reliability	Benefit cost analysis	Materials replacement	Turbine components	Protective coatings	
Aircraft engines	Reconditioning																						
Service life	Maintenance																						
Life cycle costs	Design																						
Defense economics	Safety engineering																						
Damage control	Tolerances (mechanics)																						
Durability	Fatigue (materials)																						
Performance	Cost effectiveness																						
Reliability	Benefit cost analysis																						
Materials replacement	Turbine components																						
Protective coatings																							
14. Abstract	<p>Contains the papers presented at the Workshop on Qualification of Life Extension Schemes for Engine Components, organized by the Applied Vehicle Technology Panel of RTO, in Corfu, Greece, 5-6 October 1998.</p> <p>The replacement cost of service-damaged components contributes significantly to the life cycle costs of an aero-engine. Damaged engine components also impact on the reliability and safety of aircraft. The papers discuss component damage management in turbines, including life management aspects of high cycle fatigue, and techniques for extending lives of service-damaged parts to achieve engine life cycle cost reductions, without compromising safety. Operators' needs and benefits accruing from component life extension are discussed. Various technologies available to life cycle managers for component life extension are described. The technologies include surface modification treatments and coatings, repair and refurbishment procedures, as well as improved component life cycle management practices based on damage tolerance and inspection. Emphasis is placed on the qualification testing requirements that must be satisfied to ensure that repaired or modified parts, or parts for which new life cycle management practices are applied, remain safe and reliable when returned to service.</p>																						



RESEARCH AND TECHNOLOGY ORGANIZATION

BP 25 • 7 RUE ANCELLE

F-92201 NEUILLY-SUR-SEINE CEDEX • FRANCE

Télécopie 0(1)55.61.22.99 • Téléc 610 176

DIFFUSION DES PUBLICATIONS

RTO NON CLASSIFIEES

L'Organisation pour la recherche et la technologie de l'OTAN (RTO), détient un stock limité de certaines de ses publications récentes, ainsi que de celles de l'ancien AGARD (Groupe consultatif pour la recherche et les réalisations aérospatiales de l'OTAN). Celles-ci pourront éventuellement être obtenues sous forme de copie papier. Pour de plus amples renseignements concernant l'achat de ces ouvrages, adressez-vous par lettre ou par télécopie à l'adresse indiquée ci-dessus. Veuillez ne pas téléphoner.

Des exemplaires supplémentaires peuvent parfois être obtenus auprès des centres nationaux de distribution indiqués ci-dessous. Si vous souhaitez recevoir toutes les publications de la RTO, ou simplement celles qui concernent certains Panels, vous pouvez demander d'être inclus sur la liste d'envoi de l'un de ces centres.

Les publications de la RTO et de l'AGARD sont en vente auprès des agences de vente indiquées ci-dessous, sous forme de photocopie ou de microfiche. Certains originaux peuvent également être obtenus auprès de CASI.

CENTRES DE DIFFUSION NATIONAUX

ALLEMAGNE

Fachinformationszentrum Karlsruhe
D-76344 Eggenstein-Leopoldshafen 2

BELGIQUE

Coordinateur RTO - VSL/RTO
Etat-Major de la Force Aérienne
Quartier Reine Elisabeth
Rue d'Evere, B-1140 Bruxelles

CANADA

Directeur - Gestion de l'information
(Recherche et développement) - DRDGI 3
Ministère de la Défense nationale
Ottawa, Ontario K1A 0K2

DANEMARK

Danish Defence Research Establishment
Ryvangs Allé 1
P.O. Box 2715
DK-2100 Copenhagen Ø

ESPAGNE

INTA (RTO/AGARD Publications)
Carretera de Torrejón a Ajalvir, Pk.4
28850 Torrejón de Ardoz - Madrid

ETATS-UNIS

NASA Center for AeroSpace Information (CASI)
Parkway Center, 7121 Standard Drive
Hanover, MD 21076-1320

FRANCE

O.N.E.R.A. (Direction)
29, Avenue de la Division Leclerc
92322 Châtillon Cedex

GRECE

Hellenic Air Force
Air War College
Scientific and Technical Library
Dekelia Air Force Base
Dekelia, Athens TGA 1010

ISLANDE

Director of Aviation
c/o Flugrad
Reykjavik

ITALIE

Aeronautica Militare
Ufficio Stralcio RTO/AGARD
Aeroporto Pratica di Mare
00040 Pomezia (Roma)

LUXEMBOURG

Voir Belgique

NORVEGE

Norwegian Defence Research Establishment
Attn: Biblioteket
P.O. Box 25
N-2007 Kjeller

PAYS-BAS

NDRCC
DGM/DWOO
P.O. Box 20701
2500 ES Den Haag

PORTUGAL

Estado Maior da Força Aérea
SDFA - Centro de Documentação
Alfragide
P-2720 Amadora

ROYAUME-UNI

Defence Research Information Centre
Kentigern House
65 Brown Street
Glasgow G2 8EX

TURQUIE

Millî Savunma Başkanlığı (MSB)
ARGE Dairesi Başkanlığı (MSB)
06650 Bakanlıklar - Ankara

AGENCES DE VENTE

NASA Center for AeroSpace Information (CASI)

Parkway Center
7121 Standard Drive
Hanover, MD 21076-1320
Etats-Unis

The British Library Document Supply Centre

Boston Spa, Wetherby
West Yorkshire LS23 7BQ
Royaume-Uni

Canada Institute for Scientific and Technical Information (CISTI)

National Research Council
Document Delivery,
Montreal Road, Building M-55
Ottawa K1A 0S2
Canada

Les demandes de documents RTO ou AGARD doivent comporter la dénomination "RTO" ou "AGARD" selon le cas, suivie du numéro de série (par exemple AGARD-AG-315). Des informations analogues, telles que le titre et la date de publication sont souhaitables. Des références bibliographiques complètes ainsi que des résumés des publications RTO et AGARD figurent dans les journaux suivants:

Scientific and Technical Aerospace Reports (STAR)

STAR peut être consulté en ligne au localisateur de ressources uniformes (URL) suivant:

<http://www.sti.nasa.gov/Pubs/star/Star.html>

STAR est édité par CASI dans le cadre du programme

NASA d'information scientifique et technique (STI)

STI Program Office, MS 157A

NASA Langley Research Center

Hampton, Virginia 23681-0001

Etats-Unis

Government Reports Announcements & Index (GRA&I)

publié par le National Technical Information Service
Springfield

Virginia 2216

Etats-Unis

(accessible également en mode interactif dans la base de données bibliographiques en ligne du NTIS, et sur CD-ROM)



Imprimé par le Groupe Communication Canada Inc.
(membre de la Corporation St-Joseph)

45, boul. Sacré-Cœur, Hull (Québec), Canada K1A 0S7



RESEARCH AND TECHNOLOGY ORGANIZATION

BP 25 • 7 RUE ANCELLE

F-92201 NEUILLY-SUR-SEINE CEDEX • FRANCE

Telefax 0(1)55.61.22.99 • Telex 610 176

DISTRIBUTION OF UNCLASSIFIED
RTO PUBLICATIONS

NATO's Research and Technology Organization (RTO) holds limited quantities of some of its recent publications and those of the former AGARD (Advisory Group for Aerospace Research & Development of NATO), and these may be available for purchase in hard copy form. For more information, write or send a telefax to the address given above. **Please do not telephone.**

Further copies are sometimes available from the National Distribution Centres listed below. If you wish to receive all RTO publications, or just those relating to one or more specific RTO Panels, they may be willing to include you (or your organisation) in their distribution.

RTO and AGARD publications may be purchased from the Sales Agencies listed below, in photocopy or microfiche form. Original copies of some publications may be available from CASI.

NATIONAL DISTRIBUTION CENTRES

BELGIUM

Coordinateur RTO - VSL/RTO
Etat-Major de la Force Aérienne
Quartier Reine Elisabeth
Rue d'Evere, B-1140 Bruxelles

CANADA

Director Research & Development
Information Management - DRDIM 3
Dept of National Defence
Ottawa, Ontario K1A 0K2

DENMARK

Danish Defence Research Establishment
Ryvangs Allé 1
P.O. Box 2715
DK-2100 Copenhagen Ø

FRANCE

O.N.E.R.A. (Direction)
29 Avenue de la Division Leclerc
92322 Châtillon Cedex

GERMANY

Fachinformationszentrum Karlsruhe
D-76344 Eggenstein-Leopoldshafen 2

GREECE

Hellenic Air Force
Air War College
Scientific and Technical Library
Dekelia Air Force Base
Dekelia, Athens TGA 1010

ICELAND

Director of Aviation
c/o Flugrad
Reykjavik

ITALY

Aeronautica Militare
Ufficio Stralcio RTO/AGARD
Aeroporto Pratica di Mare
00040 Pomezia (Roma)

LUXEMBOURG

See Belgium

NETHERLANDS

NDRCC
DGM/DWOO
P.O. Box 20701
2500 ES Den Haag

NORWAY

Norwegian Defence Research Establishment
Attn: Biblioteket
P.O. Box 25
N-2007 Kjeller

PORTUGAL

Estado Maior da Força Aérea
SDFA - Centro de Documentação
Alfragide
P-2720 Amadora

SPAIN

INTA (RTO/AGARD Publications)
Carretera de Torrejón a Ajalvir, Pk.4
28850 Torrejón de Ardoz - Madrid

TURKEY

Millî Savunma Başkanlığı (MSB)
ARGE Dairesi Başkanlığı (MSB)
06650 Bakanlıklar - Ankara

UNITED KINGDOM

Defence Research Information Centre
Kentigern House
65 Brown Street
Glasgow G2 8EX

UNITED STATES

NASA Center for AeroSpace Information (CASI)
Parkway Center, 7121 Standard Drive
Hanover, MD 21076-1320

SALES AGENCIES

NASA Center for AeroSpace
Information (CASI)

Parkway Center
7121 Standard Drive
Hanover, MD 21076-1320
United States

The British Library Document
Supply Centre

Boston Spa, Wetherby
West Yorkshire LS23 7BQ
United Kingdom

Canada Institute for Scientific and
Technical Information (CISTI)

National Research Council
Document Delivery,
Montreal Road, Building M-55
Ottawa K1A 0S2
Canada

Requests for RTO or AGARD documents should include the word 'RTO' or 'AGARD', as appropriate, followed by the serial number (for example AGARD-AG-315). Collateral information such as title and publication date is desirable. Full bibliographical references and abstracts of RTO and AGARD publications are given in the following journals:

Scientific and Technical Aerospace Reports (STAR)

STAR is available on-line at the following uniform resource locator:

<http://www.sti.nasa.gov/Pubs/star/Star.html>

STAR is published by CASI for the NASA Scientific and Technical Information (STI) Program

STI Program Office, MS 157A
NASA Langley Research Center
Hampton, Virginia 23681-0001
United States

Government Reports Announcements & Index (GRA&I)

published by the National Technical Information Service

Springfield

Virginia 22161

United States
(also available online in the NTIS Bibliographic Database or on CD-ROM)



Printed by Canada Communication Group Inc.
(A St. Joseph Corporation Company)
45 Sacré-Cœur Blvd., Hull (Québec), Canada K1A 0S7